01 Apr 1968

Problems in structural diaphragm bracing 1. Beams continuously braced by diaphragms 2. I-section columns braced by girts and a diaphragm

T. V. S. R. Apparao

S. J. Errera

Gordon P. Fisher

DEPARTMENT OF STRUCTURAL ENGINEERING

SCHOOL OF CIVIL ENGINEERING

CORNELL UNIVERSITY

Report No. 331

PROBLEMS IN STRUCTURAL DIAPHRAGM BRACING

1. Beams continuously braced by diaphragms
2. I-section columns braced by girts and a diaphragm

by

T.V.S.R. Apparao

Research Assistant

Samuel J. Errera
Gordon P. Fisher

Project Directors

A research project sponsored by the

American Iron and Steel Institute

Ithaca, New York April, 1968

FOREWORD

This report was originally a thesis presented to the Faculty of the Graduate School of Cornell University for the Degree of Doctor of Philosophy (January, 1968). The helpful advice, suggestions, and criticism of Professor George Winter, Chairman of the author's academic committee, during the course of the work are gratefully acknowledged.

TABLE OF CONTENTS

ABSTRACT

Shear-resistant light-gage metal diaphragms can be very effective in increasing the load carrying capacity of beams continuously braced by diaphragms, or of columns braced by girts which in turn are braced by diaphragms, if proper connections are made between the individual elements. In this thesis, behavior of diaphragm-braced I-beams, channel beams, and Z-beams under uniform moments, and the behavior of axially loaded I-section columns braced by girts which in turn are braced by diaphragms are investigated.

Load-deflection relationships of diaphragm-braced beams are obtained taking into consideration the initial imperfections of the beams and using the equilibrium method. Critical moments of diaphragm-braced beams are derived from the load-deflection relationships by letting the initial imperfections equal zero and solving the resulting eigenvalue problem. A procedure to determine the load carrying capacities of diaphragm-braced beams is given using an assumed criteria of failure for beams and diaphragms. Using the above procedure, load carrying capacities of diaphragm-braced beams are calculated in two examples; they range from 80% to 85% of the corresponding critical moments.

A test was conducted on an assembly of four diaphragm-braced I-beams, and the moment sustained by the beams was 10% smaller than the predicted critical moment. Three tests were conducted on assemblies of two diaphragm-braced channel beams,

and the moments sustained by the beam assemblies ranged from 75% to 99.6% of the corresponding critical moments. Tests conducted on assemblies of two diaphragm-braced I-beams are also reported here. In general, the experimental and predicted load-deflection relationships are in fairly good agreement for both diaphragm-braced I-beam and channel beam assemblies.

Load-deflection relationships of columns braced by girts and diaphragms are obtained taking into consideration the initial imperfections of the columns and using the energy method. The Rayleigh-Ritz technique is used to obtain an approximate solution. Similar to the case of beam assemblies, critical loads of column assemblies are derived from the load-deflection relationships. A procedure to determine the load carrying capacity of columns braced by girts and diaphragms is given using assumed criteria of failure of columns, girts, and diaphragms. Using the above procedure, load carrying capacities of two different wall columns are calculated and they range from 68% to 83% of the corresponding critical loads.

Three tests were conducted on columns braced by two intermediate girts which in turn were braced by diaphragms, and the failure loads of the column assemblies ranged from 84% to 94% of the corresponding critical loads. Fully flexible, fully rigid, and semi-rigid girt-column connections were used in the three tests. The experimental and theoretically predicted load-deflection relationships are in fair agreement.

Theoretical solutions for diaphragm-braced beams and for

columns braced by girts and diaphragms were developed first in the elastic range and then extended to the inelastic range by suitably modifying the elastic modulii. The plastic moment of the beams or the Euler buckling load of the columns between successive girts appears to be theoretically attainable by using the diaphragm bracing.

1. INTRODUCTION

In many structures, shear-resistant light-gage metal diaphragms, such as wall cladding, roof decking, or floor panels are connected directly to beams or columns, or to girts which in turn are connected to columns. Therefore, the beams are continuously braced by the diaphragm, and the columns are either continuously braced by the diaphragm or discretely braced by the girts which in turn are braced by a diaphragm (refer to Figs. 1-1 and 1-2). The investigation reported in this thesis had the objective of determining (1) the buckling strength of ideal members, (2) the load-deflection relationships of imperfect members, and (3) the load carrying capacities of imperfect members, when the members are directly or indirectly braced by a diaphragm. The light-gage steel wall cladding on a metal building frame can brace the girts which in turn brace the columns against buckling about their weak axes if adequate connections are provided. Similarly, light-gage steel roof decking can oppose lateral buckling of truss chords, roof beams and purlins. This investigation is directed towards the determination of the effectiveness and reliability of such bracing.

Timoshenko[1]* has discussed the buckling of bars on elastic foundations, where the foundation consists of closely

---

* Superscripts in parentheses indicate reference numbers in the Bibliography.

spaced, independently acting elastic springs whose reactions are proportional to the lateral displacement of the bar. He also considered the buckling of bars supported on several interior elastic point supports. Bleich[2] extended the theory and considered further cases of bars elastically supported at various points.

Green[3] and Winter[4] determined the behavior of columns braced by elastic supports either discretely or continuously at the center of gravity of the cross section or symmetrically about the flanges. In Ref. (4) the magnitude of the lateral forces in bracing is determined and two characteristics of lateral support are distinguished: strength and stiffness; and "full bracing" is defined as equivalent in effectiveness to immovable lateral support. Full bracing, or full lateral support, therefore, is that restraint which increases the critical load of a member from that for the unbraced mode to that corresponding to the next higher failure mode, such as attainment of full plastic moment in a beam, or strong axis critical load in a column. For discrete spring-type bracing, Winter concluded that to provide less than "full bracing" for a member generally would be uneconomical.

Larson[5], in a discussion of Ref. (4), extended Winter's analysis to shear type lateral supporting media, including diaphragms continuously connected to columns or beams. In this case, the restraint is a function of the slope, or the rate of change of lateral deflection of the member, rather than the lateral deflection itself. Pincus and Fisher[6] have

presented an independent analysis for beams and columns braced by continuous shear-rigid diaphragms, and introduced the concept of "partial lateral support" for this type of bracing. Partial lateral support is defined as that restraint which results in member failure at a load higher than that for the unbraced condition, but in the same mode. For example, a partially braced column may fail by weak-axis buckling, but at a load which is intermediate between the unbraced weak-axis failure load and the strong-axis failure load, and which may be called the "increased or augmented weak-axis buckling load". In many present forms of construction, such partial restraint may be available, and if accounted for, may result in more economical design.

In 1961, an investigation of diaphragm-braced members was initiated at Cornell University under the direction of Professor Gordon P. Fisher, leading to doctoral theses by Pincus[7] in 1963 and by Errera[8] in 1965. From the general energy expression for a beam-column, and using Euler-Lagrange conditions from the calculus of variations, Pincus obtained a theoretical solution to the problem of a centrally loaded elastic column braced by shear-resistant diaphragms symmetrically located with respect to the centroid; that is, with a diaphragm on each flange of the column. An approximate solution was obtained by Pincus for the case of bracing on one flange only, by neglecting twist of the column. Pincus showed that his approach could be used to determine the critical moment to cause lateral buckling of a simply supported elastic beam

with diaphragm bracing. Ref. (9) includes four tests in addition to those presented in Ref. (7) and summarizes the progress to that date. Ref. (6) is a summary of Refs. (7) and (9).

Errera[8] corrected and modified some of the solutions presented by Pincus using the same general procedure. In addition, he presented, (1) the solution for the problem of lateral buckling of diaphragm-braced beams with ends fixed about the vertical and longitudinal axes and subjected to uniform bending moment, using the Rayleigh-Ritz technique; (2) a solution giving the critical buckling load for diaphragm-braced columns with an enforced axis of rotation; and (3) a consideration of the behavior of diaphragm-braced beams and columns in the inelastic range. Theoretical results were compared with experimental results.

Dooley's[10] solution for the problem of an axially loaded column attached at finite intervals to sheeting rails and shear-stiff cladding became known to the author after the author had already obtained a much more general solution for the problem of an axially loaded column braced by girts which in turn are braced by a shear diaphragm. The solution to the above problem obtained by the author is presented in the following as a part of this thesis. This solution (1) permits the movement of the flange at the points of attachment to the intermediate girts relative to the ends of the column (Dooley's solution does not permit this movement), (2) uses a better approximation of the deflection functions, (3) considers the initial imperfec-

tions of the column, and (4) includes the case of sidesway of the column. Further, the load carrying capacity of an imperfect column braced by girts which in turn are braced by a diaphragm is determined basing the failure of the column-girt-diaphragm assembly on either (1) yield failure of the column, or (2) shear failure of the diaphragm, or (3) failure by bending of the intermediate girts.

The investigation reported in this present thesis comprises the following:

A) For diaphragm-braced beams either "simply supported" (i.e. flexurally simply supported twist is zero and warping unrestrained at ends) or "fixed" (i.e. fixed about the vertical and longitudinal axes and simply supported about the horizontal axis at ends) subjected to uniform bending moment using the equilibrium method,

1. a solution for load-deflection relationships for imperfect Z-beams, I-beams and channel beams,

2. a solution for buckling loads of ideal Z-beams, I-beams and channel beams,

3. an investigation of the load-carrying capacity of imperfect I-beams and channel beams based on failure by yielding of the beams or failure by shear of the diaphragm.

B) For an axially loaded I-section column with "hinged" ends (i.e. flexurally hinged; twist is zero and warping is unrestrained at ends) braced by girts which in turn are braced by a diaphragm using an energy method and the Rayleigh-Ritz technique,

1. a solution for the load-deflection relationships of an imperfect column,

2. a solution for the buckling load of an ideal column,

3. an investigation of the load-carrying capacity of an imperfect column based on failure by yielding of the column, or failure by shear of the diaphragm, or failure of the girts in bending.

C) For an axially loaded I-section column, with the ends flexurally hinged and torsionally "fixed" (i.e. twist and first derivative of twist are zero and warping restrained), braced by two girts which in turn are braced by a diaphragm,

1. a solution for the load-deflection relationships of an imperfect column,

2. a solution for the buckling load of an ideal column.

D) Consideration of inelastic behavior of diaphragm-braced beams, and of columns braced by girts which in turn are braced by a diaphragm.

Three tests on diaphragm-braced 6 [8.5 double-beam assemblies, and three tests on 8Jr6.5 I-section columns braced by girts which in turn are braced by a diaphragm were conducted to verify the respective theories developed for the behavior of the members.

The theory for predicting the buckling loads of diaphragm-braced ideal I-beam assemblies has been developed by Errera[8] and verified by experiments on diaphragm-braced double 8Jr6.5 I-beam assemblies. Tests conducted by Errera

on diaphragm-braced 10B17 double I-beam assemblies are reported in this thesis to verify the theory developed by the author for the prediction of load-deflection relationships in addition to the comparison of the failure loads of the beam assemblies with the theoretically predicted buckling loads. Further, a test was conducted on an assembly of four diaphragm-braced 8Jr6.5 I-beams and a comparison of the failure load of the diaphragm-braced beam with its theoretically predicted buckling load is presented in this report.

Notation: The symbols adopted for use in this thesis are defined where they first appear and are listed alphabetically in Appendix I.

2. DIAPHRAGM-BRACED BEAMS UNDER UNIFORM MOMENT

2.1 Elastic Theory

2.1.1 General Formulation of the Problem by Equilibrium Method

A model of the diaphragm-braced beams chosen for the purposes of the theoretical analysis is shown in Fig. 2-1. It consists of two beams braced at their compression flanges by a diaphragm. For the case of uniform moments applied at the ends in a plane parallel to the planes of the webs of the beams, the critical moment of the double-beam assembly is obtained by using an equilibrium approach. The following forces are considered to describe the equilibrium of one of the beams when the assembly is under load:

1. Components of uniform moments applied at the ends in the directions of the principal axes ξ, η, and ζ of the deflected beam at the particular section under consideration. The deflected shape of the beam assembly under load is shown in Fig. 2-2 along with the coordinate axes. The vectorial components of the uniform moments are shown in Figs. 2-3.

2. Distributed force on the beam perpendicular to its longitudinal axis at the level of the diaphragm due to shear in the diaphragm in the deflected beam assembly. To evaluate this force consider the deflected shape of the diaphragm in plan as shown in Fig. 2-4. At the cross section AA the net force on the beam due to shear in the diaphragm is the difference in the shear forces contributed by the two adjacent shear panels 1 and

2 as shown in Fig. 2-4. In obtaining a continuous distributed force per unit length of the beam the difference in the above forces can be treated as the first derivative of the shear force at the particular cross section. Shear force S_b on one beam at the cross section is given by

$$S_b = \tau t w \tag{2-1}$$

where

τ is the shear stress in the diaphragm

t is the thickness of the diaphragm

and w is the width of the diaphragm contributing to the bracing of one beam.

Further,

$$\tau = G_{eff} r \tag{2-2}$$

where

G_{eff} is the effective shear modulus of the diaphragm[8]

and r is the shear strain at section AA.

Therefore,

$$S_b = G_{eff} t w r$$

$$= Q r \tag{2-3}$$

where $$Q = G_{eff} t w \tag{2-4}$$

Note that Q is the shear rigidity[8] of the diaphragm contributing to the bracing of one member. Hence the distributed force q on one beam perpendicular to its longitudinal axis and in the plane of the diaphragm due to shear in the diaphragm is given by

$$q = \frac{d}{dz}(Qr)$$

$$= Qr' \qquad (2\text{-}5)$$

The direction of the force is shown in Fig. 2-4. It can be observed from Fig. 2-4 that the longitudinal component of the complementary shear in the diaphragm balances in itself if the total length of the beam is considered.

3. Distributed twist restraint on the beam due to the cross bending rigidity[8] F of the diaphragm. F is defined as the restraining moment per unit twist of the beam.

4. Internal resistance of the beam.

The general equations of equilibrium[1] for a beam bent about both the principal axes and twisted may be written as

$$EI_\xi v_1^{IV} = (-M_\xi)'' + q_\eta \qquad (2\text{-}6)$$

$$EI_\eta u_1^{IV} = (M_\eta)'' + q_\xi \qquad (2\text{-}7)$$

and

$$GK\beta'' - E\Gamma\beta^{IV} = \frac{dM_\xi}{dz} + F\beta - qe \qquad (2\text{-}8)$$

where

EI_ξ is the strong-axis bending rigidity

EI_η is the weak-axis bending rigidity

$E\Gamma$ is the warping rigidity

GK is the torsional rigidity

M_ξ, M_η, and M_ζ are the vectorial components of the externally applied end moments at the particular cross section under consideration

e is the distance from the center of gravity (C.G.) of the beam to the plane of the diaphragm

q, q_ξ, and q_η are the equivalent distributed loads as shown in Fig. 2-5.

and u_i, v_i, and β are the displacements in the directions shown in Figs. 2-3 and 2-5.

Approximations which are consistent with the small deflection theory are used wherever necessary without explicit statement.

The quantities on the right hand side of Eqs. 2-6 through 2-8 are evaluated explicitly for the problem of diaphragm-braced Z-beams in the following, and the solution for the behavior of

diaphragm-braced Z-beams under uniform moments is obtained. The behavior of diaphragm-braced I-beams and channel beams will be derived from the above solution as a particular case.

Case a. Ideal Z-beams. To realize a pure buckling problem of ideal Z-beams[11] braced by a diaphragm on one flange only, in addition to the uniform moments parallel to the webs of the beams at the ends, moments in the horizontal plane at the supports have to be applied in such an amount that the beams bend vertically until they buckle. Moments in the horizontal plane are required because the principal axes of a Z-section are not parallel and perpendicular to the plane of its web.

The horizontal moment M_s to be offered by the support for each beam at its ends so that the beams bend vertically before they buckle is worked out in Appendix II and is given by

$$M_s = \frac{M \sin\alpha \cos\alpha \ (I_{x_1} - I_{y_1})}{I_{x_1} \cos^2\alpha + I_{y_1} \sin^2\alpha} \qquad (2\text{-}9)$$

where M is the moment applied at the ends on each beam in a plane parallel to the plane of the web, X_1 and Y_1 are the principal axes, X and Y are respectively the axes perpendicular and parallel to the web of the Z-section as shown in Fig. 2-2, and α is the angle between X and X_1. The components of M and M_s in the principal directions are given by

$$M_{x_1} = M\cos\alpha + M_s \sin\alpha$$

$$= M\left\{\frac{1}{\cos\alpha + \frac{I_{y_1} \sin^2\alpha}{I_{x_1} \cos\alpha}}\right\} \qquad (2\text{-}10)$$

and $$M_{y_1} = M \sin\alpha - M_s \cos\alpha$$

$$= M \left\{ \frac{1}{\sin\alpha + \frac{I_{x_1} \cos^2\alpha}{I_{y_1} \sin\alpha}} \right\} \qquad (2\text{-}11)$$

Fig. 2-4 shows the deflected shape of one of the Z-beams along with the direction of measurement of displacements u_1 and β along the principal axes. ξ and η represent the principal axes of the Z-section in its deflected shape. The shear strain γ in this case is given by

$$\gamma = \frac{d}{dz} \left\{ u_1 \cos\alpha + v_1 \sin\alpha + e\beta \right\} \qquad (2\text{-}12)$$

or

$$\gamma = u_1' \cos\alpha + v_1' \sin\alpha + e\beta' \qquad (2\text{-}13)$$

Therefore,

$$q_f = Q \left(u_1'' \cos\alpha + v_1'' \sin\alpha + e\beta'' \right) \qquad (2\text{-}14)$$

considering the deflected shape of the beam shown in Fig. 2-5, distributed forces q_{f_ξ} and q_{f_η} may be written as

$$\left.\begin{aligned} q_{f_\xi} &= q_f \cos(\alpha - \beta) \\ \text{and} \quad q_{f_\eta} &= q_f \sin(\alpha - \beta) \end{aligned}\right\}$$

As an approximation, letting $\sin\beta = \beta$ and $\cos\beta = 1$, and neglecting $\beta\sin\alpha$ and $\beta\cos\alpha$ because they are smaller order terms compared to $\sin\alpha$ and $\cos\alpha$, q_{f_ξ} and q_{f_η} may

be approximated as

$$\left.\begin{aligned} q_\xi &= q\cos\alpha \\ q_\eta &= q\sin\alpha \end{aligned}\right\} \quad \text{and} \qquad (2\text{-}15)$$

The components of moments at the ends along the principal axes of the Z-beam may be obtained, by referring to Fig. 2-3, as

$$\begin{aligned} M_\xi &= M_{x_1}\cos\beta - M_{y_1}\sin\beta \\ &\cong M_{x_1} - M_{y_1}\beta \end{aligned} \qquad (2\text{-}16)$$

$$\begin{aligned} M_\eta &= M_{x_1}\sin\beta + M_{y_1}\cos\beta \\ &\cong M_{x_1}\beta + M_{y_1} \end{aligned} \qquad (2\text{-}17)$$

and

$$M_\xi = M_{x_1}u_1' - M_{y_1}v_1' \qquad (2\text{-}18)$$

After substituting the above values, simplifying and rearranging the terms, Eqs. 2-6 through 2-8 may be written as

$$EI_{x_1}v_1^{IV} - Q\left(u_1''\cos\alpha + v_1''\sin\alpha + e\beta''\right)\sin\alpha - M_{y_1}\beta'' = 0 \qquad (2\text{-}19)$$

$$EI_{y_1}u_1^{IV} - Q\left(u_1''\cos\alpha + V_1''\sin\alpha + e\beta''\right)\cos\alpha + M_{x_1}\beta'' = 0 \qquad (2\text{-}20)$$

and

$$G K \beta'' - E \Gamma \beta^{IV} + Qe\left(u_1'' \cos\alpha + v_1'' \sin\alpha + e\beta''\right) - F\beta - M_{x_1} u_1'' + M_{y_1} v_1'' = 0 \qquad (2\text{-}21)$$

(Note that I_ξ is replaced by I_x and I_η by I_y.)

It may be observed that Eqs. 2-19 through 2-21 are coupled in u_1, v_1, and β, and they describe a pure buckling problem as desired.

Case b. Imperfect Z-beams. The equations describing the load-deflection relationships of a diaphragm-braced imperfect Z-beam can be obtained from Eqs. 2-19 through 2-21 by modifying the terms containing the components of applied moments as follows:

$$E I_{x_1} v_1^{IV} - Q\left(u_1'' \cos\alpha + v_1'' \sin\alpha + e\beta''\right) \sin\alpha - M_{y_1}\left(\beta'' + \beta_o''\right) = 0 \qquad (2\text{-}22)$$

$$E I_{y_1} u_1^{IV} - Q\left(u_1'' \cos\alpha + v_1'' \sin\alpha + e\beta''\right) \cos\alpha + M_{x_1}\left(\beta'' + \beta_o''\right) = 0 \qquad (2\text{-}23)$$

$$G K \beta'' - E \Gamma \beta^{IV} + Qe\left(u_1'' \cos\alpha + v_1'' \sin\alpha + e\beta''\right) - F\beta - M_{x_1}\left(u_1'' + u_{10}''\right) + M_{y_1}\left(v_1'' + v_{10}''\right) = 0 \qquad (2\text{-}24)$$

Where u_{10}, v_{10}, and β_o are the initial imperfections corresponding to the displacements u_1, v_1, and β respectively.

2.1.2 Load-Deflection Relationships for Diaphragm-Braced Imperfect Beams

Case a. Z-Beams. The load-deflection relationships for Z-beams are obtained for the following end conditions by solv-

ing Eqs. 2-22 through 2-24.

a-1. "Simply Supported" ends. (i.e. ends of the section are free to warp and free to rotate about the X_1 and Y_1 axes but cannot rotate about the Z axis or deflect in the X_1 and Y_1 directions.) For this case,

$$\left.\begin{aligned} u_1 = v_1 = \beta = 0 \qquad & \text{at } z = 0 \text{ and } z = L \\ \frac{d^2u_1}{dz^2} = \frac{d^2v_1}{dz^2} = \frac{d^2\beta}{dz^2} = 0 \qquad & \text{at } z = 0 \text{ and } z = L \end{aligned}\right\} \quad (2\text{-}25)$$

The general solution for Eqs. 2-22 through 2-24 and the above end conditions is given by

$$\left.\begin{aligned} u_1 &= C_n \sin\frac{n\pi z}{L} \\ v_1 &= E_n \sin\frac{n\pi z}{L} \\ \text{and} \quad \beta &= D_n \sin\frac{n\pi z}{L} \end{aligned}\right\} \quad (2\text{-}26)$$

(where C_n, D_n, and E_n are the amplitudes of the unknown additional deflections) when the initial imperfections are of similar form, and given by

$$\left.\begin{aligned} u_{10} &= \delta_{u_{1,n}} \sin\frac{n\pi z}{L} \\ v_{10} &= \delta_{v_{1,n}} \sin\frac{n\pi z}{L} \\ \text{and} \quad \beta_0 &= \delta_{\beta_n} \sin\frac{n\pi z}{L} \end{aligned}\right\} \quad (2\text{-}27)$$

where $\delta_{u_{1,n}}$, $\delta_{v_{1,n}}$, and δ_{β_n} are the amplitudes of

the initial imperfections. When there are no intermediate equidistant supports and when the initial imperfections are given by

$$\left.\begin{aligned} u_{10} &= \delta_{u_{1,1}} \sin\frac{\pi z}{L} \\ V_{10} &= \delta_{V_{1,1}} \sin\frac{\pi z}{L} \end{aligned}\right\} \qquad (2\text{-}28)$$

and

$$\beta_0 = \delta_{\beta_1} \sin\frac{\pi z}{L}$$

the solution to Eqs. 2-22 through 2-24 and the above boundary conditions is given by the additional deflection pattern:

$$\left.\begin{aligned} u_1 &= C_1 \sin\frac{\pi z}{L} \\ V_1 &= E_1 \sin\frac{\pi z}{L} \\ \beta &= D_1 \sin\frac{\pi z}{L} \end{aligned}\right\} \qquad (2\text{-}29)$$

a-2. "Fixed" ends. (i.e. the ends are free to rotate about the X_1 axis but are fixed about the Y_1 and Z axes and cannot deflect in the X_1 direction.) For this case,

$$\left.\begin{aligned} u_1 = V_1 = \beta = 0 \qquad & \text{at } z = 0 \text{ and } z = L \\ \frac{du_1}{dz} = \frac{dV_1}{dz} = \frac{d\beta}{dz} = 0 \qquad & \text{at } z = 0 \text{ and } z = L \end{aligned}\right\} \qquad (2\text{-}30)$$

Similar to case a-1, when there are no lateral intermediate equidistant supports and when the initial imperfections are given by

$$\left.\begin{aligned} u_{10} &= \delta_{u_{1,1}}\left(1-\cos\frac{2\pi z}{L}\right)\\ v_{10} &= \delta_{v_{1,1}}\left(1-\cos\frac{2\pi z}{L}\right)\\ \text{and}\qquad \beta_0 &= \delta_{\beta_1}\left(1-\cos\frac{2\pi z}{L}\right)\end{aligned}\right\} \tag{2-31}$$

the solution to Eqs. 2-22 through 2-24 and the above boundary conditions is given by the additional deflection pattern:

$$\left.\begin{aligned} u_1 &= C_1\left(1-\cos\frac{2\pi z}{L}\right)\\ v_1 &= E_1\left(1-\cos\frac{2\pi z}{L}\right)\\ \beta &= D_1\left(1-\cos\frac{2\pi z}{L}\right)\end{aligned}\right\} \tag{2-32}$$

if the term containing the cross bending rigidity F of the diaphragm is dropped. This may be justified by considering two facts: (1) the spacing of the connectors may be considerable and therefore the effective bending rigidity will be small, and (2) the flanges of the beams may rotate with respect to the webs of the beams. Note that because the initial imperfection pat-

tern is affine to the additional deflection pattern, the additional deflections determined will be a conservatively high estimate.

The total deflections u_{1t} , v_{1t} , and β_t of the beam are given by

$$\left.\begin{aligned} u_{1t} &= u_{10} + u_1 \\ v_{1t} &= v_{10} + v_1 \\ \text{and} \quad \beta_t &= \beta_0 + \beta \end{aligned}\right\} \qquad (2\text{-}33)$$

Considering the deflection pattern given by Eqs. 2-29 and 2-32, the maximum shear strain r_{max} of the diaphragm is given by (using Eq. 2-13)

$$r_{max} = \frac{n\pi}{L}\left(C_1 \cos\alpha + E_1 \sin\alpha + e D_1\right) \qquad (2\text{-}34)$$

where $n = 1$ if the ends are "simply supported", or $n = 2$ if the ends are "fixed".

Substitution of the values of u_1 , v_1 , β , u_{10} , v_{10} , and β_0 either from Eqs. 2-28 and 2-29 or from Eqs. 2-31 and 2-32 in Eqs. 2-22 through 2-24 gives the load-deflection relationships of a diaphragm-braced Z-beam as

$$\begin{bmatrix} EI_{y_1}\left(\frac{n\pi}{L}\right)^2 + Q\cos^2\alpha & Q\sin\alpha\cos\alpha & Qe\cos\alpha - K_1 M \\ Q\sin\alpha\cos\alpha & EI_{x_1}\left(\frac{n\pi}{L}\right)^2 + Q\sin^2\alpha & Qe\sin\alpha + K_2 M \\ Qe\cos\alpha - K_1 M & Qe\sin\alpha + K_2 M & EI'\left(\frac{n\pi}{L}\right)^2 + GK + Qe^2 \end{bmatrix} \begin{Bmatrix} C_1 \\ E_1 \\ D_1 \end{Bmatrix} = M \begin{Bmatrix} K_1\delta_{\beta_1} \\ K_2\delta_{\beta_1} \\ K_1\delta_{u_{1,1}} - K_2\delta_{v_{1,1}} \end{Bmatrix} \qquad (2\text{-}35)$$

where the term containing the flexural rigidity of the diaphragm is dropped, and

$$K_1 = \frac{1}{\cos\alpha + \dfrac{I_{y_1}\sin^2\alpha}{I_{x_1}\cos\alpha}}$$

and

$$K_2 = \frac{1}{\sin\alpha + \dfrac{I_{x_1}\cos^2\alpha}{I_{y_1}\sin\alpha}}$$

Eq. 2-35 enables one to evaluate the amplitudes of the additional deflections C_1, D_1, and E_1 for a diaphragm-braced Z-beam if the amplitudes of the initial imperfections $\delta_{u_{1,1}}$, $\delta_{v_{1,1}}$ and δ_β are known.

Case b. I-beams and Channel beams. The load-deflection relationships of diaphragm-braced I-beams and channel beams can be derived from Eq. 2-35 by letting $\alpha = 0$, where α is the angle between the X_1 and X axes. Consequently, $K_1 = 1$, $K_2 = 0$, $\sin\alpha = 0$, and $\cos\alpha = 1$. After simplification the amplitudes of additional deflections C_1 and D_1 can be expressed as

$$C_1 = \frac{M\delta_\beta\left\{E\Gamma\left(\frac{n\pi}{L}\right)^2 + GK + Qe^2\right\} + M\delta_u(M - Qe)}{\left\{EI_y\left(\frac{n\pi}{L}\right)^2 + Q\right\}\left\{E\Gamma\left(\frac{n\pi}{L}\right)^2 + GK + Qe^2\right\} - (M - Qe)^2} \quad (2\text{-}36)$$

and

$$D_1 = \frac{M\delta_u\left\{EI_y\left(\frac{n\pi}{L}\right)^2 + Q\right\} + M\delta_\beta(M - Qe)}{\left\{EI_y\left(\frac{n\pi}{L}\right)^2 + Q\right\}\left\{E\Gamma\left(\frac{n\pi}{L}\right)^2 + GK + Qe^2\right\} - (M - Qe)^2} \quad (2\text{-}37)$$

where δ_u and δ_β are the amplitudes of initial imperfections of either an I-beam or a channel beam corresponding to $\delta_{u_{1,1}}$ and δ_{β_1} of a Z-beam.

Note that the amplitude of the uncoupled deflection E_1 cannot be derived from Eq. 2-35 using the above approach, but can be readily evaluated as the vertical deflection of a beam under uniform moment.

When there is no diaphragm bracing, i.e. when $Q = 0$, Eqs. 2-36 and 2-37 check with those obtained by Massey[12] for imperfect I-beams and channel beams under uniform moment.

Maximum shear strain γ_{max} of the diaphragm can be derived from Eq. 2-34 by letting $\alpha = 0$ and is given by

$$\gamma_{max} = \frac{n\pi}{L}\left(C_1 + eD_1\right) \qquad (2\text{-}38)$$

2.1.3 Critical Moment for Diaphragm-Braced Ideal Beams

Case a. Z-Beams. The critical moment for diaphragm-braced Z-beams can be derived from Eq. 2-35 by setting the amplitudes of the initial imperfections $\delta_{u_{1,1}}$, $\delta_{v_{1,1}}$, and δ_{β_1} equal to zero and solving the resulting eigenvalue problem for a non-trivial solution. Then the critical moment is given by

$$\begin{vmatrix} EI_y\left(\frac{n\pi}{L}\right)^2 + Q\cos^2\alpha & Q\sin\alpha\cos\alpha & Qe\cos\alpha - K_1M \\ Q\sin\alpha\cos\alpha & EI_x\left(\frac{n\pi}{L}\right)^2 + Q\sin^2\alpha & Qe\sin\alpha + K_2M \\ Qe\cos\alpha - K_1M & Qe\sin\alpha + K_2M & EI_\omega\left(\frac{n\pi}{L}\right)^2 + GK + Qe^2 \end{vmatrix} = 0 \qquad (2\text{-}39)$$

When there is no diaphragm bracing, i.e. when $Q = 0$, Eq. 2-39 checks with that obtained by Hill[11] for the critical moment of ideal Z-beams.

Case b. I-Beams and Channel Beams. The critical moment for diaphragm-braced ideal I-beams and channel beams can be derived from Eq. 2-39 by letting $\alpha = 0$. After simplification, the critical moment M_{cn} is given by

$$M_{cn} = \sqrt{\left\{EI_y\left(\frac{n\pi}{L}\right)^2 + Q\right\}\left\{EI_x\left(\frac{n\pi}{L}\right)^2 + GK + Qc^2\right\}} + Qe \qquad (2\text{-}40)$$

The above equation agrees with the equation developed by Errera[8] for diaphragm-braced ideal I-beams using an energy method.

When there is no diaphragm bracing, i.e. when $Q = 0$, Eq. 2-40 checks with that obtained in the conventional theory for the critical moment in lateral buckling of ideal I-beams and channel beams.

2.2 Inelastic Theory

The bilinear stress-strain relation shown in Fig. 2-6 is assumed for the inelastic theory presented in this section. Further, residual stresses are not considered. Therefore the inelastic theory is concerned with the beams subjected to moments M greater than the yield moments M_y and smaller than the plastic moments M_{pl} . The diaphragm bracing is assumed to be in the elastic range even if the beams are in the inelastic range or have attained the plastic moment.

a. Diaphragm-Braced I-Beams and Channel Beams

The modulus of elasticity E and the shear modulus G are replaced by the reduced modulii E_{nx} or E_{ny} and G_n respectively in all the equations of the elastic theory given in the previous sections, to describe the behavior of the diaphragm-

braced beams in the inelastic range. The reduced modulii $E_{\pi x}$, $E_{\pi y}$, and G_{π} are defined as

$$E_{\pi x} = E \frac{(I_x)_{\text{elastic portion of the section}}}{(I_x)_{\text{total section}}} \quad (2\text{-}41)$$

$$E_{\pi y} = E \frac{(I_y)_{\text{elastic portion of the section}}}{(I_y)_{\text{total section}}} \quad (2\text{-}42)$$

and $$G_{\pi} = G\left(\frac{E_{\pi y}}{E}\right) \quad (2\text{-}43)$$

where I_x and I_y are the moments of inertia of the cross section about the X and Y axes respectively. E is replaced by $E_{\pi x}$ in the term EI_x and E is replaced by $E_{\pi y}$ in the terms EI_y and $E\Gamma$ because bending about the Y axis and twisting of the beam are coupled in the lateral buckling of beams.

Bleich uses $G_{\pi} = G\left(E_t/E\right)$ in the inelastic range of lateral buckling of beams. However, in most cases of lateral torsional-flexural buckling the critical moment depends more on $E_{\pi y}$ than on G_{π}. This is due to the fact that only the last of the three deformations--bending, warping, and twisting--depends on the torsional stiffness GK[13]. The choice of value G_{π} is therefore less critical than that of $E_{\pi y}$. For the purposes of simplicity the expression for G_{π} in Eq. 2-43 is used in the inelastic range.

To determine the critical moments of diaphragm-braced ideal I-beams and channel beams the following procedure is followed.

Depending on the value of the shear rigidity Q of the diaphragm the beam buckles either elastically or inelastically or it reaches its plastic moment. The minimum value of shear rigidity Q_y required for a beam to reach the yield moment can be obtained from Eq. 2-40 as follows:

$$Q_y = \frac{M_y^2 - EI_y\left(\frac{n\pi}{L}\right)^2\left\{Er\left(\frac{n\pi}{L}\right)^2 + GK\right\}}{EI_y\left(\frac{n\pi}{L}\right)^2 e^2 + 2M_y e + Er\left(\frac{n\pi}{L}\right)^2 + GK} \qquad (2\text{-}44)$$

The minimum value of shear rigidity Q_{pl} required for a beam to reach its plastic moment is obtained from Eq. 2-44 by letting $E = G = 0$ and replacing M_y by M_{pl}, and is given by

$$Q_{pl} = \frac{M_{pl}}{2e} \qquad (2\text{-}45)$$

Then, for

$Q \leq Q_y$	the beam buckles in the elastic range, $M_{cr} \leq M_y$
$Q_y < Q < Q_{pl}$	the beam buckles in the inelastic range, $M_y < M_{cr} < M_{pl}$
$Q \geq Q_{pl}$	the beam attains its plastic moment, $M_{cr} = M_{pl}$

where Q is the shear rigidity of the diaphragm contributing to the support of one beam. If the beam buckles in the elastic range its critical moment is evaluated straightforward by using Eq. 2-40.

But if the beam buckles in the inelastic range its critical moment is given by

$$M_{cr} = \sqrt{\left\{E_{ry} I_y \left(\frac{n\pi}{L}\right)^2 + Q\right\}\left\{E_{ry}\Gamma\left(\frac{n\pi}{L}\right)^2 + G_r K + Qe^2\right\}} + Qe \quad (2\text{-}46)$$

and a trial and error procedure has to be used because the values E_{ry} and G_r are unknown until the critical moment M_{cr} is known. The trial and error procedure of determining the critical moment will be tedious. Therefore, an approximate and simple procedure to determine the critical moment is suggested in the following.

The shear rigidity Q can be expressed as (from Eq. 2-46)

$$Q = \frac{M_{cr}^2 - E_{ry} I_y \left(\frac{n\pi}{L}\right)^2 \left\{E_{ry}\Gamma\left(\frac{n\pi}{L}\right)^2 + G_r K\right\}}{E_{ry} I_y \left(\frac{n\pi}{L}\right)^2 e^2 + 2 M_{cr} e + E_{ry}\Gamma\left(\frac{n\pi}{L}\right)^2 + G_r K} \quad (2\text{-}47)$$

Now, a particular depth of penetration of yielding $\left(\frac{d}{2} - y\right)$ (refer to Fig. 2-7) may be assumed and the moment M, E_{ry}, and G_r can be calculated for this particular case. Then, Q is computed for the moment M using Eq. 2-47 and replacing M_{cr} by M. If the critical moment is required for a particular value of Q, two values Q_1 and Q_2 are obtained from Eq. 2-47 such that $Q_1 \leq Q \leq Q_2$, and Q_1 and Q_2 are in the close neighborhood of Q. Let the moments corresponding to Q_1 and Q_2 be M_1 and M_2 respectively. By linear interpolation, the critical moment M_{cr} for the shear rigidity Q is given by

$$M_{cr} = M_1 + \frac{(M_2 - M_1)(Q - Q_1)}{(Q_2 - Q_1)} \qquad (2\text{-}48)$$

This type of procedure to obtain the critical moments in the inelastic range is illustrated in the examples of the following section.

Also, the additional deflections C_1 and D_1 of imperfect diaphragm-braced beams under uniform moment M in the inelastic range are given by (refer to Eqs. 2-36 and 2-37)

$$C_1 = \frac{M\delta_\beta\left\{E_{ry}\Gamma\left(\frac{n\pi}{L}\right)^2 + G_r K + Qe^2\right\} + M\delta_u\,(M - Qe)}{\left\{E_{ry}I_y\left(\frac{n\pi}{L}\right)^2 + Q\right\}\left\{E_{ry}\Gamma\left(\frac{n\pi}{L}\right)^2 + G_r K + Qe^2\right\} - (M - Qe)^2} \qquad (2\text{-}49)$$

and

$$D_1 = \frac{M\delta_u\left\{E_{ry}I_y\left(\frac{n\pi}{L}\right)^2 + Q\right\} + M\delta_\beta\,(M - Qe)}{\left\{E_{ry}I_y\left(\frac{n\pi}{L}\right)^2 + Q\right\}\left\{E_{ry}\Gamma\left(\frac{n\pi}{L}\right)^2 + G_r K + Qe^2\right\} - (M - Qe)^2} \qquad (2\text{-}50)$$

b. Diaphragm-Braced Z-beams

The procedure for determining the behavior of diaphragm-braced Z-beams in the inelastic range is similar to that presented above and the load-deflection relationships of a diaphragm-braced imperfect Z-beam are given by

$$\begin{bmatrix} E_{ny_1} I_{y_1}\left(\frac{n\pi}{L}\right)^2 + Q\cos^2\alpha & Q\sin\alpha\cos\alpha & Qe\cos\alpha - K_1 M \\ Q\sin\alpha\cos\alpha & E_{nx_1} I_{x_1}\left(\frac{n\pi}{L}\right)^2 + Q\sin^2\alpha & Qe\sin\alpha + K_2 M \\ Qe\cos\alpha - K_1 M & Qe\sin\alpha + K_2 M & E_{n\gamma_1}\Gamma\left(\frac{n\pi}{L}\right)^2 + G_x K + Qe^2 \end{bmatrix} \begin{Bmatrix} C_1 \\ E_1 \\ D_1 \end{Bmatrix} = M \begin{Bmatrix} K_1\delta_{\beta_1} \\ -K_2\delta_{\beta_1} \\ K_1\delta_{u_{1,1}} \\ -K_2\delta_{r_{1,1}} \end{Bmatrix} \tag{2-51}$$

where the term containing the flexural rigidity F of the diaphragm has been dropped (refer to page 18). In Eq. 2-51,

n = 1 if the ends are simply supported (i.e. twist is zero and warping is unrestrained at the ends)

n = 2 if the ends are "fixed" (i.e. fixed about the vertical and longitudinal axes)

$$E_{nx_1} = E\,\frac{(I_{x_1})\text{ elastic portion of the cross section}}{(I_{x_1})\text{ total cross section}}$$

$$E_{ny_1} = E\,\frac{(I_{y_1})\text{ elastic portion of the cross section}}{(I_{y_1})\text{ total cross section}}$$

$$G_n = G\left(\frac{E_{ny_1}}{E}\right)$$

$E_{nx_1} I_{x_1}$ is the flexural rigidity of the beam about the principal axis X_1

$E_{ny_1} I_{y_1}$ is the flexural rigidity of the beam about the principal axis Y_1

$E_{n Y_1} \Gamma$ is the warping rigidity of the beam

$G_n K$ is the torsional rigidity of the beam

Q is the shear rigidity of the diaphragm

e is the distance from the C.G. of the beam to the plane of the diaphragm

$$K_1 = \frac{1}{\cos\alpha + \frac{I_{Y_1} \sin^2\alpha}{I_{X_1} \cos\alpha}}$$

$$K_2 = \frac{1}{\sin\alpha + \frac{I_{X_1} \cos^2\alpha}{I_{Y_1} \sin\alpha}}$$

$\delta_{u_{1,1}}$, $\delta_{v_{1,1}}$, and δ_{β_1} are the amplitudes of the initial imperfections (refer to Eqs. 2-28 and 2-31) and C_1, D_1, and E_1 are the amplitudes of the additional deflections (refer to Eqs. 2-29 and 2-32).

The critical moment for a diaphragm-braced ideal Z-beam can be derived from Eq. 2-51 by letting the initial imperfections equal zero and solving for the nontrivial solution of the resulting eigenvalue problem. The critical moment is given by

$$\begin{vmatrix} E_{n Y_1} I_{Y_1} \left(\frac{n\pi}{L}\right)^2 + Q\cos^2\alpha & Q\sin\alpha\cos\alpha & Qe\cos\alpha - K_1 M \\ Q\sin\alpha\cos\alpha & E_{n X_1} I_{X_1} \left(\frac{n\pi}{L}\right)^2 + Q\sin^2\alpha & Qe\sin\alpha + K_2 M \\ Qe\cos\alpha - K_1 M & Qe\sin\alpha + K_2 M & E_{n Y_1} \Gamma \left(\frac{n\pi}{L}\right)^2 + G_n K + Qe^2 \end{vmatrix} = 0$$

2.3 Investigation of Load Carrying Capacity of Diaphragm-Braced Imperfect I-Beams and Channel Beams

In this section the load carrying capacity of diaphragm-braced imperfect I-beams and channel beams is determined considering that the load carrying capacity is based on either the failure of the beam by yielding or the failure of the diaphragm in shear. The criteria for both of the above failures established for the purposes of investigation in this section are described in the following.

1. Failure of the beam by yielding. For the purposes of the following investigation a beam is considered as failed when the moment M in the vertical plane of the beam reaches the yield moment M_y of the beam. In fact, a beam could carry its plastic moment M_{pl} if it bends only in the vertical plane. However, the effect of lateral bending and twist of an imperfect beam contributes towards the failure of the beam by yielding. To account for this the beam is considered as failed if the moment about the strong axis of the beam reaches its yield moment M_y.

2. Failure of the diaphragm in shear. To establish the failure of the diaphragm in a diaphragm-braced beam assembly the individual characteristics of the diaphragm in shear must be known. From experience in testing shear diaphragms at Cornell University[14,15] it can be stated that two identical and relatively flexible shear diaphragms may give considerably different load-deflection relationships at higher load levels, say, beyond 80% of ultimate load. Therefore, the shear rigidity Q_d and

the average shear strain γ_d at 80% of ultimate shear load of the diaphragm are taken as the characteristics to be used for the purposes of investigation in this section in the computations for the failure of all types (whether relatively flexible or rigid) of diaphragms in shear. Q_d and γ_d are determined from the load-deflection curve (refer to Fig. 2-8) and the geometry of the shear diaphragm as follows:

Shear stiffness G_d [14] is defined as, $G_d = \frac{P_d\, a}{\Delta_d\, b}$

where

P_d is 80% of the ultimate load

Δ_d is the shear deflection at 80% of the ultimate load

a is the dimension of the shear panel perpendicular to the direction of the applied shear load

and b is the dimension of the shear panel along the direction of the applied shear load.

(Note that the subscript ' d ' refers to the values at 80% of the ultimate load)

Then,

Shear rigidity [8] $\quad Q_d = G_d W \quad$ and

Shear Strain $\quad \gamma_d = \frac{\Delta_d}{a}$

where

W is the width of the shear diaphragm contributing to the bracing of one member.

Now, the diaphragm in a diaphragm-braced beam assembly is considered as failed if the maximum shear strain γ_{max} (computed using $Q = Q_d$ in the equations) in the diaphragm at a certain

moment M on the assembly exceeds the shear strain γ_d .

All the assumptions made in the elastic and inelastic theories, presented in the previous sections, are also applicable in this section.

In evaluating the additional deflections C_1 and D_1 , the amplitude of lateral imperfection δ_u is taken as the tolerance limit of sweep for a length L of the beam as specified in the AISC manual[16] and the amplitude of initial twist δ_β is arbitrarily taken as equal to 0.01 radian (0°34'22.6").

The following procedure is used to arrive at the load carrying capacity of diaphragm-braced I-beams and channel beams.

1. The individual shear characteristics Q_d and γ_d of the diaphragm employed in the beam assembly are determined from an independent shear diaphragm test as described above.

2. The critical moment M_{cr} of the diaphragm-braced ideal beam is determined for the shear rigidity Q_d using Eqs. 2-47 and 2-48.

3. If $M_{cr} > M_y$ the maximum shear strain γ_{max} of the diaphragm at yield moment M_y on the beam is determined. If $\gamma_{max} \leq \gamma_d$, then, the moment carrying capacity of the diaphragm-braced beam is M_y and the beam fails before the diaphragm does. Otherwise, the moment carrying capacity is less than M_y and the diaphragm fails before the beam does. In this event, the moment carrying capacity is the moment M at which γ_{max} just reaches the value γ_d .

4. If $M_{cr} < M_y$ the diaphragm fails before the beam does. The moment carrying capacity is the moment M at which

the maximum shear strain γ_{max} just reaches the shear strain γ_d.

Two examples are worked out in Appendix II to illustrate the above procedure. The results of the two examples are presented and discussed in the following.

Summary of Results

Example	1. 14x4Bx17.2# I-beam, 12' long, 6' spacing of beams, 22g. roof deck	2. 18x6x70# I-beam, 18' long, 6' spacing of beams, 22g. roof deck
(1) Shear Rigidity Q_d (kips)	152.5	152.5
(2) Yield Moment M_y (kip-in)	756	3668
(3) Plastic Moment M_{pl} (kip-in)	889	4457
(4) Shear Rigidity Q_y (kips)	30.2	42.6
(5) Shear Rigidity Q_{pl} (kips)	63.5	247
(6) Critical Moment $M_{cr} \leq M_{pl}$ (kip-in)	889	3844
(7) Critical Moment $M_{cr,u}$ (without bracing) (kip-in)	329	2780
(8) Load Carrying Capacity (kip-in)	756	3063
(9) Failure	Beam	Diaphragm
(10) $\frac{(8)}{(6)}$	0.85	0.80

Discussion: Diaphragm bracing being the same, the heavier the beams are the more critical will be the failure of the dia-

phragm. In other words, the heavier beams require stronger bracing to reach their maximum moment carrying capacities.

2.4 Tests on I-Beams and Channel Beams

2.4.1 Description of Tests

The general arrangement for the double-beam flexure tests made as part of this investigation is shown in Fig. 2-9. Each test assembly comprises either two 10B17 I-beams or two 6[8.2 beams of A-441 steel, and a 30 gage plenum form cross-corrugated steel diaphragm attached to the compression flanges, with the corrugations transverse to the longitudinal axes of the beams. Loads were applied to the beams two feet inboard from each end support. The two beams were rigidily battened together in the two feet end lengths with 1/4 inch steel plates welded in place. The length of the beam between applied loads thus is subjected to uniform moment, with its ends "fixed" against lateral torsional buckling, but free to rotate about the major bending axis. This arrangement was selected as the simplest one to give well-defined and controllable conditions of loading and support as related to the theoretical assumptions. In the absence of diaphragm bracing, such an arrangement provides an effective laterally unsupported length of half the distance between the load points.

Each pair of beams was tested first with no diaphragm bracing, and then with diaphragm bracing of given width and connector spacing. Power driven pins of 1/4-inch diameter were used in all the double-beam flexure tests except in one test where #14 screws were used. A span of 30 feet was used for 10B17 beam

assemblies, giving an effective laterally unsupported length of 15 feet, and Ld/nA_f ratio of 1381. In the case of 6[8.2 beam assemblies a span of 24 feet was used, giving an effective laterally unsupported length of 12 feet, and Ld/nA_f ratio of 1311. Diaphragms used were 28 and 17-3/4 inches wide, with distances between the pins of 25-3/4 and 15-7/8 inches, for 10B17 and 6[8.2 beam assemblies respectively. A description of the double-beam flexure test specimens is given in Tables 3 and 6.

Lateral deflections were measured at several points at the levels of top and bottom flanges along the length of each beam using a surveying transit and scale, and vertical deflections were read with a level and a scale. The lateral deflections taken at zero load level enable one to compute the initial lateral imperfections and the initial twist of the beams. Level bars were used to measure web rotations at each end, each quarter point, and midspan of both the beams. In the case of 10B17 beam assemblies a total of eight resistance strain gages were mounted on the flange tips of both the beams at midspan. In the case of 6[8.2 beam assemblies resistance strain gages were mounted on the flange tips and on outside corners of flange and web intersections for both channels at midspan. Readings of all instruments were taken at several increments of load before failure.

The diaphragm-braced four-beam assembly similar to the two-beam assembly is shown in Fig. 2-10. The beams were 8Jr6.5 I-sections made of A-441 steel and the diaphragm is 26 gage steel panels (inverted) connected by #14 screws to the beams at every rib (8" spacing). A span of 20 feet was used for the 8Jr6.5

beam assembly giving an effective laterally unsupported length of 10 feet and Ld/nA_f ratio of 2232. The beams were 3'8" apart giving a total diaphragm width of (3'8") x 3 + 2-1/4" = 134-1/4". It is assumed that a width of (134-1/4")/4 $\cong$ 33.5" of the diaphragm contributes towards the shear rigidity for each beam. This assumption would give a larger value of the predicted critical moment for a diaphragm-braced beam than when a diaphragm width of (3'8")/2 = 22" contributing towards the shear rigidity for an end beam is assumed.

Strains were measured at the flange tips of each beam at midspan using resistance strain gages. The lateral deflections, vertical deflections, and twist of the webs were measured for the outer beams similar to the procedure in a double-beam assembly test.

2.4.2 Predicted Load-Deflection Relationships and Critical Moment for Diaphragm-Braced Beams; and Southwell Plot for Unbraced Beams

The load-deflection relationships for either diaphragm-braced I-beams or channel beams used to predict the behavior of the beams in the tests are given by

$$C_1 = \frac{M\delta_\beta\left\{E\Gamma\left(\frac{2\pi}{L}\right)^2 + GK + Qe^2\right\} + M\delta_u\{M-Qe\}}{\left\{EI_y\left(\frac{2\pi}{L}\right)^2 + Q\right\}\left\{E\Gamma\left(\frac{2\pi}{L}\right)^2 + GK + Qe^2\right\} - (M-Qe)^2} \qquad (2\text{-}36)$$

and

$$D_1 = \frac{M\delta_u\left\{EI_y\left(\frac{2\pi}{L}\right)^2 + Q\right\} + M\delta_\beta(M-Qe)}{\left\{EI_y\left(\frac{2\pi}{L}\right)^2 + Q\right\}\left\{E\Gamma\left(\frac{2\pi}{L}\right)^2 + GK + Qe^2\right\} - (M-Qe)^2} \qquad (2\text{-}37)$$

(Note that 2 is substituted for n.)

The critical moments for either diaphragm-braced I-beams or channel beams used for comparison with the failure loads of beams in the tests were derived from

$$M_{cr} = \sqrt{\left\{E_{ry} I_y \left(\frac{2\pi}{L}\right)^2 + Q\right\}\left\{E_{ry}\Gamma\left(\frac{2\pi}{L}\right)^2 + G_r K + Qe^2\right\}} + Qe \qquad (2\text{-}46)$$

Computations in evaluating the critical moments and load-deflection relationships for unbraced or diaphragm-braced beams were performed on a digital computer whenever necessary.

A Southwell plot suggested by Massey[12] for the elastic lateral instability of I-beams can be used in the case of tests on unbraced I-beams and channel beams. The following derivation indicates the basis of the Southwell plot.

The amplitude of additional twist D_1 of either an unbraced I-beam or channel beam in the elastic range can be derived from Eq. 2-37 by letting $Q = 0$ and may be written as

$$D_1 = \frac{M\delta_u\left\{EI_y\left(\frac{n\pi}{L}\right)^2\right\} + M^2\delta_\beta}{M_{cr,u}^2 - M^2}$$

where

$$M_{cr,u} = \sqrt{\left\{EI_y\left(\frac{n\pi}{L}\right)^2\right\}\left\{E\Gamma\left(\frac{n\pi}{L}\right)^2 + GK\right\}}$$

The above equation may be rearranged in a form suitable for a Southwell plot as follows:

$$\frac{D_1}{M} = \frac{M(D_1+\delta_\beta)}{M^2_{cr,u}} + \frac{\delta_u\left\{EI_y\left(\frac{n\pi}{L}\right)^2\right\}}{M^2_{cr,u}}$$

In the above equation the term $\frac{\delta_u\left\{EI_y\left(\frac{n\pi}{L}\right)^2\right\}}{M^2_{cr,u}}$ is constant within the elastic range so that a plot of $M(D_1+\delta_\beta)$ against $\frac{D_1}{M}$ will produce a straight line with a slope equal to the square of the critical moment.

The above type of Southwell plot was used to obtain the critical moments of unbraced I-beams and channel beams from experimental data from tests which were not carried to failure.

2.4.3 Beam Test Results

(a) Double I-beam or channel beam assemblies. Results of the tests with and without diaphragm bracing are summarized in Tables 4 and 7. For the unbraced beams, failure always was by elastic lateral buckling at very low stresses, and the test was arbitrarily stopped before the lateral deflections and stresses became excessive, in order that the same beams could be used for the braced beam tests. Upon removal of the load, the beams returned almost exactly to their no-load condition. Buckling always occurred in the direction of initial crookedness, if such crookedness was at all pronounced. Figs. 2-11 and 2-12 illustrate the lateral deflection of the centroid of typical unbraced beams at zero load and at or near the maximum applied load. The test arrangement was designed to simulate the condition of full fixity against lateral buckling, and Figs. 2-11 and 2-12 indicate

that the deflected shape of the unbraced beams reasonably approximates a displaced cosine curve. Figs 2-13 and 2-14 show typical plots of load versus lateral deflection of the top and bottom flanges of unbraced beams at mid span, and Figs. 2-15 and 2-16 show moment versus midspan vertical deflections. Figs. 2-17 through 2-20 show moment-deflection relationships for the unbraced beams. Southwell plots for the lateral instability of the unbraced beams are shown in Figs. 2-21 and 2-22.

Figs. 2-23 through 2-32 present similar information for the same beams discussed above with diaphragm bracing (except for the Southwell plots). Comparing a braced beam with an identical unbraced beam, the maximum load and vertical deflections before failure are much larger, and the lateral deflections are much smaller. It should be noted that the compression flange (braced flange) deflects more than the tension flange (unbraced flange) in agreement with the assumption made in the analysis.

For failure moments below the yield moment the diaphragm fails by tearing or popping of the pins before the beam fails by yielding (refer to Section 2-3), therefore, there was a sudden lateral deflection of the beams after the failure of the diaphragm. For failure moments higher than the yield moments the beams fail initially by yielding. After yielding the beams deflect laterally much faster than before yielding until the diaphragm fails suddenly in shear. A photograph of a double-beam assembly after failure is shown in Fig. 2-33. Figs. 2-34 and 2-35 show a comparison of the critical loads of the beams and their experimental failure loads.

(b) Four-beam assembly. The behavior of the four-beam assembly was similar to that of a double-beam assembly. Failure occurred above the yield moment at 90% of M_{pl}, and was by local buckling at a quarter point, which is also the location of a #14 screw, of the east beam. Fig. 2-36 shows a comparison of the critical load and the experimental failure load of the four-beam assembly. A photograph of the four-beam assembly after failure and the local buckling are shown in Figs. 2-37 and 2-38 respectively.

2.4.4 Discussion of Beam Test Results

a. Unbraced Beams

The maximum moments applied to the unbraced beams with their initial imperfections were 3% to 12% lower than the predicted critical moments for 10B17 I-beams, 19% to 26% lower than the predicted critical moments in the case of 6[8.2 beams and 25% lower than the predicted critical moment in the case of 8Jr6.5 I-beams. The predicted critical moments are based on the classical lateral buckling theory for ideal beams. As indicated in Section 2.4.3 these tests were arbitrarily stopped before a true maximum load was reached, in order that the same beams could be used with diaphragm bracing. It can be seen that, in the case of an unbraced I-beam, the load (240 in-kips) at which the test is arbitrarily stopped was very close to the critical moment (246 in-kips) given by the Southwell plot shown in Fig. 2-21. However, in the case of an unbraced channel beam test, the load (66 in-kips) at which the test was arbitrarily stopped was not as close to the critical moment (81.7 in-kips)

given by the Southwell plot (refer to Fig. 2-22) as in the case of an unbraced I-beam. The reason lies in the fact that in the case of channel beam tests the precritical deflections increased faster with the increase of load than in the case of I-beams. The above indicates that the test setup functioned better for the case of I-beams than for the case of channel beams, but for both sections the behavior was considered satisfactory.

b. Diaphragm-Braced Beams

In Tables 4, 7 and 9, and in Figs. 2-34, 2-35, and 2-36 the maximum moments sustained by beams are compared with the predicted critical moments from Eq. 2-46. In the case of 10B17 I-beams the predicted critical moments underestimate the failure moments of the beams in the elastic range by about 20% to 24%. This can be attributed, probably, to the fact that the cross-bending rigidity of the diaphragm is not considered in the predicted critical moments. In the case of 10B17 I-beam tests the moments sustained by the beams in the inelastic range were smaller than the predicted critical moments by about 3% to 5%. Similarly, in the case of channel beam tests the moments sustained by the beams were smaller than the predicted critical moments by about 0% to 25%. In the case of 8Jr6.5 I-beam test the moment sustained by the diaphragm-braced beam was smaller than the predicted critical moment by 10%. The following reasons may be given for the moments sustained by the beams at failure being smaller than the predicted critical moments:

1. Eq. 2-46 was developed assuming the response of the diaphragm bracing remains elastic until failure. This is probably

not true at very high moments.

2. Eq. 2-46 gives the critical moment for an ideal beam. Actually imperfections exist and it is shown in Section 2.3 that these imperfections cause the failure of the beam assembly at lower moments than the critical moments.

3. Any deviation of the plane of the applied uniform moment (refer to Fig. 2-9) from the vertical is more critical in the case of channel beams than in the case of I-beams because of the unsymmetry of the channel section.

Figs. 2-27 and 2-28 indicate that the theoretical and actual vertical deflections of the beams agreed quite well. The theoretical vertical deflections of the braced beams were computed neglecting the small contribution of the diaphragm, which acts as a very flexible cover plate.

Theoretical lateral deflection of the C.G. of the cross section and the twist of the beams at midspan were computed at the desired moment levels using the elastic theory. The initial imperfections were computed from the measurements of the positions of the beams at zero load level. The amplitudes of the initial imperfections used in the computations of load-deflection relationships were the maximum values of the average initial imperfections of the two beams, so that the computed deflections should usually give a high estimate of the actual deflections. Figs. 2-17, 2-18, 2-29, 2-30, and 2-32 show that the theoretically predicted deflections of the beams were larger than the actual experimental deflections. But, Figs. 2-19, 2-20, and 2-31 show that the theoretically predicted deflections are smaller

than the actual experimental deflections. This, probably, may be attributed to reason 3 on page 41.

3. AXIALLY LOADED I-SECTION COLUMNS BRACED BY GIRTS WHICH IN TURN ARE BRACED BY A DIAPHRAGM

3.1 Elastic Theory

3.1.1 General Formulation of the Problem by Energy Method

A model consisting of two columns braced by girts which in turn are braced by a diaphragm will be considered for the purposes of analysis of the above problem. A sketch of the above model is shown in Fig. 3-1 along with the sets of axes X, Y, Z and X_1, Y_1, Z_1, and their corresponding displacements u, v, β and u_1, v_1, β_1 respectively. In the following analysis the total energy U related to one column with j intermediate girts is formulated and the Rayleigh-Ritz technique is used to obtain an approximate solution. The analysis is based on small deflection theory.

The total energy U related to one column can be expressed as

$$U = V + U_w + B_s + B_t \qquad (3\text{-}1)$$

where

V is the internal strain energy of the column

U_w is the potential energy of the axial load

B_s is the energy due to shear in the diaphragm

and B_t is the energy of bending of the girts due to twist of the column.

Case a. Ideal Columns. Internal strain energy of the column. The general expression for the internal energy of

an elastic column bent about both the principal axes, and twisted, is[2]

$$V = \frac{1}{2}\int_0^L \left(EI_y u''^2 + EI_x v''^2 + E\Gamma \beta''^2 + GK\beta'^2 + EA\epsilon^2\right) dz \qquad (3\text{-}2)$$

where

EI_y is the weak-axis bending rigidity

EI_x is the strong-axis bending rigidity

$E\Gamma$ is the warping rigidity

GK is the torsional rigidity

E is Young's Modulus

A is the cross sectional area of the column

ϵ is the axial strain

L is the total length of the column

and u, v, and β are the displacements as shown in Fig. 3-1.

Considering only the change in energy from the stable compressed position to the unstable compressed and deflected position, the term in ϵ can be omitted from Eq. 3-2, and in subsequent expressions. Further, in this problem, the strong-axis flexural buckling is independent of bending about the weak axis and twisting of the column. The strong-axis flexural buckling load can be evaluated using Euler's equation. Bending about the weak axis and twist of the column are considered in the following. Eq. 3-2 then reduces to

$$V = \frac{1}{2}\int_0^L \left(EI_y u''^2 + E\Gamma \beta''^2 + GK\beta'^2\right) dz \qquad (3\text{-}3)$$

Potential Energy of an Axial Load. The general expression for the change in potential energy of an axial load from

the compressed stable position to the compressed and deflected unstable position, for an unsymmetrical column section, is[2]

$$U_w = \frac{1}{2}\int_0^L \left[-\sigma A\,(u'^2+v'^2) - 2\sigma A\,\gamma_o u'\beta' + 2\sigma A\,x_o v'\beta' - \sigma I_p \beta'^2\right] dz \qquad (3\text{-}4)$$

where

σ is the average compressive stress on the column

I_p is the polar moment of inertia of the section

and x_o and γ_o are the distances from the C.G. of the section to the shear center in the X and Y directions respectively.

Considering only bending about the weak-axis and twist of the axially loaded doubly-symmetric I-section column, Eq. 3-4 reduces to

$$U_w = -\frac{1}{2}\int_0^L \left(Pu'^2 + P\frac{I_p}{A}\beta'^2\right) dz \qquad (3\text{-}5)$$

where P is the axial load on the column.

Energy B_s due to shear in the diaphragm. The relative movement of the girts causes shear in the diaphragm, and this shear is transferred through the girts as resistive forces to the lateral movement of the column when the latter is under load. Therefore, the energy due to shear in the diaphragm is given by

$$B_s = \sum_{i=0}^{j+1} \frac{1}{2} R_{i\ell}\, u_{1,i\ell} \qquad (3\text{-}6)$$

where

ℓ is the spacing of girts ($= \frac{L}{j+1}$)

$R_{i\ell}$ is the resistive force on the column at $z = i\ell$

and $u_{1,il}$ is the lateral deflection of the column parallel to x_1 axis at $z_1 = z = il$

The resistive force offered by a girt, due to shear in the diaphragm, to the lateral movement of the column can be expressed as

$$R_{il} = \frac{Q}{l}\left\{[u_{1,il} - u_{1,(i-1)l}] + [u_{1,il} - u_{1,(i+1)l}]\right\}$$

$$= \frac{Q}{l}\left\{2u_{1,il} - u_{1,(i-1)l} - u_{1,(i+1)l}\right\} \qquad (3\text{-}7)$$

where Q is the shear rigidity[8] of the diaphragm contributing to the support of one column. (Note: $u_{1,-l}$ and $u_{1,(j+2)l}$ should be taken as equal to zero).

Energy B_t due to bending of the girts. The bending stiffness of the girts offers twist restraints m to the column under load. The energy due to bending of the girts is given by

$$B_t = \sum_{i=0}^{j+1} \frac{1}{2} m \beta_{il}^2 \qquad (3\text{-}8)$$

where

m is the stiffness of the girts bracing the column at $z = il$, for $i = 0, 1, \ldots, j+1$

Thus, the total energy for an axially loaded doubly symmetric ideal I-section column braced by girts which in turn are braced by a diaphragm is given by

$$U = \frac{1}{2}\int_0^L \left(EI_y u''^2 + E\Gamma\beta''^2 + GK\beta'^2 - Pu'^2 - P\frac{I_p}{A}\beta'^2\right) dz$$

$$+ \frac{1}{2}\sum_{i=0}^{j+1} R_{il}\, u_{1,il} + \frac{1}{2}\sum_{i=0}^{j+1} m\, \beta_{il}^2 \qquad (3\text{-}9)$$

(Note that $u_{1,-\ell}$ and $u_{1,(j+2)\ell}$ should be taken as zero).

Case b. Imperfect Columns. The total energy expression given by Eq. 3-9 can be modified for the case of an imperfect column to be

$$U = \frac{1}{2}\int_0^L \left\{ EI_y u''^2 + E\Gamma \beta''^2 + GK\beta'^2 - P\left(u_t'^2 - u_o'^2\right) - P\frac{I_p}{A}\left(\beta_t'^2 - \beta_o'^2\right)\right\} dz$$

$$+ \frac{1}{2}\sum_{i=0}^{j+1} R_{i\ell}\, u_{1,i\ell} \quad + \frac{1}{2}\sum_{i=0}^{j+1} m\, \beta_{i\ell}^2 \qquad (3\text{-}10)$$

where

u_t is the total deflection of the column in the X-direction

u_o is the initial lateral imperfection of the column in the X-direction

β_t is the total twist of the column

and β_o is the initial imperfection of the column in twist.

Further, it may be noted that

$$u_t = u_o + u \qquad (3\text{-}11)$$

and

$$\beta_t = \beta_o + \beta \qquad (3\text{-}12)$$

Using Eqs. 3-11 and 3-12, Eq. 3-10 may be simplified and expressed as

$$U = \frac{1}{2}\int_0^L \left\{ EI_y u''^2 + E\Gamma \beta''^2 + GK\beta'^2 - P\left(u'^2 + 2u_o' u'\right) - P\frac{I_p}{A}\left(\beta'^2 + 2\beta_o'\beta'\right)\right\} dz$$

$$+ \frac{1}{2}\sum_{i=0}^{j+1} R_{i\ell}\, u_{1,i\ell} \quad + \frac{1}{2}\sum_{i=0}^{j+1} m\, \beta_{i\ell}^2 \qquad (3\text{-}13)$$

(Note that $u_{1,-\ell}$ and $u_{1,(j+2)\ell}$ should be taken as zero).

It may be observed that when the column is perfect; i.e. $u_0 = 0$ and $\beta_0 = 0$, Eq. 3-13 reduces to Eq. 3-9 as expected.

The connection between the columns and the girts is assumed to be such that, prior to the connection of the diaphragm to the assembly, the column could sway along with the girts in the plane of the assembly with negligible shear restraint compared to that of a light-gage steel diaphragm. The expression of total energy U given by Eq. 3-13 will be used in the following to derive the load-deflection relationships of imperfect columns braced by one or two intermediate girts and a diaphragm. The buckling loads of ideal columns will be derived from the load-deflection relationships by letting the initial imperfections equal zero. The ends of the columns are assumed to be "hinged", i.e. flexurally hinged, twist is zero and warping is unrestrained at the ends.

3.1.2 Load-Deflection Relationships for Imperfect Columns

Case a. With Sidesway. The most general deflection pattern to obtain a conservative estimate (i.e. an upper limit) of the additional deflections of the column under load may be expressed as

$$\text{Initial Imperfections:} \quad \begin{cases} u_{10} = \sum_{n=1}^{\infty} E_n \sin \frac{n\pi z}{L} + \Delta_0 \left(1 - \frac{z}{L}\right) \\ \beta_{10} = \sum_{n=1}^{\infty} F_n \sin \frac{n\pi z}{L} \end{cases} \tag{3-14}$$

$$\text{Additional Deflections:} \quad \begin{cases} u_1 = \sum_{n=1}^{\infty} C_n \sin \frac{n\pi z}{L} + \Delta \left(1 - \frac{z}{L}\right) \\ \beta_1 = \sum_{n=1}^{\infty} D_n \sin \frac{n\pi z}{L} \end{cases} \tag{3-15}$$

(Note that at every cross section of the column $z = z_1$)

where u_{10} and β_{10} are the initial imperfections corresponding to the deflections u_1 and β_1; E_n, F_n, and Δ_0 are the amplitudes of the initial imperfections; and C_n, D_n, and Δ are the unknown amplitudes of the additional deflections. Knowing the deflections u_{10}, β_{10}, u_1 and β_1 the deflections u_0, β_0, u and β of the C.G. of the column can be expressed as

$$\begin{cases} \beta_0 = \beta_{10} = \sum_{n=1}^{\infty} F_n \sin \frac{n\pi z}{L} \\ u_0 = u_{10} + e\beta_{10} = \sum_{n=1}^{\infty} (E_n + eF_n) \sin \frac{n\pi z}{L} + \Delta_0 \left(1 - \frac{z}{L}\right) \end{cases} \tag{3-16}$$

and

$$\begin{cases} \beta = \beta_1 = \sum_{n=1}^{\infty} D_n \sin \frac{n\pi z}{L} \\ u = u_1 + e\beta_1 = \sum_{n=1}^{\infty} (C_n + eD_n) \sin \frac{n\pi z}{L} + \Delta \left(1 - \frac{z}{L}\right) \end{cases} \tag{3-17}$$

where

e is the distance between the C.G. of the column section and the plane of the diaphragm.

The total energy U of the column is obtained by substituting the values given by Eqs. 3-16 and 3-17 for u_0, β_0, u, and β in Eq. 3-13. The unknown amplitudes C_n, D_n, and Δ can be determined by minimizing the total energy U and solving the resulting linear simultaneous equations in C_n, D_n, and Δ.

An approximate solution of the problem is obtained in the following by using the Rayleigh-Ritz technique. It is observed from the solutions of some practical problems using different values for n in Eqs. 3-14 and 3-15 that the con-

vergence of the solutions is quite fast. Therefore, to obtain approximate solutions of the problems with one and two intermediate girts certain values of n are chosen in the following depending on the number of intermediate girts in the problem and the type of accuracy needed.

Column with One Intermediate Girt. The assumed deflection pattern is given by

$$\text{Initial Imperfections:} \begin{cases} u_{10} = \sum_{n=1}^{3} E_n \sin \frac{n\pi z}{L} + \Delta_0 \left(1 - \frac{z}{L}\right) \\ \beta_{10} = \sum_{n=1}^{3} F_n \sin \frac{n\pi z}{L} \end{cases} \tag{3-18}$$

$$\text{Additional Deflections:} \begin{cases} u_1 = \sum_{n=1}^{3} C_n \sin \frac{n\pi z}{L} + \Delta \left(1 - \frac{z}{L}\right) \\ \beta_1 = \sum_{n=1}^{3} D_n \sin \frac{n\pi z}{L} \end{cases} \tag{3-19}$$

(Note: $L = 2\ell$).

Minimization of the total energy U using Eq. 3-13 gives the following load-deflection relationships:

$$[D11]\{X11\} = P\{V11\} \tag{3-20}$$

$$[D21]\{X21\} = P\{V21\} \tag{3-21}$$

$$(Q - P)\Delta = P\Delta_0 \tag{3-22}$$

where

$$[D11] = \begin{bmatrix} EI_y\left(\frac{\pi}{2\ell}\right)^2 - P + 8Q/\pi^2 & e\left\{EI_y\left(\frac{\pi}{2\ell}\right)^2 - P\right\} & -8Q/\pi^2 & 0 \\ e\left\{EI_y\left(\frac{\pi}{2\ell}\right)^2 - P\right\} & EI\left(\frac{\pi}{2\ell}\right)^2 + GK - P\frac{I_P}{A} + e^2\left\{EI_y\left(\frac{\pi}{2\ell}\right)^2 - P\right\} + 4m\ell/\pi^2 & 0 & -4m\ell/\pi^2 \\ -8Q/9\pi^2 & 0 & EI_y\left(\frac{3\pi}{2\ell}\right)^2 - P + 8Q/9\pi^2 & e\left\{EI_y\left(\frac{3\pi}{2\ell}\right)^2 - P\right\} \\ 0 & -4m\ell/9\pi^2 & e\left\{EI_y\left(\frac{3\pi}{2\ell}\right)^2 - P\right\} & EI\left(\frac{3\pi}{2\ell}\right)^2 + GK - P\frac{I_P}{A} + e^2\left\{EI_y\left(\frac{3\pi}{2\ell}\right)^2 - P\right\} + 4m\ell/9\pi^2 \end{bmatrix}$$

$$\{X11\} = \begin{Bmatrix} C_1 \\ D_1 \\ C_3 \\ D_3 \end{Bmatrix}$$

$$\{V11\} = \begin{Bmatrix} E_1 + eF_1 \\ \left(\frac{I_P}{A} + e^2\right)F_1 + eE_1 \\ E_3 + eF_3 \\ \left(\frac{I_P}{A} + e^2\right)F_3 + eE_3 \end{Bmatrix}$$

$$[D21] = \begin{bmatrix} EI_y\left(\frac{\pi}{\ell}\right)^2 - P & e\left\{EI_y\left(\frac{\pi}{\ell}\right)^2 - P\right\} \\ e\left\{EI_y\left(\frac{\pi}{\ell}\right)^2 - P\right\} & EI\left(\frac{\pi}{\ell}\right)^2 + GK - P\frac{I_P}{A} + e^2\left\{EI_y\left(\frac{\pi}{\ell}\right)^2 - P\right\} \end{bmatrix}$$

$$\{X21\} = \begin{Bmatrix} C_2 \\ D_2 \end{Bmatrix}$$

and

$$\{V21\} = \begin{Bmatrix} E_2 + eF_2 \\ \left(\frac{I_p}{A} + e^2\right)F_2 + eE_2 \end{Bmatrix}$$

It can be observed from Eqs. 3-20 through 3-22 that the deflections $\{X11\}$, $\{X21\}$, and Δ are not coupled. Eqs. 3-20 through 3-22, hereafter, will be known as the equations corresponding to the first mode and modified first mode, second mode, and sidesway mode respectively because of the deflection pattern associated with each of the above equations (refer to Fig. 3-2; a through c and e). Further, Eqs. 3-20 through 3-22 could have been obtained by using the following deflection pattern:

First Mode and Modified First Mode:

Initial Imperfections:

$$\begin{cases} u_{10} = E_1 \sin\frac{\pi z}{2\ell} + E_3 \sin\frac{3\pi z}{2\ell} \\ \beta_{10} = F_1 \sin\frac{\pi z}{2\ell} + F_3 \sin\frac{3\pi z}{2\ell} \end{cases} \qquad (3\text{-}23)$$

Additional Deflections:

$$\begin{cases} u_1 = C_1 \sin\frac{\pi z}{2\ell} + C_3 \sin\frac{3\pi z}{2\ell} \\ \beta_1 = D_1 \sin\frac{\pi z}{2\ell} + D_3 \sin\frac{3\pi z}{2\ell} \end{cases} \qquad (3\text{-}24)$$

Second Mode:

Initial Imperfections:

$$\begin{cases} u_{10} = E_2 \sin\frac{\pi z}{\ell} \\ \beta_{10} = F_2 \sin\frac{\pi z}{\ell} \end{cases} \qquad (3\text{-}25)$$

Additional Deflections:

$$\begin{cases} u_1 = C_2 \sin \frac{\pi z}{\ell} \\ \beta_1 = D_2 \sin \frac{\pi z}{\ell} \end{cases} \tag{3-26}$$

Sidesway:

Initial Imperfections:

$$\begin{cases} u_{10} = \Delta_0 \left(1 - \frac{z}{2\ell}\right) \\ \beta_{10} = 0 \end{cases} \tag{3-27}$$

Additional Deflections:

$$\begin{cases} u_1 = \Delta \left(1 - \frac{z}{2\ell}\right) \\ \beta_1 = 0 \end{cases} \tag{3-28}$$

Minimization of the total energy U for the deflection pattern of first mode and modified first mode, second mode, and sidesway individually in each case gives Eqs. 3-20 through 3-22 respectively.

Column with Two Intermediate Girts. As in the problem with one intermediate girt, the load-deflection relationships can be obtained in each mode separately by assuming the following deflection pattern (refer to Fig. 3-3; a through d and f). First Mode and Modified First Mode:

Initial Imperfections:

$$\begin{cases} u_{10} = E_1 \sin \frac{\pi z}{3\ell} + E_5 \sin \frac{5\pi z}{3\ell} \\ \beta_{10} = F_1 \sin \frac{\pi z}{3\ell} + F_5 \sin \frac{5\pi z}{3\ell} \end{cases} \tag{3-29}$$

Additional Deflections:

$$\begin{cases} u_1 = C_1 \sin \frac{\pi z}{3\ell} + C_5 \sin \frac{5\pi z}{3\ell} \\ \beta_1 = D_1 \sin \frac{\pi z}{3\ell} + D_5 \sin \frac{5\pi z}{3\ell} \end{cases} \tag{3-30}$$

Modified Second Mode:

Initial Imperfections:

$$\begin{cases} u_{10} = E_2 \sin\frac{2\pi z}{3\ell} + E_4 \sin\frac{4\pi z}{3\ell} \\ \beta_{10} = F_2 \sin\frac{2\pi z}{3\ell} + F_4 \sin\frac{4\pi z}{3\ell} \end{cases} \quad (3\text{-}31)$$

Additional Deflections:

$$\begin{cases} u_1 = C_2 \sin\frac{2\pi z}{3\ell} + C_4 \sin\frac{4\pi z}{3\ell} \\ \beta_1 = D_2 \sin\frac{2\pi z}{3\ell} + D_4 \sin\frac{4\pi z}{3\ell} \end{cases} \quad (3\text{-}32)$$

Third Mode:

Initial Imperfections:

$$\begin{cases} u_{10} = E_3 \sin\frac{\pi z}{\ell} \\ \beta_{10} = F_3 \sin\frac{\pi z}{\ell} \end{cases} \quad (3\text{-}33)$$

Additional Deflections:

$$\begin{cases} u_1 = C_3 \sin\frac{\pi z}{\ell} \\ \beta_1 = D_3 \sin\frac{\pi z}{\ell} \end{cases} \quad (3\text{-}34)$$

Sidesway:

Initial Imperfections:

$$\begin{cases} u_{10} = \Delta_0 \left(1 - \frac{z}{3\ell}\right) \\ \beta_{10} = 0 \end{cases} \quad (3\text{-}35)$$

Additional Deflections:

$$\begin{cases} u_1 = \Delta \left(1 - \frac{z}{3\ell}\right) \\ \beta_1 = 0 \end{cases} \quad (3\text{-}36)$$

(Note: $L = 3\ell$).

Minimization of the total energy U, for each mode separately, using Eq. 3-13 gives the following load-deflection relationships:

$$[D12]\{X12\} = P\{V12\} \tag{3-37}$$

$$[D22]\{X22\} = P\{V22\} \tag{3-38}$$

$$[D32]\{X32\} = P\{V32\} \tag{3-39}$$

$$(Q-P)\Delta = P\Delta_o \tag{3-40}$$

where

$$[D12] = \begin{bmatrix}
EI_y\left(\frac{\pi}{3\ell}\right)^2 - P + 9Q/\pi^2 & e\left\{EI_y\left(\frac{\pi}{3\ell}\right)^2 - P\right\} & -9Q/\pi^2 & 0 \\
e\left\{EI_y\left(\frac{\pi}{3\ell}\right)^2 - P\right\} & Er\left(\frac{\pi}{3\ell}\right)^2 + GK - P\frac{I_p}{A} + e^2\left\{EI_y\left(\frac{\pi}{3\ell}\right)^2 - P\right\} + 9m\ell/\pi^2 & 0 & -9m\ell/\pi^2 \\
-9Q/25\pi^2 & 0 & EI_y\left(\frac{5\pi}{3\ell}\right)^2 - P + 9Q/25\pi^2 & e\left\{EI_y\left(\frac{5\pi}{3\ell}\right)^2 - P\right\} \\
0 & -9m\ell/25\pi^2 & e\left\{EI_y\left(\frac{5\pi}{3\ell}\right)^2 - P\right\} & Er\left(\frac{5\pi}{3\ell}\right)^2 + GK - P\frac{I_p}{A} + e^2\left\{EI_y\left(\frac{5\pi}{3\ell}\right)^2 - P\right\} + 9m\ell/25\pi^2
\end{bmatrix}$$

$$[D22] = \begin{bmatrix} EI_y\left(\frac{2\pi}{3\ell}\right)^2 - P + 27Q/4\pi^2 & e\left\{EI_y\left(\frac{2\pi}{3\ell}\right)^2 - P\right\} & -27Q/4\pi^2 & 0 \\ e\left\{EI_y\left(\frac{2\pi}{3\ell}\right)^2 - P\right\} & EI\left(\frac{2\pi}{3\ell}\right)^2 + GK - P\frac{I_p}{A} + e^2\left\{EI_y\left(\frac{2\pi}{3\ell}\right)^2 - P\right\} + 9m\ell/4\pi^2 & 0 & -9m\ell/4\pi^2 \\ -27Q/16\pi^2 & 0 & EI_y\left(\frac{4\pi}{3\ell}\right)^2 - P + 27Q/16\pi^2 & e\left\{EI_y\left(\frac{4\pi}{3\ell}\right)^2 - P\right\} \\ 0 & -9m\ell/16\pi^2 & e\left\{EI_y\left(\frac{4\pi}{3\ell}\right)^2 - P\right\} & EI\left(\frac{4\pi}{3\ell}\right)^2 + GK - P\frac{I_p}{A} + e^2\left\{EI_y\left(\frac{4\pi}{3\ell}\right)^2 - P\right\} + 9m\ell/16\pi^2 \end{bmatrix}$$

$$[D32] = [D21]$$

$$\{X12\} = \begin{Bmatrix} C_1 \\ D_1 \\ C_5 \\ D_5 \end{Bmatrix}$$

$$\{V12\} = \begin{Bmatrix} E_1 + eF_1 \\ \left(\frac{I_p}{A} + e^2\right)F_1 + eE_1 \\ E_5 + eF_5 \\ \left(\frac{I_p}{A} + e^2\right)F_5 + eE_5 \end{Bmatrix}$$

$$\{X22\} = \begin{Bmatrix} C_2 \\ D_2 \\ C_4 \\ D_4 \end{Bmatrix}$$

$$\{V22\} = \begin{Bmatrix} E_2 + eF_2 \\ \left(\frac{I_P}{A} + e^2\right)F_2 + eE_2 \\ E_4 + eF_4 \\ \left(\frac{I_P}{A} + e^2\right)F_4 + eE_4 \end{Bmatrix}$$

$$\{X32\} = \begin{Bmatrix} C_3 \\ D_3 \end{Bmatrix}$$

and $$\{V32\} = \begin{Bmatrix} E_3 + eF_3 \\ \left(\frac{I_P}{A} + e^2\right)F_3 + eE_3 \end{Bmatrix}$$

It can be observed from Eqs. 3-37 through 3-40 that they are respectively the load-deflection relationships for the first mode and modified first mode, modified second mode, third mode, and sidesway for the column with two intermediate girts.

The behavior of the column in sidesway described by Eq. 3-40 (same as Eq. 3-22) may be better understood by deriving the same load-deflection relationship in a different way. It can be observed from above that the sidesway of the column is not coupled with either bending or twisting, or bending and twisting of the column. The columns and girts may be imagined to form the framework of a shear diaphragm to which a load P_{si} is applied as shown in Fig. 3-4 to produce an additional deflection Δ. The load P_{si}, neglecting any minor bending effects in columns or girts and assuming the shear restraint,

if any, of the bare frame to be equal to zero, is given by

$$P_{si} = 2 G_{eff} t w \Delta / L \qquad (3\text{-}41)$$

where

G_{eff} is the effective shear modulus of the diaphragm

t is the thickness of the diaphragm

and L and w are the dimensions as shown in Fig. 3-4.

Now, the equilibrium of one column is described by

$$P(\Delta + \Delta_o) = \tfrac{1}{2} P_{si} L = G_{eff} t w \Delta = Q\Delta$$

or

$$(Q - P)\Delta = P\Delta_o$$

where

$$Q = G_{eff} t w$$

It can be observed from the above derivation that the column is able to carry load only by virtue of the shear in the diaphragm in the case of sidesway of the column.

The deflection of the column is described by one of the Eqs. 3-20 through 3-22 for the column with one intermediate girt or one of the Eqs. 3-37 through 3-40 for the column with two intermediate girts depending on the characteristics of the bracing - shear rigidity Q, twist restraint m, and the eccentricity e - for a particular spacing of the girts. The equation which corresponds to that mode in which an identical ideal column buckles gives the load-deflection relationship of the column.

The investigation of the buckling mode of an ideal column will be treated in Section 3.1.3.

In general, if the rolled steel sections deflect in the $(j+1)$ th mode, where j is the total number of intermediate girts, the deflections will be primarily flexural. For the $(j+1)$ th mode, the following assumption of deflection pattern, a better deflection pattern than the ones given by Eqs. 3-25 and 3-26 or 3-33 and 3-34, will be used to obtain the load-deflection relationship of the column:

$$\text{Initial Imperfections:} \quad \begin{cases} u_{10} = E_1 \sin\frac{\pi z}{(j+1)\ell} + E_{j+1} \sin\frac{\pi z}{\ell} \\ \beta_{10} = 0 \end{cases} \tag{3-42}$$

$$\text{Additional Deflections:} \quad \begin{cases} u_1 = C_1^* \sin\frac{\pi z}{(j+1)\ell} + C_{j+1}^* \sin\frac{\pi z}{\ell} \\ \beta_1 = 0 \end{cases} \tag{3-43}$$

Minimization of the total energy U corresponding to the above deflection pattern gives the following load-deflection relationship:

$$\begin{bmatrix} EI_y\left\{\frac{\pi}{(j+1)\ell}\right\}^2 - P + Kz'_j Q & 0 \\ 0 & EI_y\left(\frac{\pi}{\ell}\right)^2 - P \end{bmatrix} \begin{Bmatrix} C_1^* \\ C_{j+1}^* \end{Bmatrix} = P \begin{Bmatrix} E_1 \\ E_{j+1} \end{Bmatrix} \tag{3-44}$$

where i the number of the mode of deflection and Kz_j^i is given in Section 3.3.

Case b. Without Sidesway. If the column is prevented from swaying sidewards, for example by providing X-bracing as shown in Fig. 1-1, then, the assumed deflection pattern is

given by Eqs. 3-23 through 3-26 for the column with one intermediate girt and by Eqs. 3-29 through 3-34 for the column with two intermediate girts. The corresponding load-deflection relationships are given by Eqs. 3-20 and 3-21 for the column with one intermediate girt and by Eqs. 3-37 through 3-39 for the column with two intermediate girts.

3.1.3 Critical Loads for Ideal Columns

Case a. With Sidesway. The critical load of an ideal column will be derived from the above load-deflection relationships by letting the initial imperfections equal zero.

a1. Column with One Intermediate Girt. The deflection pattern, in this case, is shown in Fig. 3-5. By letting the initial imperfections equal zero the critical loads will be obtained from Eqs. 3-20 through 3-22 as:

First Mode and Modified First Mode: $[D_{11}]\{x_{11}\} = 0$ (3-45)

Second Mode: $[D_{21}]\{x_{21}\} = 0$ (3-46)

Sidesway: $(Q-P)\Delta = 0$ (3-47)

Each one of the above equations describe an eigenvalue problem. The smallest value P of the nontrivial solution of each of the above equations gives the critical load for each of the particular modes of buckling. Hence, the critical loads are given by

First Mode and Modified First Mode: $|D_{11}| = 0$ (3-48)

Second Mode: $|D_{21}| = 0$ (3-49)

Sidesway: $(Q-P) = 0$ (3-50)

The critical load $P_{cr,1}$ of the column is the smallest of the critical loads obtained from Eqs. 3-48 through 3-50 and the column buckles in that mode from which the critical load of the column is obtained.

The possible types of behavior of the column given by Eqs. 3-48 through 3-50 under different values of stiffnesses Q and m and the value of e are represented graphically in Fig. 3-6.

The behavior of the column at the limiting values of stiffnesses Q and m and the value e is discussed in the following.

a1-1. Critical Load given by Eq. 3-50. When $Q = 0$ there is no diaphragm bracing of the column. As expected, Eq. 3-50 predicts that the column fails by sidesway and it cannot carry any load.

a1-2. Critical Load given by Eqs. 3-48 and 3-49.

a1-2.1 $e = 0$ and $Q = 0$. This corresponds to no diaphragm and girts connected to the column at the center of gravity of its section. It is shown in Appendix III-a that single half sine wave flexural buckling is predicted by Eq. 3-48, as expected.

a1-2.2 $e = 0$ and $Q > Q'_{10}$. This corresponds to "full bracing" ("full bracing" is defined as the bracing which makes an ideal column reach its Euler buckling load, $P_e = \frac{\pi^2 E I_y}{l^2}$) where Q'_{10} is the minimum stiffness so as to obtain the Euler buckling load P_e of the column. The value of Q'_{10} is obtained by solving Eq. 3-48 for Q'_{10} after letting $Q = Q'_{10}$

and $P = P_e$. A graphical representation of the above solution is shown in Fig. 3-7. It is shown in Appendix III-a that when $e = 0$ the terms corresponding to flexure separate out from the terms corresponding to torsion in Eq. 3-48, indicating pure torsional or pure flexural buckling, and the behavior of the column in flexure does not depend on the value of m .

a1-2.3 $e > 0$, $Q = 0$, and $m = 0$. This corresponds to no diaphragm and girts. As expected and shown in Appendix III-b, the critical load is given by Eq. 3-48 as the first mode pure flexural buckling load, $P_{eL} = \frac{\pi^2 E I_y}{L^2}$.

a1-2.4 $e > 0$, $Q = 0$ and $m > 0$. This corresponds to the case with no diaphragm. As expected and shown in Appendix III-b the critical load is given by Eq. 3-48 as the first mode pure flexural buckling load P_{eL} .

a1-2.5 $e > 0$, $Q > 0$, and $m = 0$. This corresponds to the case where the connection between the girts and the column is not moment resisting. There are two possible types of behavior of the ideal column as shown in Fig. 3-8, depending on the problem.

a1-2.6 $e > 0$, $Q > Q_1'(i)$, and $m > m_1'(i)$, where $i = 1, \ldots$. This corresponds to "full bracing", where $Q_1'(i)$ and $m_1'(i)$ are such a combination of minimum stiffnesses so as to obtain the maximum possible buckling load of the column with restraints. The values of combinations of $Q_1'(i)$ and $m_1'(i)$ are obtained by solving for combinations

of minimum values of Q and m from Eq. 3-48 by putting $P = P_e$, $Q = Q'_1(i)$ and $m = m'_1(i)$. A graphical representation of the above solution is shown in Fig. 3-9.

As intermediate cases consider $e > 0$, $0 < Q < Q'_1(i)$, and $0 < m < m'_1(i)$ for $i = 1, \cdots$. Critical load $P_{cr,1}$ for these cases is less than the Euler buckling load P_e .

It also can be observed from the numerical computations of particular problems that the greater the value of e, the larger the values of $Q'_1(i)$ and $m'_1(i)$ must be to provide "full bracing".

a2. Column with Two Intermediate Girts. The deflection pattern, in this case, is shown in Fig. 3-10. By letting the initial imperfections equal zero the critical loads will be obtained from Eqs. 3-37 through 3-40 as:

First Mode and Modified First Mode: $[D12]\{X12\} = 0$ (3-51)

Modified Second Mode: $[D22]\{X22\} = 0$ (3-52)

Third Mode: $[D32]\{X32\} = 0$ (3-53)

Sidesway: $(Q-P)\Delta = 0$ (3-54)

Each one of the above equations describe an eigenvalue problem. The smallest value of P of the nontrivial solution of each of the above equations gives the critical load for each of the particular modes of buckling. Hence, the critical loads are given by

First Mode and Modified First Mode: $|D_{12}| = 0$ (3-55)

Modified Second Mode: $|D_{22}| = 0$ (3-56)

Third Mode: $|D_{32}| = 0$ (3-57)

Sidesway: $(Q-P) = 0$ (3-58)

The critical load $P_{cr,2}$ of the column is the smallest of the critical loads obtained from the Eqs. 3-55 through 3-58 and the column buckles in that mode from which the critical load of the column is obtained.

The possible types of behavior of the column given by Eqs. 3-55 through 3-58 under different values of stiffnesses Q and m and the value of e are represented graphically in Fig. 3-11.

The behavior of the column with two intermediate girts at the limiting values of stiffnesses Q and m, and the value of e is discussed in the following.

a2-1. Critical load given by Eq. 3-58. When $Q=0$ there is no diaphragm bracing of the column. As expected Eq. 3-58 predicts that the column fails by sidesway and it cannot carry any load.

a2-2. Critical load given by Eqs. 3-55 through 3-57.

a2-2.1 $e=0$ and $Q=0$. This corresponds to no diaphragm and girts connected to the column at the center of gravity of its section. It is shown in Appendix III-c that Eq. 3-55 predicts single half sine wave flexural buckling as expected.

a2-2.2 $e = 0$ and $Q > Q'_{20}$. This corresponds to "full bracing" where Q'_{20} is the minimum stiffness so as to obtain the maximum possible buckling load of the column P_e . The value of Q'_{20} is obtained from Eq. 3-55 or 3-56, whichever is controlling, by letting $P = P_e$ and $Q = Q'_{20}$. A graphical representation of the above solution is shown in Fig. 3-12. It is shown in Appendix III-c that when $e = 0$ the terms corresponding to flexure separate out from those corresponding to torsion in Eqs. 3-55 and 3-56, indicating either pure flexural or pure torsional buckling, and the behavior of the column in flexure does not depend on the value of m .

a2-2.3 $e > 0$, $Q = 0$, and $m = 0$. This corresponds to the case with no diaphragm and girts. As expected, and shown in Appendix III-d the critical load $P_{cr,2}$ is given by Eq. 3-55 as the first mode pure flexural buckling load P_{eL} .

a2-2.4 $e > 0$, $Q = 0$, and $m > 0$. This corresponds to the case with no diaphragm. As expected, and shown in Appendix III-d, the critical load is given by Eq. 3-55 as the first mode pure flexural buckling load P_{eL} .

a2-2.5 $e > 0$, $Q > 0$, and $m = 0$. This corresponds to the case where the connection between the girts and the column is not moment resisting. There are four possible types of behavior of the column as shown in Fig. 3-13 depending on the problem.

a2-2.6 $e > 0$, $Q > Q'_2(i)$, and $m > m'_2(i)$ for $i = 1, \ldots$ This corresponds to the case of "full bracing" where $Q'_2(i)$

and $m'_2(i)$ are such a combination of minimum stiffnesses so as to obtain the maximum possible buckling load P_e of the column with restraints. The values of combinations of $Q'_2(i)$ and $m'_2(i)$ are obtained by solving for combinations of minimum values of Q and m from either Eq. 3-55 or 3-56 depending on the particular problem, by letting $P = P_e$, $Q = Q'_2(i)$ and $m = m'_2(i)$. A graphical representation of the above solution is shown in Fig. 3-14 for the two different possibilities.

As intermediate cases consider $e > 0$, $0 < Q < Q'_2(i)$, and $0 < m < m'_2(i)$ where $i = 1, \ldots$. The critical load $P_{cr,2}$ for these cases is less than P_e.

It can be observed from numerical computations of particular problems that the greater the value of e, the larger the values of $Q'_2(i)$ and $m'_2(i)$ must be to provide "full bracing".

Case b. Without Sidesway. If the column is prevented from swaying sidewards, for example by providing X-bracing as shown in Fig. 1-1, then, the assumed deflection pattern is given by Eqs. 3-23 through 3-28 for the column with one intermediate girt and by Eqs. 3-29 through 3-36 for the column with two intermediate girts by letting Δ, and the initial imperfections equal zero. The critical load corresponding to the above deflection pattern will be given by Eqs. 3-48 and 3-49 for the column with one intermediate girt and by Eqs. 3-55 through 3-57 for the column with two intermediate girts because Eqs. 3-50 and 3-58 become trivial when $\Delta = 0$.

The possible types of behavior described by Eqs. 3-48 and 3-49 for the column with one intermediate girt and by Eqs. 3-55 through 3-57 for the column with two intermediate girts for different values of Q, m, and e are represented graphically in Figs. 3-8 and 3-13 respectively.

The discussion of the behavior of the column at the limiting values of Q, m, and e described by Eqs. 3-48 and 3-49 and Eqs. 3-55 through 3-57 is given in Case a, and the same is applicable in this case also.

The method of analysis presented above is quite general and can be employed for a column with end conditions other than "hinged" end conditions described here.

3.2 Inelastic Theory

For stocky columns the average compressive stress may exceed the proportional limit of the stress-strain relationship of the entire cross section prior to buckling. As a result buckling will occur in the inelastic range (i.e. at stresses beyond the proportional limit) at a stress lower than that given by the elastic theory in Section 3.1. In contrast to the elastic buckling solution, no rigorous theory for obtaining the inelastic torsional-flexural buckling load exists at present. The available literature on the subject is mainly limited to the methods which use the elastic equations with the modulus of elasticity E and shear modulus G replaced by effective modulii E^* and G^*. Bleich suggests using the tangent modulus, $E_t = \frac{d\sigma}{d\epsilon}$, for E^*, and $G\sqrt{E_t/E}$ or $G\left(E_t/E\right)$ for G^*.

In most cases of torsional-flexural buckling the critical load depends more on E^* than on G^*.[13] This is due to the fact that only the last of the three deformations - bending, warping, and twisting - depends on the torsional stiffness GK. The choice of a value G^* is therefore less critical than that of E^*.

To describe the behavior of the columns braced by girts which in turn are braced by a diaphragm in the inelastic range E will be replaced by $E^* = E_t$ and G will be replaced by $G^* = G\,(E_t/E)$. Further, the diaphragm and the girts will be assumed to be in the elastic range even if the column is in the inelastic range.

It is known that E_t depends on the effective stress-strain relationship of the entire cross section. A stress-strain curve typical of those obtained for the entire cross section of hot rolled steel members is shown in Fig. 3-15. The existence of a gradual yielding region in the curve is caused by the distribution of residual cooling stresses over the cross section.

If the relation between the inelastic buckling stress and slenderness ratio is assumed to be a quadratic parabola, tangent to the abscissa, $\sigma = \sigma_Y$ (yield stress), at slenderness ratio equal to zero and intersecting the elastic curve at $\sigma = \sigma_p$ (proportional limit), then the relation between tangent modulus and stress is shown by Bleich to be given by

$$\frac{E_t}{E} = \frac{(\sigma_Y - \sigma)\sigma}{(\sigma_Y - \sigma_p)\sigma_p} \qquad (3\text{-}59)$$

where σ is the average compressive stress $\frac{P}{A}$ on the cross section.

The above relation will be used in the inelastic range to obtain E^* and G^* once the average stress on the column is known and the application will be demonstrated in two examples in Appendix III.

3.3 Investigation of Load Carrying Capacity of Imperfect Columns

In this section the load carrying capacity of an axially loaded imperfect I-section column braced by girts which in turn are braced by a diaphragm is determined considering that the load carrying capacity is based on either the failure of the column by yielding, or failure of the diaphragm in shear, or failure of the girts in bending. The criteria of the above failures established for the purposes of investigation presented in this section are discussed in the following.

1. Failure of the column by yielding. The criterion of failure established here is that of failure in combined bending and axial stresses. A column is considered as failed if any one of the following inequalities is violated:

Between girts:
$$\frac{f_a}{F_a} + \frac{f_b}{F_y} \leq 1 \qquad (3\text{-}60)$$

At braced points:
(i.e. at intermediate girts and ends)
$$\frac{f_a + f_b}{F_y} \leq 1 \qquad (3\text{-}61)$$

where

f_a is the computed axial stress

f_b is the computed bending stress at the section under consideration including the effect of additional deflections under axial load

F_a is the buckling stress

and F_y is the yield stress.

Note that the above inequalities are ultimate strength equivalents to Eqs. 7a and 7b in the AISC manual[16]. Further, since the column is bent about the Y axis, there will be no lateral torsional flexural buckling; and therefore, on the basis of ultimate strength, F_y is substituted for F_b in Eqs. 7a and 7b of the AISC manual. It is also to be noted that contribution of twist towards the failure of the column is not included in the above.

2. Failure of the diaphragm in shear. The criterion of failure of the diaphragm bracing the girts which in turn brace a column is similar to that described in 2 on page 29 for diaphragm braced beams. The diaphragm is considered as failed if the maximum shear strain γ_{max} computed using $Q = Q_d$ in the required equations, exceeds the shear strain γ_d. γ_{max} can be computed from the load-deflection relationships knowing the deflected shape of the column.

3. Failure of the girts in bending. Twist of the columns produces bending of the girts about their strong axis. Fig. 3-16 shows the bent shape of a girt bracing an imperfect column. It is seen from Fig. 3-16 that the compression flange in one

half length of the girt between the columns is not braced by the diaphragm. Therefore, to be conservative, a girt is considered as failed if any one of the following inequalities is violated:

$$\left.\begin{aligned} M_c &< M_{cr}^g \\ M_c &< M_y^g \end{aligned}\right\} \qquad (3\text{-}62)$$

where

M_c is the moment on the girt at the connection to the column due to the twisting of the column

M_{cr}^g is the critical moment of the girt of length w subjected to uniform moment

and M_y^g is the yield moment of the girt.

The deflection pattern of the column used for the analysis in this investigation contains, in general, only one term in flexure and one term in torsion as against two terms in flexure and two terms in torsion, that were used in the theory presented in the previous sections. These two approximations seemed to differ by only about 5% to 10% in critical loads. The analysis in this section is intended to enable one to compute the load-deflection relationships and the critical loads by hand. All the assumptions used in the theory presented in the previous sections are also applicable in this section.

The necessary constants for the investigation in this section are derived for a column whose ends are flexurally hinged and torsionally simple (i.e. warping is unrestrained

and twist is zero at ends) using the following deflection pattern:

For j intermediate girts and i th mode:

$i \leq j$

Initial Imperfections:

$$\begin{cases} u_{10} = E_i \sin \dfrac{i\pi z}{(j+1)\ell} \\ \beta_{10} = F_i \sin \dfrac{i\pi z}{(j+1)\ell} \end{cases} \tag{3-63}$$

Additional Deflections:

$$\begin{cases} u_1 = C_i' \sin \dfrac{i\pi z}{(j+1)\ell} \\ \beta_1 = D_i' \sin \dfrac{i\pi z}{(j+1)\ell} \end{cases} \tag{3-64}$$

$i = j+1$

Initial Imperfections:

$$\begin{cases} u_{10} = E_1 \sin \dfrac{\pi z}{(j+1)\ell} + E_{j+1} \sin \dfrac{\pi z}{\ell} \\ \beta_{10} = 0 \end{cases} \tag{3-65}$$

Additional Deflections:

$$\begin{cases} u_1 = C_1'^{*} \sin \dfrac{\pi z}{(j+1)\ell} + C_{j+1}'^{*} \sin \dfrac{\pi z}{\ell} \\ \beta_1 = 0 \end{cases} \tag{3-66}$$

The above deflection pattern gives the following load-deflection relationships after minimizing the total energy U :

$$i \leq j \quad \begin{bmatrix} K1_j^i P_e^{*} - P + K2_j^i Q & e\left(K1_j^i P_e^{**} - P\right) \\ e\left(K1_j^i P_e^{**} - P\right) & \left(a^{*} - P\frac{I_p}{A}\right) + e^2\left(K1_j^i P_e^{**} - P\right) \end{bmatrix} \begin{Bmatrix} C_i' \\ D_i' \end{Bmatrix} = P \begin{Bmatrix} E_i + eF_i \\ \left(\frac{I_p}{A} + e^2\right)F_i \\ + eE_i \end{Bmatrix} \tag{3-67}$$

$$\begin{bmatrix} KI'_j P_e^{**} - P + K2'_j Q & 0 \\ 0 & (P_e^{**} - P) \end{bmatrix} \begin{Bmatrix} C_1'^{*} \\ C_{j+1}'^{*} \end{Bmatrix} = P \begin{Bmatrix} E_1 \\ E_{j+1} \end{Bmatrix} \qquad (3\text{-}68)$$

(Note that effective modulii, E^* and G^*, are substituted for elastic modulii, E and G, after minimization of the total energy.)

where

P_e^* is the buckling load of an ideal column determined by using Euler's equation in the elastic range and the CRC formula in the inelastic range

$P_e^{**} = \frac{\pi^2 E^* I_y}{\ell^2}$; E^* depends on the average axial stress level in the column

KI_j^i, $K2_j^i$, and $K3_j^i$ are the constants KI, $K2$, and $K3$ respectively for the column with j intermediate girts and in the i th mode and are given at the end of this section

and $a^* = KI_j^i E^* \Gamma \left(\frac{\pi}{\ell}\right)^2 + G^* K + K3_j^i m$

The additional deflections C_i', D_i', $C_1'^{*}$, and $C_{j+1}'^{*}$ are derived from Eqs. 3-67 and 3-68 and are given by

$$C_i' = \frac{P \begin{vmatrix} E_i + eF_i & e(KI_j^i P_e^{**} - P) \\ \left(\frac{I_P}{A} + e^2\right)F_i + eE_i & (a^* - P\frac{I_P}{A}) + e^2(KI_j^i P_e^{**} - P) \end{vmatrix}}{DD_j^i} \qquad (3\text{-}69)$$

$$D_i' = \frac{P \begin{vmatrix} K1_j^i P_e^{**} - P + K2_j^i Q & E_i + cF_i \\ e(K1_j^i P_e^{**} - P) & \left(\frac{I_P}{A} + e^2\right)F_i + cE_i \end{vmatrix}}{DD_j^i} \qquad (3\text{-}70)$$

$$C_1'^* = \frac{E_1 P}{K1_j' P_e^{**} - P + K2_j' Q} \qquad (3\text{-}71)$$

and $$C_{j+1}'^* = \frac{E_{j+1} P}{(P_e^{**} - P)} \qquad (3\text{-}72)$$

where

$$DD_j^i = (K1_j^i P_e^{**} - P)(a^* - P\tfrac{I_P}{A}) + K2_j^i Q\{e^2(K1_j^i P_e^{**} - P) + (a^* - P\tfrac{I_P}{A})\}$$

Critical load $P_{cr,j}^i$ of a column with j intermediate girts in the i th mode will be derived from Eq. 3-67 by letting the initial imperfections equal zero when $i \leq j$, and is given by

$$P_{cr,j}^i = \left\{\frac{b^*}{2} - \sqrt{\left(\frac{b^*}{2}\right)^2 - c^*}\right\} \qquad (3\text{-}73)$$

where

$$b^* = K1_j^i P_e^{**} + K2_j^i Q\left(1 + \frac{Ae^2}{I_P}\right) + \frac{A a^*}{I_P}$$

and $$c^* = \frac{A}{I_P}\left\{K2_j^i Q\left(a^* + K1_j^i P_e^{**} e^2\right) + a^* K1_j^i P_e^{**}\right\}$$

When $i = j+1$, $P_{cr,j}^i$ is given by

$$P^{i}_{cr,j} = P^{j+1}_{cr,j} = P^{*}_{e} \qquad (3\text{-}74)$$

Then, the critical load of a column $P_{cr,j}$ with j intermediate girts is given by

$$P_{cr,j} = \text{Min}\left(P^{1}_{cr,j}, \ldots, P^{j+1}_{cr,j}\right) \qquad (3\text{-}75)$$

Note that the mode of buckling of an ideal column depends on the values of Q, m, e, and the spacing of girts, ℓ.

Further, the shear rigidity $Q^{i}_{id,j}$ required for an ideal column with j intermediate girts so that the column could reach the buckling load P^{*}_{e} in the i th mode is given by Eq. 3-73 by letting $P^{i}_{cr,j} = P^{*}_{e}$ and $Q = Q^{i}_{id,j}$. Thus

$$Q^{i}_{id,j} = \frac{-1}{K2^{i}_{j}}\left\{\frac{\left(K1^{i}_{j}P^{**}_{e} - P^{*}_{e}\right)\left(a^{*} - P^{*}_{e}\frac{I_p}{A}\right)}{e^{2}\left(K1^{i}_{j}P^{**}_{e} - P^{*}_{e}\right) + \left(a^{*} - P^{*}_{e}\frac{I_p}{A}\right)}\right\} \qquad (3\text{-}76)$$

The shear rigidity $Q_{id,j}$ required for an ideal column to reach the critical load P^{*}_{e}, irrespective of the mode, is given by

$$Q_{id\,j} = \text{Max}\left(Q^{1}_{id,j}, \ldots, Q^{j}_{id,j}\right) \qquad (3\text{-}77)$$

The difficulty in using the above Eq. 3-73 lies in the fact that one does not know the value of E^{*} before obtaining $P^{i}_{cr,j}$. Therefore, one has to use a trial value for E^{*}. After obtaining $P^{i}_{cr,j}$ one can calculate E^{*} corresponding to the load level $P^{i}_{cr,j}$. If this E^{*} agrees with the trial value then the computation of $P^{i}_{cr,j}$ is correct; otherwise

the process has to be repeated with a new rational trial value until the trial value becomes correct.

The above procedure is tedious. Therefore an approximate and easier procedure described in the following may be adopted to obtain $P^{i}_{cr,j}$.

Two values of Q namely Q_1 and Q_2 such that Q_1 and Q_2 are in close neighborhood of Q and $Q_1 \leq Q \leq Q_2$ may be calculated from Eq. 3-76 corresponding to two assumed values of loads P_1 and P_2 by replacing P^{*}_{e} with P_1 or P_2 and $Q^{i}_{id,j}$ with Q_1 or Q_2 , respectively. Then the critical load $P^{i}_{cr,j}$ is obtained by linear interpolation as

$$P^{i}_{cr,j} = \left\{ P_1 + \frac{(P_2 - P_1)(Q - Q_1)}{(Q_2 - Q_1)} \right\}_{i \text{ th mode}} \qquad (3\text{-}78)$$

The initial displacement E_{io} of the C. G. of the column section is taken as the tolerance limit of sweep specified in the AISC manual for a column length of L/i. The imperfection of the column in twist F_i is arbitrarily taken as $F_i = 0.01$ radian (=0° 34' 22.6"). Knowing E_{io} and F_i the value E_i at X_1 axis can be computed as $E_i = E_{io} - eF_i$.

The following procedure is adopted to determine the load carrying capacity of an imperfect column braced by girts which in turn are braced by a diaphragm.

1. The shear characteristics Q_d and γ_d (refer to page 29) of the diaphragm used to brace the girts which in turn brace a column are determined. The stiffness m is determined from the bending stiffness of the girts and the type of con-

nection of the girts to the column. The evaluation of m for two different types of girt-column connections is shown in one of the examples worked out in Appendix III.

2. The flexural buckling stress σ_{cr} for the slenderness ratio l/r_y is determined using Euler's equation in the elastic range or the CRC formula in the inelastic range depending on whether $\frac{l}{r_y} > \sqrt{\frac{2\pi^2 E}{F_y}}$ or $< \sqrt{\frac{2\pi^2 E}{F_y}}$. The critical load P_e^* for the ideal column is given by: $P_e^* = \sigma_{cr} A$.

3. The smallest value of shear rigidity $Q_{id,j}$, which in combination with the twist restraint m gives the critical load P_e^* is determined. In some cases there may not exist any real positive value for $Q_{id,j}$ because the column may never reach the critical load P_e^* for particular values of m whatever may be the value of Q. In such cases the critical load $P_{cr,j}$, critical load of the column with shear rigidity Q_d and twist restraint m is determined.

4. If $Q_{id,j} \leq Q_d$ the procedure given in 4a through 4d is followed, otherwise the procedure given in 5a through 5e is followed.

4a. Since the column is imperfect the load carrying capacity P of the column will be less than P_e^*. Therefore a trial value for P of about $0.7\, P_e^*$ is assumed.

4b. The stress level σ $(=\frac{P}{A})$ is computed and the ratio $\frac{E^*}{E}$ is determined from Eq. 3-59. The additional deflections $C_1'^*$ and $C_{j+1}'^*$ are determined from Eqs. 3-71 and 3-72.

4c. Knowing the values of $C_1'^*$, $C_{j+1}'^*$, E_1, and E_{j+1}, and the deflection pattern the failure of the column by yield-

ing in combined bending and axial stresses is checked using the inequalities 3-60 and 3-61. If the inequalities are satisfied, increase the value of P and repeat the procedure from 4b until the inequalities are just satisfied. If the inequalities are not satisfied reduce the value of P and repeat the procedure from 4b until the inequalities are just satisfied.

4d. Knowing the additional deflections $C_1'^*$ and $C_{j+1}'^*$, and the deflection pattern, the maximum shear strain γ_{max} in the diaphragm can be computed. For the diaphragm not to fail in shear the following condition must be satisfied.

$$\gamma_{max} \leq \gamma_d \qquad (3\text{-}79)$$

If the inequality is satisfied the load carrying capacity of the column is P . Note that the failure of the girts need not be checked because there is no twist of the column in this case. If the inequality 3-79 is not satisfied the diaphragm fails before the column does. Therefore the trial value of P is reduced and the above procedure is repeated from 4b until the inequality is just satisfied.

5a. If $Q_{id,j} > Q_d$ or $Q_{id,j}$ is not a real positive number, a trial value for the load carrying capacity P of the column is assumed to be $0.7\, P_{cr,j}$.

5b. The additional deflections C_i' and D_i' are determined using Eqs. 3-69 and 3-70.

5c. Knowing C_i', D_i', E_i and F_i, and the deflection pattern the column is checked for failure by yielding in combined bending and axial stresses using inequalities 3-60 and 3-61. Note that the inequalities are, in general, con-

servative regarding the failure of the column.[33] However, in the above, the contribution of the stresses due to the twist of the column is neglected. If the inequalities are satisfied the value of P is increased, otherwise decreased, and the procedure is repeated from 5b until the inequalities are just satisfied.

5d. Knowing the value of C'_i and the deflection pattern, the maximum shear strain in the diaphragm can be computed. If the inequality 3-79 is satisfied, the diaphragm does not fail before the column does; the failure of the girts in bending is checked in 5e. If the inequality 3-79 is not satisfied, the trial value of P is decreased and the procedure is repeated from 5b until the inequality is satisfied.

5e. Knowing D'_i and the deflection pattern, the twist of the column at the connection to the girts can be computed. Knowing the nature of the girt-column connection, the maximum moment M_c on the girt, due to the twist of the column, can be computed. If the inequalities 3-62 are satisfied the load carrying capacity of the column is P ; otherwise the trial value of P is reduced and the above procedure is repeated from 5b until the inequalities 3-62 are just satisfied.

It is to be noted that any increase in Q above $Q_{id,j}$ would, in general, result in an increased value of the load carrying capacity P of the column. However, this increase is, in general, not considerable because the column might fail in between the braced points.

The constants K1, K2, and K3 for the column with one, two, and three intermediate girts are given in the following:

K1

i \ j	1	2	3
1	$\frac{1}{4}$	$\frac{1}{9}$	$\frac{1}{16}$
2		$\frac{4}{9}$	$\frac{1}{4}$
3			$\frac{9}{16}$

K2

i \ j	1	2	3
1	$\frac{8}{\pi^2}$	$\frac{9}{\pi^2}$	$\frac{32(1-\frac{1}{\sqrt{2}})}{\pi^2}$
2		$\frac{27}{4}\pi^2$	$\frac{8}{\pi^2}$
3			$\frac{32(1+\frac{1}{\sqrt{2}})}{9\pi^2}$

K3

i \ j	1	2	3
1	$\frac{4\ell}{\pi^2}$	$\frac{9\ell}{\pi^2}$	$\frac{16\ell}{\pi^2}$
2		$\frac{9\ell}{4\pi^2}$	$\frac{4\ell}{\pi^2}$
3			$\frac{16\ell}{9\pi^2}$

Two examples are worked out in Appendix III to illustrate the above procedure, the results of the examples are presented and discussed in the following.

Summary of Results

(1) Investigation No.	(2) Example	(3) Type of Column - girt Connection	(4) Shear Rigidity, Q_d (kips)	(5) Twist Restraint, m(k-in/rad)
1	1, L=16'	I(fully rigid)	413	2325
2	1, L=16'	II(fully flexible)	413	0
3	2, L=12'	I(fully rigid)	413	2900
4	2, L=12'	I(fully rigid)	826	2900

(Continued on next page)

Summary of Results (Continued)

(6) Shear Rigidity, $Q_{id,j}$ (kips)	(7) Critical load, $P_{cr,j}$ (kips)	(8) Mode of Buckling	(9) Load Carrying Capacity (kips)	(10) Failure by Yielding at	(11) (9)/(7)
> 413	296.7	Modified Second Mode	245	at braced point	0.83
-	182.6	Modified First Mode	124	between girts	0.68
404	305.5	Third Mode	230	at braced point	0.75
404	305.5	Third Mode	240	between girts	0.79

Discussion:

(1) The load carrying capacity of an imperfect column is always less than the critical load of the corresponding ideal column. In the above two examples, the load carrying capacities varied from 68% to 83% of the corresponding critical loads.

(2) It may be observed from investigations 3 and 4 that an increased value of diaphragm rigidity shifted the location of failure from a braced point to a point between the girts. This shows that at higher values of diaphragm rigidity the failure of the column takes place between the braced points before the critical load of the ideal column is reached, and this is expected in the case of an imperfect column.

(3) The load carrying capacity in investigation 3 should

have been higher than that in investigation 1 but for the fact that the assumption of initial imperfections in the third mode is more conservative than in the modified second mode.

3.4 Tests on Columns

3.4.1 Description of Tests

To corroborate the theoretical predictions of load-deflection relationships and buckling loads of axially loaded columns braced by girts which in turn are braced by a diaphragm, three tests were performed on the specimens shown schematically in Fig. 3-17. All test assemblies consisted of two equally and axially loaded 8Jr6.5 I-section columns, made of ASTM A-441 low alloy high strength steel, braced by two intermediate girts which in turn are braced by a 26 gage standard corrugated steel diaphragm. The diaphragm was attached to the girts with #14 screws at every third valley. In tests 1 and 3 wherein an unusual connection between the girts and the columns was provided (refer to Fig. 3-17), to simulate known twist restraints on the columns, the girts were 6 [13 rolled steel sections whereas in test 2, where the girts were welded to the columns, the girts were 6 [2.26 light-gage steel sections. An unusual column-girt connection was provided in tests 1 and 3 because it was desired to have fully flexible and semi-rigid (with known restraints) connections, respectively, in these tests. The column-girt connection in test 2 is, in general, considered as a fully rigid connection. Note that

the connection in test 3 was designed to provide an intermediate case between the two extremes (fully flexible and fully rigid). The total length of each column between knife edges was 12' 7" and the spacing of columns in all the tests was 6'.

The column assemblies were tested in a frame constructed for the purpose. The test frame consists of two 6 WF 25 columns spaced 12' apart. Rolled steel channel sections, 18" deep, were connected to the columns one on each side of the flanges and perpendicular to the longitudinal axes of the columns, one pair of channels at the bottom and the other at the top such that there was a clear height of 15' 8" between the top pair and bottom pair of channels. Two 50 ton hydraulic jacks with hydraulic load cells were connected to the top channel beams such that the center lines of the jacks coincide with the longitudinal axes of the test columns. The test column assemblies were always situated at the center of the space between the columns of the test frame. The two jacks were connected to a common pump so that the loading on both columns would be equal at all times. The test columns were individually supported on knife edges parallel to the web. The jacks apply load on the top knife edges whereas the bottom knife edges rest on the bottom channel beams of the test frame. The load was read on an Emery console.

The plane of the test frame was in the north-south direction. The weight of the girts and the diaphragm tend to tilt the assembly to the west. The assembly was tied at the top

to the wall beam of the laboratory and thus the tilt of the assembly in all the tests was avoided.

A minimum of seven dial gages on each column reading to 0.001" were used in each test to measure the deflections of the columns at both the flanges parallel to the X-axis of the section. Twist of the columns can be computed from the above measurement of deflections. In all the tests, one dial gage at the top knife edge of each column was used to measure its movement parallel to the plane of the assembly. All the dial gages were supported by an independent framing system.

A total of eight electrical resistance strain gages were located at mid height of the column on the inside of each flange tip.

A suitable centering procedure developed in connection with this type of test was used in an effort to obtain concentricity of loading on each column[6]. However, the centering procedure was not carried up to high load levels, compared to the buckling loads of the columns, because the warping stresses due to precritical twist of the column form a considerable proportion of the average axial stress on the column in tests GT-1 and GT-3.

After centering the columns, the position of the flanges of the columns was noted by taking readings on a horizontal scale held perpendicular to the flange at the tip of the flange with the help of a transit in a vertical plane. The initial imperfections of the column (i.e. initial lateral deflection and twist) can be computed from the above readings.

In test 3 two springs were arranged on each side of the hinges at the connection of the girts to the columns. Springs were calibrated before use in the test and each has an average stiffness of k = 0.626 kip/in. The springs were 3 1/4" long and they were precompressed by 1/4" before they fit in between the plates of the connection arrangement. The distance between the springs on either side of the hinges is 7 3/8". This provided a value of twist restraint m = 26 kip-in./radian.

In test 2 the girts were 6 [2.26 light gage steel sections. By virtue of their bending stiffness they provided a value of twist restraint m = 7750 kip-in./radian.

3.4.2 Predicted Load-Deflection Relationships and Critical Loads for Columns

The ends of the columns were flexurally hinged. Twist is zero and warping is restrained at the ends. For these end conditions the assumed deflection pattern is given by

First Mode and Modified First Mode:

$$\text{Initial Imperfections:} \quad \begin{cases} u_{10} = E_1 \sin \frac{\pi z}{3\ell} \\ \beta_{10} = F_1 \left(1 - \cos \frac{2\pi z}{3\ell}\right) \end{cases} \tag{3-80}$$

$$\text{Additional Deflections:} \quad \begin{cases} u_1 = C_1 \sin \frac{\pi z}{3\ell} + C_5 \sin \frac{5\pi z}{3\ell} \\ \beta_1 = D_2 \left(1 - \cos \frac{2\pi z}{3\ell}\right) + D_6 \left(1 - \cos \frac{6\pi z}{3\ell}\right) \end{cases} \tag{3-81}$$

Modified Second Mode:

$$\text{Initial Imperfections:} \quad \begin{cases} u_{10} = 0 \\ \beta_{10} = 0 \end{cases} \tag{3-82}$$

$$\text{Additional Deflections:} \quad \begin{cases} u_1 = C_2 \sin \frac{2\pi z}{3\ell} \\ \beta_1 = D_1 \cos \frac{\pi z}{\ell} - \frac{2D_1}{3\ell}\left(\frac{3\ell}{2} - z\right) \end{cases} \tag{3-83}$$

(It will be seen that buckling of the columns in tests 1 and 3 occurs in the modified first mode and the buckling of the columns in test 2 occurs in the third mode. Therefore the load-deflection relationships in the modified second mode are not of practical importance and the initial imperfections are assumed to be zero in the above.) Minimization of the total energy U associated with the above deflection pattern gives the following load-deflection relationships for the column:

First Mode and Modified First Mode: $[DW12]\{XW12\} = P\{VW12\}$ (3-84)

Modified Second Mode: $[DW22]\{XW22\} = 0$ (3-85)

(Note that buckling of columns in all the three tests occurs in the elastic range.)

where

$$[DW12] = \begin{bmatrix} EI_y\left(\frac{\pi}{3\ell}\right)^2 - P + \frac{9Q}{\pi^2} & \frac{16e}{3\pi}\left\{EI_x\left(\frac{\pi}{3\ell}\right)^2 - P\right\} & -\frac{9Q}{\pi^2} & \frac{144e}{35\pi}\left\{EI_y\left(\frac{\pi}{3\ell}\right)^2 - P\right\} \\ \frac{4e}{3\pi}\left\{EI_y\left(\frac{\pi}{3\ell}\right)^2 - P\right\} & e^2\left\{EI_x\left(\frac{\pi}{3\ell}\right)^2 - P\right\} + E\Gamma\left(\frac{2\pi}{3\ell}\right)^2 + GK - P\frac{I_p}{A} + \frac{27m\ell}{4\pi^2} & -\frac{20e}{21\pi}\left\{EI_x\left(\frac{5\pi}{3\ell}\right)^2 - P\right\} & 0 \\ \frac{-9Q}{25\pi^2} & -\frac{16e}{105\pi}\left\{EI_x\left(\frac{5\pi}{3\ell}\right)^2 - P\right\} & EI_x\left(\frac{5\pi}{3\ell}\right)^2 - P + \frac{9Q}{25\pi^2} & \frac{144e}{55\pi}\left\{EI_y\left(\frac{5\pi}{3\ell}\right)^2 - P\right\} \\ \frac{4e}{35\pi}\left\{EI_y\left(\frac{\pi}{3\ell}\right)^2 - P\right\} & 0 & \frac{20e}{11\pi}\left\{EI_y\left(\frac{5\pi}{3\ell}\right)^2 - P\right\} & e^2\left\{EI_x\left(\frac{6\pi}{3\ell}\right)^2 - P\right\} + E\Gamma\left(\frac{6\pi}{3\ell}\right)^2 + GK - P\frac{I_p}{A} \end{bmatrix}$$

$$[XW12] = \begin{Bmatrix} C_1 \\ D_2 \\ C_5 \\ D_6 \end{Bmatrix}$$

$$[YW12] = \begin{Bmatrix} E_1 + \frac{16eF_1}{3\pi} \\ \frac{I_p}{A}F_1 + \frac{4eE_1}{3\pi} + e^2F_1 \\ -\frac{16eF_1}{35\pi} \\ \frac{4eE_1}{35\pi} \end{Bmatrix}$$

$$[DW22] = \begin{bmatrix} EI_y\left(\frac{2\pi}{3\ell}\right)^2 - P + \frac{27Q}{4\pi^2} & -\frac{18e}{5\pi}\left\{EI_y\left(\frac{2\pi}{3\ell}\right)^2 - P\right\} \\ -\frac{8e}{5\pi}\left\{EI_y\left(\frac{2\pi}{3\ell}\right)^2 - P\right\} & e^2\left\{EI_y\left(\frac{\pi}{\ell}\right)^2 - P\left(1-\frac{8}{9\pi^2}\right)\right\} \\ & + E\Gamma\left(\frac{\pi}{\ell}\right)^2 + \left(GK - P\frac{I_p}{A}\right)\left(1-\frac{8}{9\pi^2}\right) \\ & + \frac{64\,m\ell}{27\pi^2} \end{bmatrix}$$

and $\{XW22\} = \begin{Bmatrix} C_2 \\ D_1 \end{Bmatrix}$

The load-deflection relationships of a column with two intermediate girts in the third mode are the same as those given by Eq. 3-44 whether warping is restrained or unrestrained at the ends because the buckling is purely flexural. Further, the load-deflection relationships in sidesway are the same as given by Eq. 3-40. The load-deflection relationships may be restated as

Third Mode: $$[DM32]\ \{XM32\} = P\{VM32\} \qquad (3\text{-}86)$$

Sidesway: $$(Q - P)\ \Delta = P\,\Delta_o \qquad (3\text{-}40)$$

where

$$[DM32] = \begin{bmatrix} EI_y\left(\frac{\pi}{3\ell}\right)^2 - P + \frac{9Q}{\pi^2} & 0 \\ 0 & EI_y\left(\frac{\pi}{\ell}\right)^2 - P \end{bmatrix}$$

$$\{XM32\} = \begin{Bmatrix} C_1^* \\ C_3^* \end{Bmatrix}$$

and $$\{VM32\} = \begin{Bmatrix} E_1 \\ E_3 \end{Bmatrix}$$

By setting the initial imperfections equal to zero in Eqs. 3-84, 3-86 and 3-40, the critical loads will be obtained from Eqs. 3-84 through 3-86 and 3-40 as

First Mode and Modified First Mode: $[DW12]\{XW12\} = 0$ (3-87)

Modified Second Mode: $[DW22]\{XW22\} = 0$ (3-88)

Third Mode: $[DM32]\{XM32\} = 0$ (3-89)

Sidesway: $(Q-P)\Delta = 0$ (3-54)

Each one of the above equations describe an eigenvalue problem. The smallest value of P of the nontrivial solution of each of the above equations gives the critical load for each of the particular modes of buckling. Hence, the critical loads are given by

First Mode and Modified First Mode: $|DW12| = 0$ (3-90)

Modified Second Mode: $|DW22| = 0$ (3-91)

Third Mode: $|DM32| = 0$ (3-92)

Sidesway: $(Q-P) = 0$ (3-58)

$$\{XM32\} = \begin{Bmatrix} C_1^* \\ C_3^* \end{Bmatrix}$$

and $$\{VM32\} = \begin{Bmatrix} E_1 \\ E_3 \end{Bmatrix}$$

By setting the initial imperfections equal to zero in Eqs. 3-84, 3-86 and 3-40, the critical loads will be obtained from Eqs. 3-84 through 3-86 and 3-40 as

First Mode and Modified First Mode: $[DW12]\{XW12\} = 0$ (3-87)

Modified Second Mode: $[DW22]\{XW22\} = 0$ (3-88)

Third Mode: $[DM32]\{XM32\} = 0$ (3-89)

Sidesway: $(Q-P)\Delta = 0$ (3-54)

Each one of the above equations describe an eigenvalue problem. The smallest value of P of the nontrivial solution of each of the above equations gives the critical load for each of the particular modes of buckling. Hence, the critical loads are given by

First Mode and Modified First Mode: $|DW12| = 0$ (3-90)

Modified Second Mode: $|DW22| = 0$ (3-91)

Third Mode: $|DM32| = 0$ (3-92)

Sidesway: $(Q-P) = 0$ (3-58)

The critical load $P_{crw,z}$ of the column is the smallest of the critical loads obtained from the Eqs. 3-90 through 3-92 and 3-58, and the column buckles in that mode from which the critical load of the column is obtained.

Computations in evaluating critical loads and load deflection relationships of columns braced by girts which in turn are braced by a diaphragm were performed on a digital computer whenever necessary.

3.4.3 Column Test Results

The description and the results of the three tests are given in Table 8. The predicted critical loads and the experimental failure loads are shown in Figs. 3-18 through 3-20. The experimental failure loads of columns ranged from 84% to 94% of the corresponding critical loads.

In all the three tests the in-plane shear deflection of the diaphragm was very small and almost no damage to the diaphragm was observed even after the columns had failed. Photographs of the column assembly before and after test GT-1 are shown in Figs. 3-21 and 3-22. A photograph of failure of the column assembly in Test GT-2 is shown in Fig. 3-23.

In test 3, because of the large twist of the columns the precompressed springs on one side of the girt-column connection hinges were found to be released when a load of 25 kips was reached on each column. But the columns could take an additional load of 0.5 kip before they failed. This shows that before the column failed the twist restraint was reduced to 13 kip-in/radian from 26 kip-in/radian because the springs

on one side of the girt-column connection hinges were released. Therefore, the failure load of the column is compared with the critical load of the column having a twist restraint of 13 kip-in/radian. The initial imperfections, deflection pattern at 23 kips load (the last load level at which the deflection measurements of the columns were taken with the springs on both sides of the girt-column connections operative) on each column, and the load-deflection curves for the north column in test 3 are shown in Figs. 3-24 through 3-27 respectively.

3.4.4 Discussion of Column Test Results

The buckling modes of failure in all the three tests were the same as predicted by the theory. As mentioned in Section 3.4.3 the experimental failure loads of columns ranged from 84% to 94% of the corresponding critical loads. The maximum amplitudes of initial imperfections used in the computations of the theoretical load-deflection relationships were the maximum values of the initial imperfections along the length of the column, so that the theoretical deflections would be a conservative estimate of the actual experimental deflections. Figs. 3-26 and 3-27 show a comparison between the theoretical load-deflection curves and the actual experimental load-deflection curves. It can be seen from the figures that the theoretical deflections are a conservative estimate of the actual experimental deflections except at very high load levels. At very high load levels the deflections of the column become large and certain portions of the cross section of the column might have yielded even if the average stress level on the

column is in the elastic range. At these high load levels the assumption of small deflection theory in the analysis may not be valid. The above reason probably explains why the experimental deflections at very high loads are larger than the theoretically predicted values.

4. SUMMARY AND CONCLUSIONS

4.1 Summary of Current Investigation

4.1.1 Diaphragm-Braced Beams Under Uniform Moment

The critical moment for I-beams continuously braced by a diaphragm on the compression flanges and subjected to uniform moment was obtained by Errera[8] using an energy method. In the present investigation, the solution for a more general problem--the load-deflection relationships of an imperfect Z-beam continuously braced by a diaphragm on the compression flange and subjected to uniform moments--was obtained by using the equilibrium method. The load-deflection relationships for diaphragm-braced imperfect I-beams and channel beams, the critical moment for a diaphragm-braced ideal Z-beam, and the critical moment for diaphragm-braced ideal I-beams and channel beams were derived as particular cases from the load-deflection relationships of a diaphragm-braced imperfect Z-beam.

The principal axes of the Z-beam are inclined at an angle α to the vertical and horizontal planes. In the theoretical analysis, uniform moment in the horizontal plane was applied in addition to the uniform moment in the vertical plane in such an amount that a diaphragm-braced ideal Z-beam bends vertically before it buckles. The uniform moment in the horizontal plane vanishes for diaphragm-braced I-beams and channel beams. The load-deflection relationships for a diaphragm-braced Z-beam are given by

$$\begin{bmatrix} E_{n\gamma_1} I_{Y_1}\left(\frac{n\pi}{L}\right)^2 + Q\cos^2\alpha & Q\sin\alpha\cos\alpha & Qe\cos\alpha - K_1 M \\ Q\sin\alpha\cos\alpha & E_{nx_1} I_{x_1}\left(\frac{n\pi}{L}\right)^2 + Q\sin^2\alpha & Qe\sin\alpha + K_2 M \\ Qe\cos\alpha - K_1 M & Qe\sin\alpha + K_2 M & E_{n\gamma_1}\Gamma\left(\frac{n\pi}{L}\right)^2 + G_n K + Qe^2 \end{bmatrix} \begin{Bmatrix} C_1 \\ E_1 \\ D_1 \end{Bmatrix} = M \begin{Bmatrix} K_1\delta_{\beta_1} \\ -K_2\delta_{\beta_1} \\ K_1\delta_{u_{1,1}} - K_2\delta_{v_{1,1}} \end{Bmatrix}$$

(4-1)

where the term containing the flexural rigidity F of the diaphragm is dropped (refer to page 18) and

n = 1 if the ends are simply supported (i.e. twist is zero and warping is unrestrained at the ends)

n = 2 if the ends are "fixed" (i.e. fixed about the vertical and longitudinal axes)

$$E_{nx_1} = E\,\frac{(I_{x_1})\ \text{elastic portion of the cross section}}{(I_{x_1})\ \text{total cross section}}$$

$$E_{n\gamma_1} = E\,\frac{(I_{\gamma_1})\ \text{elastic portion of the cross section}}{(I_{\gamma_1})\ \text{total cross section}}$$

$$G_n = G\left(\frac{E_{n\gamma_1}}{E}\right)$$

$E_{nx_1} I_{x_1}$ is the flexural rigidity of the beam about the principal axis X_1

$E_{n\gamma_1} I_{\gamma_1}$ is the flexural rigidity of the beam about the principal axis Y_1

$E_{\pi Y_1}\Gamma$ is the warping rigidity of the beam

$G_\pi K$ is the torsional rigidity of the beam

Q is the shear rigidity of the diaphragm

e is the distance from the C.G. of the beam to the plane of the diaphragm

$$K_1 = \frac{1}{\cos\alpha + \frac{I_{y_1}\sin^2\alpha}{I_{x_1}\cos\alpha}}$$

$$K_2 = \frac{1}{\sin\alpha + \frac{I_{x_1}\cos^2\alpha}{I_{y_1}\sin\alpha}}$$

$\delta_{u_{1,1}}$, $\delta_{v_{b1}}$, and δ_{β_1} are the amplitudes of the initial imperfections (refer to Eqs. 2-28 and 2-31) and C_1 , D_1 , and E_1 are the amplitudes of the additional deflections (refer to Eqs. 2-29 and 2-32).

The load-deflection relationships of diaphragm-braced imperfect I-beams and channel beams were derived by letting $\alpha = 0$, and $E_{\pi Y_1} = E_{\pi Y}$, in Eq. 4-1. After simplification the amplitudes of the additional deflections are given by

$$C_1 = \frac{M\delta_\beta\left\{E_{\pi Y}\Gamma\left(\frac{n\pi}{L}\right)^2 + G_\pi K + Qe^2\right\} + M\delta_u(M-Qe)}{\left\{E_{\pi Y}I_Y\left(\frac{n\pi}{L}\right)^2 + Q\right\}\left\{E_{\pi Y}\Gamma\left(\frac{n\pi}{L}\right)^2 + G_\pi K + Qe^2\right\} - (M-Qe)^2} \qquad (4\text{-}2)$$

and

$$D_1 = \frac{M\delta_u\left\{E_{ry}I_y\left(\frac{n\pi}{L}\right)^2+Q\right\}+M\delta_\beta\,(M-Qe)}{\left\{E_{ry}I_y\left(\frac{n\pi}{L}\right)^2+Q\right\}\left\{E_{ry}\Gamma\left(\frac{n\pi}{L}\right)^2+G_rK+Qe^2\right\}-(M-Qe)^2} \tag{4-3}$$

where δ_u and δ_β are the amplitudes of initial imperfections of either an I-beam or a channel beam corresponding to $\delta_{u_{1,1}}$ and δ_{β_1} of a Z-beam.

The critical moment for a diaphragm-braced ideal Z-beam was derived from Eq. 4-1 by letting the initial imperfections equal zero and solving for the nontrivial solution of the resulting eigenvalue problem. The critical moment is given by

$$\begin{vmatrix} E_{ry_1}I_{y_1}\left(\frac{n\pi}{L}\right)^2+Q\cos^2\alpha & Q\sin\alpha\cos\alpha & Qe\cos\alpha-K_1M \\ Q\sin\alpha\cos\alpha & E_{rx_1}I_{x_1}\left(\frac{n\pi}{L}\right)^2+Q\sin^2\alpha & Qe\sin\alpha+K_2M \\ Qe\cos\alpha-K_1M & Qe\sin\alpha+K_2M & E_{ry_1}\Gamma\left(\frac{n\pi}{L}\right)^2+G_rK+Qe^2 \end{vmatrix} = 0 \tag{4-4}$$

The critical moment for diaphragm-braced ideal I-beams and channel beams was derived from Eq. 4-4 by letting $\alpha = 0$ and $E_{ry_1} = E_{ry}$. After simplification the critical moment is given by

$$M_{cr} = \sqrt{\left\{E_{ry}I_y\left(\frac{n\pi}{L}\right)^2+Q\right\}\left\{E_{ry}\Gamma\left(\frac{n\pi}{L}\right)^2+G_rK+Qe^2\right\}}+Qe$$

The load carrying capacity of diaphragm-braced imperfect I-beams and channel beams was determined on the basis of one of the two failures described below, whichever occurs first.

1. Failure of the beam by yielding. The beam is considered as failed if the uniform moment on the beam reaches the yield moment M_y of the beam.

2. Failure of the diaphragm in shear. The diaphragm is considered as failed if the maximum shear strain γ_{max} of the diaphragm in the diaphragm-braced beam assembly exceeds the shear strain γ_d of the diaphragm determined in an independent cantilever or simple beam shear diaphragm test described in Appendix IV. The maximum shear strain γ_{max} can be calculated by using Eqs. 4-2 and 4-3 and knowing the deflected shape of the diaphragm-braced I-beams and channel beams.

A comparison between the theoretically predicted critical moments and experimental failure moments from four diaphragm-braced double 10B17 I-beam tests conducted by Errera is presented in Fig. 2-34. The predicted critical moments underestimate the failure moments of the beams in the elastic range by about 20% to 24%. This can be attributed, probably, to the fact that the cross-bending rigidity of the diaphragm is not considered in the predicted critical moments. However, in the inelastic range the moments sustained by the beams were smaller than the predicted critical moments by about 3% to 5%.

Three diaphragm-braced 6[8.2 double-beam tests were made and the comparison between the theoretically predicted critical moments and the experimental failure moments are shown in Fig. 2-35.

The moments sustained by the beams in the above tests ranged from 75% to 99.6% of the predicted critical moments of the beams.

A comparison between the theoretically predicted critical moment and the experimental failure moment for a diaphragm-braced beam assembly comprising of four 8Jr6.5 I-beams is presented in Fig. 2-36. The moment sustained by the beam assembly was 90% of the predicted critical moment.

The load carrying capacities of two different diaphragm-braced I-beams were calculated in Appendix II to exhibit the behavior of the imperfect beams and the diaphragm under load. In one of the examples the beam fails before the diaphragm does whereas in the other example the diaphragm fails before the beam does. It is seen that the type of failure which determines the load carrying capacity of the diaphragm-braced beam assembly depends on the relative strength and stiffness of the diaphragm and the beam.

4.1.2 Axially Loaded I-Section Columns Braced by Girts Which in Turn are Braced by a Diaphragm

The load-deflection relationship of an axially loaded imperfect I-section column with "hinged" (i.e. flexurally hinged, twist is zero and warping is unrestrained) ends braced by one or two intermediate girts which in turn are braced by a diaphragm was obtained by minimizing the total energy U (given by Eq. 3-13) associated with one column of the assembly, using the Rayleigh-Ritz technique. The assumed deflection pattern of the column is given by Eqs. 3-18 and 3-19, and 3-29 through 3-36. The load-

deflection relationships of an axially loaded imperfect I-section column are given by

Column with one intermediate girt:

First Mode and Modified First Mode: $$[D_{11}]\{x_{11}\} = P\{V_{11}\} \quad (4\text{-}5)$$

Second Mode: $$[D_{21}]\{X_{21}\} = P\{V_{21}\} \quad (4\text{-}6)$$

Sidesway: $$(Q-P)\Delta = P\Delta_o \quad (4\text{-}7)$$

Column with two intermediate girts:

First Mode and Modified First Mode: $$[D_{12}]\{x_{12}\} = P\{V_{12}\} \quad (4\text{-}8)$$

Modified Second Mode: $$[D_{22}]\{x_{22}\} = P\{V_{22}\} \quad (4\text{-}9)$$

Third Mode: $$[D_{32}]\{X_{32}\} = P\{V_{32}\} \quad (4\text{-}10)$$

Sidesway $$(Q-P)\Delta = P\Delta_o \quad (4\text{-}11)$$

(Refer to Section 3.1.2 for the matrices D_{11}, D_{21}, D_{12}, D_{22}, D_{32}, X_{11}, X_{21}, X_{12}, x_{22}, x_{32}, V_{11}, V_{21}, V_{12}, V_{22}, and V_{32}.)

It was seen in Section 3.1.3 that when the column sways it neither bends nor twists, and, also, if the column bends or twists, or bends and twists, it does not sway. The deflection mode for an imperfect column braced by girts which in turn are braced by a diaphragm is the same as the buckling mode for an identical ideal column with the identical bracing. If the column is prevented from swaying in the plane of the diaphragm, for example, by using X-bracing (refer to Fig. 1-1), then, the load-deflection relationships are given by Eqs. 4-5 and 4-6, and Eqs. 4-8 through 4-10.

The critical load of an axially loaded ideal column braced by girts which in turn are braced by a diaphragm was obtained by letting the initial imperfections equal zero in Eqs. 4-5 through 4-11 and solving the resulting eigenvalue problem for the non-trivial solution. The critical load is obtained from:

Column with one intermediate girt:

First Mode and Modified First Mode: $|D_{11}| = 0$ (4-12)

Second Mode: $|D_{21}| = 0$ (4-13)

Sidesway: $(Q-P) = 0$ (4-14)

Column with two intermediate girts:

First Mode and Modified First Mode: $|D_{12}| = 0$ (4-15)

Modified Second Mode: $|D_{22}| = 0$ (4-16)

Third Mode: $|D_{32}| = 0$ (4-17)

Sidesway: $(Q-P) = 0$ (4-18)

The critical load is given by the smallest value of P obtained from Eqs. 4-12 through 4-14 for the ideal column with one intermediate girt and from Eqs. 4-15 through 4-18 for the ideal column with two intermediate girts. The ideal column buckles in that mode from which the smallest value of P is obtained. If the sidesway is prevented, the critical load is given by Eqs. 4-12 or 4-13 for the column with one intermediate girt and by Eqs. 4-15, 4-16, or 4-17 for the column with two intermediate girts.

In the inelastic range the above equations are modified by replacing the modulus of elasticity E and the shear modulus G by $E^* = E\frac{\sigma(\sigma_y-\sigma)}{\sigma_p(\sigma_y-\sigma_p)}$ and $G^* = G\left(\frac{E^*}{E}\right)$, where σ, σ_p, and σ_y are the average axial stress on the column, proportional limit of the stress-strain relationship of the cross section, and the yield stress of the material. The proportional limit was assumed to be equal to $\frac{\sigma_y}{2}$ in the analysis herein.

The load carrying capacity of an axially loaded imperfect I-section column was based on one of the three failures given below, whichever occurs first.

1. Failure of the column by yielding. The criterion of failure established here is that of failure in combined bending and axial stresses. A column is considered as failed if any one of the following inequalities is violated:

Between girts: $$\frac{f_a}{F_a} + \frac{f_b}{F_y} \leq 1 \qquad (4\text{-}19)$$

At braced points (i.e., at intermediate girts and ends): $$\frac{f_a + f_b}{F_y} \leq 1 \qquad (4\text{-}20)$$

where

f_a is the computed axial stress

f_b is the computed bending stress at the section under consideration including the effect of additional deflections under axial load

F_a is the buckling stress

and F_y is the yield stress.

Note that the above inequalities are ultimate strength equivalents to Eqs. 7a and 7b in the AISC manual. Further, since the column is bent about the Y axis, there will be no lateral torsional flexural buckling; and therefore on the basis of ultimate strength F_y is substituted for F_b in Eqs. 7a and 7b of the AISC manual. It is to be noted that contribution of twist towards failure of the column is not included in the above.

2. Failure of the diaphragm in shear. The criterion of failure of the diaphragm bracing the girts which in turn brace a column is similar to that described in 2 on page 29 for diaphragm-braced beams. The diaphragm is considered as failed if the maximum shear strain r_{max} computed using $Q = Q_d$ in the required equations, exceeds the shear strain r_d .

r_{max} can be computed from the load-deflection relationships knowing the deflected shape of the column.

3. Failure of the girts in bending. Twist of the columns produces bending of the girts about their strong axis. Fig. 3-16 shows the bent shape of a girt bracing an imperfect column. It is seen from Fig. 3-16 that the compression flange in one half length of the girt between the columns is not braced by the diaphragm. Therefore, to be conservative, a girt is considered as failed if any one of the following inequalities is violated:

$$\left.\begin{aligned} M_c &< M_{cr}^g \\ M_c &< M_y^g \end{aligned}\right\} \qquad (4\text{-}21)$$

where

M_c is the moment on the girt at the connection to the column due to the twisting of the column

M_{cr}^{g} is the critical moment of the girt of length w subjected to uniform moment (refer to Fig. 3-16)

and M_y^g is the yield moment of the girt.

Three tests were conducted on 8Jr6.5 I-section columns braced by girts which in turn were braced by a 26 gage standard corrugated steel diaphragm. The variable in the three tests was the twist restraint m on the column. The ends of the column were flexurally hinged. Warping was restrained and twist was zero at the ends of the columns. Load-deflection relationships and the critical loads were derived in Section 3.4.2 for the column in the three tests using the general procedure given in Section 3.1. A comparison of theoretically predicted critical loads and experimental failure loads of the columns are shown in Figs. 3-18 through 3-20. The axial loads sustained by the columns in the tests ranged from 84% to 94% of the critical loads. The theoretical and experimental load-deflection relationships are shown graphically in Figs. 3-26 and 3-27.

4.2 Conclusions

Present theory and test results demonstrate conclusively that shear-rigid diaphragms properly attached can effectively brace slender beams against lateral buckling, and can increase the critical moments of ideal beams to their plastic moments.

It was shown that the theoretical failure loads of imperfect beams subjected to uniform moments can be computed analytically for assumed criteria of failure of the beams and the bracing, and the theoretical failure load of the beam assembly is always less than the critical moment of the corresponding ideal beam assembly. In the case of particular examples worked out in Appendix II the theoretical failure loads of the beam assemblies were smaller than the corresponding critical moments by about 15% to 20%.

Further, present theory and test results demonstrate that properly attached diaphragms can brace girts which in turn can effectively brace columns if proper moment resistant column-girt connections are provided. Such diaphragms and girts can reliably increase the critical loads of columns to the Euler buckling loads of the columns of a length equal to the spacing of the girts. It was shown that the failure loads of axially loaded imperfect I-section columns braced by girts which in turn are braced by a diaphragm can be computed analytically for assumed criteria of failure of the column and the bracing, and the theoretical failure load of the assembly is always less than the critical load of the corresponding ideal column assembly. In the case of particular examples worked out in Appendix III the theoretical failure loads of the column assemblies were smaller than the corresponding critical loads by about 17% to 32%.

Where present forms of construction provide adequate diaphragm bracing to beams or columns, or where minor modifications in construction practice would accomplish this, the above infor-

mation could serve as the basis for increased design load capacity, or elimination of other types of bracing.

APPENDIX I

NOTATION

A	cross-sectional area
B_s	energy due to shear in the diaphragm
B_t	energy of bending of the girts
C	amplitude of additional lateral deflection
D	amplitude of additional twist
$Dij, DWij, DMij$ $(i=1,\cdots; j=1,\cdots)$	matrices
E	modulus of elasticity
E_t	tangent modulus
E^*	effective modulus for weak-axis buckling
E_r	reduced modulus in bending
$E_1, E_2, \cdots$	amplitudes of initial lateral deflection of column
F	flexural parameter of diaphragm
F_a	buckling stress
F_Y	yield stress
$F_1, F_2, \cdots$	amplitudes of initial twist of column
G	shear modulus
G_{eff}	effective shear modulus of diaphragm
G'	shear stiffness of diaphragm
G_r	reduced shear modulus
G^*	inelastic shear modulus
I	moment of inertia
I_p	polar moment of inertia
K	torsional constant

$K1, K2, K3$	constants
K_1, K_2, K_3	constants
L	length
M	moment
M_{cr}	critical moment
M_o	end moment
M_{pl}	plastic moment
M_y	yield moment
N	number of corrugations between successive connectors
P	load
Q	effective shear rigidity of diaphragm
R	resistive force on the column due to the girts
S_x	elastic section modulus about X-axis
S_b	shear force of the diaphragm
U	total potential energy in a system
U_w	potential energy of external loads
V	internal strain energy of column
$Vij, VWij, VMij$ $(i=1,\cdots; j=1,\cdots)$	column matrices
X, Y, Z X_1, Y_1, Z_1	coordinate axes
$Xij, XWij, XMij$ $(i=1,\cdots; j=1,\cdots)$	column matrices
Z_x	plastic section modulus about X-axis
a	length of shear panel perpendicular to load direction
a^*	$= K1_j^i E^* r \left(\frac{\pi}{l}\right)^2 + G^* k + K3_j^i m$

b	length of shear panel parallel to load direction
b^*	$= K1_j^i P_e^{**} + K2_j^i Q\left(1+\frac{A}{I_p}e^2\right) + \frac{A}{I_p}a^*$
c^*	$= \frac{A}{I_p}\left\{K2_j^i Q\left(a^* + K1_j^i P_e^{**} e^2\right) + a^* K1_j^i P_e^{**}\right\}$
d	depth of beam section
e	distance between the plane of bracing and C.G. of member section
f_a	average axial stress of the member
f_b	bending stress at the extreme fiber of the member
i	mode number
j	number of intermediate girts
ℓ	spacing of girts
m	twist restraint
q_f	equivalent distributed force for shear of diaphragm
r_y	weak-axis radius of gyration
t	thickness of diaphragm
u, u_1	deflections of member parallel to X and X_1 axes respectively
v, v_1	deflections of member parallel to Y and Y_1 axes respectively
w	width of diaphragm contributing to bracing of one member
x_o, y_o	distances from center of gravity to shear center of a section along X and Y principal axes respectively.

α	angle between the principal and horizontal or vertical axes for a Z-beam
β	twist of member
γ	shear strain
Γ	warping constant
δ	initial imperfection or deflection of Z-section
Δ	sidesway or shear deflection
ϵ	axial strain
σ	average axial stress
σ_P	proportional limit
σ_Y	yield stress
τ	shear stress

APPENDIX II

ABOUT DIAPHRAGM-BRACED BEAMS

Deflections in the directions of the principal axes of a Z-beam are given by

Deflection in +ve Y_1 direction due to M, $\delta_{Y_1}^{M} = K_3 \frac{M \cos\alpha}{I_{X_1}}$

Deflection in +ve Y_1 direction due to M_S, $\delta_{Y_1}^{M_S} = K_3 \frac{M_S \cos\alpha}{I_{X_1}}$

Deflection in -ve X_1 direction due to M, $\delta_{X_1}^{M} = K_3 \frac{M \sin\alpha}{I_{Y_1}}$

Deflection in -ve X_1 direction due to M_S, $\delta_{X_1}^{M_S} = K_3 \frac{M_S \sin\alpha}{I_{Y_1}}$

where K_3 is a constant.

The total deflections δ_{X_1} and δ_{Y_1} in the X_1 and Y_1 directions respectively are as shown in Fig. 2-3 and are given by

$$\delta_{X_1} = \delta_{X_1}^{M} + \delta_{X_1}^{M_S}$$

$$\delta_{Y_1} = \delta_{Y_1}^{M} + \delta_{Y_1}^{M_S}$$

For no horizontal deflection before buckling the following condition should hold:

$$\frac{\delta_{X_1}}{\delta_{Y_1}} = \frac{\sin\alpha}{\cos\alpha} \qquad \text{(II-1)}$$

But,

$$\frac{\delta_{X_1}}{\delta_{Y_1}} = \frac{\delta_{X_1}^{M} + \delta_{X_1}^{M_S}}{\delta_{Y_1}^{M} + \delta_{Y_1}^{M_S}} = \frac{I_{X_1}}{I_{Y_1}} \left\{ \frac{M \sin\alpha - M_S \cos\alpha}{M \cos\alpha + M_S \sin\alpha} \right\} \qquad \text{(II-2)}$$

Using Eqs. II-1 and II-2, M_S can be computed as

$$M_s = \frac{M \sin\alpha \cos\alpha \{I_{x_1} - I_{y_1}\}}{\{I_{x_1} \cos^2\alpha + I_{y_1} \sin^2\alpha\}}$$

Example 1. The roof of a building is spanned by 14 x 4B x 17.2# I-section beams 12' long. The beams are braced by a 22 gage wide rib roof deck (12' long sheets) welded as shown in Fig. II-1. It is required to determine the moment carrying capacity of an end beam. Beams are made of A36 steel. Beams can be considered as "simply supported" (simply supported about the horizontal and vertical axes, twist is zero and warping unrestrained) at ends.

Shear Diaphragm Characteristics (refer to page 29 and Fig. II-2):

80% of ultimate shear load = 0.8 x 3.43

= 2.74 kips

Shear deflection at 80% of ultimate load (neglecting bending effect of the frame) = 0.54"

Shear stiffness, $G'_d = \frac{2.74}{0.54}(\frac{10}{12}) = 4.24$ K/in

Shear rigidity, Q_d (Considering that 3' width of diaphragm contributes to the support of an end beam) = 4.24 x 36

= 152.5 kips

Shear strain $\gamma_d = \frac{0.54}{10 \times 12} = 0.0045$

Critical Moment $M_{cr,u}$ of the Beam (no bracing):

$Q = 0$ and $F = 0$

Using Eq. 2-46, $M_{cr,u} = 329$ K-in

Critical Moment M_{cr} of the Beam with Q_d = 152.5 kips:

$M_y = 36 \times 21.0 = 756$ K-in

$M_{pl} = 36 \times 24.7 = 889$ K-in

Using Eq. 2-44, $Q_y = 30.2$ kips

Using Eq. 2-45, $Q_{pl} = 63.5$ kips

$Q_d > Q_{pl}$,

Therefore, $M_{cr} = M_{pl} = 889$ K-in

Failure Moment of the Beam:

Maximum Shear Strain γ_{max} at M_y:

Initial lateral imperfection $\delta_u = \frac{1}{8} \times \frac{12}{10} = 0.15"$

Initial twist $\delta_\beta = 0.01$ radian

Using Eq. 2-36, $C_1 = 0.0232"$

Using Eq. 2-37, $D_1 = 0.0102$

Using Eq. 2-38, $\gamma_{max} = 0.00206 < \gamma_d$

Therefore, moment carrying capacity of the beam = $M_y = 756$ K-in.

Vertical Deflection at Midspan of the Beam at M_y:

$$\text{Vertical deflection at midspan} = \frac{M_y \ell^2}{8EI_x} = \frac{756 \times 144 \times 144}{8 \times 29000 \times 147.3} = 0.458"$$

Allowable deflection at failure moment:

$$= \frac{144}{360 \times 0.66} = 0.606 > 0.458$$

Result:

The beam fails before the diaphragm does and the moment carrying capacity of the beam = $M_y = 756$ K-in.

Example 2. The roof of a building is spanned by 18 x 6 x 70# I-beams 18' long. The beams are braced by a 22 gage wide rib roof deck (12' long sheets) welded as shown in Fig. II-1. It is required to determine the moment carrying capacity of an end beam. Beams are made of A36 steel. Beams can be considered as "simply supported" (simply supported about the horizontal and vertical axes, twist is zero and warping unrestrained) at the ends.

Shear Diaphragm Characteristics:

Same as in Example 1.

Q_d = 152.5 kips, and γ_d = 0.0045

Critical Moment $M_{cr,u}$ of the Beam (no bracing):

$Q = 0$, and $F = 0$

Using Eq. 2-46, $M_{cr,u}$ = 2780 K-in

Critical Moment M_{cr} of the Beam with Q_d = 152.5 kips:

M_y = 36 x 101.9 = 3668 K-in

M_{pl} = 36 x 123.8 = 4456 K-in

Using Eq. 2-44, Q_y = 42.6 kips

Using Eq. 2-45, Q_{pl} = 247 kips

Now, $Q_y < Q < Q_{pl}$

Therefore, the beam buckles in the inelastic range and $M_{cr} > M_y$.

Using Eq. 2-47, for

M = 3823 K-in, Q = 109 kips

M = 3867 K-in, Q = 200 kips

Using Eq. 2-48, M_{cr} = 3844 K-in.

Failure Moment of the Beam:

Maximum Shear Strain γ_{max} :

Initial lateral imperfection $\delta_u = \frac{1}{8} \times \frac{18}{10} = 0.225"$.

Initial twist $\delta_\beta = 0.01$ radian

It is found that the maximum shear strain $\gamma_{max} > \gamma_d$ at M_y. Therefore, the moment carrying capacity of the beam is smaller than M_y.

Using Eqs. 2-36 through 2-38, γ_{max} at moment M = 3063 K-in is found to be: $\gamma_{max} = 0.0045 = \gamma_d$.

Therefore, the moment carrying capacity of the beam = 3063 K-in.

Vertical Deflection at Midspan of the Beam:

Allowable vertical deflection at failure moment =

$$\frac{18 \times 12}{360 \times 0.66} = 0.909"$$

Vertical deflection at M = 3063 K-in:

$$\frac{3063 \times (18 \times 12)^2}{8 \times 29000 \times 917.5} = 0.671" < .909"$$

Result: The diaphragm fails before the beam does and the moment carrying capacity of the beam = 3063 K-in.

APPENDIX III

ABOUT COLUMNS BRACED BY GIRTS WHICH IN TURN ARE BRACED BY A DIAPHRAGM

III-a Column with One Intermediate Girt, Cases a1-2.1 and a1-2.2

When $e = 0$, Eqs. 3-48 and 3-49 give

$$|D_{11}| = \left\{\left[EI_y\left(\frac{\pi}{2\ell}\right)^2 - P + \frac{8Q}{\pi^2}\right]\left[EI_y\left(\frac{3\pi}{2\ell}\right)^2 - P + \frac{8Q}{9\pi^2}\right] - \left(\frac{-8Q}{\pi^2}\right)\left(\frac{-8Q}{9\pi^2}\right)\right\}$$

$$\left\{\left[E\Gamma\left(\frac{\pi}{2\ell}\right)^2 + Gk - P\frac{I_p}{A} + \frac{4m\ell}{\pi^2}\right]\left[E\Gamma\left(\frac{3\pi}{2\ell}\right)^2 + Gk - P\frac{I_p}{A} + \frac{4m\ell}{9\pi^2}\right] - \left(\frac{-4m\ell}{\pi^2}\right)\left(\frac{-4m\ell}{9\pi^2}\right)\right\} = 0$$

and

$$|D_{21}| = \left[EI_y\left(\frac{\pi}{\ell}\right)^2 - P\right]\left[E\Gamma\left(\frac{\pi}{\ell}\right)^2 + Gk - P\frac{I_p}{A}\right] = 0$$

It can be observed from the above equations that buckling will be either purely flexural or purely torsional and the critical load for a rolled steel column is, generally, given by (for case a1-2.2)

$$\text{either} \quad \left\{\left[EI_y\left(\frac{\pi}{2\ell}\right)^2 - P + \frac{8Q}{\pi^2}\right]\left[EI_y\left(\frac{3\pi}{2\ell}\right)^2 - P + \frac{8Q}{9\pi^2}\right] - \left(\frac{8Q}{\pi^2}\right)\left(\frac{8Q}{9\pi^2}\right)\right\} = 0$$

$$\text{or} \quad \left[EI_y\left(\frac{\pi}{\ell}\right)^2 - P\right] = 0$$

whichever gives the smaller value of P.

When $Q = 0$ (Case a1-2.1), the critical load is given by

$$\left[EI_y\left(\frac{\pi}{2\ell}\right)^2 - P\right] = 0$$

III-b Column with One Intermediate Girt, Cases a1-2.3 and a1-2.4

When $Q = 0$, Eqs. 3-48 and 3-49 give

$$\begin{aligned}|D11| = {} & \left[\left[EI_y\left(\frac{\pi}{2\ell}\right)^2 - P\right]\left\{\left[E\Gamma\left(\frac{\pi}{2\ell}\right)^2 + GK - P\frac{I_p}{A} + \frac{4m\ell}{\pi^2}\right] + e^2\left[EI_y\left(\frac{\pi}{2\ell}\right)^2 - P\right]\right\}\right. \\ & \left. - e^2\left[EI_y\left(\frac{\pi}{2\ell}\right)^2 - P\right]^2\right]\left[\left[EI_y\left(\frac{3\pi}{2\ell}\right)^2 - P\right]\left\{\left[E\Gamma\left(\frac{3\pi}{2\ell}\right)^2 + GK - P\frac{I_p}{A} + \frac{4m\ell}{9\pi^2}\right]\right.\right. \\ & \left.\left. + e^2\left[EI_y\left(\frac{3\pi}{2\ell}\right)^2 - P\right]\right\} - e^2\left[EI_y\left(\frac{3\pi}{2\ell}\right)^2 - P\right]^2\right] - \left[EI_y\left(\frac{\pi}{2\ell}\right)^2 - P\right] \\ & \left[EI_y\left(\frac{3\pi}{2\ell}\right)^2 - P\right]\left[\frac{-4m\ell}{\pi^2}\right]\left[\frac{-4m\ell}{9\pi^2}\right] = 0\end{aligned}$$

and

$$\begin{aligned}|D21| = {} & \left[EI_y\left(\frac{\pi}{\ell}\right)^2 - P\right]\left\{\left[E\Gamma\left(\frac{\pi}{\ell}\right)^2 + GK - P\frac{I_p}{A}\right] + e^2\left[EI_y\left(\frac{\pi}{\ell}\right)^2 - P\right]\right\} \\ & - e^2\left[EI_y\left(\frac{\pi}{\ell}\right)^2 - P\right]^2 = 0\end{aligned}$$

After simplification and rearranging the terms the above equations reduce to

$$|D11| = \left[EI_y\left(\frac{\pi}{2\ell}\right)^2 - P\right]\left[EI_y\left(\frac{3\pi}{2\ell}\right)^2 - P\right]\left\{\begin{array}{l}\left[E\Gamma\left(\frac{\pi}{2\ell}\right)^2 + GK - P\frac{I_p}{A} + \frac{4m\ell}{\pi^2}\right] \\ \left[E\Gamma\left(\frac{3\pi}{2\ell}\right)^2 + GK - P\frac{I_p}{A} + \frac{4m\ell}{9\pi^2}\right] \\ -\left[\frac{4m\ell}{\pi^2}\right]\left[\frac{4m\ell}{9\pi^2}\right]\end{array}\right\} = 0$$

and

$$|D21| = \left[EI_y\left(\frac{\pi}{\ell}\right)^2 - P\right]\left[E\Gamma\left(\frac{\pi}{\ell}\right)^2 + GK - P\frac{I_p}{A}\right] = 0$$

From the above equations, for $m \neq 0$ (Case a1-2.4) or $m = 0$ (Case a1-2.3), the critical load for a rolled steel column is, generally, given by

$$\left[EI_y\left(\frac{\pi}{2\ell}\right)^2 - P\right] = 0$$

III-c Column with Two Intermediate Girts, Cases a2-2.1 and a2-2.2

When $e = 0$, Eqs. 3-55 through 3-57 give

$$\left|D12\right| = \left\{\left[EI_y\left(\frac{\pi}{3\ell}\right)^2 - P + \frac{9Q}{\pi^2}\right]\left[EI_y\left(\frac{5\pi}{3\ell}\right)^2 - P + \frac{9Q}{25\pi^2}\right] - \left[\frac{-9Q}{\pi^2}\right]\left[\frac{-9Q}{25\pi^2}\right]\right\}$$
$$\left\{\left[E\Gamma\left(\frac{\pi}{3\ell}\right)^2 + GK - P\frac{I_p}{A} + \frac{9m\ell}{\pi^2}\right]\left[E\Gamma\left(\frac{5\pi}{3\ell}\right)^2 + GK - P\frac{I_p}{A} + \frac{9m\ell}{25\pi^2}\right] - \left[\frac{-9m\ell}{\pi^2}\right]\left[\frac{-9m\ell}{25\pi^2}\right]\right\} = 0$$

$$\left|D22\right| = \left\{\left[EI_y\left(\frac{2\pi}{3\ell}\right)^2 - P + \frac{27Q}{4\pi^2}\right]\left[EI_y\left(\frac{4\pi}{3\ell}\right)^2 - P + \frac{27Q}{16\pi^2}\right] - \left[\frac{-27Q}{4\pi^2}\right]\left[\frac{-27Q}{16\pi^2}\right]\right\}$$
$$\left\{\left[E\Gamma\left(\frac{2\pi}{3\ell}\right)^2 + GK - P\frac{I_p}{A} + \frac{9m\ell}{4\pi^2}\right]\left[E\Gamma\left(\frac{4\pi}{3\ell}\right)^2 + GK - P\frac{I_p}{A} + \frac{9m\ell}{16\pi^2}\right] - \left[\frac{-9m\ell}{4\pi^2}\right]\left[\frac{-9m\ell}{16\pi^2}\right]\right\} = 0$$

and

$$\left|D32\right| = \left[EI_y\left(\frac{\pi}{\ell}\right)^2 - P\right]\left[E\Gamma\left(\frac{\pi}{\ell}\right)^2 + GK - P\frac{I_p}{A}\right] = 0$$

it can be observed from the above equations that buckling will be either purely flexural or purely torsional and the critical load for a rolled steel column is, generally, given by (for Case a2-2.2)

either $\left[EI_y\left(\frac{\pi}{3\ell}\right)^2 - P + \frac{9Q}{\pi^2}\right]\left[EI_y\left(\frac{5\pi}{3\ell}\right)^2 - P + \frac{9Q}{25\pi^2}\right] - \left[\frac{9Q}{\pi^2}\right]\left[\frac{9Q}{25\pi^2}\right] = 0$

or $\left[EI_y\left(\frac{2\pi}{3\ell}\right)^2 - P + \frac{27Q}{4\pi^2}\right]\left[EI_y\left(\frac{4\pi}{3\ell}\right)^2 - P + \frac{27Q}{16\pi^2}\right] - \left[\frac{27Q}{4\pi^2}\right]\left[\frac{27Q}{16\pi^2}\right] = 0$

or $\left[EI_y\left(\frac{\pi}{\ell}\right)^2 - P\right] = 0$

whichever gives the smallest value of P.

When $Q = 0$, (Case a2-2.1) the critical load is given by

$$E I_y \left(\frac{\pi}{3\ell}\right)^2 - P \quad = 0$$

III-d Problem with Two Intermediate Girts, Cases a2-2.3 and a2-2.4

When $Q = 0$, Eqs. 3-55 through 3-57 give

$$\left|D12\right| = \left[\left[EI_y\left(\frac{\pi}{3\ell}\right)^2-P\right]\left\{\left[E\Gamma\left(\frac{\pi}{3\ell}\right)^2+GK-P\frac{I_p}{A}+\frac{9m\ell}{\pi^2}\right]+e^2\left[EI_y\left(\frac{\pi}{3\ell}\right)^2-P\right]\right\}-e^2\left[EI_y\left(\frac{\pi}{3\ell}\right)^2-P\right]^2\right]$$
$$\left[\left[EI_y\left(\frac{5\pi}{3\ell}\right)^2-P\right]\left\{\left[E\Gamma\left(\frac{5\pi}{3\ell}\right)^2+GK-P\frac{I_p}{A}+\frac{9m\ell}{25\pi^2}\right]+e^2\left[EI_y\left(\frac{5\pi}{3\ell}\right)^2-P\right]\right\}-e^2\left[EI_y\left(\frac{5\pi}{3\ell}\right)^2-P\right]^2\right]$$
$$-\left[EI_y\left(\frac{\pi}{3\ell}\right)^2-P\right]\left[EI_y\left(\frac{5\pi}{3\ell}\right)^2-P\right]\left[\frac{-9m\ell}{\pi^2}\right]\left[\frac{-9m\ell}{25\pi^2}\right] = 0$$

$$\left|D22\right| = \left[\left[EI_y\left(\frac{2\pi}{3\ell}\right)^2-P\right]\left\{\left[E\Gamma\left(\frac{4\pi}{3\ell}\right)^2+GK-P\frac{I_p}{A}+\frac{9m\ell}{4\pi^2}\right]+e^2\left[EI_y\left(\frac{2\pi}{3\ell}\right)^2-P\right]\right\}-e^2\left[EI_y\left(\frac{2\pi}{3\ell}\right)^2-P\right]^2\right]$$
$$\left[\left[EI_y\left(\frac{4\pi}{3\ell}\right)^2-P\right]\left\{\left[E\Gamma\left(\frac{4\pi}{3\ell}\right)^2+GK-P\frac{I_p}{A}+\frac{9m\ell}{16\pi^2}\right]+e^2\left[EI_y\left(\frac{4\pi}{3\ell}\right)^2-P\right]\right\}-e^2\left[EI_y\left(\frac{4\pi}{3\ell}\right)^2-P\right]^2\right]$$
$$-\left[EI_y\left(\frac{2\pi}{3\ell}\right)^2-P\right]\left[EI_y\left(\frac{4\pi}{3\ell}\right)^2-P\right]\left[\frac{-9m\ell}{4\pi^2}\right]\left[\frac{-9m\ell}{16\pi^2}\right] = 0$$

and

$$\left|D32\right| = \left[EI_y\left(\frac{\pi}{\ell}\right)^2-P\right]\left\{\left[E\Gamma\left(\frac{\pi}{\ell}\right)^2+GK-P\frac{I_p}{A}\right]+e^2\left[EI_y\left(\frac{\pi}{\ell}\right)^2-P\right]\right\}-e^2\left[EI_y\left(\frac{\pi}{\ell}\right)^2-P\right]^2 = 0$$

After simplification and rearranging the terms the above equations reduce to

$$\left|D12\right| = \left[EI_y\left(\frac{\pi}{3\ell}\right)^2-P\right]\left[EI_y\left(\frac{5\pi}{3\ell}\right)^2-P\right]\begin{Bmatrix}\left[E\Gamma\left(\frac{\pi}{3\ell}\right)^2+GK-P\frac{I_p}{A}+\frac{9m\ell}{\pi^2}\right]\\ \left[E\Gamma\left(\frac{5\pi}{3\ell}\right)^2+GK-P\frac{I_p}{A}+\frac{9m\ell}{25\pi^2}\right]\\ -\left[\frac{9m\ell}{\pi^2}\right]\left[\frac{9m\ell}{25\pi^2}\right]\end{Bmatrix} = 0$$

$$\left|D22\right| = \left[EI_y\left(\frac{2\pi}{3\ell}\right)^2 - P\right]\left[EI_y\left(\frac{4\pi}{3\ell}\right)^2 - P\right]\left\{\begin{array}{l}\left[E\Gamma\left(\frac{2\pi}{3\ell}\right)^2 + GK - P\frac{I_p}{A} + \frac{9m\ell}{4\pi^2}\right] \\ \left[E\Gamma\left(\frac{4\pi}{3\ell}\right)^2 + GK - P\frac{I_p}{A} + \frac{9m\ell}{16\pi^2}\right] \\ -\left[\frac{9m\ell}{4\pi^2}\right]\left[\frac{9m\ell}{16\pi^2}\right]\end{array}\right\} = 0$$

and

$$\left|D32\right| = \left[EI_y\left(\frac{\pi}{\ell}\right)^2 - P\right]\left\{\left[E\Gamma\left(\frac{\pi}{\ell}\right)^2 + GK - P\frac{I_p}{A}\right] + e^2\left[EI_y\left(\frac{\pi}{\ell}\right)^2 - P\right]\right\} - e^2\left[EI_y\left(\frac{\pi}{\ell}\right)^2 - P\right]^2 = 0$$

From the above equations, for $m \neq 0$ (Case a2-2.4) or $m = 0$ (Case a2-2.3) the critical load for a rolled steel column is, generally, given by

$$\left[EI_y\left(\frac{\pi}{3\ell}\right)^2 - P\right] = 0$$

Example 1. The 14 WF 30 columns in a building are 19'4" apart and 16' high. Three 6"x1-1/2"[14 gage intermediate girts spaced at 4' intervals brace the columns. The girts are braced by a diaphragm, whose shear characteristics are: Q_d = 413 kips (for the end column), and r_d = 1.103 x 10^{-2} (refer to page 29 for Q_d and r_d). It is desired to determine the load carrying capacity of an end column in the case of two types of girt-column connections shown in Fig. III-1. The ends of the column may be considered as flexurally hinged and torsionally simple (i.e. twist is zero and warping unrestrained). A36 steel is used for all the members. E = 29000 ksi. Refer to Fig. III-1 for a sketch of the problem.

Properties of 14 WF 30 Column Section and Other Constants:

$$\Gamma = 935 \text{ in}^6$$

$$K = 0.343 \text{ in}^4$$

$$\frac{I_p}{A} = 34.9 \text{ in}^2$$

$$E\Gamma\left(\frac{\pi}{\ell}\right)^2 = 116300 \text{ K-in}^{4r2}$$

$$GK = 3830 \text{ K-in}^2$$

Torsional Restraint m :

(a) Connection Type-I (refer to Fig. III-1)

Bending stiffness of the girt at the end column =

$$\frac{6 \times 29000 \times 3.10}{232} = 2325 \text{ K-in/rad}$$

In order to ascertain rigidity of the connection a model of the connection shown in Fig. III-1 is considered.

Assume 100 K-in moment on the connection due to the twist of the column. This means a twist of $\frac{100}{2325} = 0.043$ rad.

Force in 6"x1-1/2"[$= \frac{100}{8.86} = 11.28$K (Tension)

Force in 3"x3"x3/8 L $= (11.28)\sqrt{2} = 15.96$K (Compression)

Extension in [section $= \frac{11.28 \times 8.86}{0.65 \times 29000} = 0.0053"$

Compression in L section $= \frac{15.96 \times 12.52}{1.44 \times 29000} = 0.00478"$

Twist of I-section due to axial stresses in [and L sections $= \frac{(0.0053 + 0.00478/\sqrt{2})}{8.86} = 0.001093$ rad.

Note that 0.001093 rad. is negligible compared to the twist of 0.043 rad. of the column. Therefore, this type of connection is considered as fully rigid, and the twist restraint m on the

column is given by

$$m = 2325 \text{ K-in/rad}$$

(b) Connection Type-II (refer to Fig. III-1)

This type of connection, in general, is considered as fully flexible. Therefore, $m = 0$.

Flexural Buckling Load P_e^* :

Referring to page 73, P_e^* can be computed as

$$P_e^* = 305.5 \text{ kips}$$

Load Carrying of the Column with Connection Type-I:

Using Eq. 3-76, $Q'_{id,3} = 337$ kips

$$Q^2_{id,3} = 454 \text{ kips}$$

It can be seen from the above values of $Q^{i=1,2}_{id,3}$ that the critical load is not given by the modified first mode.

For $Q_d = 413$ kips and $m = 2325$, and using Eq. 3-73,

$$P^2_{cr,3} = 296.7 \text{ kips}$$

$$P^3_{cr,3} \cong P_e^* = 305.5 \text{ kips}$$

Therefore, the critical load is given by the modified second mode, and $P_{cr,3} = P^2_{cr,3} = 296.7$ kips.

The column deflects in the modified second mode because the buckling load of the ideal column is obtained from the modified second mode.

Initial Imperfections: $\begin{cases} E_{20} = \frac{1}{8} \times \frac{16/2}{10} = 0.1" \\ F_2 = 0.01 \end{cases}$

Therefore, $E_2 = 0.1 - 8 \times 0.01 = 0.02"$

Assume the load carrying capacity P = 245 kips.

Using Eq. 3-69, $C_2' = 0.044"$

Using Eq. 3-70, $D_2' = 0.004$

The failure of the column is checked at the critical locations (1) and (2) as shown in Fig. III-2.

Using Eq. 3-61 at (1), $f_a + f_b = 35.87 < 36.0$

Using Eq. 3-60 at (2), $\frac{f_a}{F_a} + \frac{f_b}{F_y} = 0.9852 < 1.0$

Diaphragm shear strain $\gamma_{max} = C_2' \times \frac{\pi}{2\ell} = 0.044 \frac{\pi}{96}$

$= 0.144 \times 10^{-2} < \gamma_d$

M_y^g of 6 [14 gage girt = $36 \times 1.03 = 37.1$ K-in

M_{cr}^g of 6 [14 gage girt of length $\frac{19'4"}{2}$ can be computed using the conventional theory of lateral buckling.

$$M_{cr}^g = 8.0 \text{ K-in}$$

Using Eq. 3-62, $M_c = M_{cr}^g = 8.0$ K-in.

Allowable slope of bending of the girt before it buckles =

$$\frac{8.0 \times 116}{2 \times 29000 \times 3.10} = 0.00515$$

Note that $D_2' < 0.00515$

It can be seen from the above computations that the column is very near to failure, and the diaphragm and the girts do not fail before the column does. Therefore, the load carrying capacity of the column will be taken as 245 kips.

Further, it was seen from the computations (not included

here) that increase of P beyond 245 kips would bring about the failure of the column at (1).

Load Carrying Capacity of the Column with Connection Type-II

Because $m = 0$, the column buckles in the modified first mode in this problem.

Using Eq. 3-76, for $P_1 = 180$ kips, $Q_1 = 139.2$ kips

Using Eq. 3-76, for $P_2 = 190$ kips, $Q_2 = 1181$ kips

Using Eq. 3-78, for $Q_d = 413$ kips, $P_{cr,3} = P'_{cr,3} = 182.6$ kips

Initial Imperfections: $\begin{cases} E_{10} = \frac{1}{8} \times \frac{16}{10} = 0.2" \\ F_1 = 0.01 \end{cases}$

Therefore, $E_1 = 0.2 - 8 \times 0.01 = 0.12"$

Assume $P = 125$ kips.

Using Eq. 3-69, $C'_1 = 0.0553"$

Using Eq. 3-70, $D'_1 = 0.0332$

The failure of the column is checked at the critical locations (1) and (2). Refer to Fig. III-3.

Using Eq. 3-61, at (1), $f_a + f_b = 26.52 < 36$

Using Eq. 3-60, at (2), $\frac{f_a}{F_a} + \frac{f_b}{F_y} = 1.001 > 1$

Diaphragm Shear Strain $\gamma_{max} = C'_1 \frac{\pi}{4\ell} = \frac{0.0553 \times \pi}{192}$

$= 0.089 \times 10^{-2} < \gamma_d$

Because $m = 0$, the girts are not loaded by the twist of the column. Therefore, there is no failure of the girts.

It is seen in the above computations that the column just fails at (2).

If P = 124 kips the column will not fail at (2). The computations for this case are not included here. Therefore, the load carrying capacity of the column = 124 kips.

Example 2. The 14 WF 30 columns in a building are 15'6" apart and 12' high. Two 6" x 1-1/2" [14 gage intermediate girts spaced at 4' intervals brace the columns. The girts are braced by a diaphragm whose shear characteristics are: Q_d = 413 kips (for the end column), and $r_d = 1.103 \times 10^{-2}$ (refer to page 29 for Q_d and r_d). It is desired to determine the load carrying capacity of an end column when the column-girt connection is connection type-I. The ends of the column may be considered as flexurally hinged and torsionally simple (i.e. twist is zero and warping is unrestrained). A36 steel is used for all the members. E = 29000 ksi. Refer to Fig. III-4.

Properties of 14 WF 30 column section and other constants are the same as given in Example 1.

Twist Restraint m : It was seen in Example 1 that the connection type-I can be considered as fully rigid.

Therefore, m (for an end column) = $\frac{6 \times 29000 \times 3.10}{186}$ =

2900 K-in/rad

From Example 1, $P_e^* = 305.5$ kips

Using Eq. 3-76, $Q'_{id,2} = 350$ kips $< Q_d$

$Q''_{id,2} = 404$ kips $< Q_d$

Therefore, buckling occurs in the third mode.

Load Carrying Capacity of the Column (Q = 413, m = 2900)

Initial Imperfections : $\begin{cases} E_1 = \frac{1}{8} \times \frac{12}{10} = 0.15" \\ E_3 = \frac{1}{8} \times \frac{4}{10} = 0.05" \end{cases}$

Assume $P = 230$ kips.

Using Eq. 3-71, $C_1'^* = 0.1018"$

Using Eq. 3-72, $C_3'^* = 0.00768"$

The failure of the column was checked at locations (1), (2), and (3) (refer to Fig. III-5). It was found that location (2) was more critical than location (3).

Using Eq. 3-61, at (1), $f_a + f_b = 35.75 < 36$

Using Eq. 3-60, at (2), $\frac{f_a}{F_a} + \frac{f_b}{F_y} = 0.9915 < 1.0$

Diaphragm Shear Strain $\gamma_{max} = C_1'^* \frac{\pi}{3\ell} + C_3'^* \frac{\pi}{\ell}$

$= 0.27 \times 10^{-2} < \gamma_d = 1.103 \times 10^{-2}$

There is no twist of the column because the column buckles in a pure flexural mode. Therefore, there is no failure of the girts.

It is seen from the above computations that the column is about to fail at (1). Therefore, the load carrying capacity of the column will be taken as 230 kips.

Further, if the load P is increased it will be seen that the column fails first at (1).

Load Carrying Capacity of the Column (Q = 826, m = 2900)

Assume $P = 245$ kips

Using Eq. 3-71, $C_1'^* = 0.0542"$

Using Eq. 3-72, $C_3'^* = 0.00962"$

Similar to the above case, when $Q = 413$, it was found that (1) and (2) (refer to Fig. III-5) are the critical locations for failure of the column.

Using Eq. 3-61, at (1), $f_a + f_b = 35.57 < 36$

Using Eq. 3-60, at (2), $\frac{f_a}{F_a} + \frac{f_b}{F_y} = 1.104 > 1$

Diaphragm Shear Strain $\gamma_{max} = C_1'^* \frac{\pi}{3\ell} + C_3'^* \frac{\pi}{\ell}$

$= 0.181 \times 10^{-2} < \gamma_d = 1.103 \times 10^{-2}$

There is no twist of the column because the column buckles in a pure flexural mode. Therefore, there is no failure of the girts.

It is seen from the above computations that the column fails first at location (2) if $P = 245$ kips. It was seen, by making a similar computation (not included here), that the column does not fail at $P = 240$ kips. Therefore the load carrying capacity of the colum will be taken as 240 kips.

APPENDIX IV

DETERMINATION OF MATERIAL PROPERTIES

IV-a Diaphragm Rigidity: Double-Beam Shear Tests

The distinguishing feature of the diaphragm bracing discussed in this report is that the increased buckling loads and load-deflection relationships are a function of the shear rigidity and the shear strength of the bracing, rather than the stiffness and strength of an elastic spring, or Winkler, support. The effective shear rigidity Q of the diaphragm has been defined as

$$Q = A G_{eff} \qquad \text{(IV-1)}$$

where A is the cross sectional area of the diaphragm (normal to the column or beam axis) contributing to the support of one member and G_{eff} is the effective shear modulus of the diaphragm for given width, thickness, corrugation form, and connector details. As indicated in the above definition the effective shear modulus appears to be a function of the width, thickness and the cross sectional shape of the diaphragm, as well as the type, number and location of the fasteners used in connecting the diaphragm to the edge members. In this investigation, double-beam shear tests as developed by Fisher and Pincus[6] and shown in Fig. IV-1 were used to determine G_{eff} and Q experimentally. The shear rigidity of a given diaphragm can be obtained from the double-beam shear tests using the following expression, also obtained from energy considerations:

$$Q = \frac{4M_o}{\pi\Delta} - \frac{\pi^2 E I_y}{L^2}$$

where M_o and Δ are the applied end moments and midspan deflection of the beams, respectively. G_{eff} is obtained from Eq. IV-1. Table 2 contains the pertinent results from tests of 30 gage plenum form cross-corrugated steel diaphragm material. The corrugations of the plenum material are 17/32" deep, with a pitch of 1-13/16" (measured values). The diaphragms were attached to the rolled shapes with 1/4-inch Pow-R-Set pins at the junction of the flange and web, in the valley of the sheet.

The 30 gage plenum material has a nominal thickness of 0.012". The measured thickness was 0.0129 and was used in the calculations. The strong influence of fastener spacing N and the diaphragm width w on the effective shear modulus may be noted from Table 2.

IV-b Diaphragm Rigidity: Simple Beam Shear Test

Several shear diaphragm tests have been conducted by Nilson[17] and Luttrell[14] to determine the shear stiffness and strength of light gage steel diaphragms. They were either simple beam shear tests or cantilever shear tests. Luttrell defined the shear stiffness G' as

$$G' = \frac{Pa}{\Delta b} \qquad \text{(IV-3)}$$

where

P is the 0.4 (ultimate shear load of the diaphragm)

Δ is the shear deflection of the diaphragm at 0.4 (ulti-

mate shear load) along the load direction. ($\Delta = \frac{1}{2}\{D_2 + D_3 - D_1 - D_4\}$, where D_1 , D_2 , D_3 , and D_4 are the deflections of the diaphragm in the directions indicated in Fig. IV-2)

a is the shear span of the diaphragm perpendicular to the load direction (refer to Fig. IV-2)

and b is the diaphragm length along the load direction (refer to Fig. IV-2).

Now the diaphragm rigidity[8] Q may be defined as

$$Q = G'W \qquad \text{(IV-4)}$$

where G' and W are respectively the shear stiffness and width of the diaphragm perpendicular to the member (beam or column) contributing to the support of one member.

Shear rigidity used in computations to evaluate the critical loads of columns braced by girts which in turn are braced by a diaphragm was obtained experimentally using a simple beam shear test as shown in Fig. IV-2. Table 2 shows pertinent results from the test of a 26 gage standard corrugated steel diaphragm. The diaphragm was attached to the rolled steel channels with #14 screws in every third valley of the sheets.

IV-c Diaphragm Shear Rigidity: Cantilever Shear Test

The end shear panels of a simple beam shear test are actually cantilevers. The middle panel does not carry any shear because of the symmetry of loading. Therefore, the shear rigidity Q of a diaphragm can also be obtained by testing a single can-

tilever panel. The plan of an inverted 26 gage Armco Econorib shear panel in a cantilever shear test is shown schematically in Fig. IV-3. The frame members were connected in such a way that the frame offers no restraint to in-plane shear loads before it is connected to the diaphragm. The diaphragm is connected by #14 screws to the frame as shown in Fig. IV-3. Neglecting any minor bending effects of the frame the shear deflection is given by

$$\Delta = D_3 - \left\{ D_1 + \frac{a}{b} (D_2 + D_4) \right\} \qquad \text{(IV-5)}$$

where D_1, D_2, D_3, and D_4 are the deflections of the diaphragm at the locations 1, 2, 3, and 4 and in the directions indicated in the Fig. IV-3.

Shear rigidity Q of the diaphragm can be computed using Eqs. IV-3 through IV-5. The details and results of the cantilever shear test on an inverted 26 gage Armco Econorib diaphragm is described in Table 2 and the value of the shear rigidity obtained in the test was used in the analysis of a four-beam test described in Section 2.4.

IV-d Residual Stress Measurements

Residual stress measurements were made by Errera[8] on the 8Jr6.5 sections used in the column test program and 10B17 sections used in the beam test program. Both shapes were ASTM A-441 low alloy high strength steel. The method of sectioning[18] was used to determine the residual stresses; readings were measured with a 10-inch Wittemore gage.

Residual stress measurements made on the 8Jr6.5 sections

gave consistent and smooth residual stress patterns, as indicated in Figs. IV-4 and IV-5. The stresses are shown in two parts, those that were observed when the 11" section was freed from a longer length, and the total measured residual stresses upon final sectioning of the member into strips. It will be noted that the flanges of the 8Jr6.5 sections are in residual tension, and the webs are mostly in residual compression, with a maximum measured value of 20 Ksi tension in the flanges, and 20 Ksi compression in the webs. This is in contrast to most rolled shapes which usually have some residual compressive stresses in the flanges, particularly in the flange tips[19].

The residual stresses measured in the 10B17 sections are shown in Figs. IV-6 and IV-7. It will be noted that some parts of the flanges are in residual tension, and the webs are mostly in residual compression, with maximum measured values of 8.5 Ksi tension in the flanges, and 8 Ksi compression in the webs.

IV-e Stub Column Tests

Stub column tests were made by Errera[8] on the 8Jr6.5 sections. The dimensions of the 8Jr6.5 sections are such that the recommendations for stub column tests[20] regarding requirements to avoid local buckling and end effects cannot be satisfied simultaneously. If this shape is tested in the usual manner premature buckling of the slender web occurs. To avoid this, an arrangement as shown in Fig. IV-8 was used. The test section, with waterproofed resistance strain gages in place, was well greased and placed within a steel tube formed by welding two channels toe to toe. Hydrostone, often used as a cap-

ping material for concrete test cylinders, was poured between the test piece and steel channels, and allowed to harden. The test piece protruded from the steel tube 1/4 inch at each end. A similar arrangement, developed at Cornell, is often used for compression tests of light gage steel sections when the basic compressive properties of the material, rather than the buckling properties of the section, are under investigation. Typical results of stub column tests of 8Jr6.5 sections without and with hydrostone encasement are shown in Figs. IV-8 and IV-9. An elastic limit of about 45 Ksi is indicated for the section with hydrostone encasement.

IV-f Tension Coupon Tests

Tension coupon tests were made on 10B17 section by Errera, and on the 6[8.2 section by the author as part of the present investigation. The results, together with the mill reports and chemical analysis, are given in Tables 1 and 5. The 10 inch and 6 inch shapes showed average yield points of 64.8 Ksi and 57.2 Ksi, respectively.

BIBLIOGRAPHY

1. Timoshenko, S., Theory of Elastic Stability. McGraw-Hill, New York, 1936.

2. Bleich, F., Buckling of Metal Structures. McGraw-Hill, New York, 1952.

3. Green, G. G., "Lateral Buckling of Elastically Braced Columns", Ph.D. Dissertation. Cornell University, 1948.

4. Winter, George, "Lateral Buckling of Columns and Beams", Transactions ASCE, Vol. 125, 1960.

5. Larson, M. A., Discussion of "Lateral Buckling of Columns and Beams", Transactions ASCE, Vol. 125, 1960.

6. Pincus, G., and Fisher, G. P., "Behavior of Diaphragm-Braced Columns and Beams", Proceedings ASCE, Vol. 92, ST2, April, 1966.

7. Pincus, G., "The Performance of Columns and Beams Continuously Braced with Diaphragms", Ph.D. Dissertation, Cornell University, 1963.

8. Errera, S. J., "The Performance of Beams and Columns Continuously Braced with Diaphragms", Ph.D. Dissertation, Cornell University, 1965. (Same as Report No. 321, Department of Structural Engineering, Cornell University, Ithaca, New York, October, 1965).

9. Fisher, G. P., and Pincus, G., "The Performance of Beams and Columns Continuously-Braced with Diaphragms", Report No. 313, Department of Structural Engineering, Cornell University, September, 1963.

10. Dooley, J. F., "On the Torsional Buckling of Columns of I-Section Restrained at Finite Intervals", International Journal of Mechanical Sciences, Vol. 9, No. 1. Jan., 1967.

11. Hill, H. N., "Lateral Buckling of Channels and Z-Beams", Transactions ASCE, 118, 337, 1953.

12. Massey, C., "Elastic and Inelastic Lateral Instability of I-Beams", The Engineer, October, 1963.

13. Chajes, A., Fang, P. J., and Winter, G., "Torsional Flexural Buckling, Elastic and Inelastic, of Cold Formed Thin Walled Columns", Cornell Engineering Research Bulletin, 66-1, Ithaca, New York, August, 1966.

14. Luttrell, L. D., "Structural Performance of Light Gage Steel Diaphragms", Ph.D. Dissertation, Cornell University, 1965. (Same as Report No. 319, Department of Structural Engineering, Cornell University, Ithaca, New York, August, 1965.)

15. Apparao, T.V.S.R., "Tests on Light Gage Steel Diaphragms", Report No. 328, Department of Structural Engineering, Cornell University, Ithaca, New York, December, 1966.

16. Manual of Steel Construction, AISC, Sixth Edition, 1966.

17. Nilson, A. H., "Diaphragm Action in Light Gage Steel Construction", Presented at Regional Technical Meeting of American Iron and Steel Institute, October 13, 1960.

18. Huber, A., and Beedle, L. S., "Residual Stress and Compressive Strength of Steel", Welding Journal Research Supplement, December, 1954.

19. Beedle, L. S., and Tall, L., "Basic Column Strength", ASCE Proceedings, Vol. 86, ST7, July, 1960.

20. Tall, L., "Stub Column Test Procedure", Fritz Laboratory Report No. 220 A.36, Lehigh University, February, 1961.

21. Errera, S. J., "The Performance of Beams and Columns Continuously Braced with Diaphragms", Report No. 316, Department of Structural Engineering, Cornell University, Ithaca, New York, August, 1964.

22. Errera, S. J., Pincus, G., and Fisher, G. P., "Columns and Beams Braced by Diaphragms", Proceedings ASCE, Vol. 93, ST1, February, 1967.

23. Goodier, J. N., "Torsional and Flexural Buckling of Bars of Thin Walled Open Section Under Compressive and Bending Loads", Journal of Applied Mechanics, September, 1942.

24. Winter, G., "Strength of Slender Beams", Transactions ASCE, Vol. 109, 1944.

25. Green, G. G., Winter, G., and Cuykendall, T. R., "Light Gage Steel Columns in Wall Braced Panels", Cornell University Engineering Experimental Station Bulletin, No. 35/2, 1947.

26. Zuk, W., "Lateral Support Forces on Beams and Columns", Ph.D. Thesis, Cornell University, Ithaca, New York, 1955.

27. Zuk, W., "Lateral Bracing Forces on Beams and Columns", Proceedings ASCE, EM3, Paper 1032, July, 1956.

28. Flint, A. R., "The Influence of Restraints on the Stability of Beams", Structural Engineer, 29, 235, England, September, 1951.

29. Flint, A. R., "The Stability and Strength of Slender Beams", Engineering, 170, 545, England, 1950.

30. Schmidt, L. C., "Restraints against Elastic Lateral Buckling", Proceedings ASCE, EM6, December, 1965.

31. Lee, G. C., "A Survey of Literature on the Lateral Instability of Beams", Welding Research Council Bulletin No. 63, August, 1960.

32. Taylor, A. C., and Ojalvo, M., "Torsional Restraint of Lateral Buckling", Proceedings ASCE, Vol. 92, ST2, April, 1966.

33. Beedle, L. S., et al, "Structural Steel Design", The Ronald Press Company, New York, N.Y., 1964.

Table 1 10B17 Tension Coupon Test Results and Mill Report

Tension Coupon Test Results

Beam	Coupon	Yield Point (ksi)	Tensile Strength (ksi)
a	1	61.4	82.8
	2	69.1	87.5
	3	64.9	84.5
	4	61.6	82.1
g	1	64.0	83.3
	2	67.9	87.3
	3	66.8	84.5
	4	64.8	81.5
Average		64.8	84.2
Mill Report		67.35	90.23

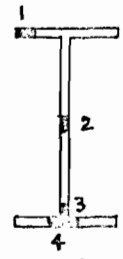

Location of Coupons

Chemical Analysis

C	Mn	P	S	Si	Cu	V
0.20	1.22	0.010	0.035	0.092	0.25	0.077

Table 2 Summary of Shear Tests

Double-Beam Shear Tests

Material	Width (in.)	Area (in^2)	Connector Spacing, N	Shear Rigidity, Q (kips)	Effective Shear Modulus, G_{eff} (ksi)
30 g. Plenum Galv.Steel	28	0.361	4	62.7	173.6
"	"	"	2	181.2	502.0
"	"	"	6	27.5	76.2*
"	$17\frac{3}{4}$	0.229	4	27.7	120.8
"	"	"	2	60.2	263.0

Simple Beam and Cantilever Shear Tests

Material	Size of Shear Panel (length x width)	Type of Connection	Shear Stiffness G' (lbs/in)	Ultimate Load (lbs)	Strength (plf)
		Simple Beam Shear Test			
26 g. Standard Corrugated Galvanized Steel	4' x 6'	#14 screws at every third valley	6000	2740	457
		Cantilever Shear Test			
26 gage Armco Econo Rib Panels (inverted)	12'x10'	#14 screws at every 8"	6320	2980	248

* Extrapolated from the other two tests having the same width.

Table 3 Description of 10B17 Double-Beam Flexure Test Specimens

Beam Section: 10B17, A441 Steel, d = 10.12", A_f = 1.318 in.^{2}, $\frac{d}{A_f}$ = 7.67.

Diaphragm Material: 30 gage Granco Plenum Cross-Corrugated Steel.

Test No.	Test Length, L (in)	Ld/nA_f*	Diaphragm Width (in)	Connector Spacing, N	Q (kips)
1	360	1381	None		0
2	"	"	28	6	13.8
3	"	"	None		0
4	"	"	28	4	31.4
5	"	"	None		0
6	"	"	28	2	90.6
7	"	"	None		0
8	"	"	28	4	31.4

* Beams were "fixed" against lateral buckling, hence n = 2 was used to obtain Ld/nA_f ratios shown.

Table 4 Summary of 10B17 Double-Beam Flexure Tests, Predicted Critical Moments and Actual Failure Loads

Beam Section: 10B17, A441 Steel

Diaphragm Material: 30 gage Granco Plenum Cross-Corrugated Steel

Test No.	Test Length, L (in)	Ld/nA_f	Q (kips)	Predicted M_{cr} (1) (in-kips)	Max.Test Load (in-kips)	Test/Pred.
1	360	1381	0	266(2)	240 (246*)	0.90(2)
2	"	"	13.8	414	498	1.20
3	"	"	0	266(2)	233	0.88(2)
4	"	"	31.4	598	570	0.95
5	"	"	0	266(2)	252	0.95(2)
6	"	"	90.6	1056	1019	0.97
7	"	"	0	266(2)	257	0.97(2)
8	"	"	31.4	598.1	740	1.24

(1) $$M_{cr} = \sqrt{\left\{E_{ry} I_y \left(\frac{2\pi}{L}\right)^2 + Q\right\}\left\{E_{ry}\Gamma\left(\frac{2\pi}{L}\right)^2 + G_r K + Qe^2\right\}} + Qe \leq M_{p\ell}$$

(2) Tests of unbraced beams were arbitrarily stopped to avoid beam damage and permit use of same beams with diaphragm bracing.

* Critical Moment obtained from Southwell Plot.

Table 5 6 [8.2 Tension Coupon Test Results and Mill Report

Tension Coupon Test Results

Beam	Coupon	Yield Point (ksi)	Tensile Strength (ksi)
a	1	54.8	77.5
	2	61.2	82.1
	3	60.5	81.0
	4	55.7	79.8
d	1	55.6	78.4
	2	54.1	75.0
	3	59.0	75.8
	4	56.5	77.6
Average		57.2	78.4
Mill Report		59.43	81.64

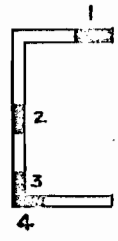

Location of Coupons

Chemical Analysis

C	Mn	P	S	Si	Cu	V
0.20	1.12	0.013	0.025	0.066	0.22	0.059

Table 6 Description of 6 [8.2 Double-Beam Flexure Test Specimens

Beam Section: 6 [8.2, A441 Steel, d = 6.00", A_f = 0.658 in^2, $\frac{d}{A_f}$ = 9.11

Diaphragm Material: 30 gage Granco Plenum Cross-Corrugated Steel

Test No.	Test Length, L (in)	Ld/nA_f*	Diaphragm Width (in)	Connector Spacing N	Q (kips)
		Connectors: Power Driven Pins			
1	288	1311	None		0
2	"	"	$17\frac{3}{4}$	4	13.9
3	"	"	None		0
4	"	"	$17\frac{3}{4}$	2	30.1
		Connectors: #14 Screws			
5	288	1311	None		0
6	"	"	$17\frac{3}{4}$	2	30.1

* Beams were "fixed" against lateral buckling, hence n = 2 was used to obtain Ld/nA_f ratios shown.

Table 7 Summary of 6 [8.2 Double-Beam Flexure Tests, Predicted Critical Moments and Actual Failure Loads

Beam Section: 6 [8.2, A441 Steel

Diaphragm Material: 30 gage Granco Plenum Cross-Corrugated Steel

Test No.	Test Length, L (in)	Ld/nA_f	Q (kips)	Predicted M_{cr} (1) (in-kips)	Max. Test Load (in-kips)	Test/Pred.
			Connectors: Power Driven Pins			
1	288	1311	0	89	66(2)	0.74(2)
2	"	"	13.9	190.8	143	0.75
3	"	"	0	89	66(2) (81.7*)	0.74(2)
4	"	"	30.1	253.1	227	0.90
			Connectors: #14 Screws			
5	"	"	0	89	72(2)	0.81(2)
6	"	"	30.1	253.1	252	0.996

(1) $$M_{cr} = \sqrt{\left\{E_{ry} I_y \left(\frac{2\pi}{L}\right)^2 + Q\right\}\left\{E_{ry}\Gamma \left(\frac{2\pi}{L}\right)^2 + G_r K + Qe^2\right\}} + Qe \leq M_{p\ell}$$

(2) Tests of unbraced beams were arbitrarily stopped to avoid beam damage and permit use of same beams with diaphragm bracing.

* Critical Moment obtained from Southwell Plot.

Table 8 Description of Test Specimens and Summary of Test Results of Columns Braced by Girts which in Turn are Braced by a Diaphragm

Column Section: 8JR6.5, A441 Steel

Diaphragm Material: 26 gage Standard Corrugated Galvanized Steel

Girt Section: 6 [13 for GT-1 and GT-3; and 6 [2.26 (14 ga.) for GT-2

Connection of Diaphragm to Girts: #14 Screws at every third valley

Width of Diaphragm (for two members) : 6'

Diaphragm Rigidity Q: Q = 216 kips

Column End Conditions: Flexurally hinged, warping restrained, twist is zero.

Total Length of Column L: L = 12' - 7"

Number of Intermediate Girts: 2

Ave. Unbraced Length of Column: 4' - 2 1/3"

Test	Twist Restraint, m(kip-in/rad.)	Failure Mode	Distance, e (in)	Predicted Critical Load (kips)	Max. Test Load (kips)	Test/Pred.
GT-1	0	Modified First Mode (Tor-Flex)	6	21.4	17.7	0.84
GT-2	7750	Third Mode (Flexural)	10	39.9	37.3	0.94
GT-3	13	Modified First Mode (Tor-Flex)	6	29.6	25.5	0.86

Table 9 Description and Summary of Test Results of a Diaphragm-Braced four-Beam Assembly

Beam: 8JR6.5 I-section; A441 Steel

Diaphragm: 26 gage Econorib Panels, Inverted

Connectors: #14 Screws at every 8"

Spacing of Beams: 3' - 8"

Test No.	Test Length, L (in)	Ld/nA_f	Shear Rigidity Q (kips)	Predicted M_{cr} (1) (in-kips)	Max. Test Load (in.-kips)	Test/Pred.
1	240	2232	0	47.7 (2)	35.8	0.75 (2)
2	240	2232	212.0	290	259.8	0.90

(1) $$M_{cr} = \sqrt{\left\{E_{ry}I_y\left(\frac{2\pi}{L}\right)^2 + Q\right\}\left\{E_{ry}\Gamma\left(\frac{2\pi}{L}\right)^2 + G_rK + Qe^2\right\}} + Qe \leq M_{p\ell}$$

(2) Test of unbraced beams was arbitrarily stopped to avoid beam damage and permit use of same beams with diaphragm bracing.

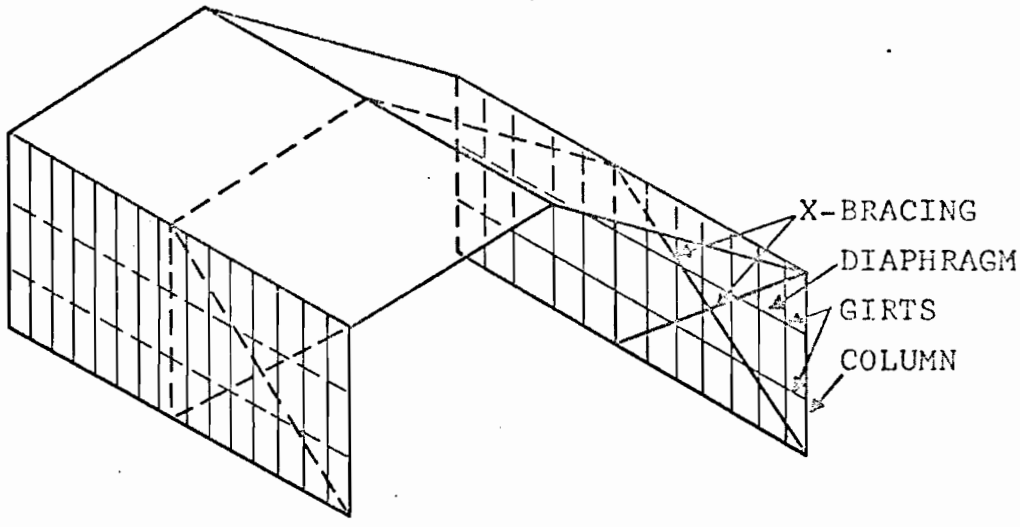

FIG. 1-1 BUILDING WITH X-BRACING

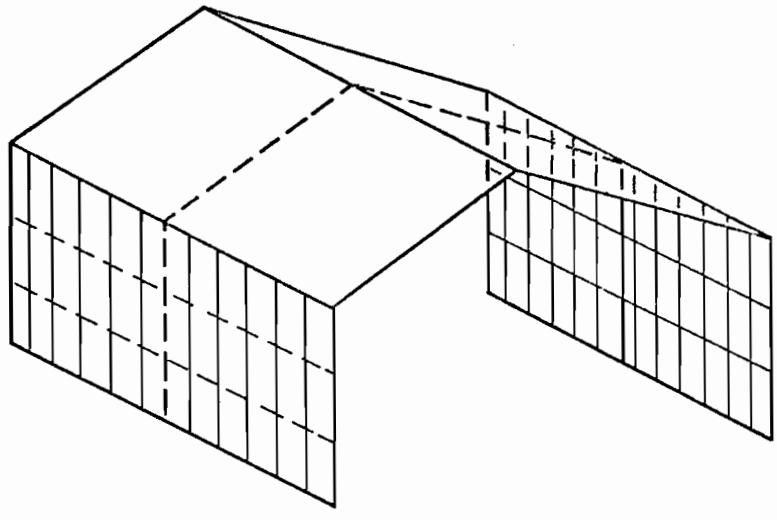

FIG. 1-2 BUILDING WITHOUT X-BRACING

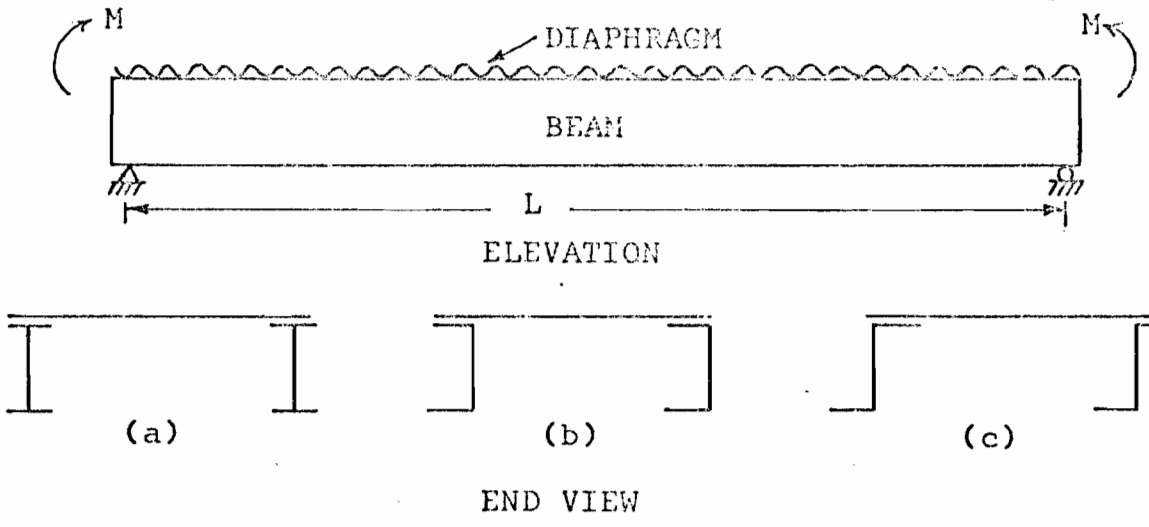

FIG. 2-1 MODELS OF DIAPHRAGM-BRACED BEAM ASSEMBLIES

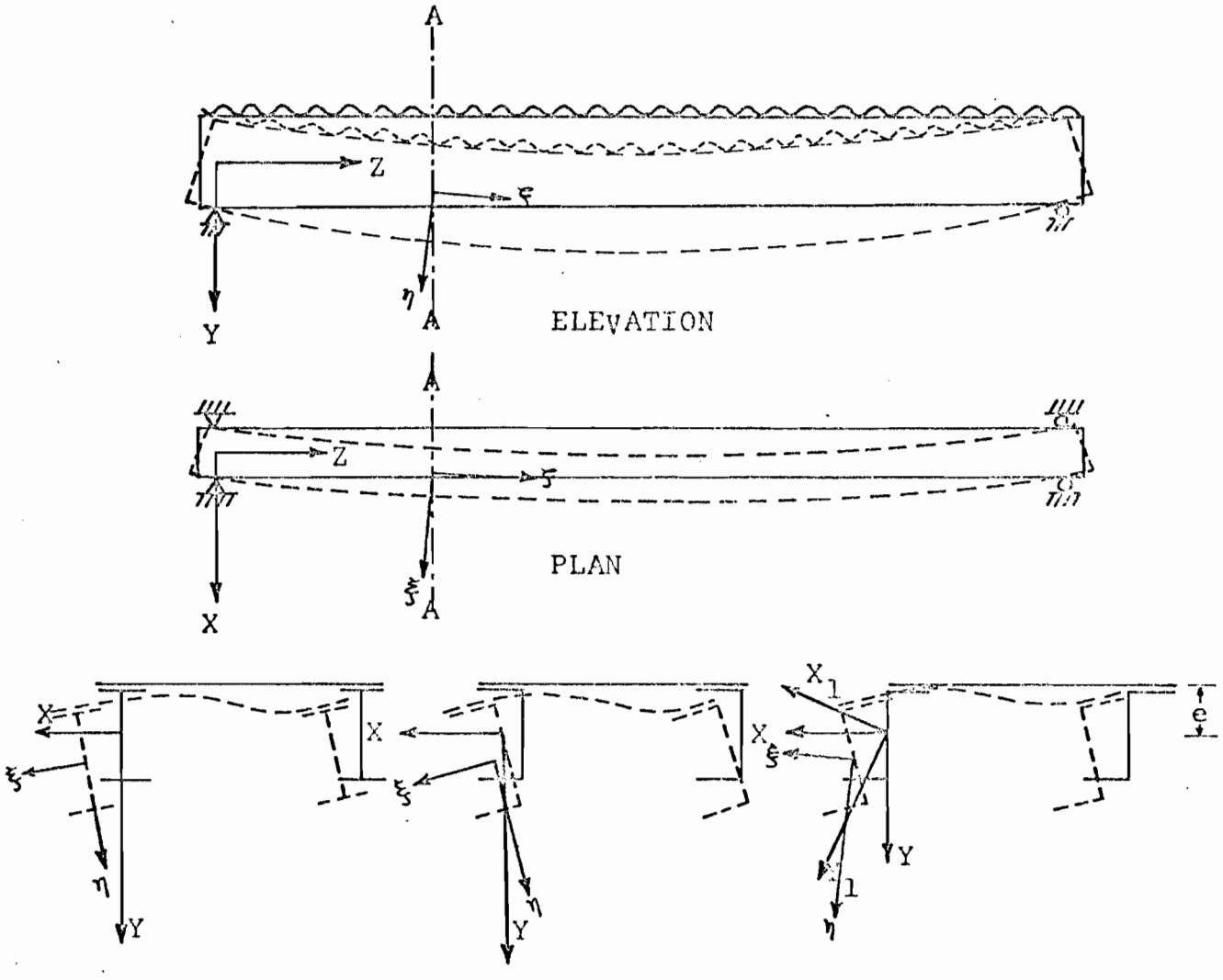

FIG. 2-2 COORDINATE AXES OF DIAPHRAGM-BRACED DOUBLE-BEAM ASSEMBLIES

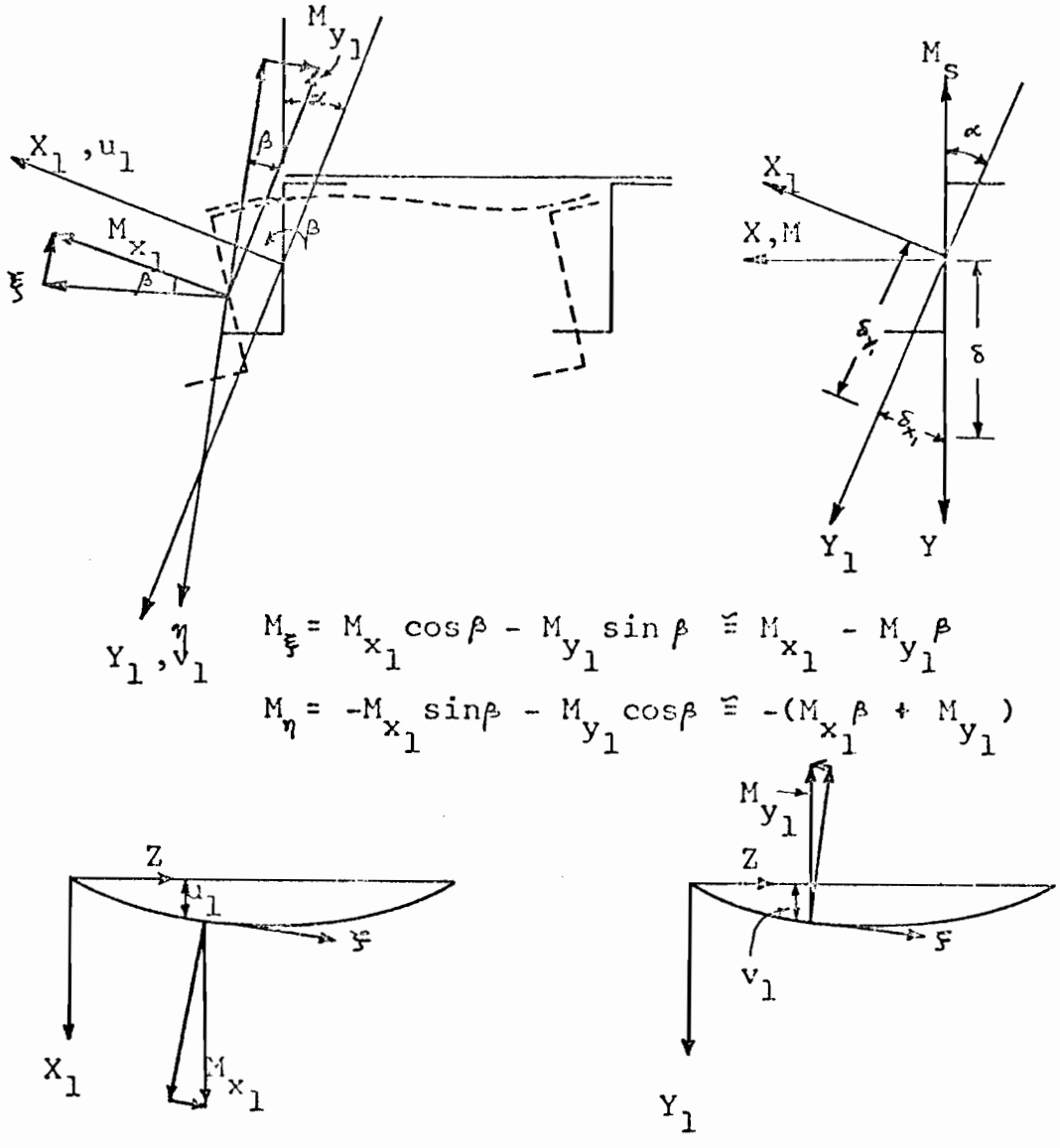

FIG. 2-3 DEFLECTIONS AND MOMENT COMPONENTS FOR A DIAPHRAGM-BRACED BEAM

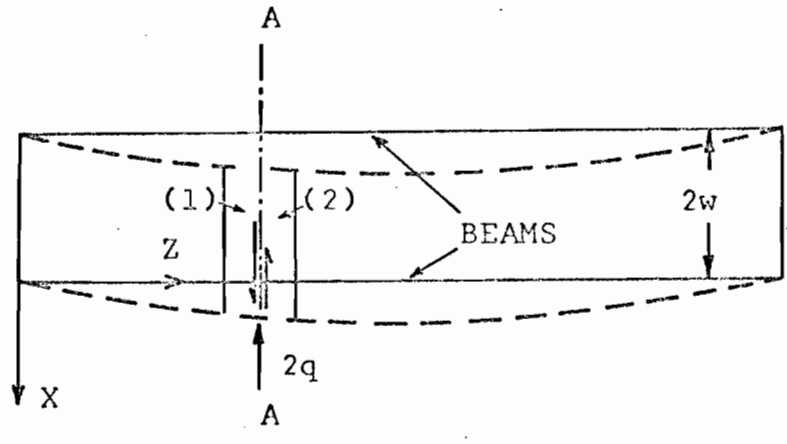

SHEAR PERPENDICULAR TO BEAMS

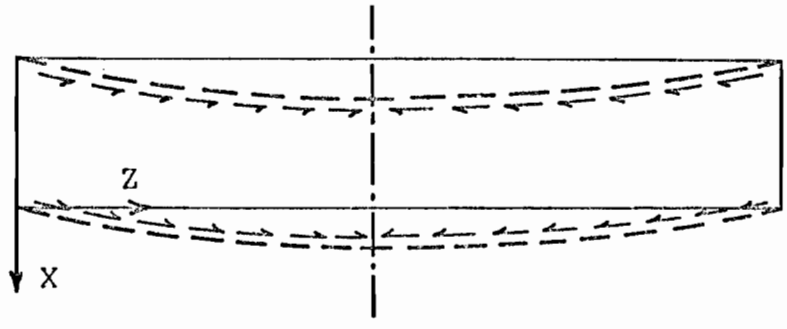

LONGITUDINAL SHEAR ON BEAMS

FIG. 2-4 SHEAR ON DIAPHRAGM-BRACED BEAMS

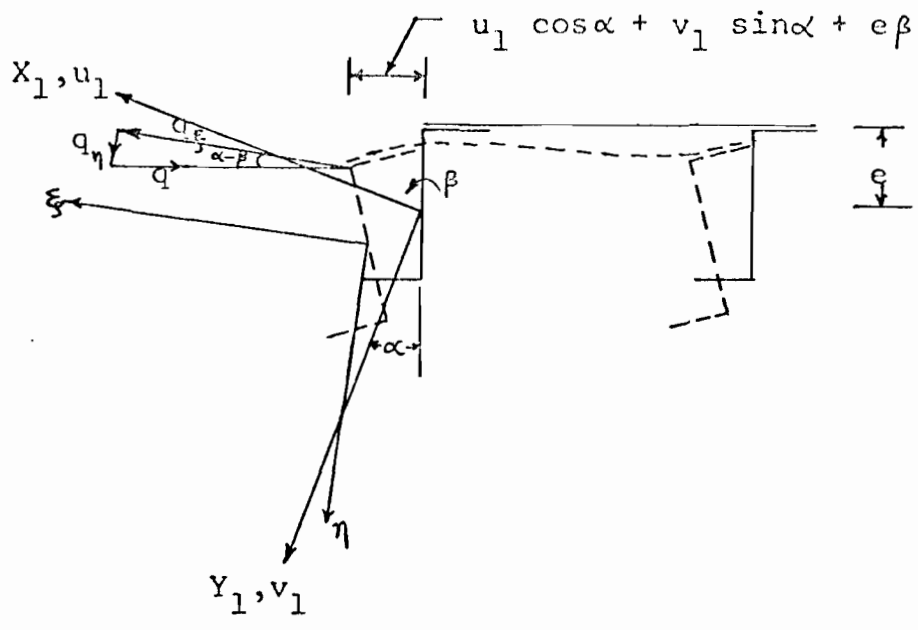

FIG. 2-5 DEFLECTIONS AND FORCE COMPONENTS FOR A DIAPHRAGM-BRACED BEAM

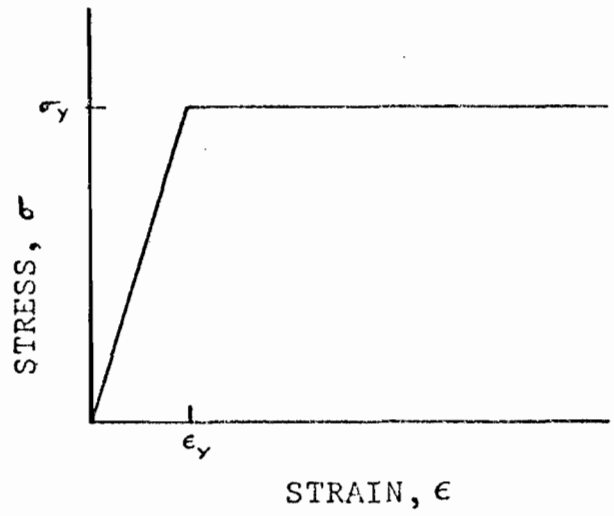

FIG. 2-6 BILINEAR STRESS-STRAIN DIAGRAM

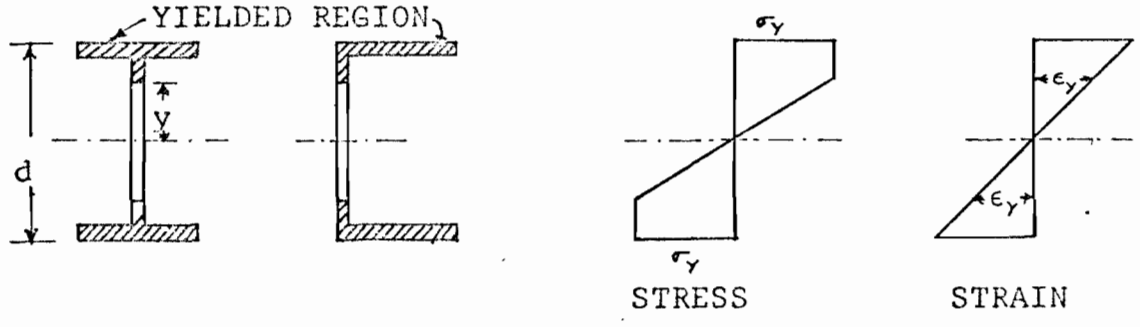

FIG. 2-7 DISTRIBUTION OF STRESS AND STRAIN FOR PARTIALLY YIELDED CROSS SECTIONS

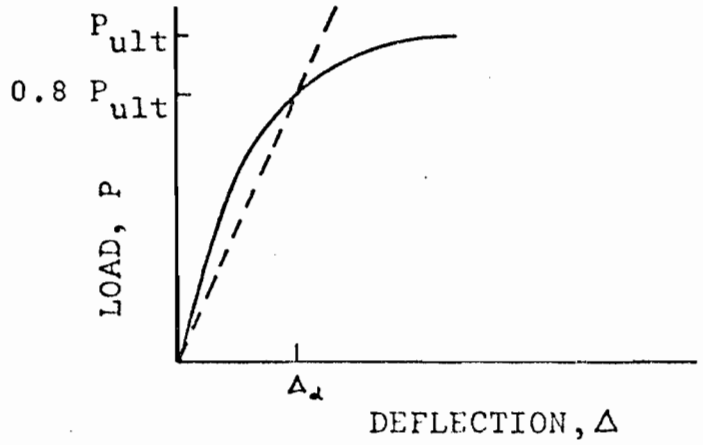

FIG. 2-8 LOAD-DEFLECTION DIAGRAM FOR A SHEAR DIAPHRAGM

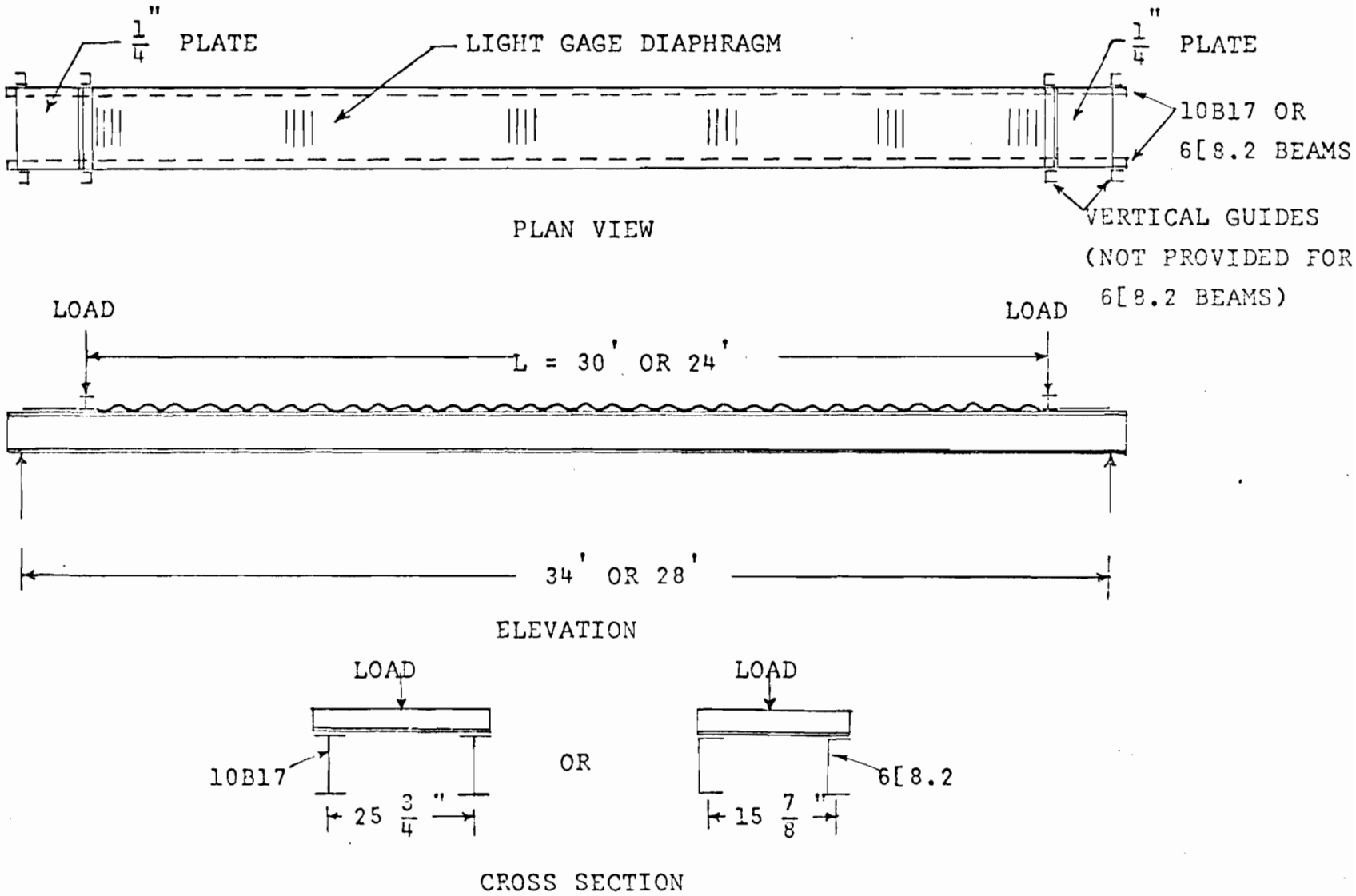

FIG. 2-9 ARRANGEMENT FOR DOUBLE-BEAM FLEXURE TESTS

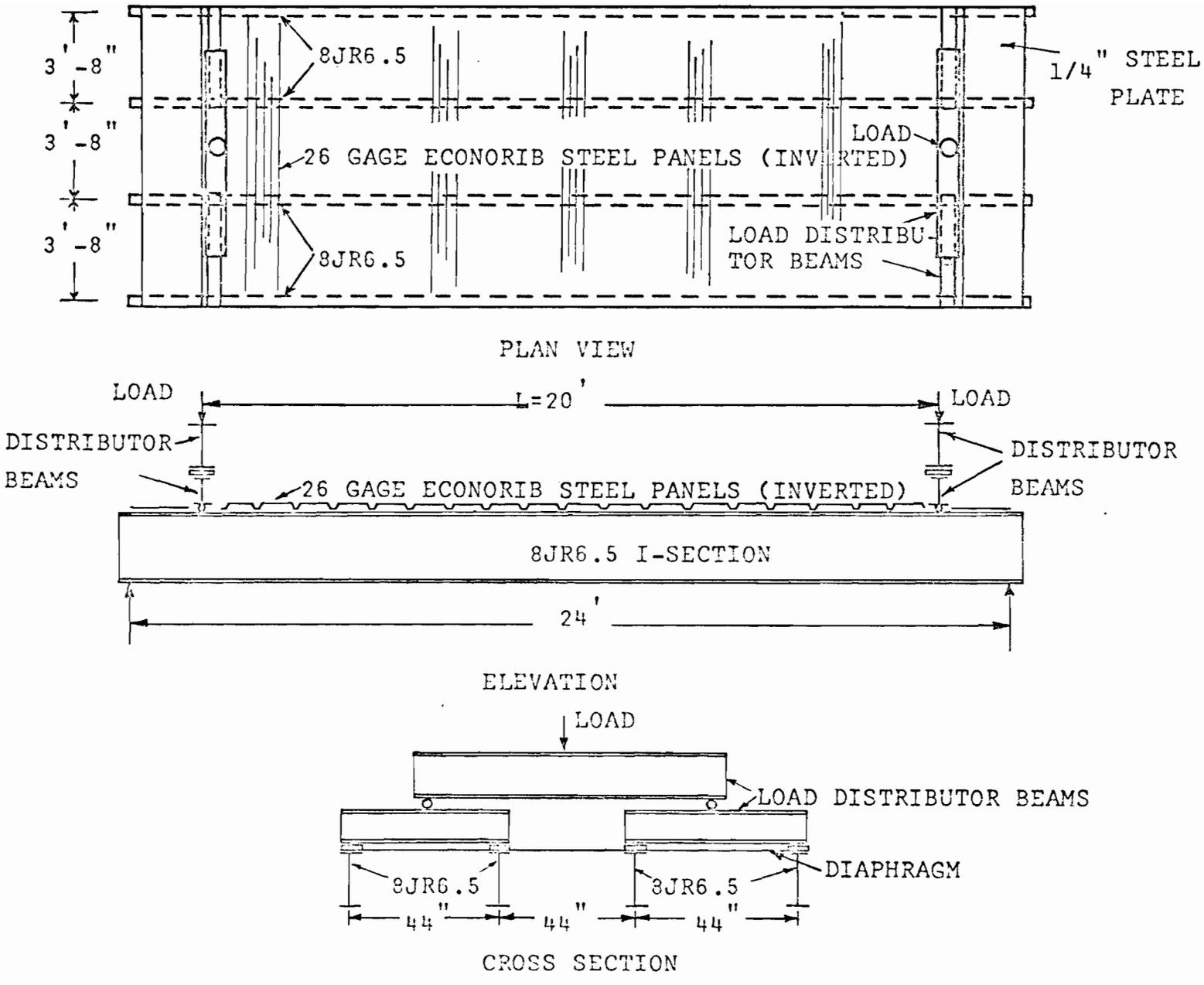

FIG. 2-10 ARRANGEMENT FOR DIAPHRAGM-BRACED FOUR-BEAM FLEXURE TEST

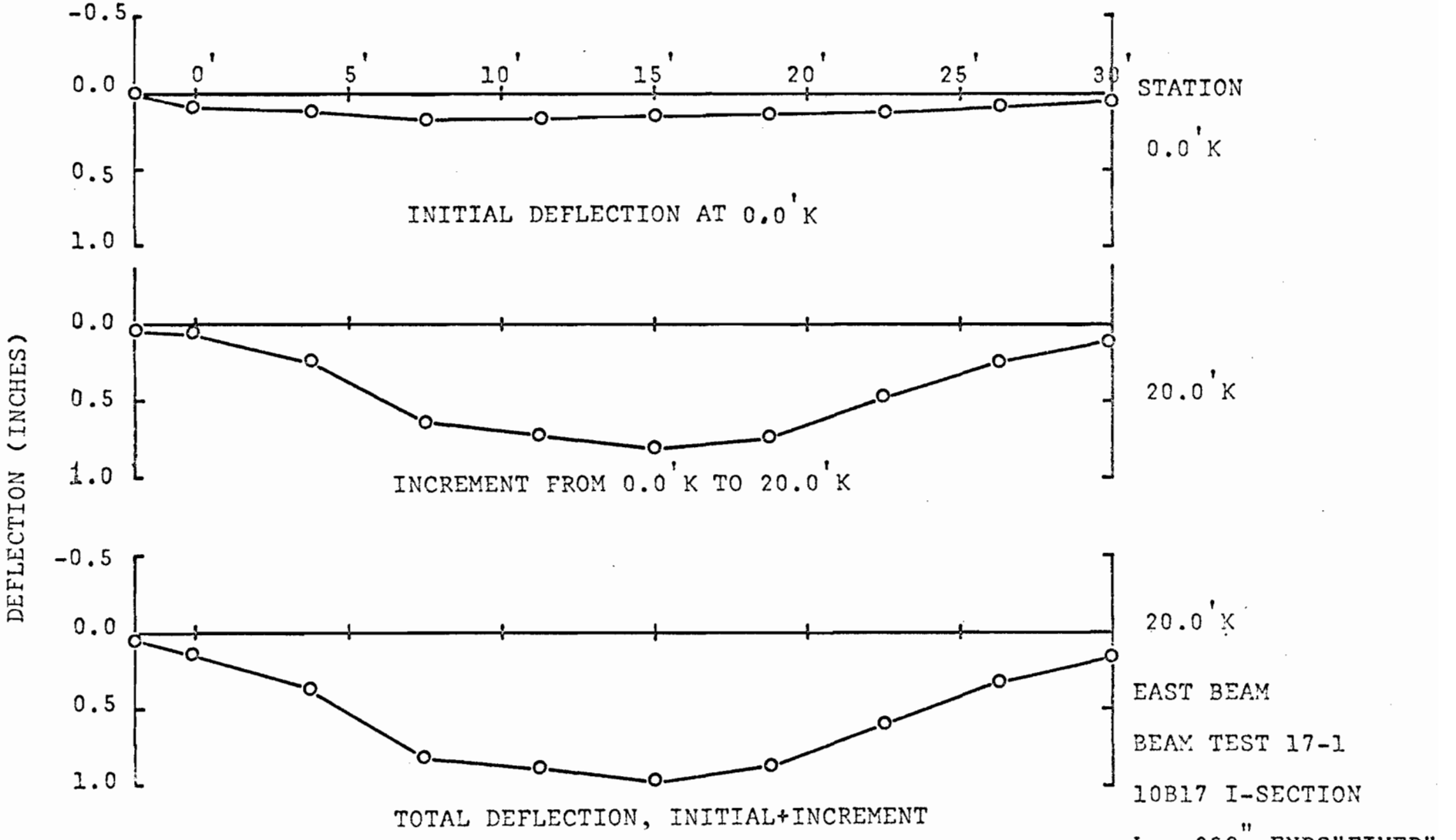

FIG. 2-11 LATERAL DEFLECTIONS OF CENTROIDAL AXIS OF AN UNBRACED 10B17 I-BEAM

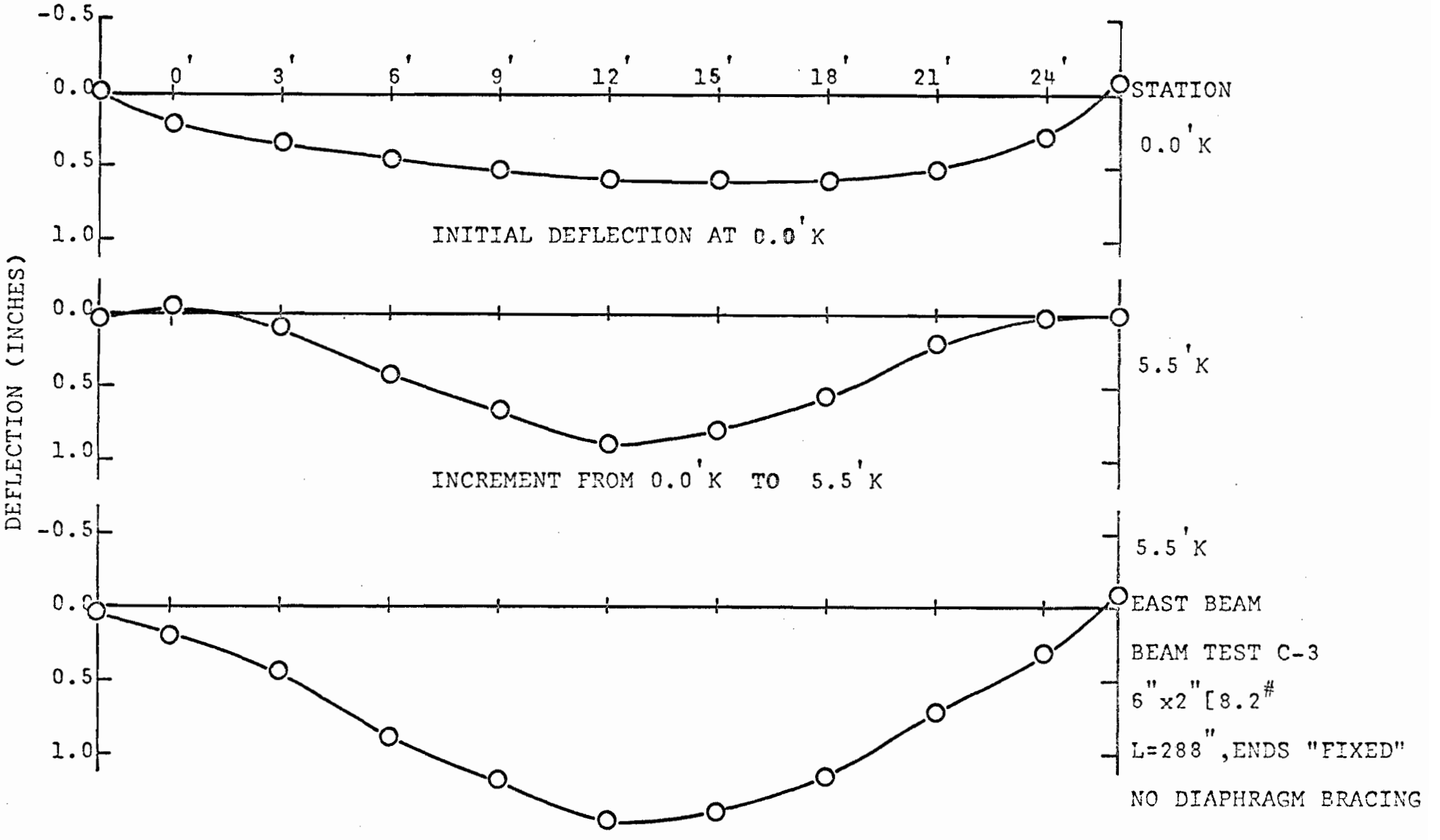

FIG. 2-12 LATERAL DEFLECTIONS OF CENTROIDAL AXIS OF AN UNBRACED 6[8.2 BEAM

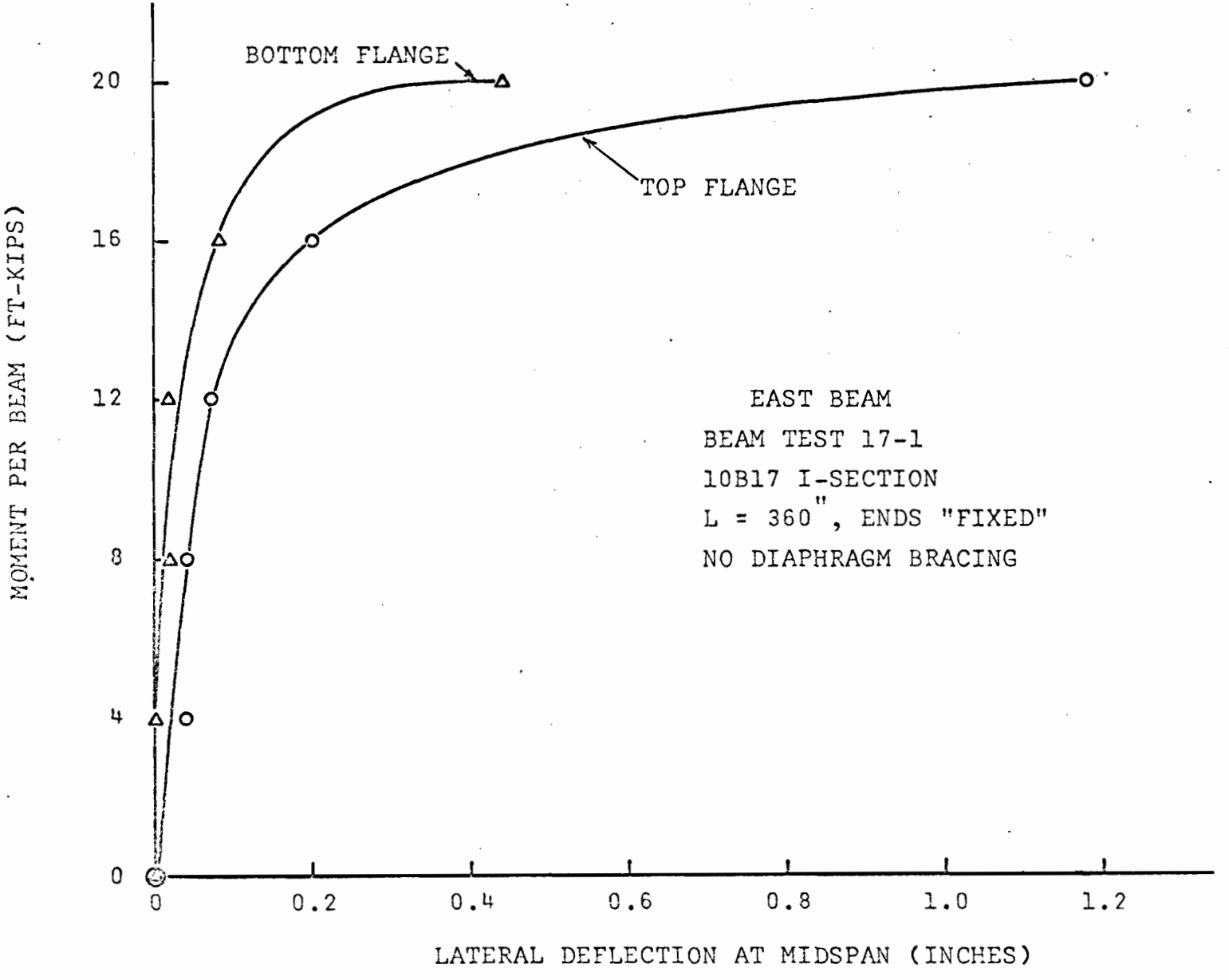

FIG. 2-13 LATERAL DEFLECTION VERSUS MOMENT FOR AN UNBRACED 10B17 I-BEAM

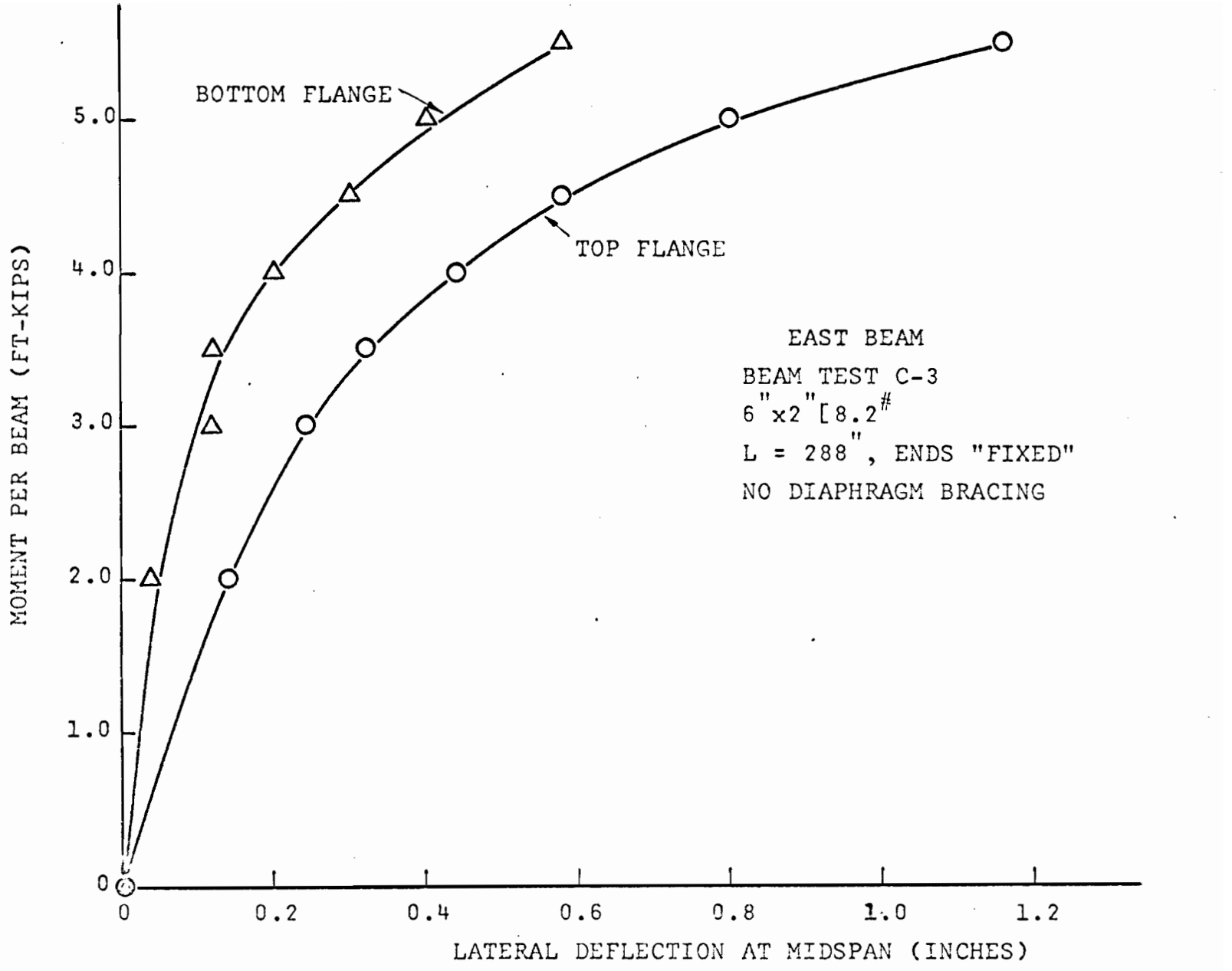

FIG. 2-14 LATERAL DEFLECTION VERSUS MOMENT FOR AN UNBRACED 6[8.2 BEAM

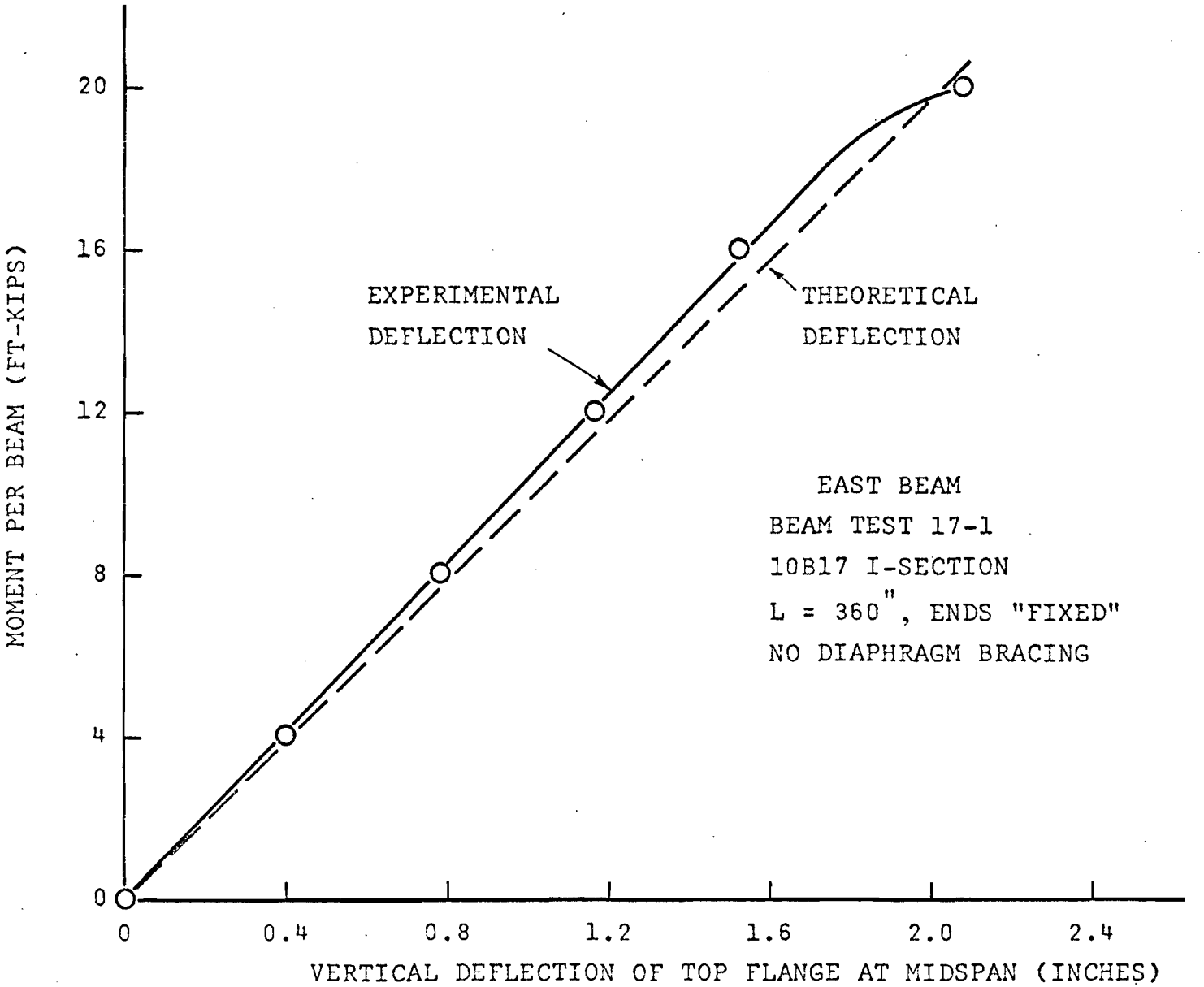

FIG. 2-15 VERTICAL DEFLECTION VERSUS MOMENT FOR AN UNBRACED 10B17 I-BEAM

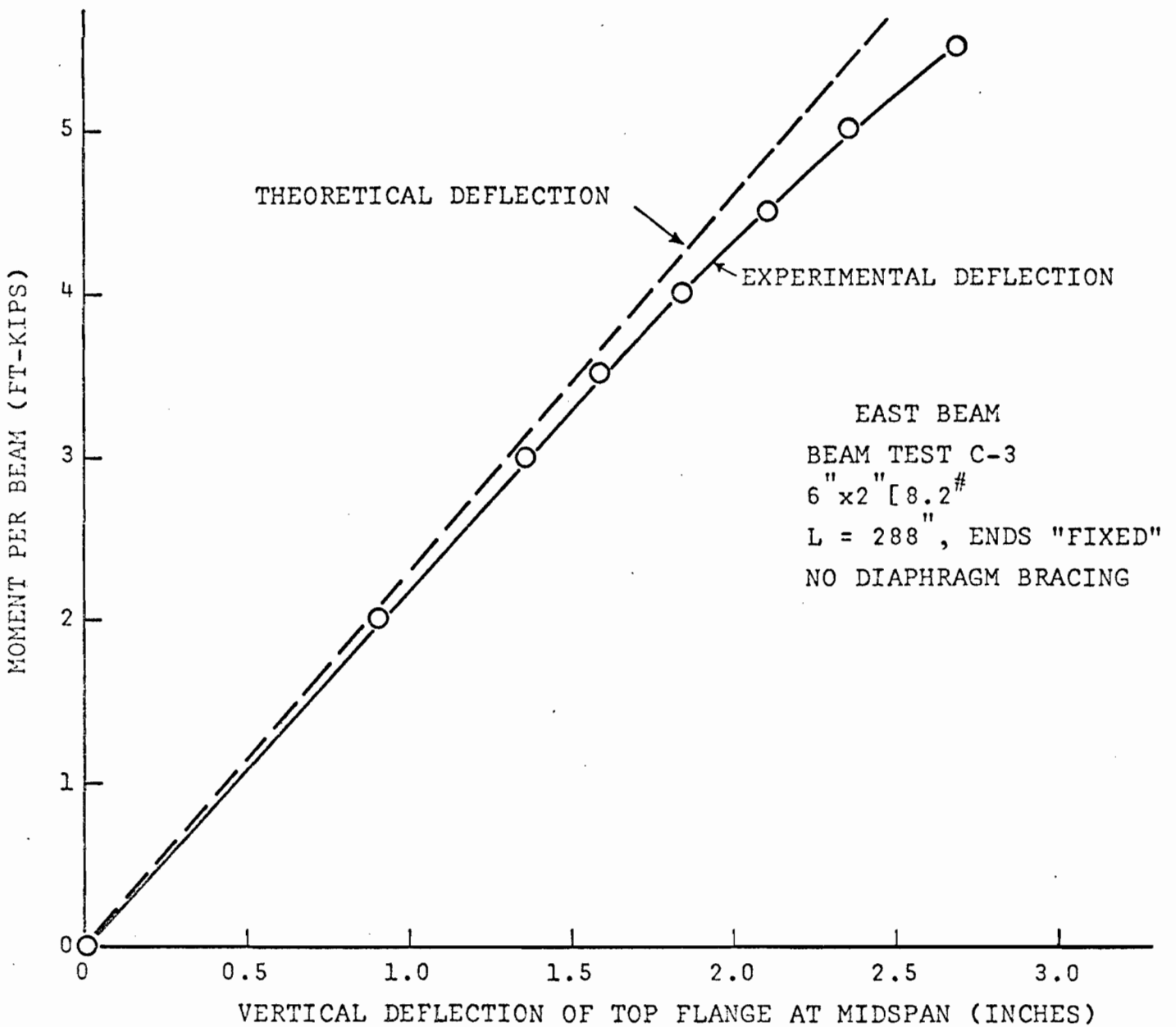

FIG. 2-16 VERTICAL DEFLECTION VERSUS MOMENT FOR AN UNBRACED 6[8.2 BEAM

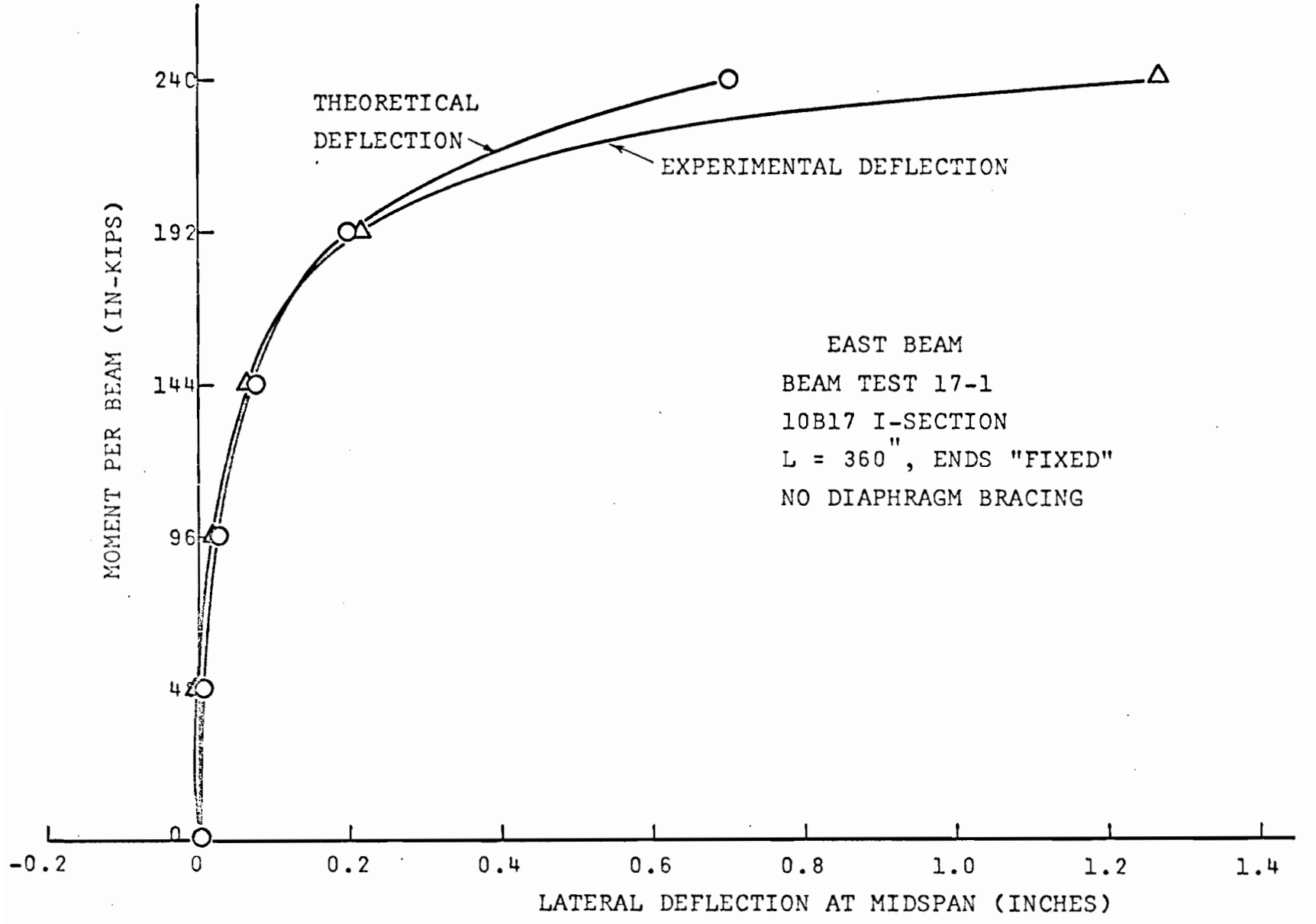

FIG. 2-17 LATERAL DEFLECTION VERSUS MOMENT FOR AN UNBRACED 10B17 I-BEAM

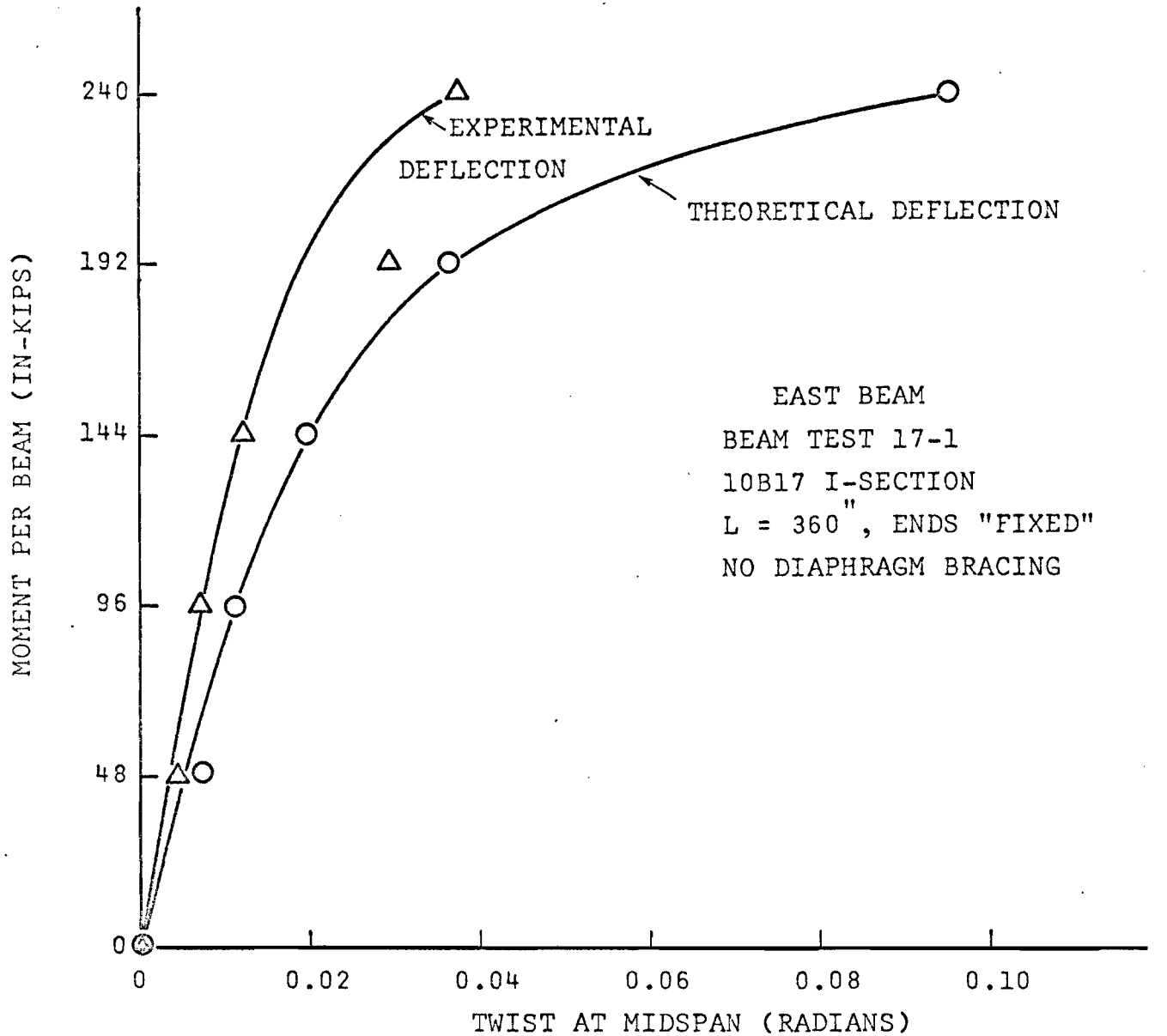

FIG. 2-18 TWIST VERSUS MOMENT FOR AN UNBRACED 10B17 I-BEAM

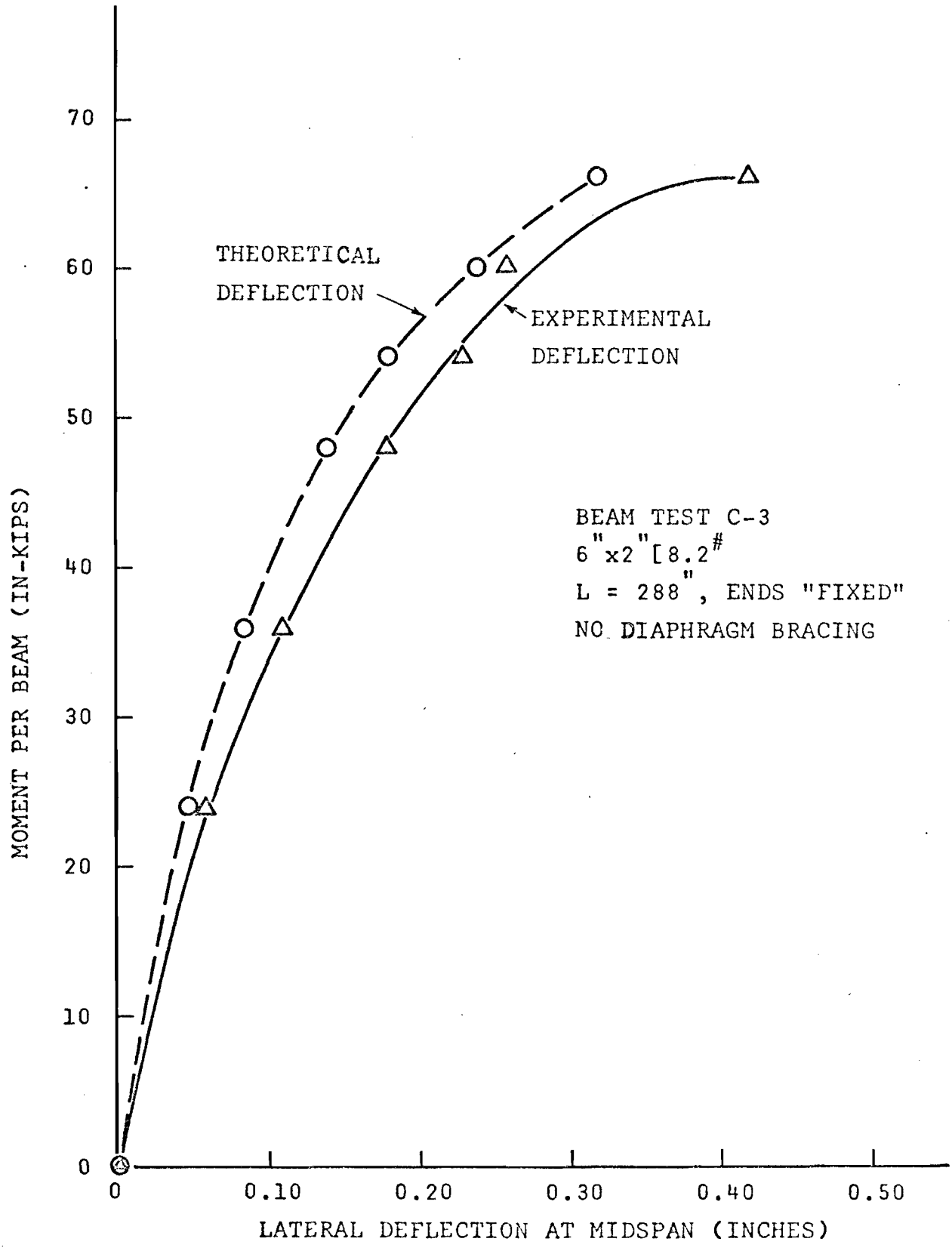

FIG. 2-19 LATERAL DEFLECTION VERSUS MOMENT FOR AN UNBRACED 6[8.2 BEAM

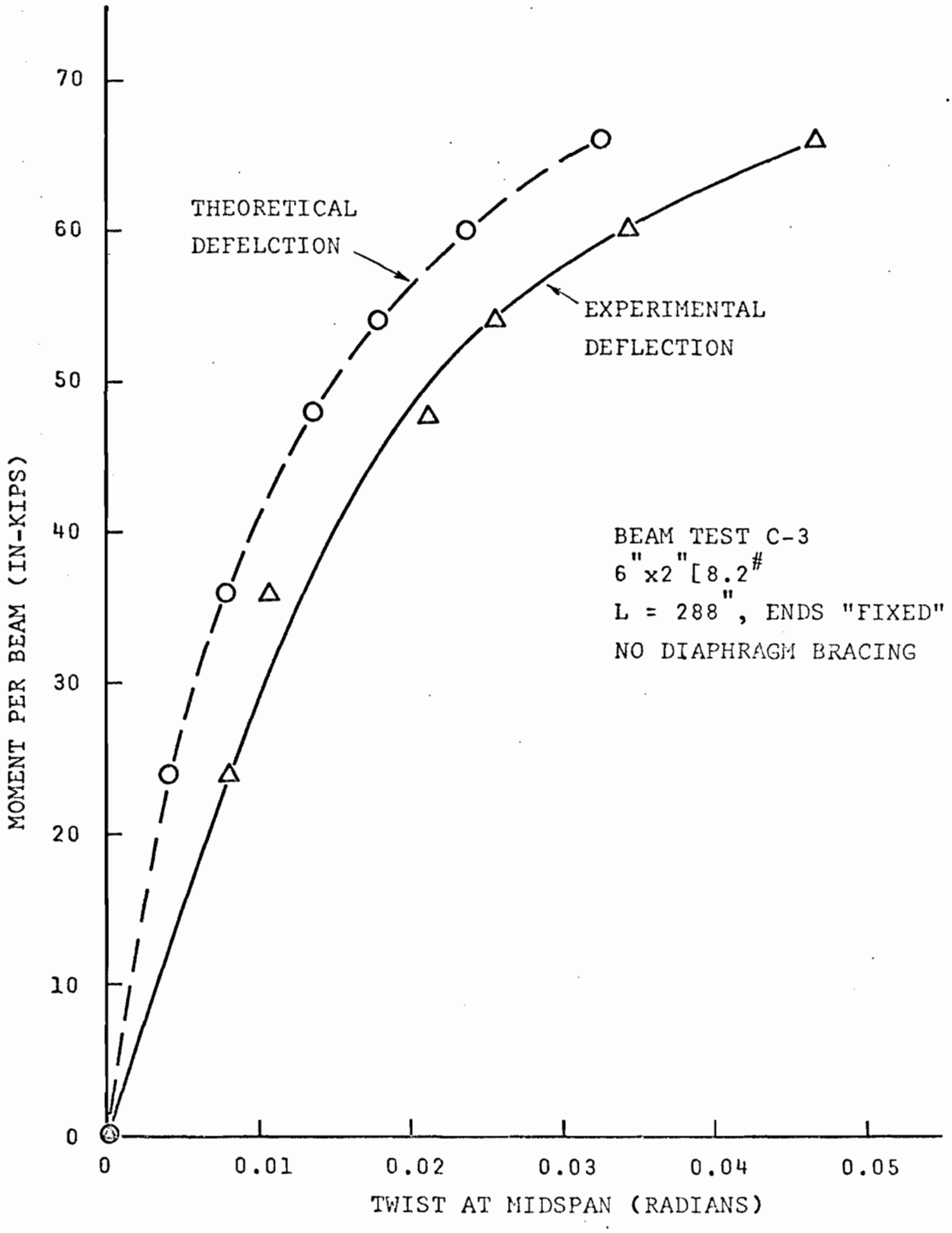

FIG. 2-20 TWIST VERSUS MOMENT FOR AN UNBRACED 6[8.2 BEAM

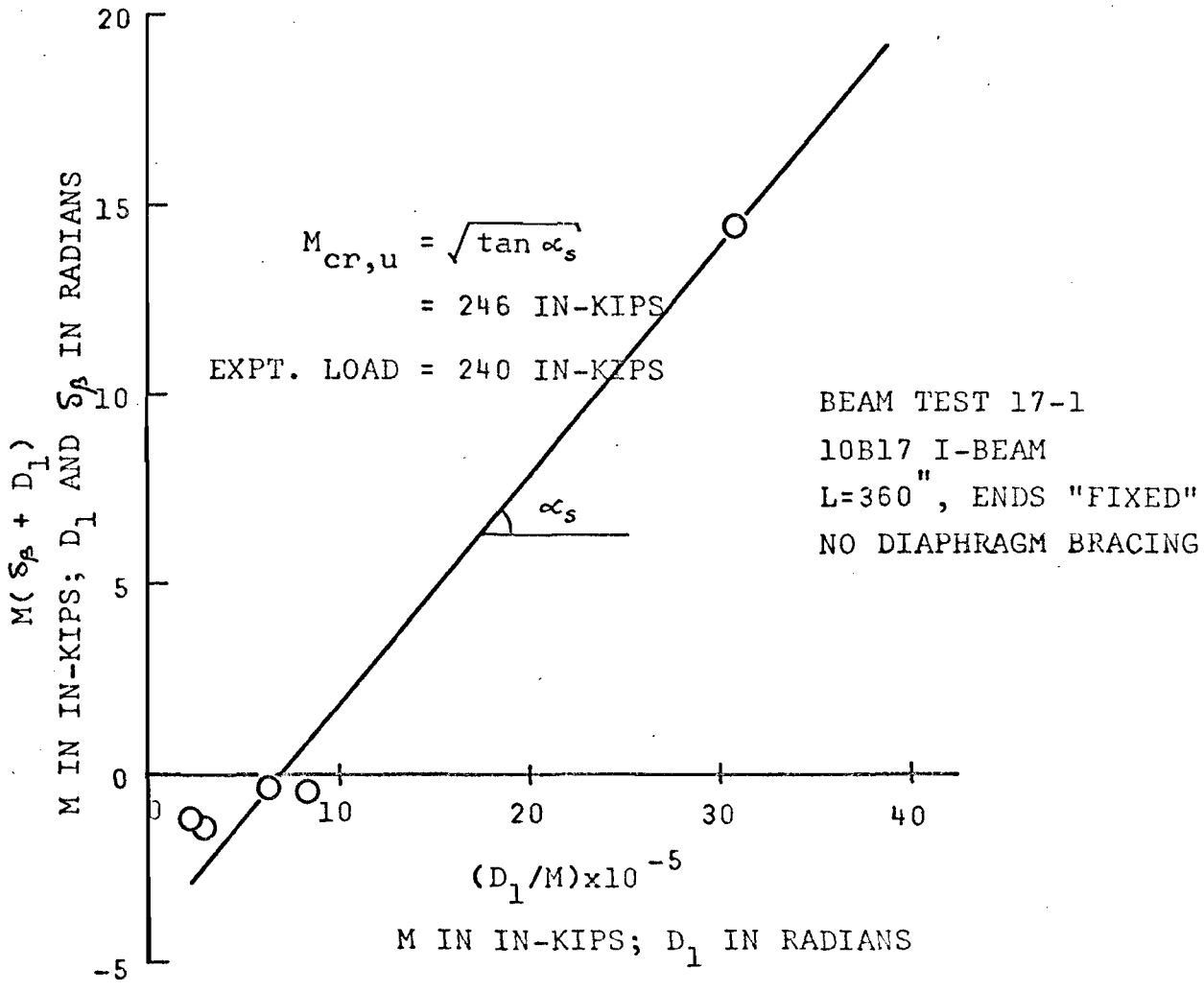

FIG. 2-21 SOUTHWELL PLOT FOR LATERAL INSTABILITY OF AN UNBRACED 10B17 I-BEAM

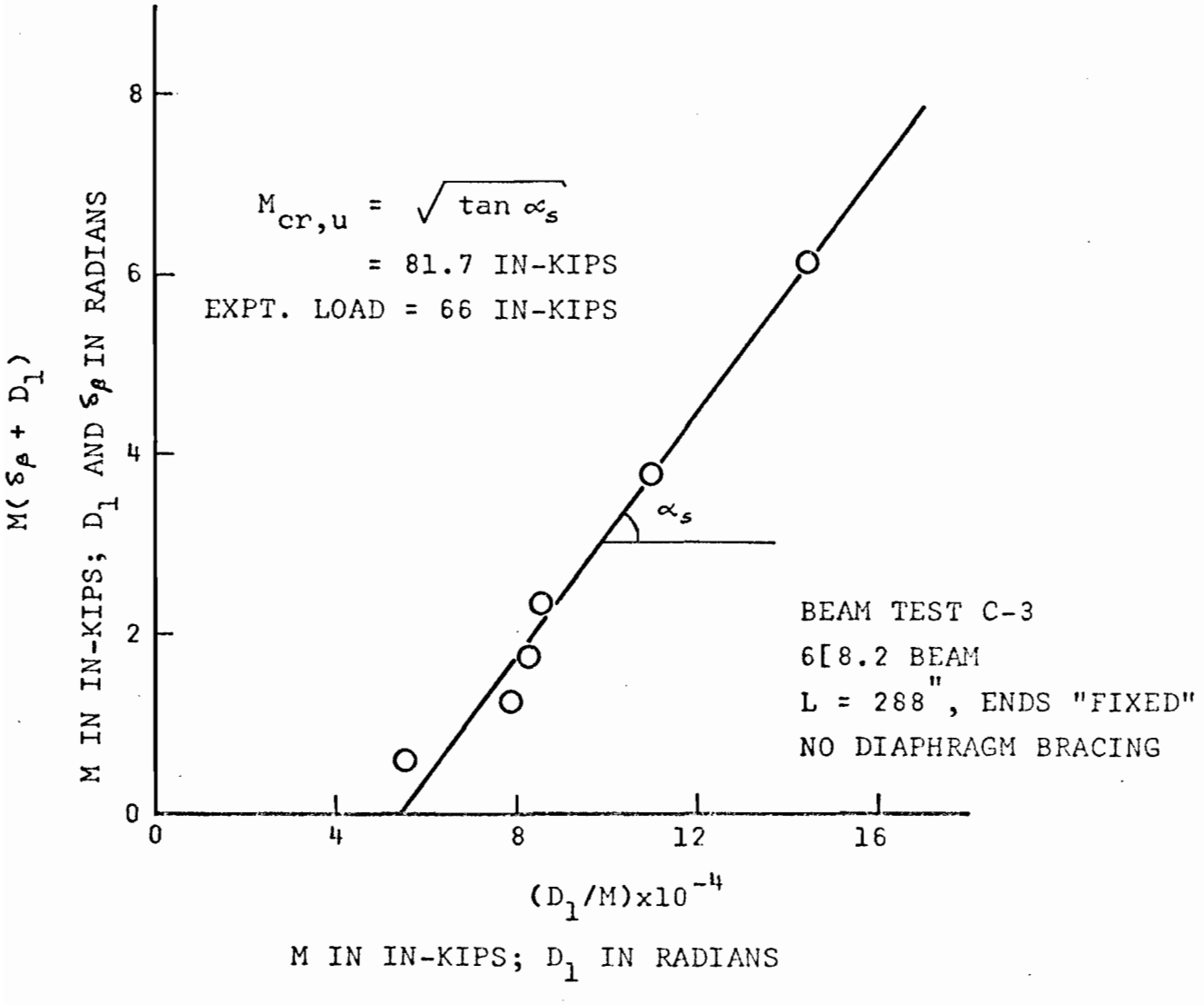

M IN IN-KIPS; D_1 IN RADIANS

FIG. 2-22 SOUTHWELL PLOT FOR LATERAL INSTABILITY OF AN UNBRACED 6[8.2 BEAM

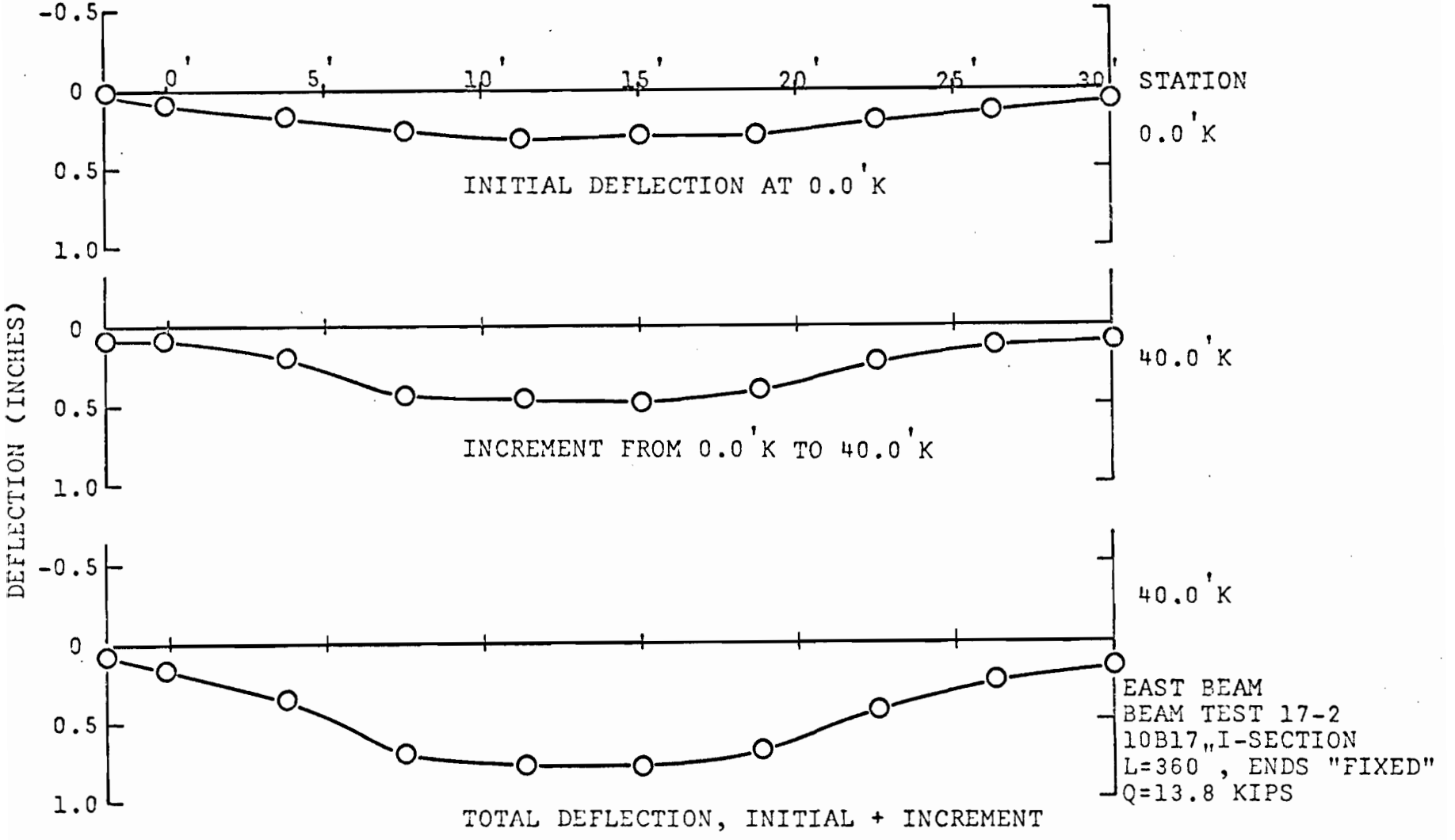

FIG. 2-23 LATERAL DEFLECTIONS OF CENTROIDAL AXIS OF A DIAPHRAGM-BRACED 10B17 I-BEAM

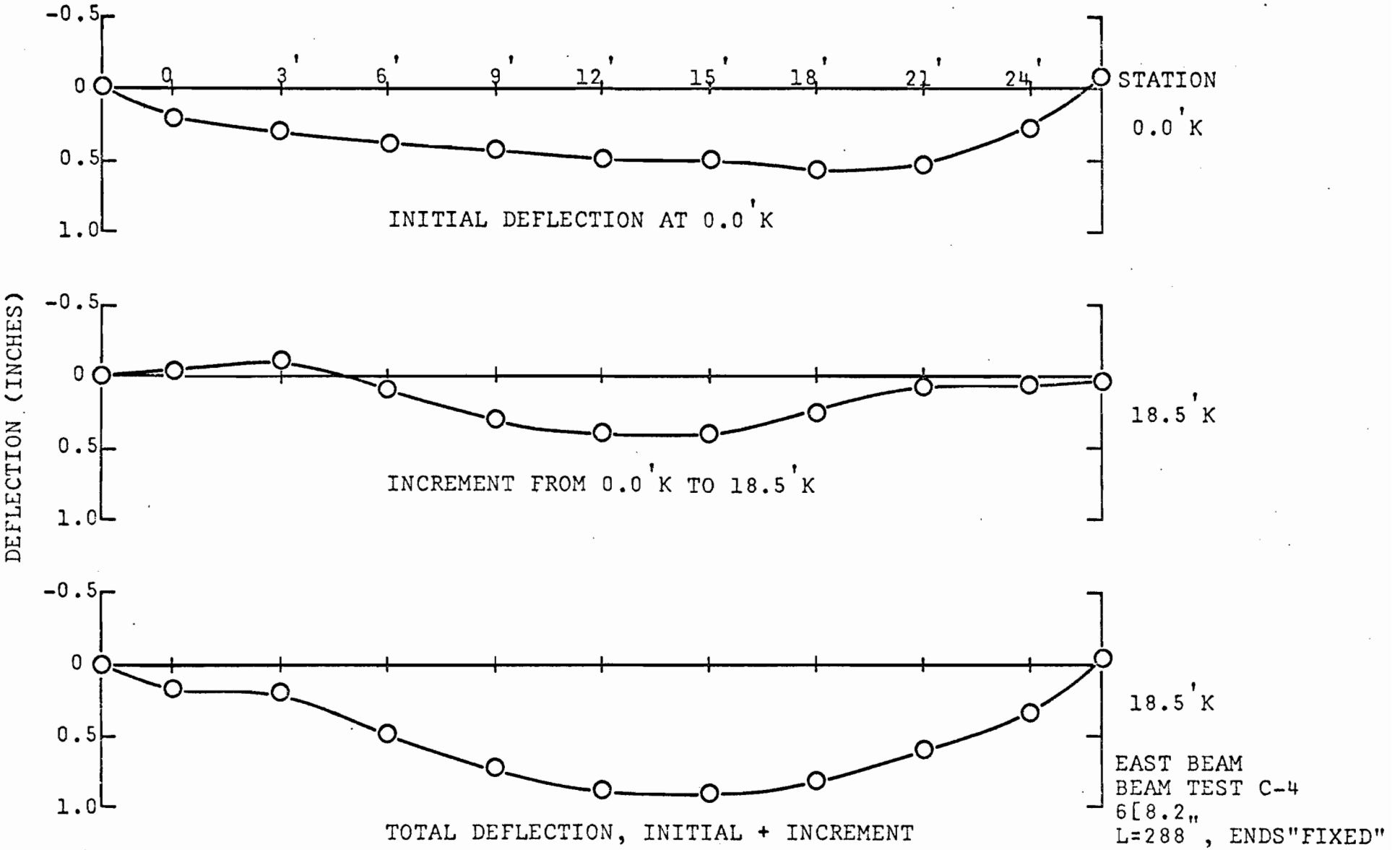

FIG. 2-24 LATERAL DEFLECTIONS OF CENTROIDAL AXIS OF A DIAPHRAGM-BRACED 6[8.2 BEAM

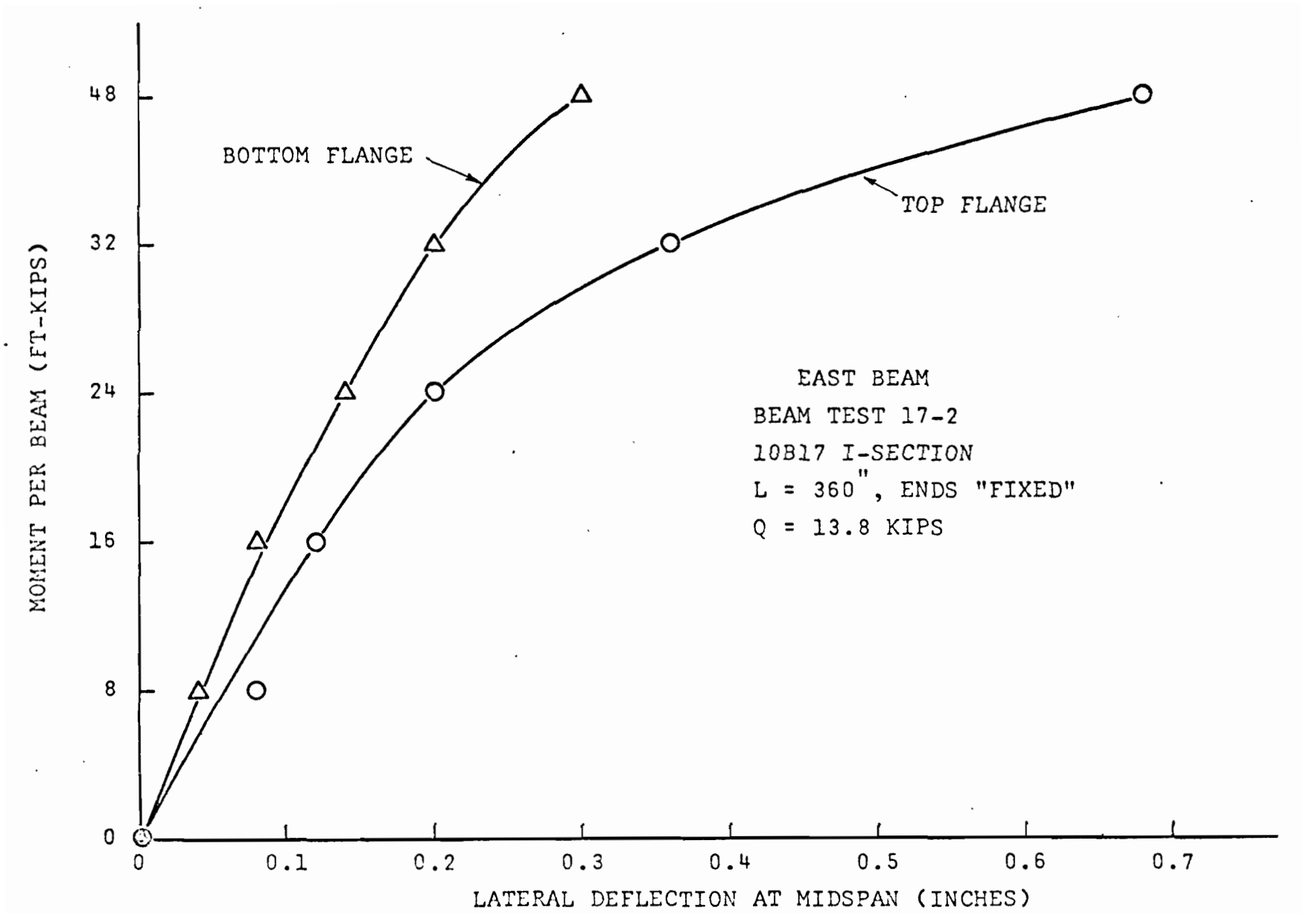

FIG. 2-25 LATERAL DEFLECTION VERSUS MOMENT FOR A DIAPHRAGM-BRACED 10B17 I-BEAM

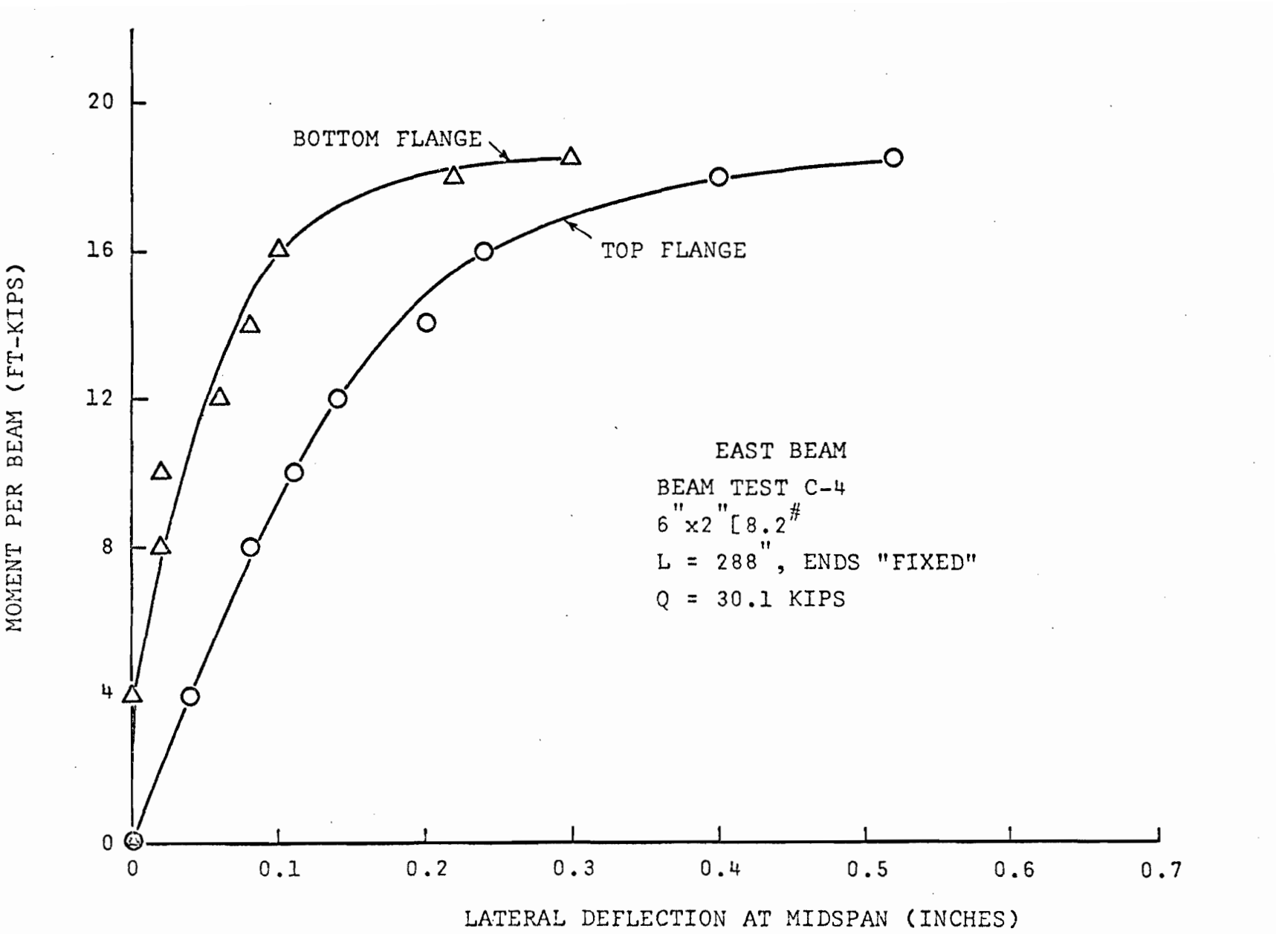

FIG. 2-26 LATERAL DEFLECTION VERSUS MOMENT FOR A DIAPHRAGM-BRACED 6[8.2 BEAM

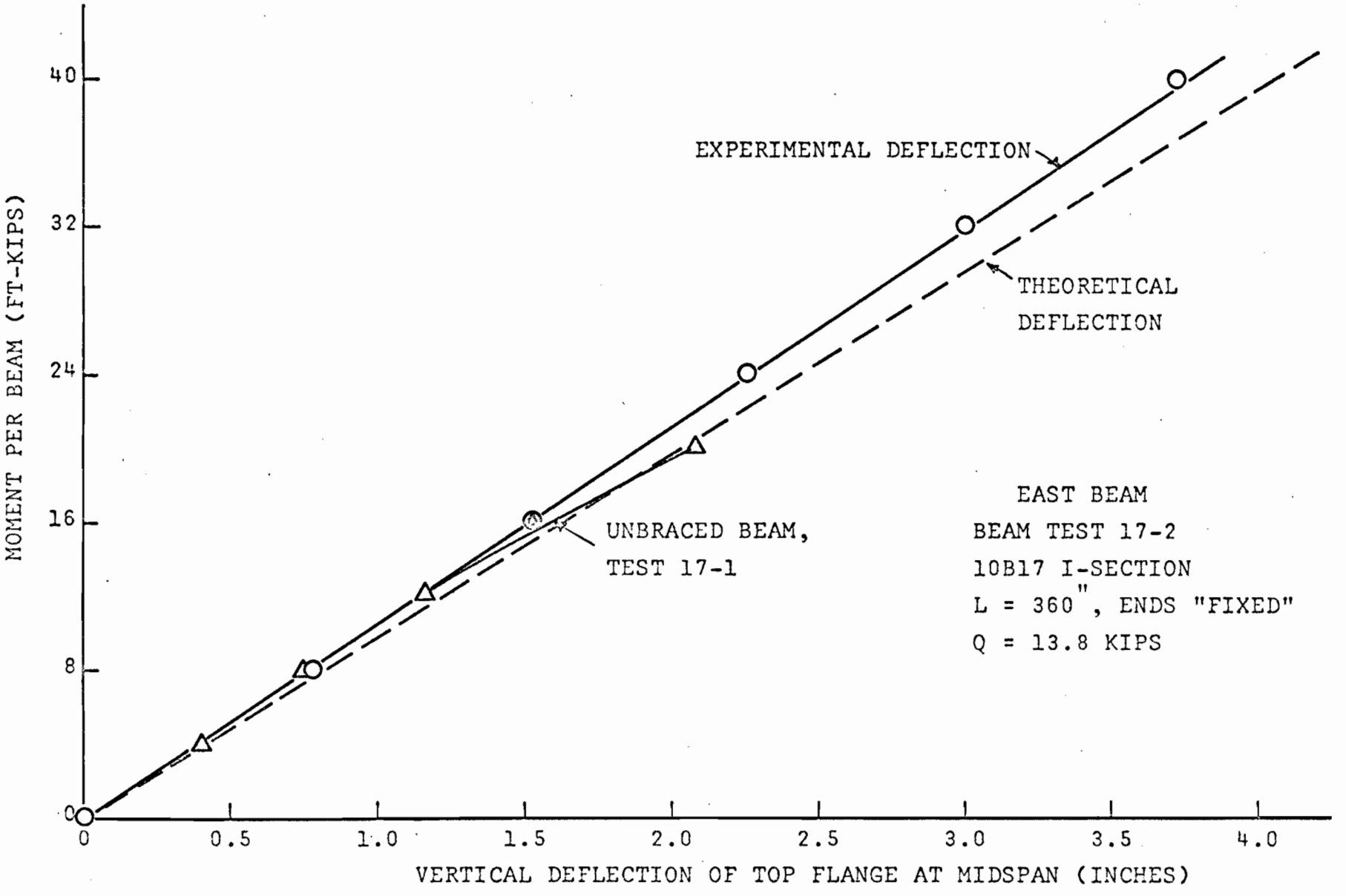

FIG. 2-27 VERTICAL DEFLECTION VERSUS MOMENT FOR A DIAPHRAGM-BRACED 10B17 I-BEAM

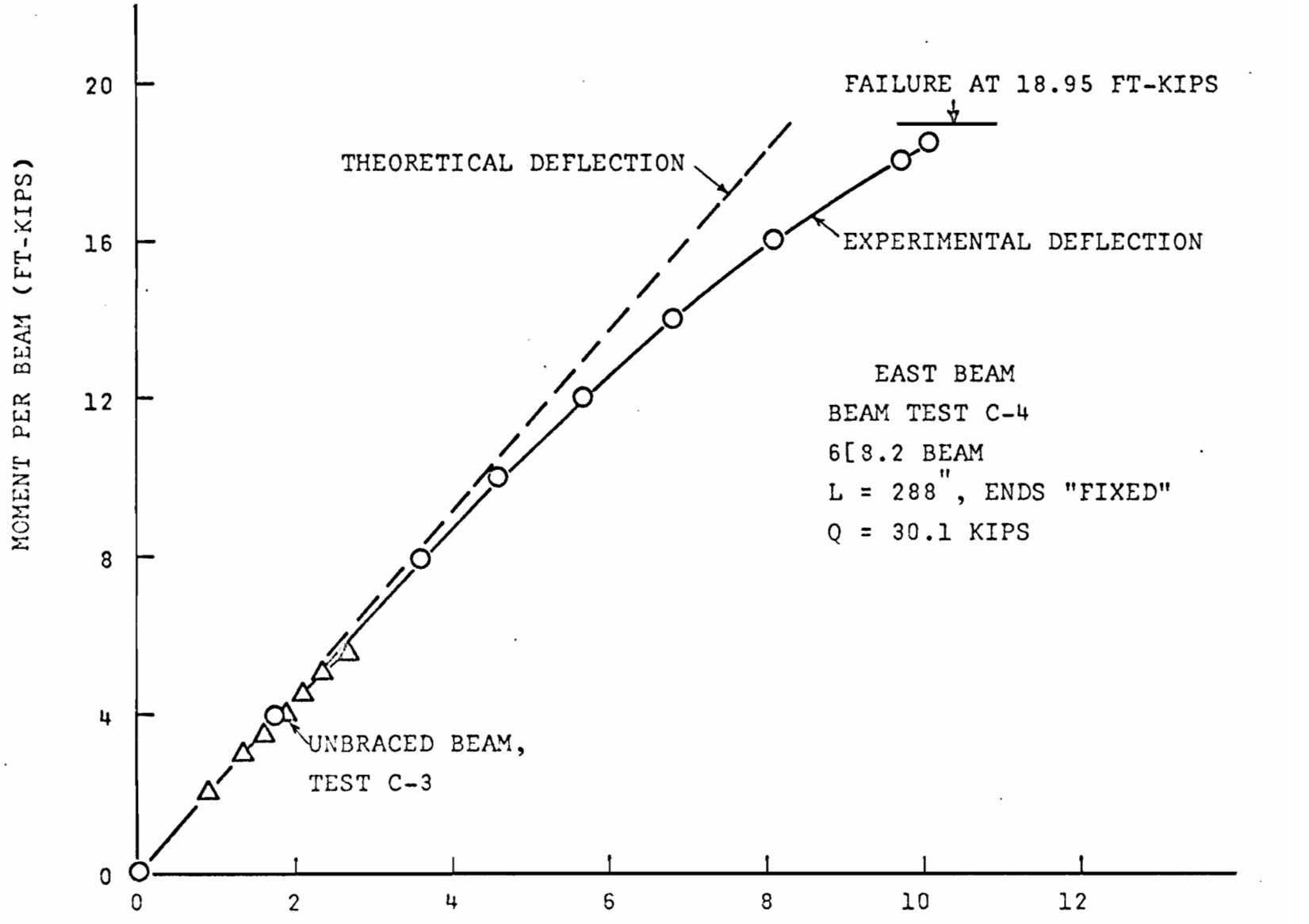

FIG. 2-28 VERTICAL DEFLECTION VERSUS MOMENT FOR A DIAPHRAGM-BRACED 6[8.2 BEAM

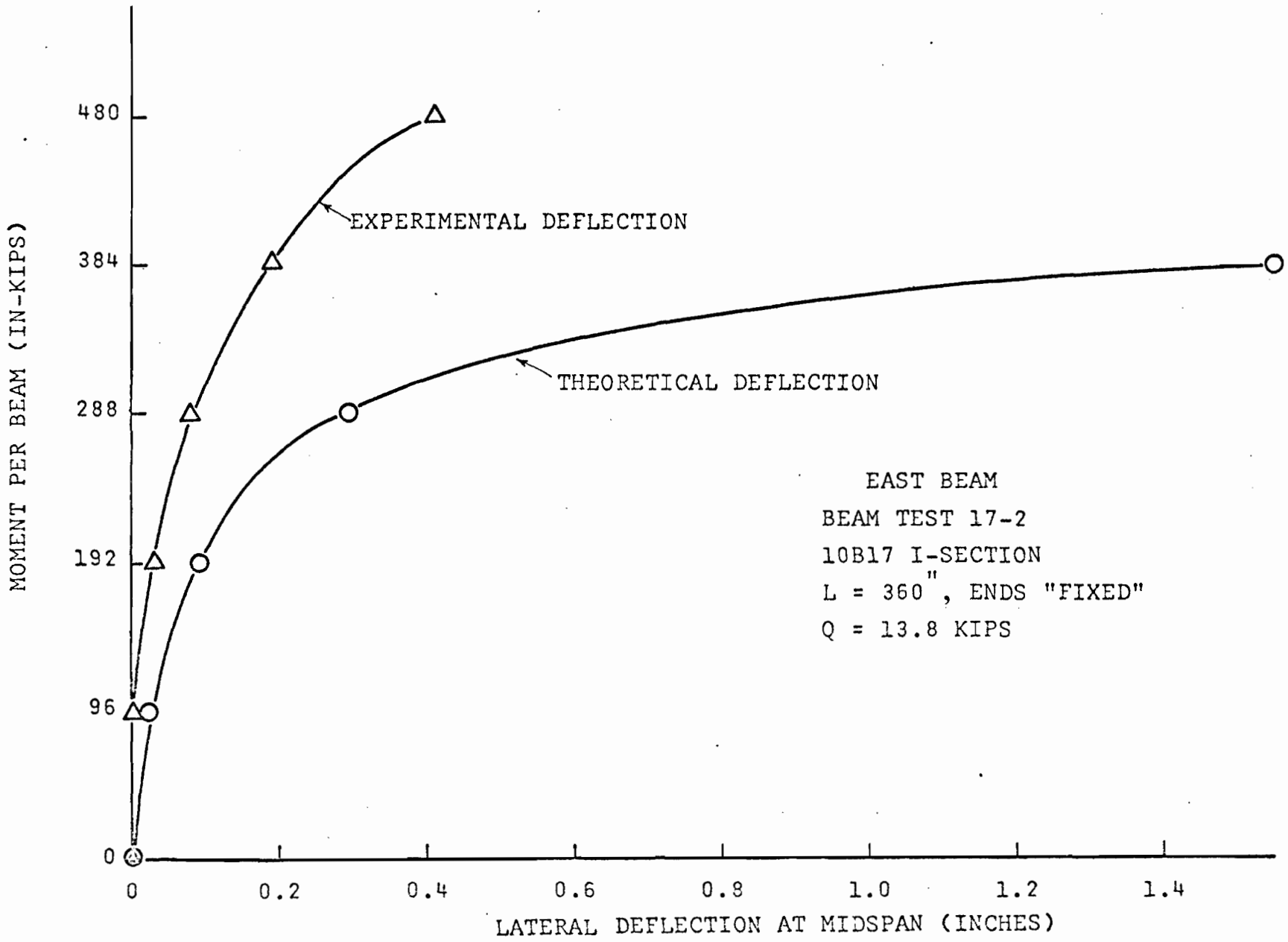

FIG. 2-29 LATERAL DEFLECTION VERSUS MOMENT FOR A DIAPHRAGM-BRACED 10B17 I-BEAM

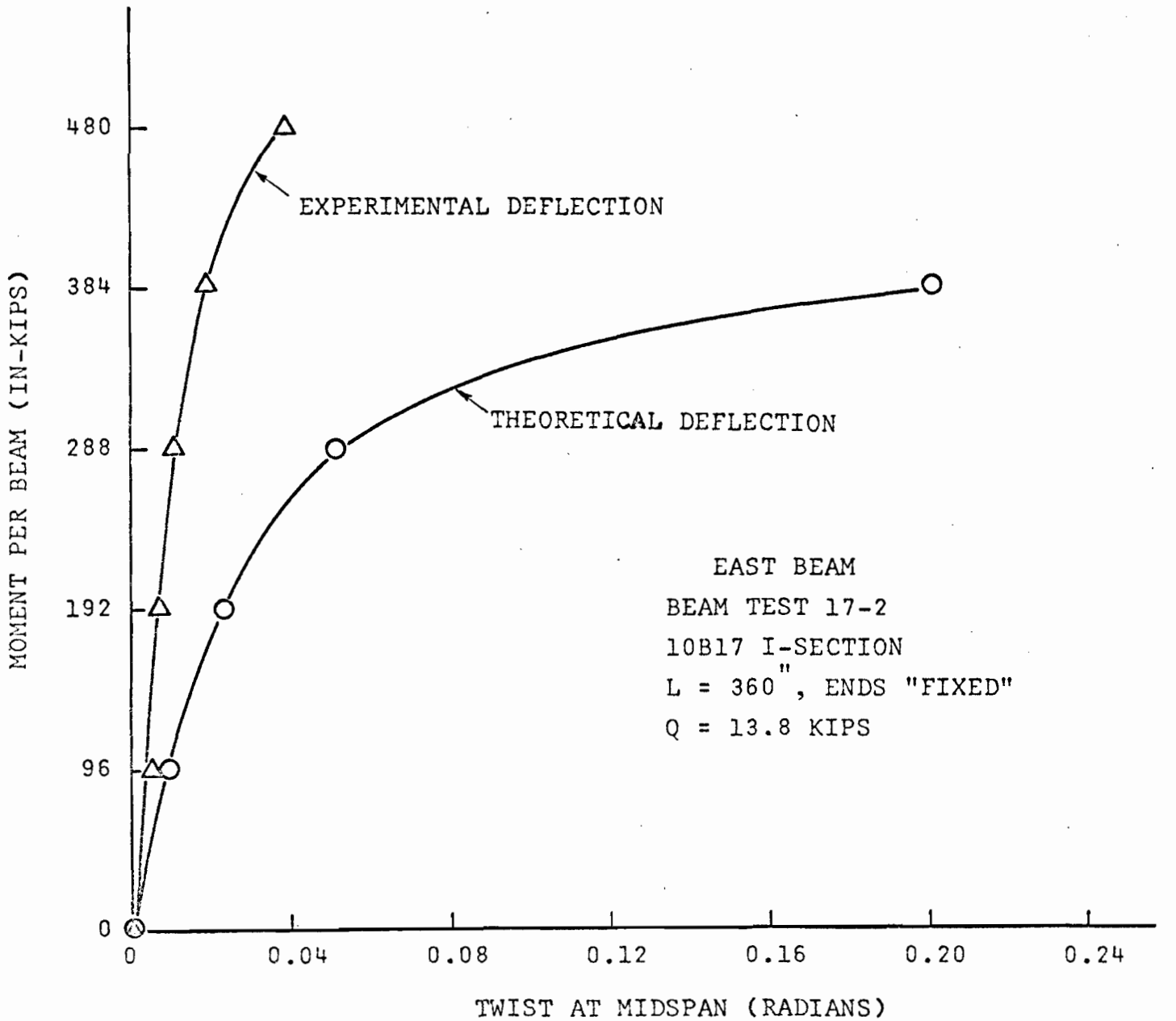

FIG. 2-30 TWIST VERSUS MOMENT OF A DIAPHRAGM-BRACED 10B17 I-BEAM

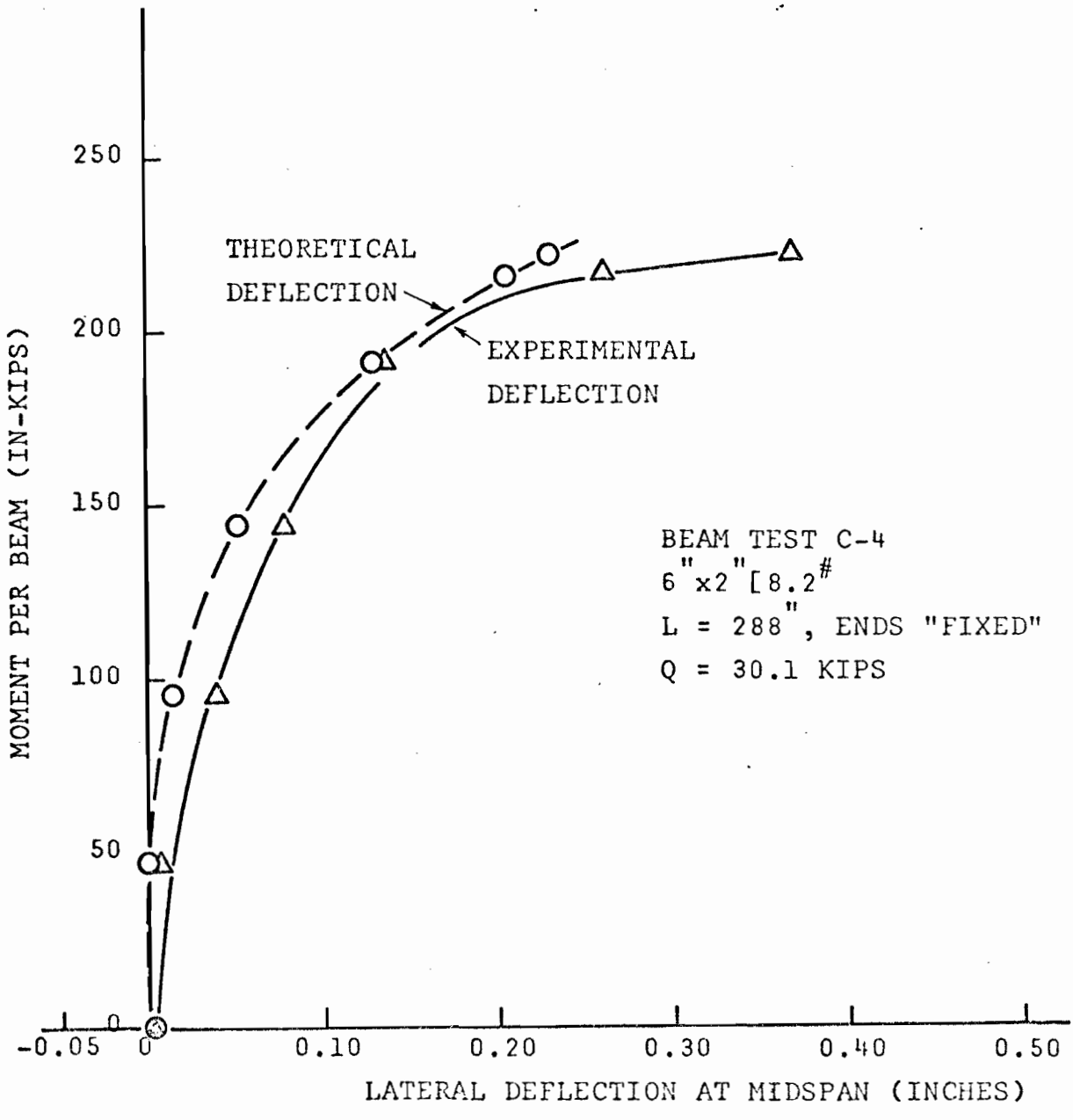

FIG. 2-31 LATERAL DEFLECTION VERSUS MOMENT FOR A DIAPHRAGM-BRACED 6[8.2 BEAM

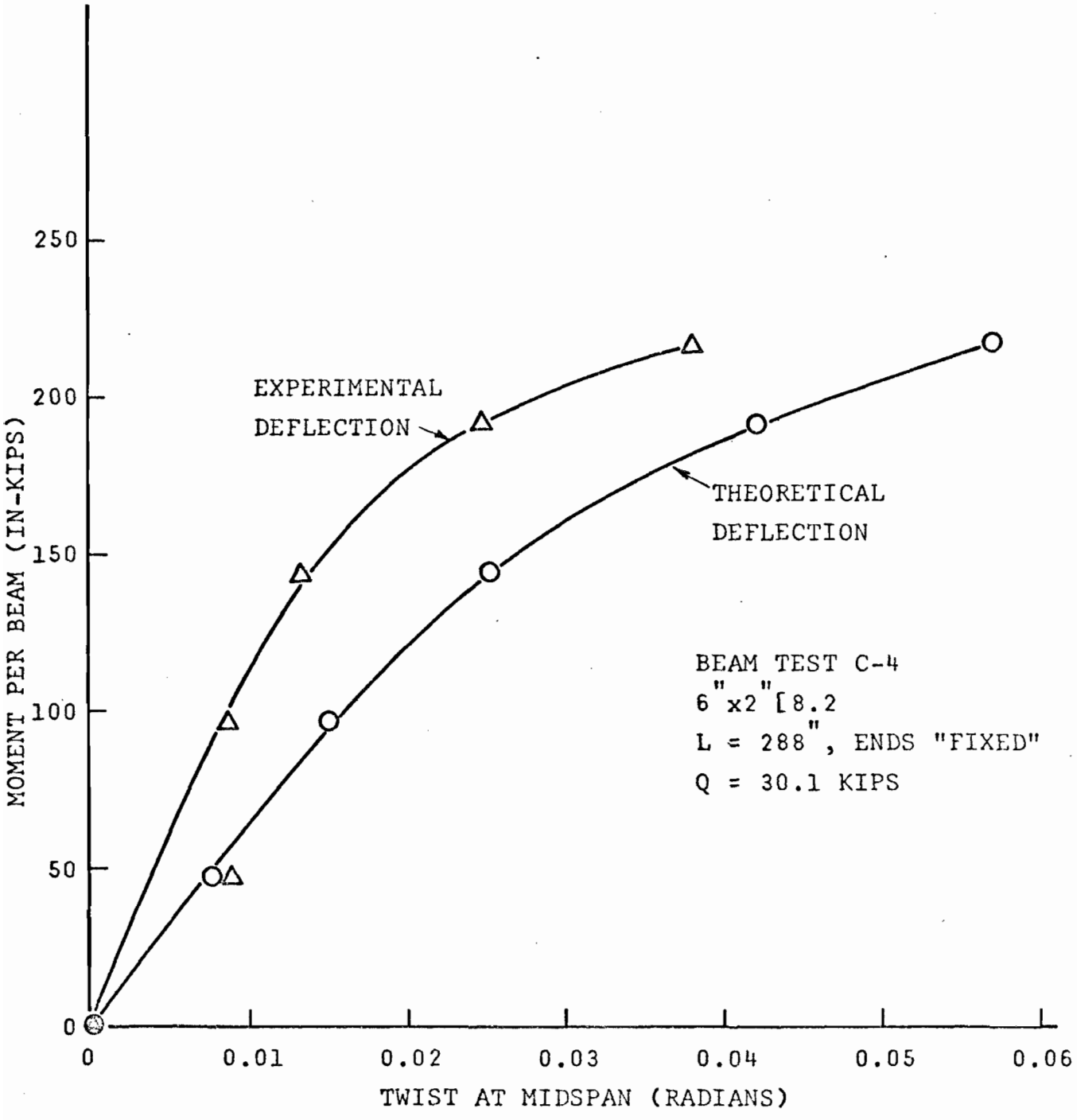

FIG. 2-32 TWIST VERSUS MOMENT FOR A DIAPHRAGM-BRACED 6[8.2 BEAM

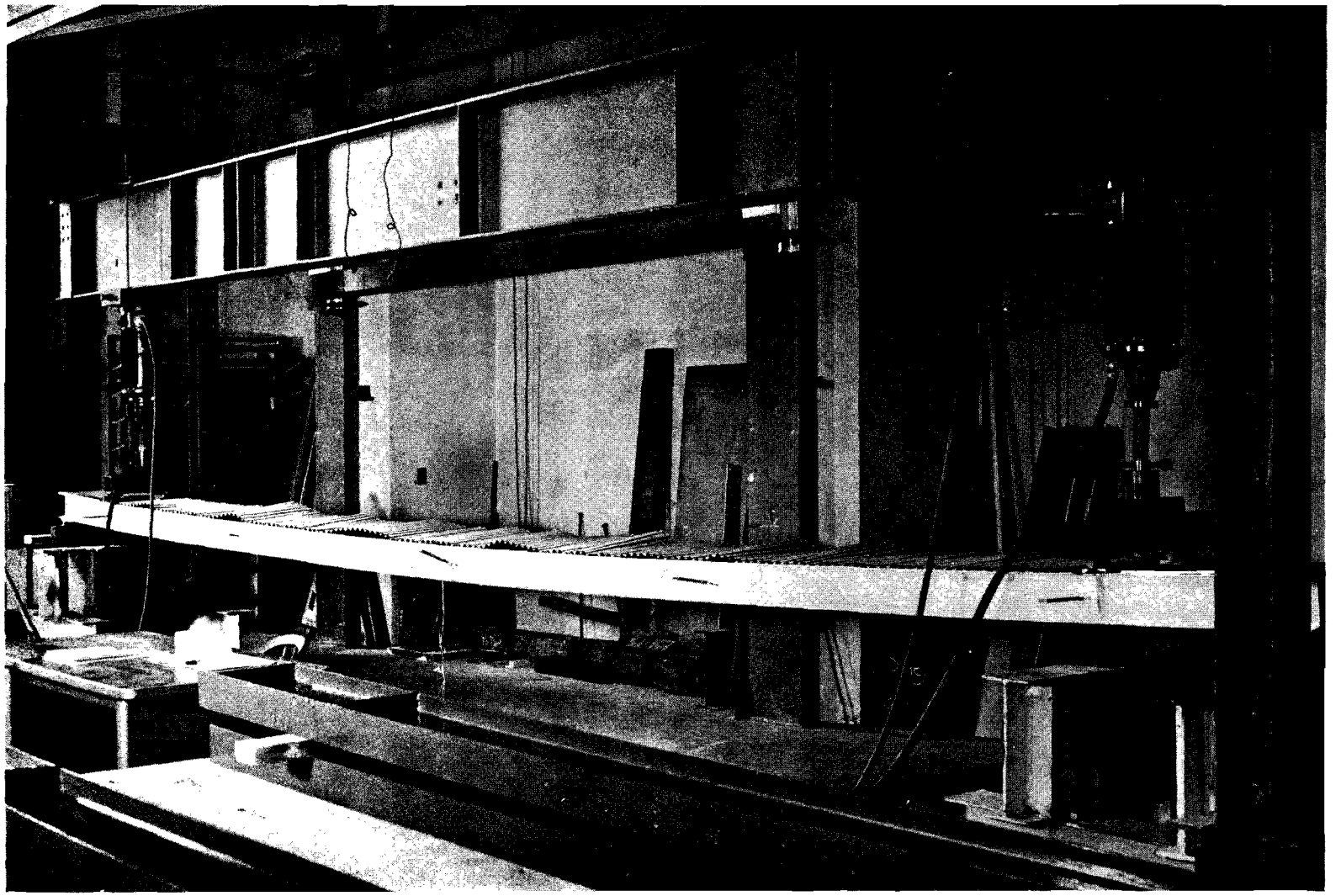

FIG. 2-33 6[8.2 BEAM ASSEMBLY AFTER FAILURE

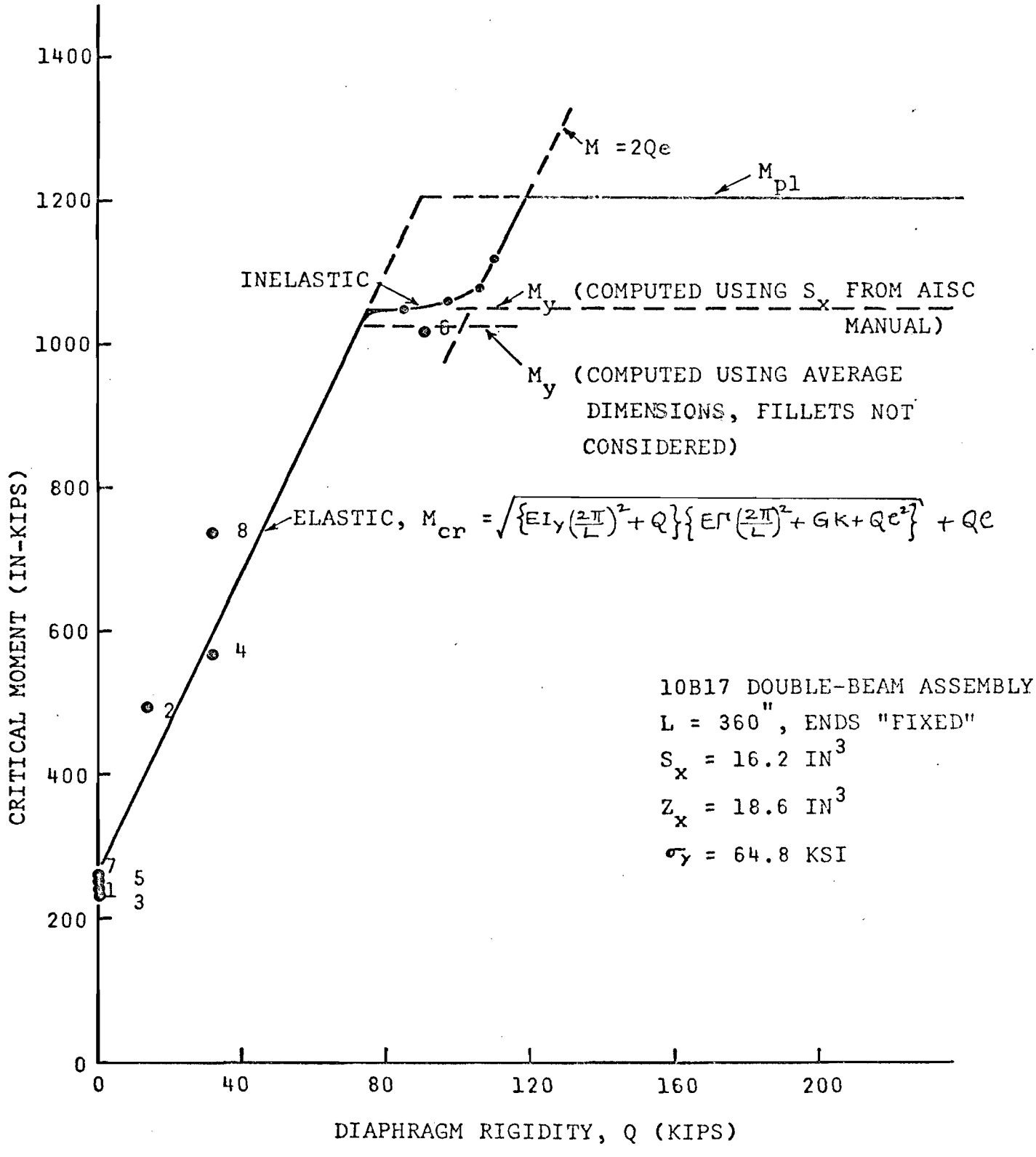

FIG. 2-34 COMPARISON OF 10B17 I-BEAM TEST RESULTS WITH PREDICTED CRITICAL MOMENTS, L = 360"

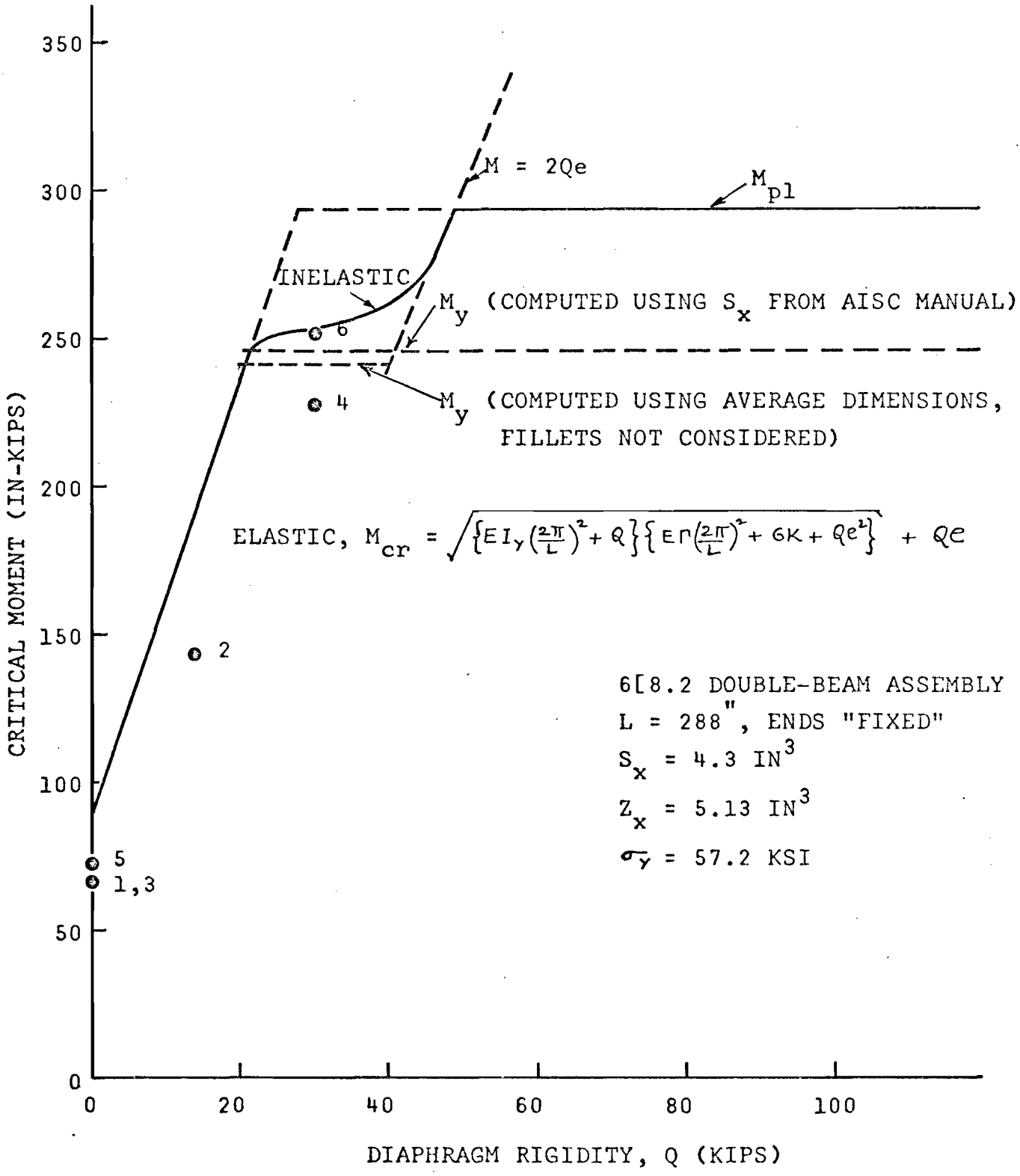

FIG. 2-35 COMPARISON OF 6[8.2 BEAM TEST RESULTS WITH PREDICTED CRITICAL MOMENTS, L = 288"

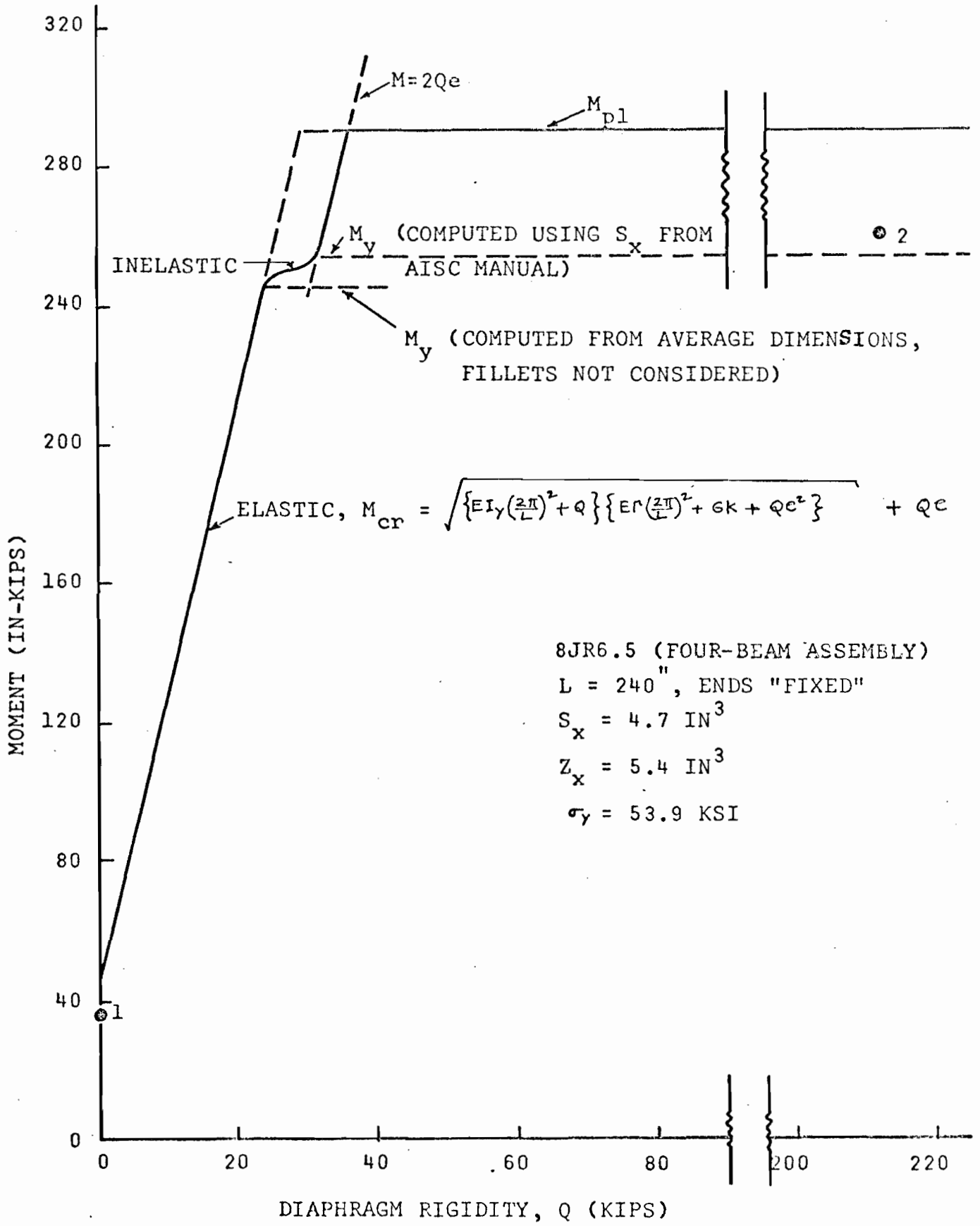

FIG. 2-36 COMPARISON OF 8JR6.5 I-BEAM TEST RESULTS WITH PREDICTED CRITICAL MOMENTS, L = 240"

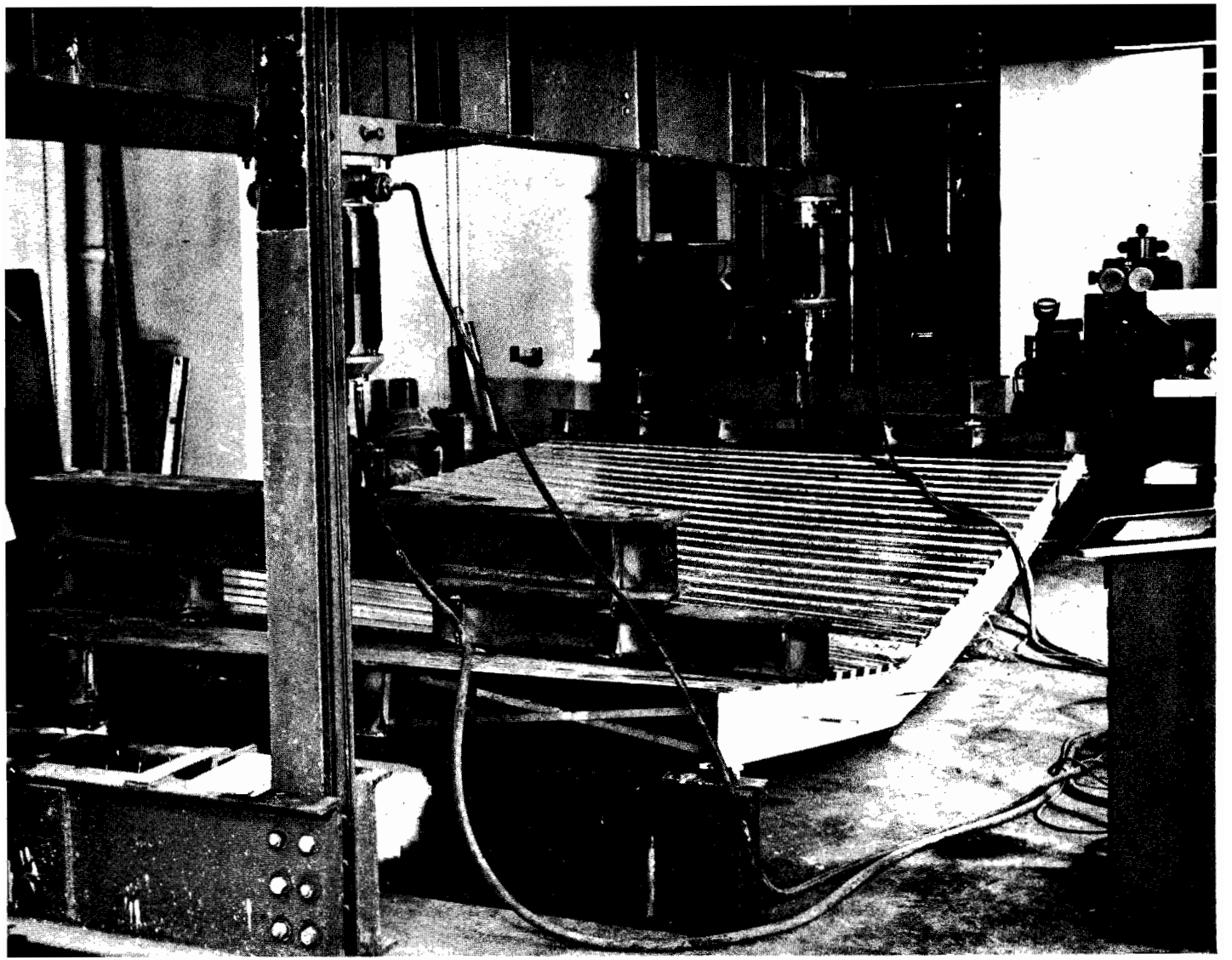

FIG. 2-37 FOUR-BEAM ASSEMBLY AFTER FAILURE

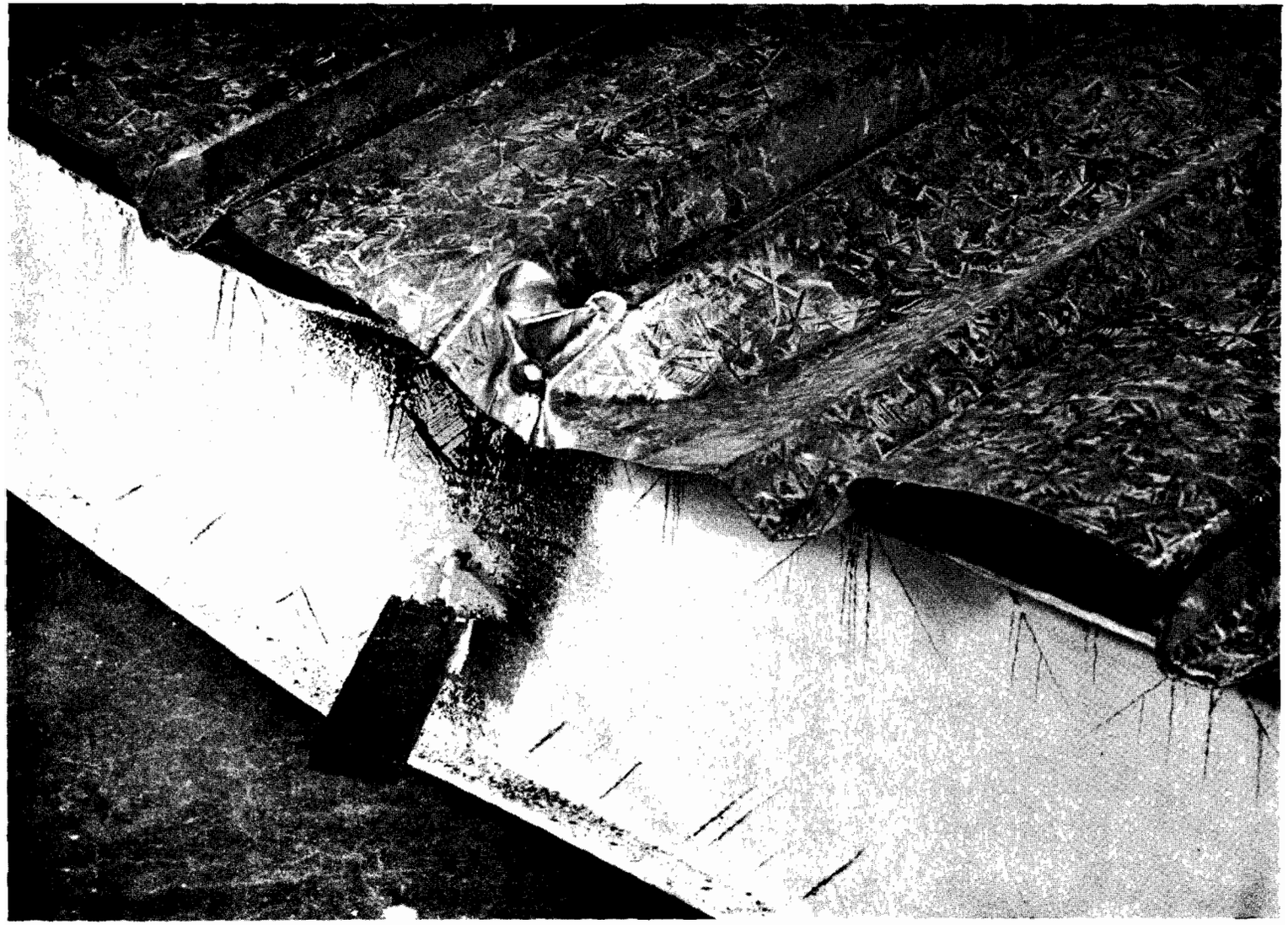

FIG. 2-38 LOCAL BUCKLING OF EAST BEAM IN THE FOUR-BEAM ASSEMBLY TEST

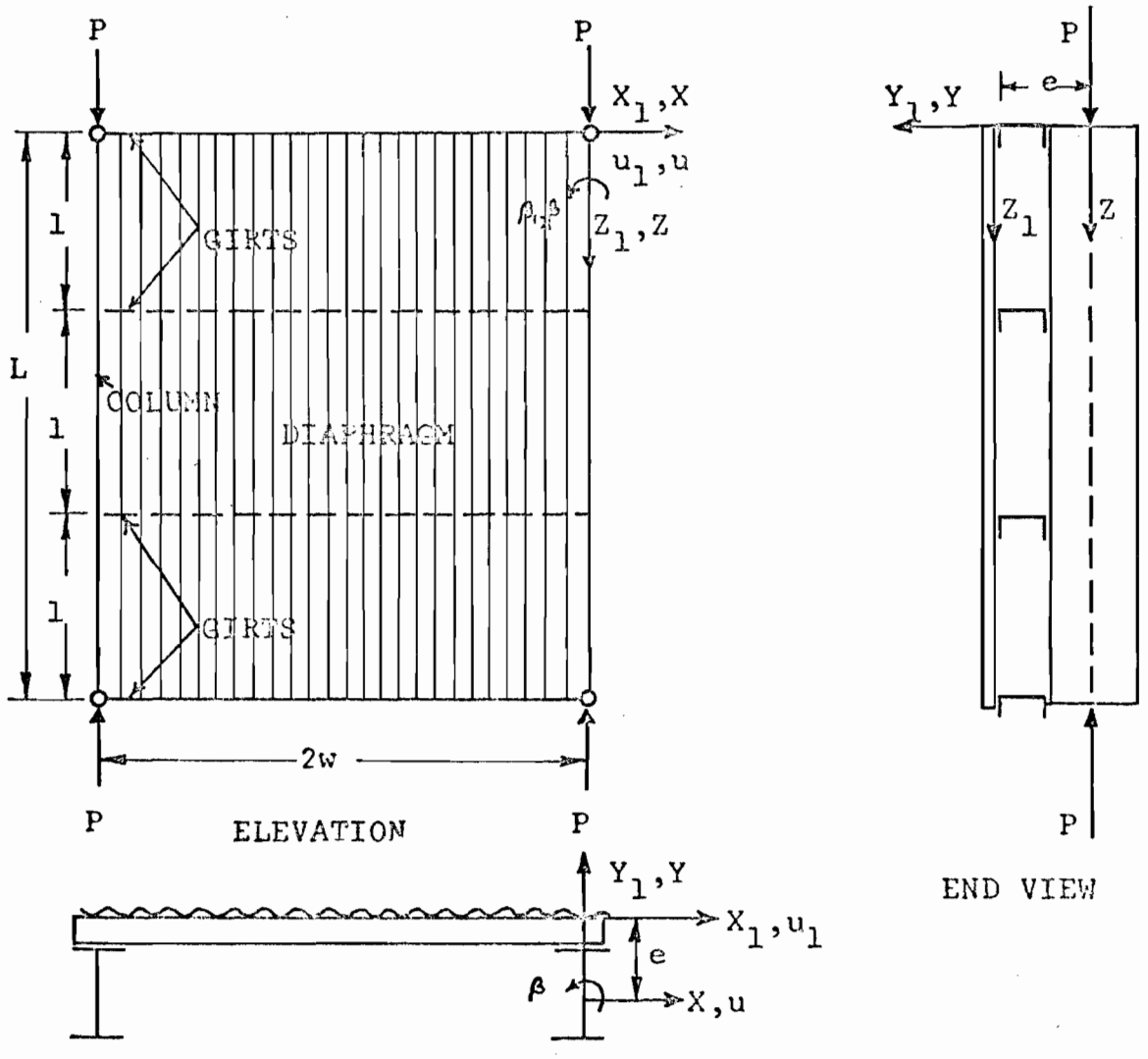

FIG. 3-1 A MODEL OF COLUMN-GIRT-DIAPHRAGM ASSEMBLY

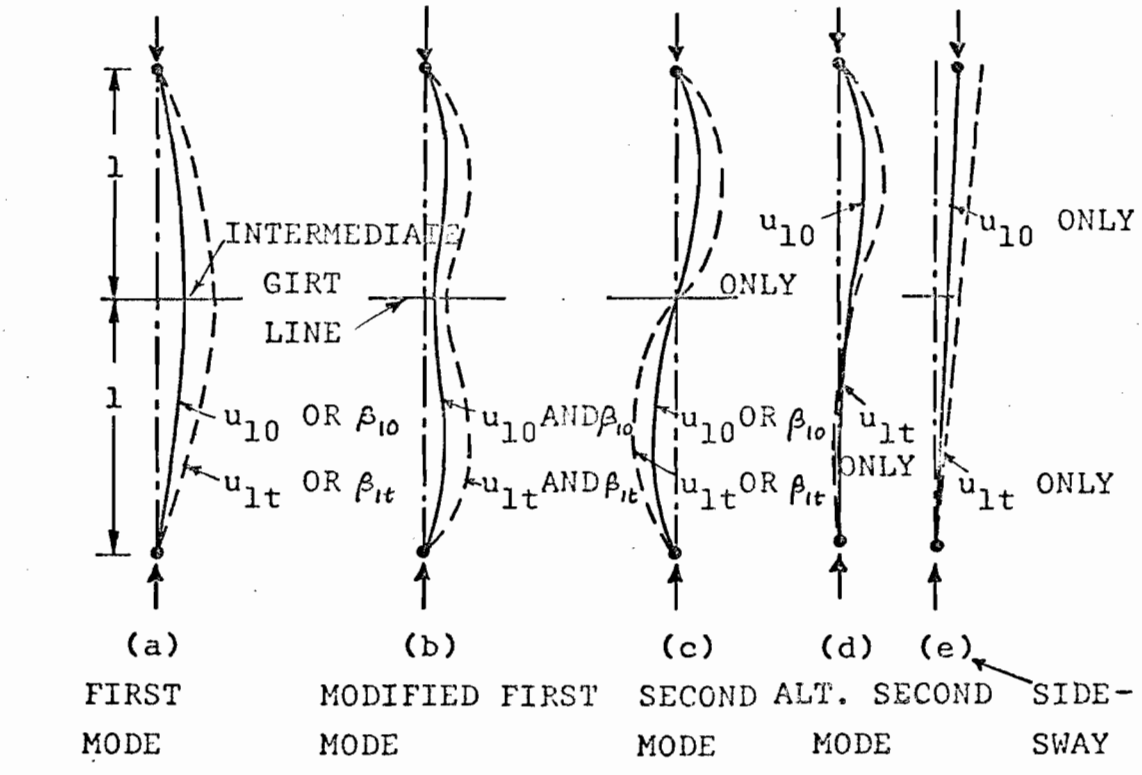

—— INITIAL POSITION; – – – DEFLECTED POSITION; $(u_{1t}=u_{10}+u_1)$ AND $\beta_{1t}=\beta_{10}+\beta_1$

FIG. 3-2 IMPERFECT COLUMN WITH ONE INTERMEDIATE GIRT

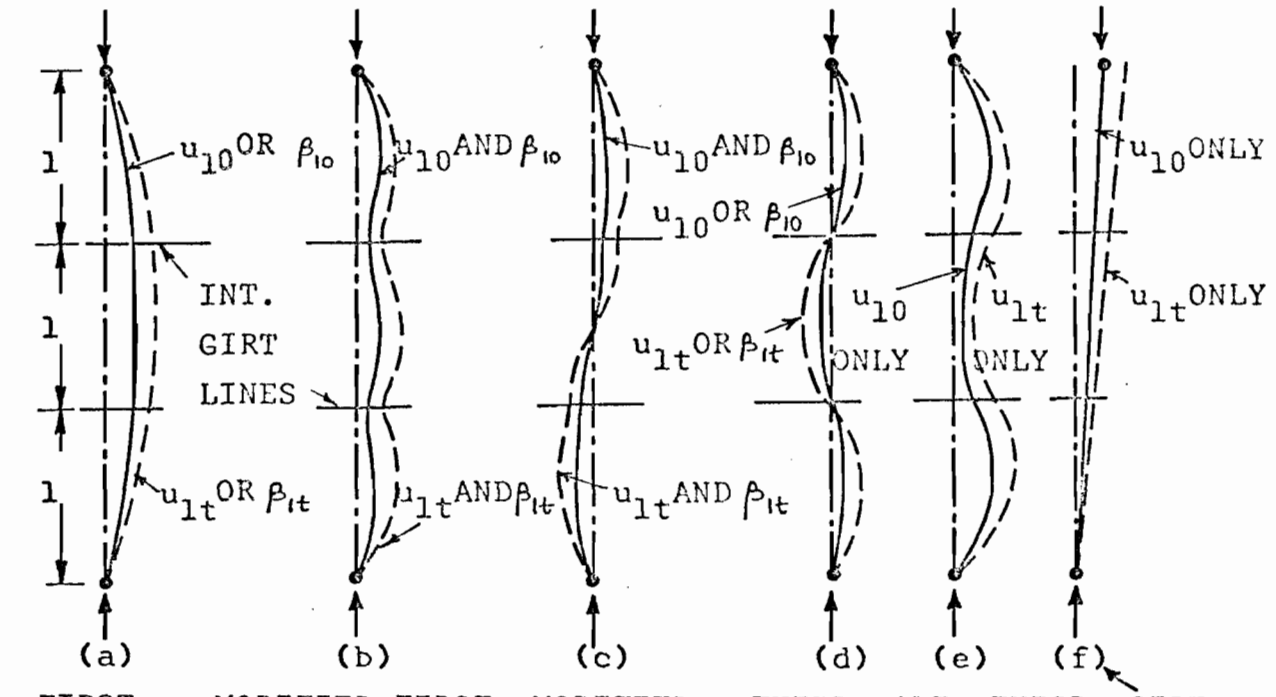

—— INITIAL POSITION; – – – DEFLECTED POSITION; $(u_{1t}=u_{10}+u_1)$ AND $\beta_{1t}=\beta_{10}+\beta_1$

FIG. 3-3 IMPERFECT COLUMN WITH TWO INTERMEDIATE GIRTS

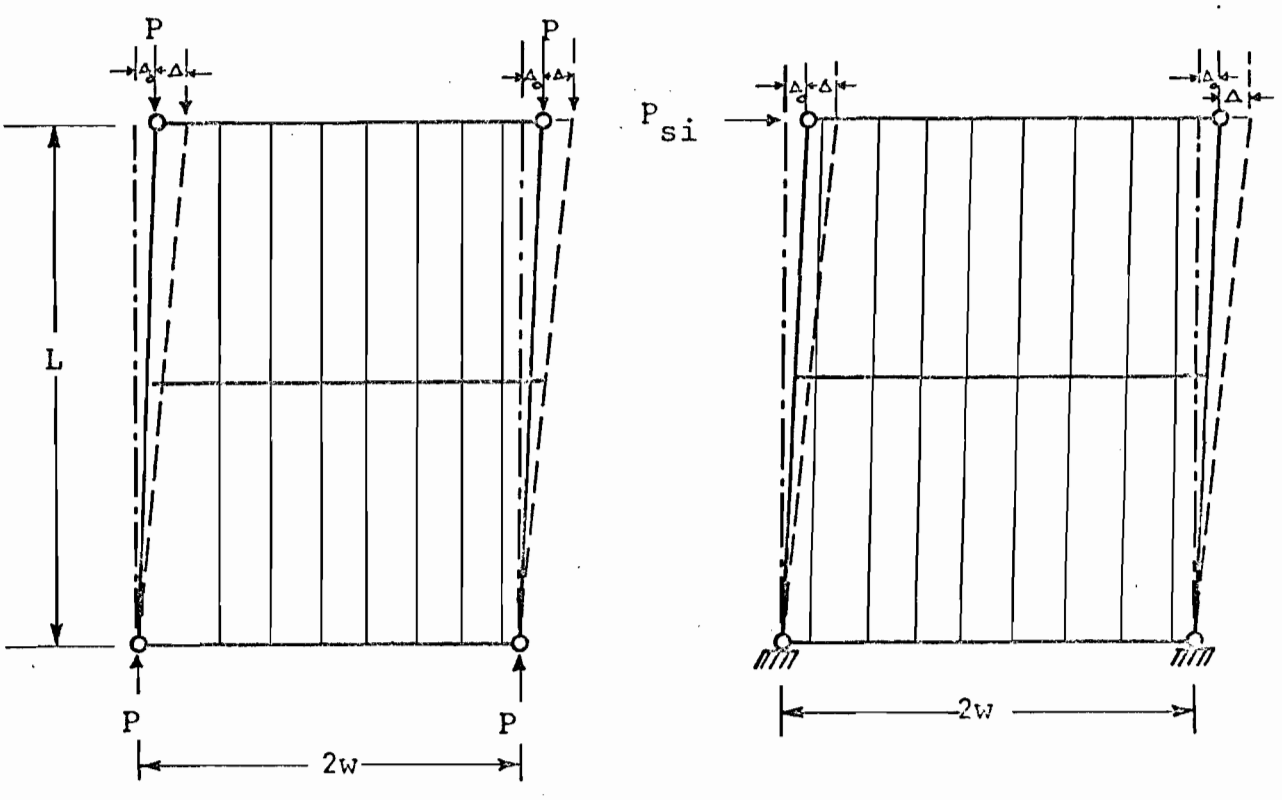

FIG. 3-4 SIDESWAY OF COLUMNS

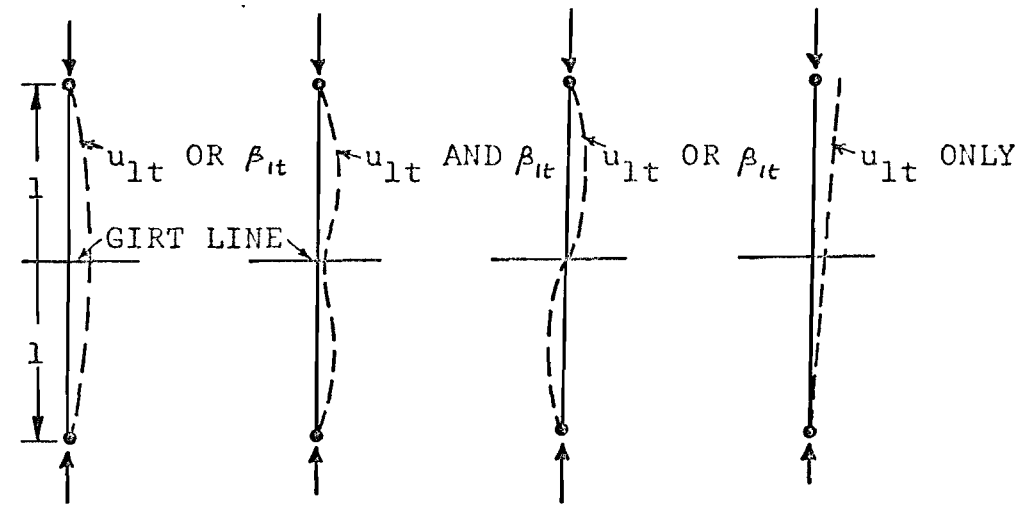

——— INITIAL POSITION; – – – DEFLECTED POSITION

$$u_{1t} = u_1 \text{ AND } \beta_{1t} = \beta_1$$

FIG. 3-5 IDEAL COLUMN WITH ONE INTERMEDIATE GIRT

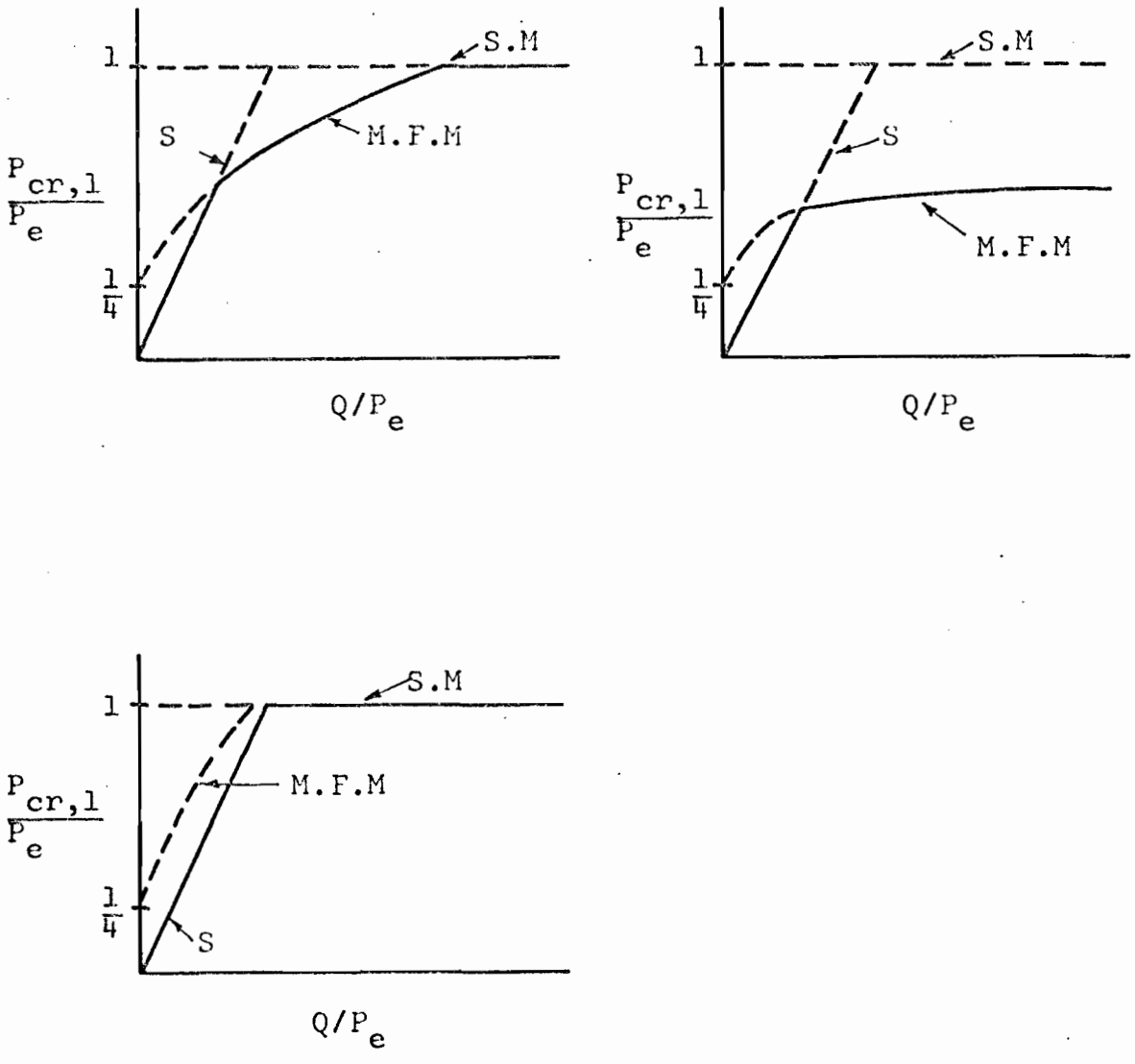

LEGEND:

M.F.M - MODIFIED FIRST MODE; S.M - SECOND MODE;

S - SIDESWAY

FIG. 3-6 POSSIBLE TYPES OF BEHAVIOR OF A COLUMN WITH ONE INTERMEDIATE GIRT

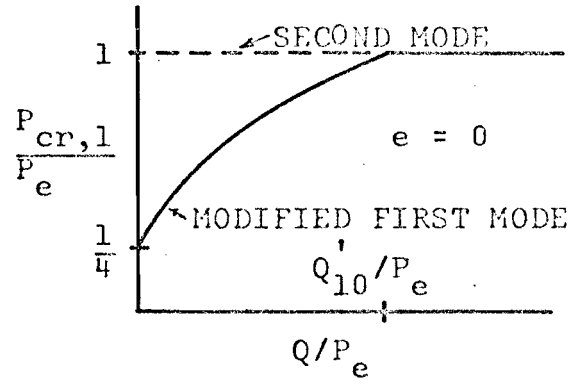

FIG. 3-7 BEHAVIOR OF A COLUMN WITH ONE INTERMEDIATE GIRT, e = 0

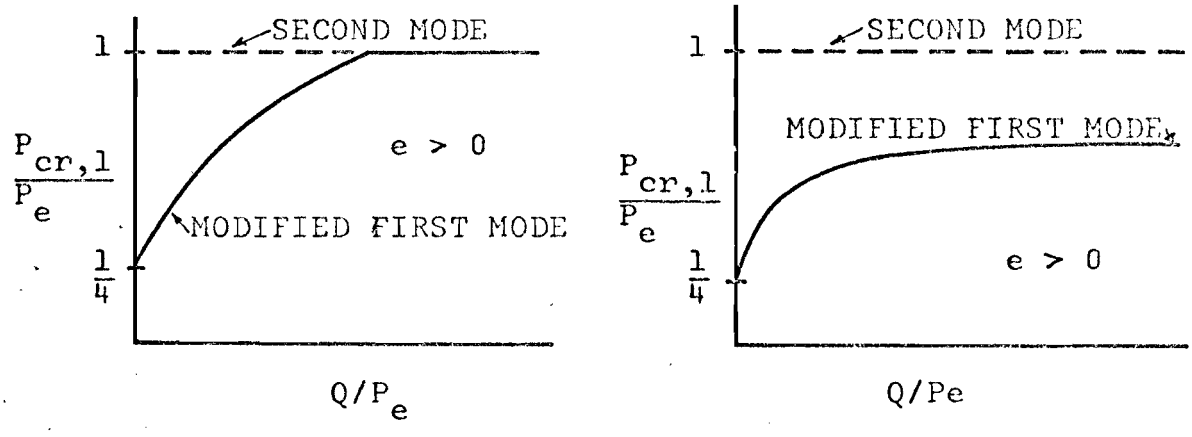

FIG. 3-8 BEHAVIOR OF A COLUMN WITH ONE INTERMEDIATE GIRT, e > 0

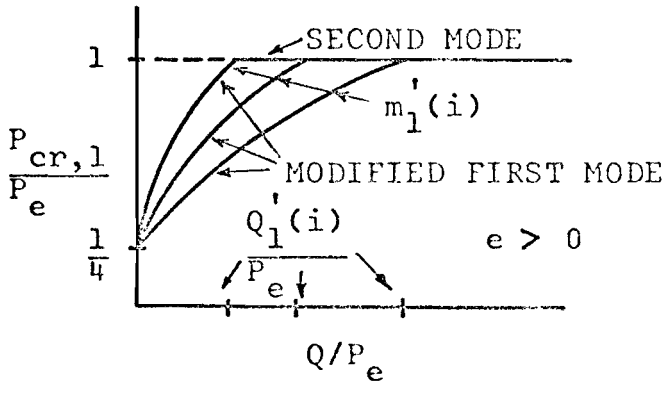

FIG. 3-9 BEHAVIOR OF A COLUMN WITH ONE INTERMEDIATE GIRT FOR DIFFERENT VALUES OF TWIST RESTRAINT m, e > 0

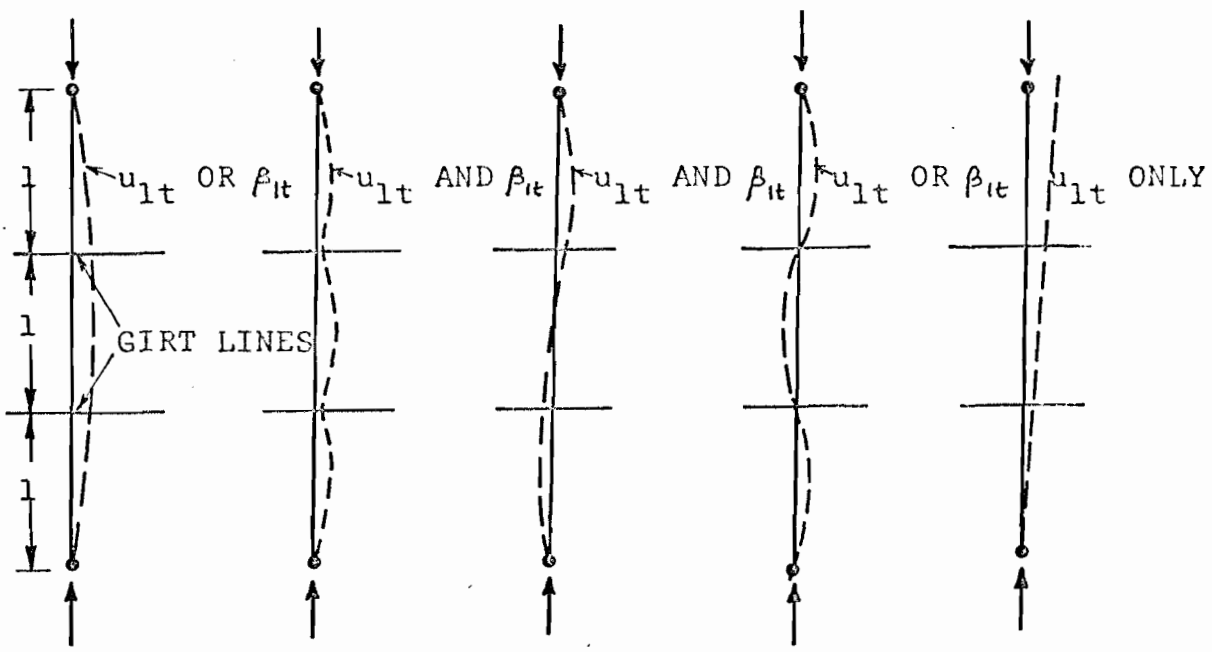

——— INITIAL POSITION; — — — DEFLECTED POSITION

$u_{1t} = u_1$ AND $\beta_{1t} = \beta_1$

FIG. 3-10 IDEAL COLUMN WITH TWO INTERMEDIATE GIRTS

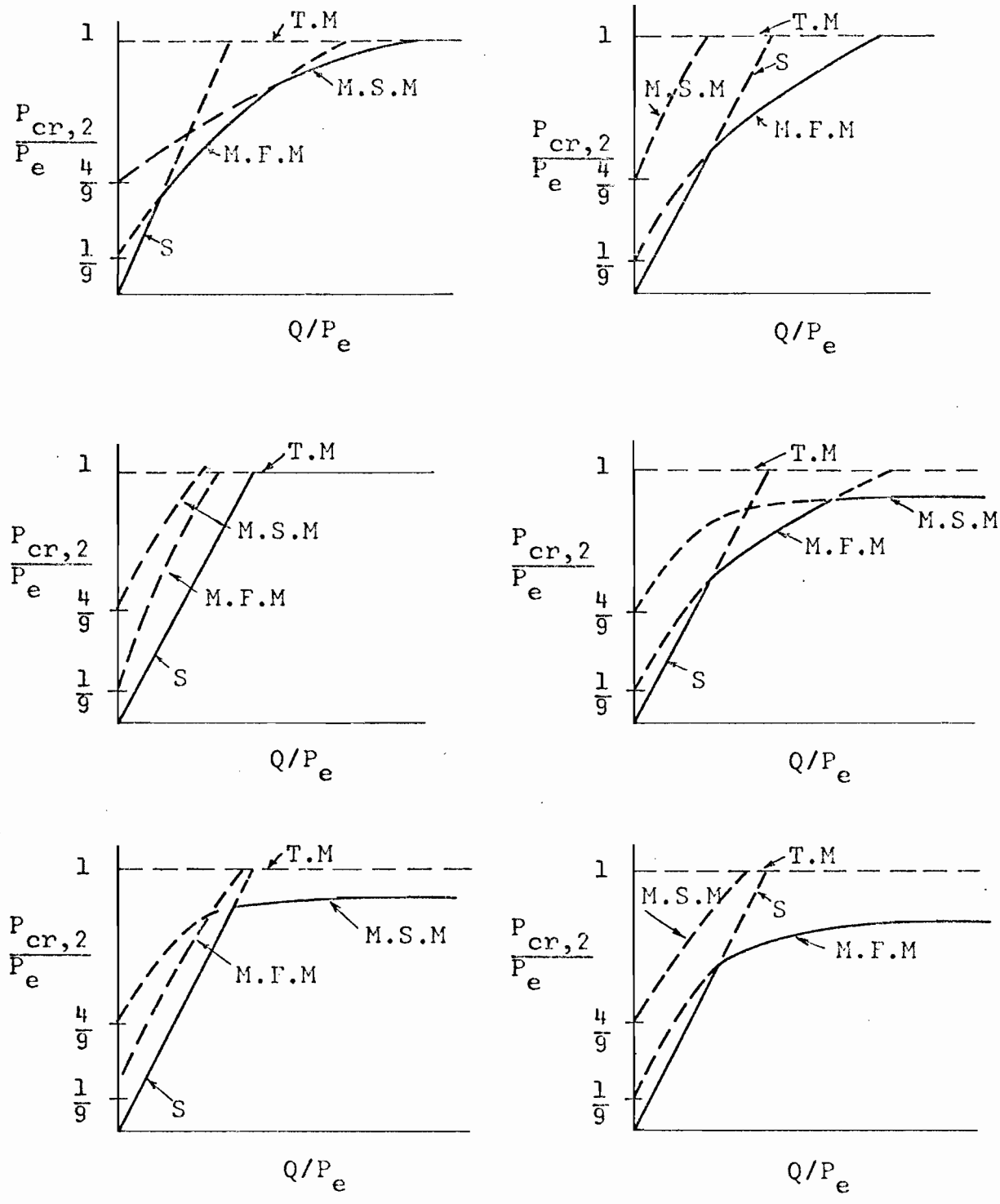

LEGEND:

M.F.M - MODIFIED FIRST MODE; M.S.M - MODIFIED SECOND MODE;
T.M - THIRD MODE; S - SIDESWAY ; $P_e = \frac{\pi^2 E I_y}{\ell^2}$

FIG. 3-11 POSSIBLE TYPES OF BEHAVIOR OF A COLUMN WITH TWO INTERMEDIATE GIRTS

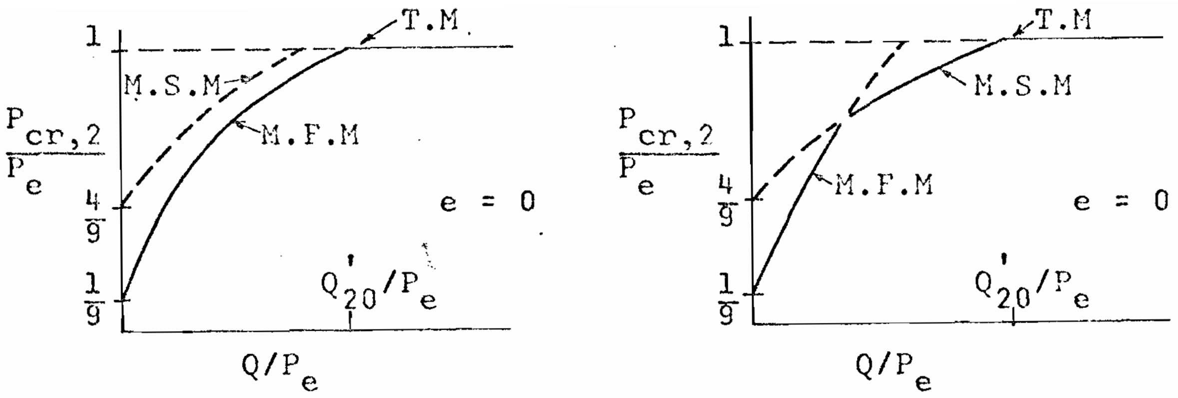

FIG. 3-12 BEHAVIOR OF A COLUMN WITH TWO INTERMEDIATE GIRTS, e=0

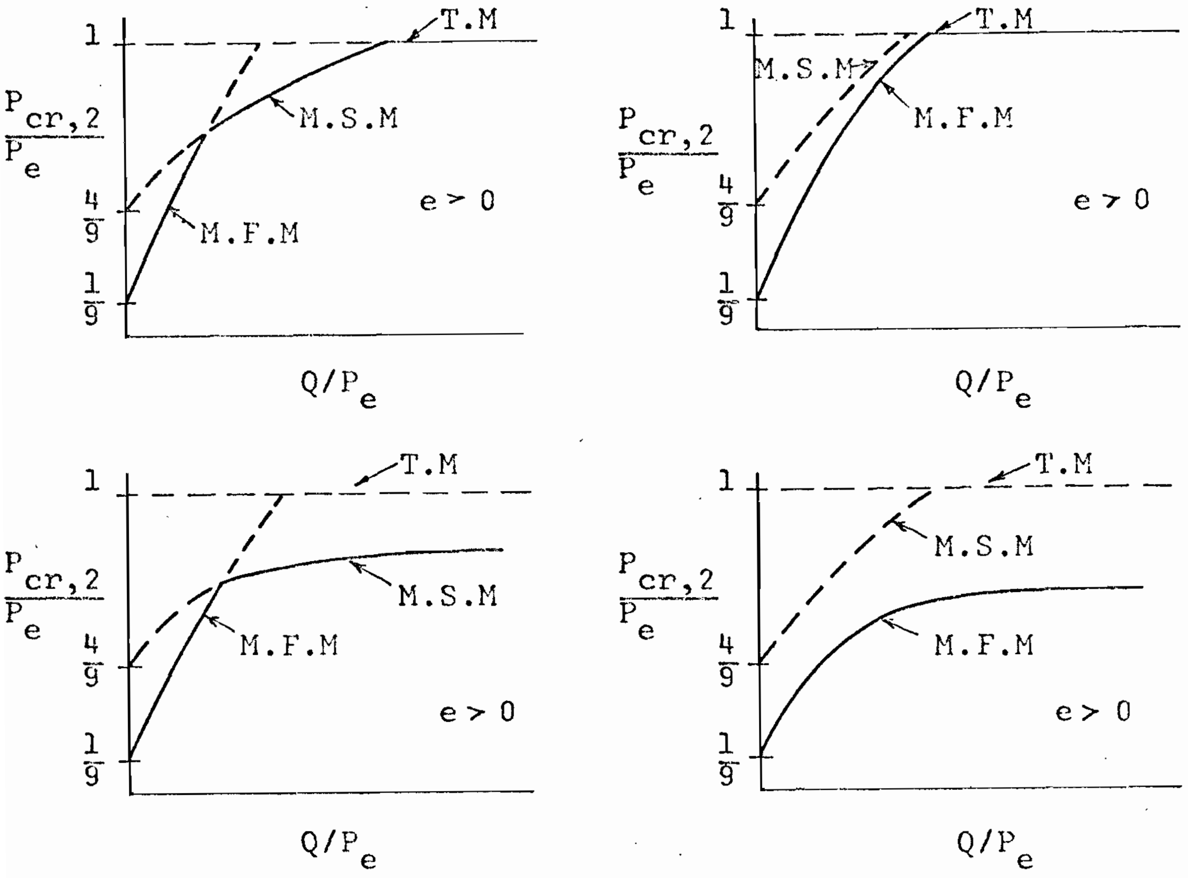

LEGEND FOR FIGS. 3-12 AND 3-13:

M.F.M - MODIFIED FIRST MODE; M.S.M - MODIFIED SECOND MODE;

T.M - THIRD MODE; $P_e = \frac{\pi^2 EI_y}{\ell^2}$

FIG. 3-13 BEHAVIOR OF A COLUMN WITH TWO INTERMEDIATE GIRTS, e > 0

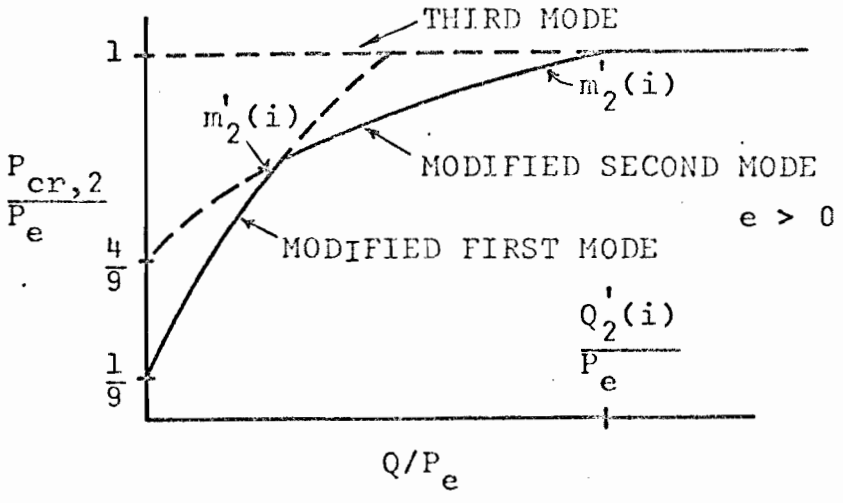

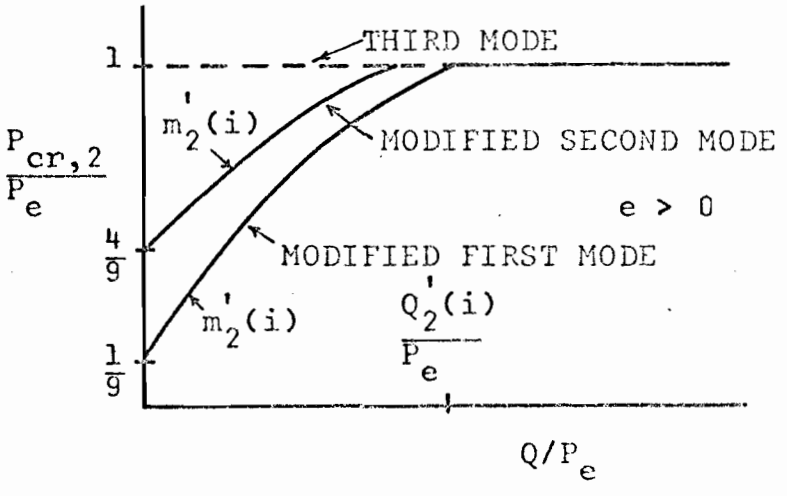

FIG. 3-14 BEHAVIOR OF A COLUMN WITH TWO INTERMEDIATE GIRTS FOR THE TWIST RESTRAINT, $m_2'(i)$; e > 0

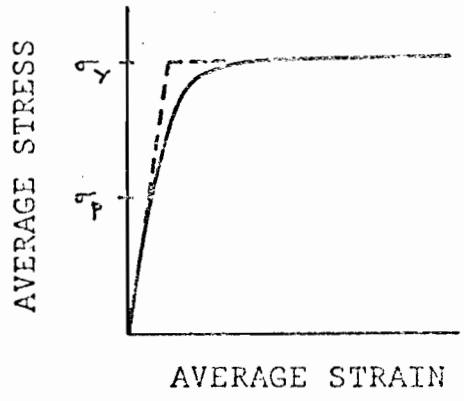

FIG. 3-15 TYPICAL STRESS-STRAIN DIAGRAM

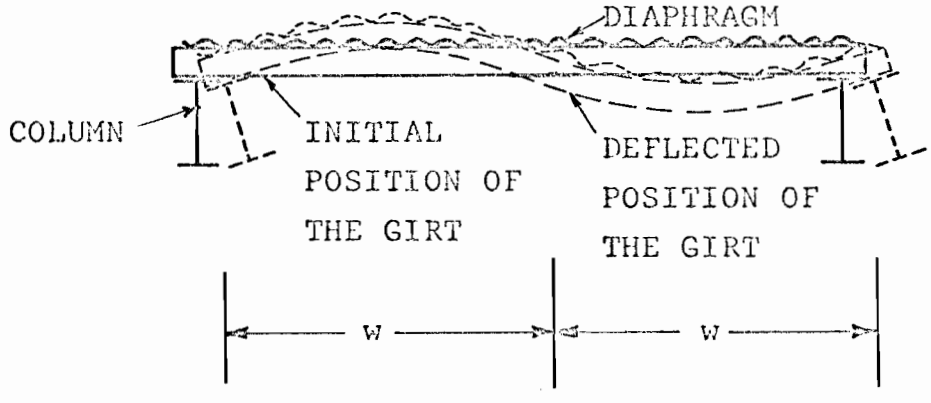

FIG. 3-16 DEFLECTED SHAPE OF A GIRT

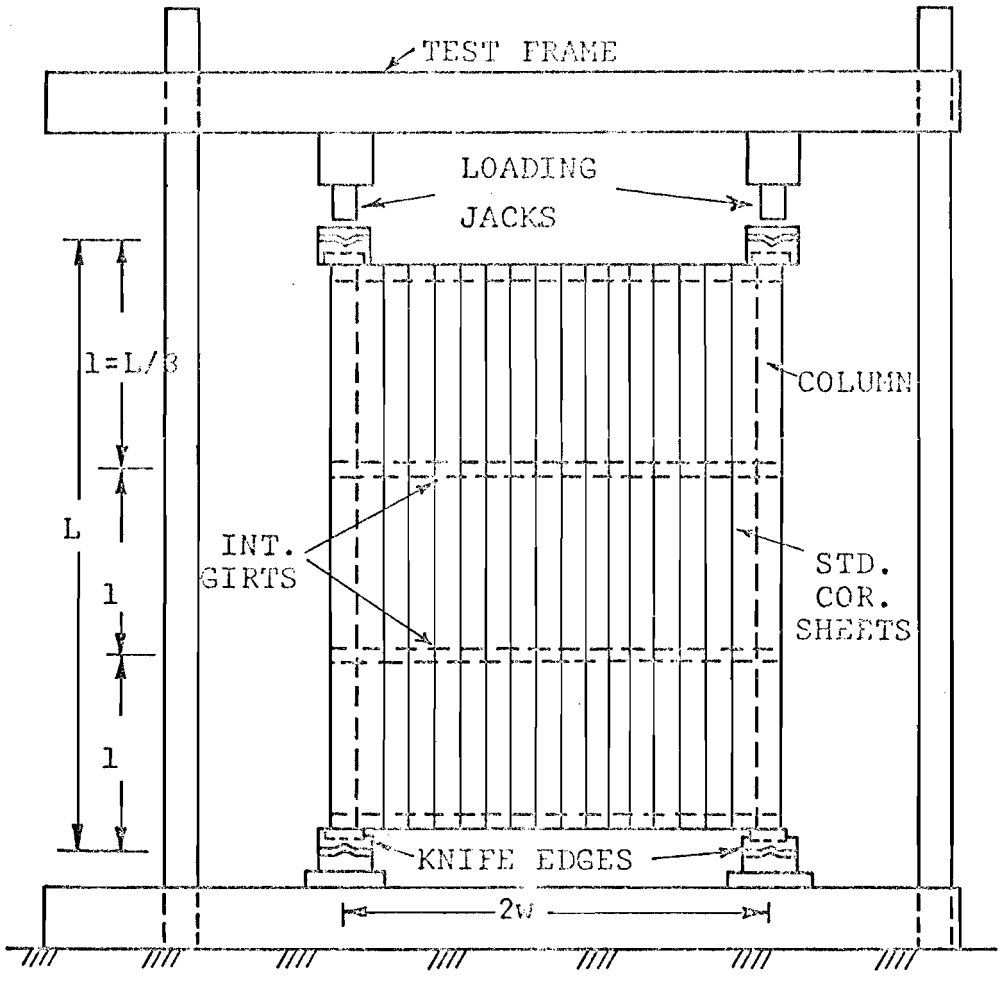

ELEVATION

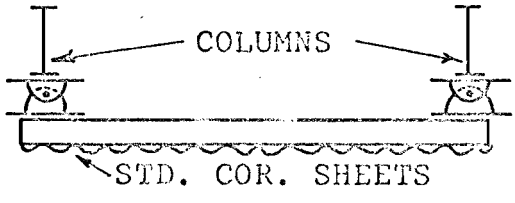

CONNECTION FOR TEST GT-1 (PLAN)

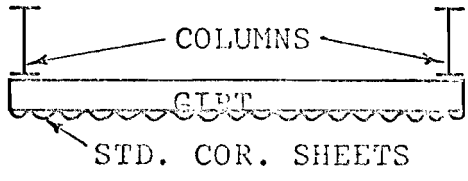

CONNECTION FOR TEST GT-2 (PLAN)

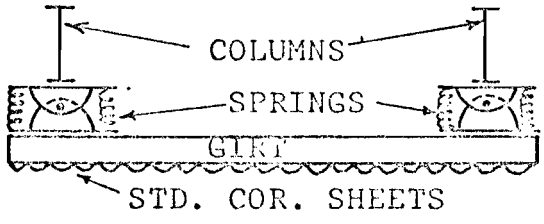

CONNECTION FOR TEST GT-3 (PLAN)

FIG. 3-17 TEST SETUP FOR COLUMNS

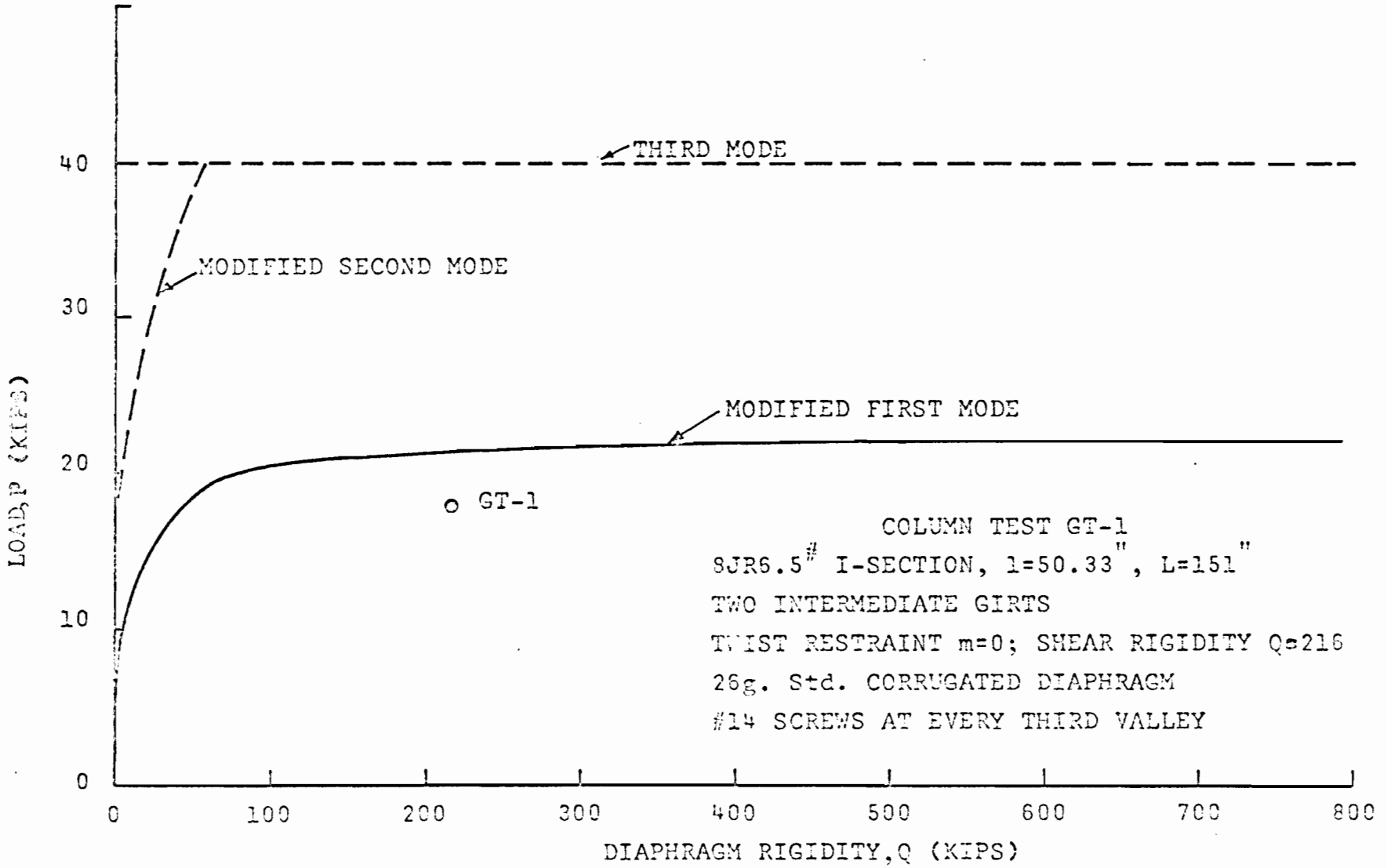

FIG. 3-18 COMPARISON OF FAILURE LOAD WITH THE PREDICTED LOAD OF AN 8JR6.5 I-SECTION COLUMN

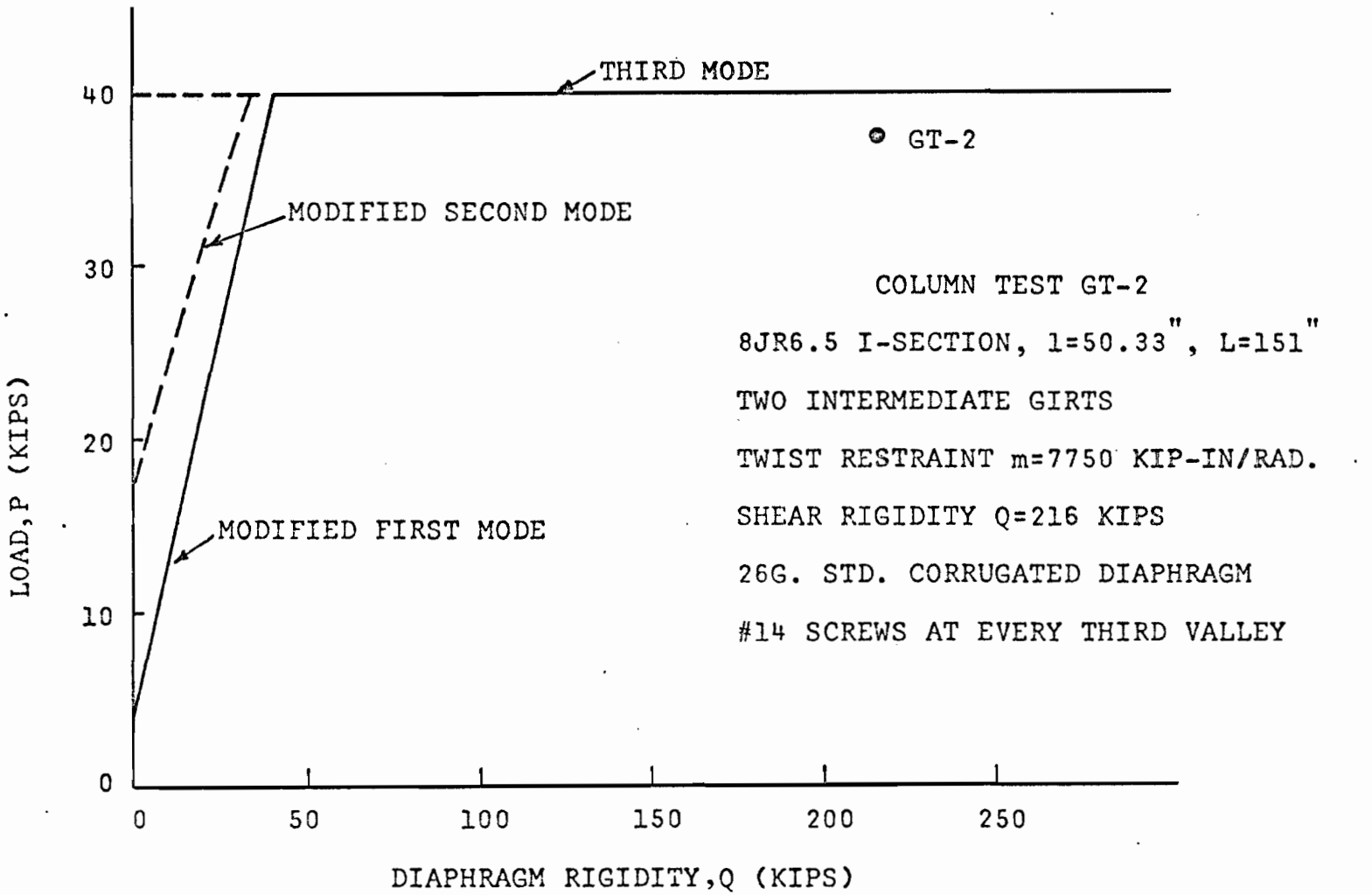

FIG. 3-19 COMPARISON OF FAILURE LOAD WITH THE PREDICTED CRITICAL LOAD OF AN 8JR6.5 I-SECTION COLUMN

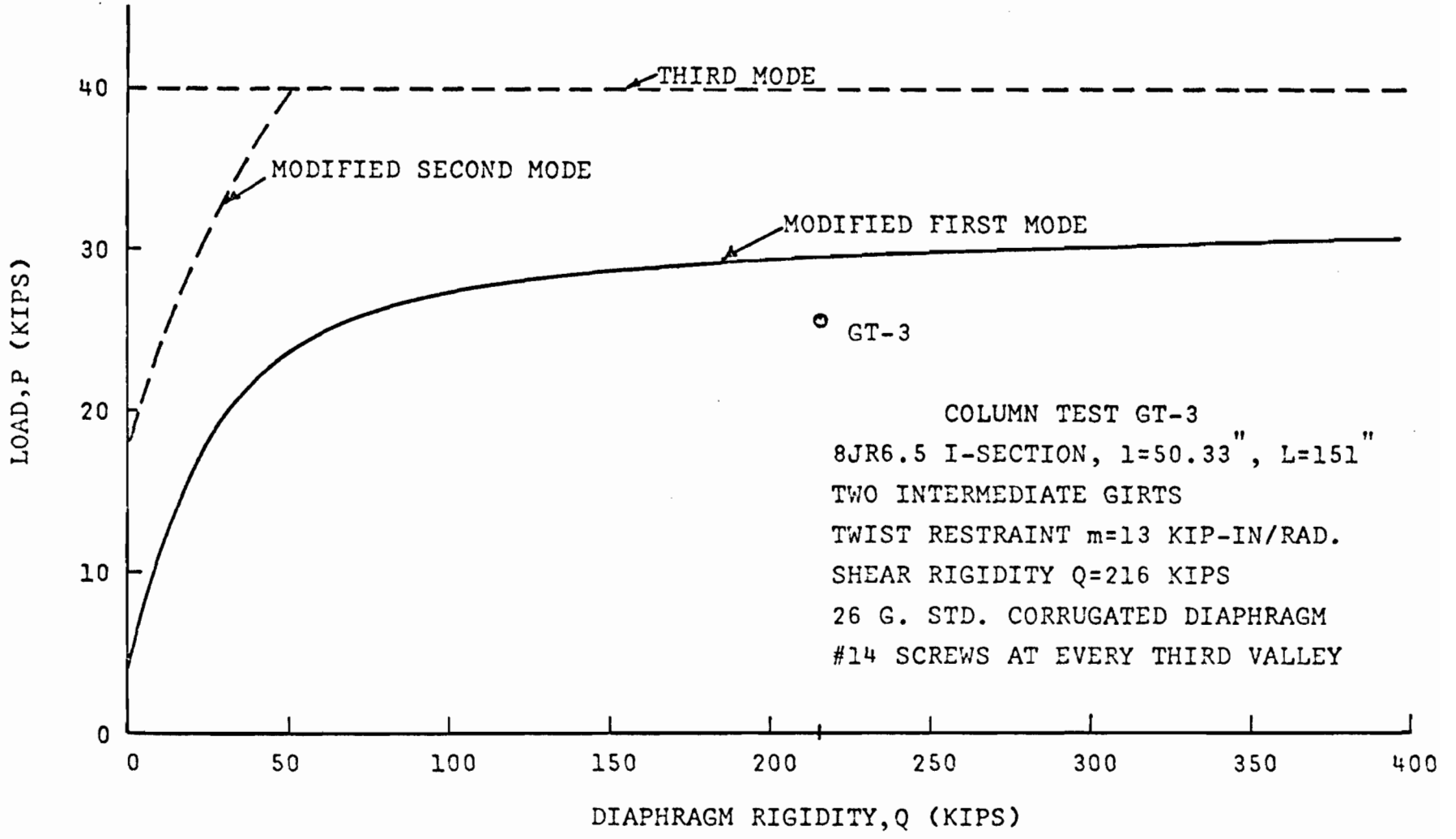

FIG. 3-20 COMPARISON OF FAILURE LOAD WITH THE PREDICTED CRITICAL LOAD OF AN 8JR6.5 I-SECTION COLUMN

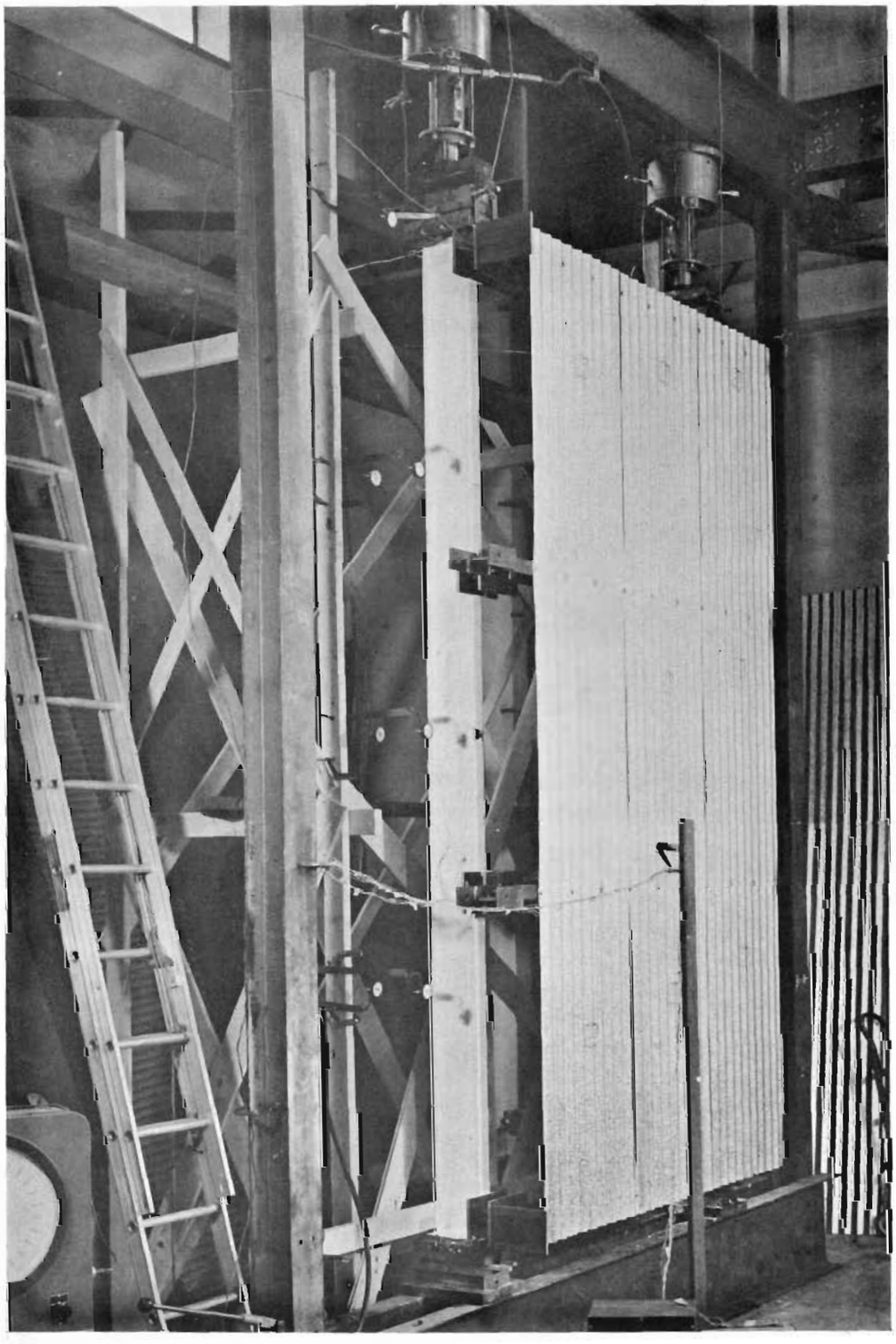

FIG. 3-21 COLUMN-GIRT-DIAPHRAGM ASSEMBLY BEFORE FAILURE, TEST GT-1

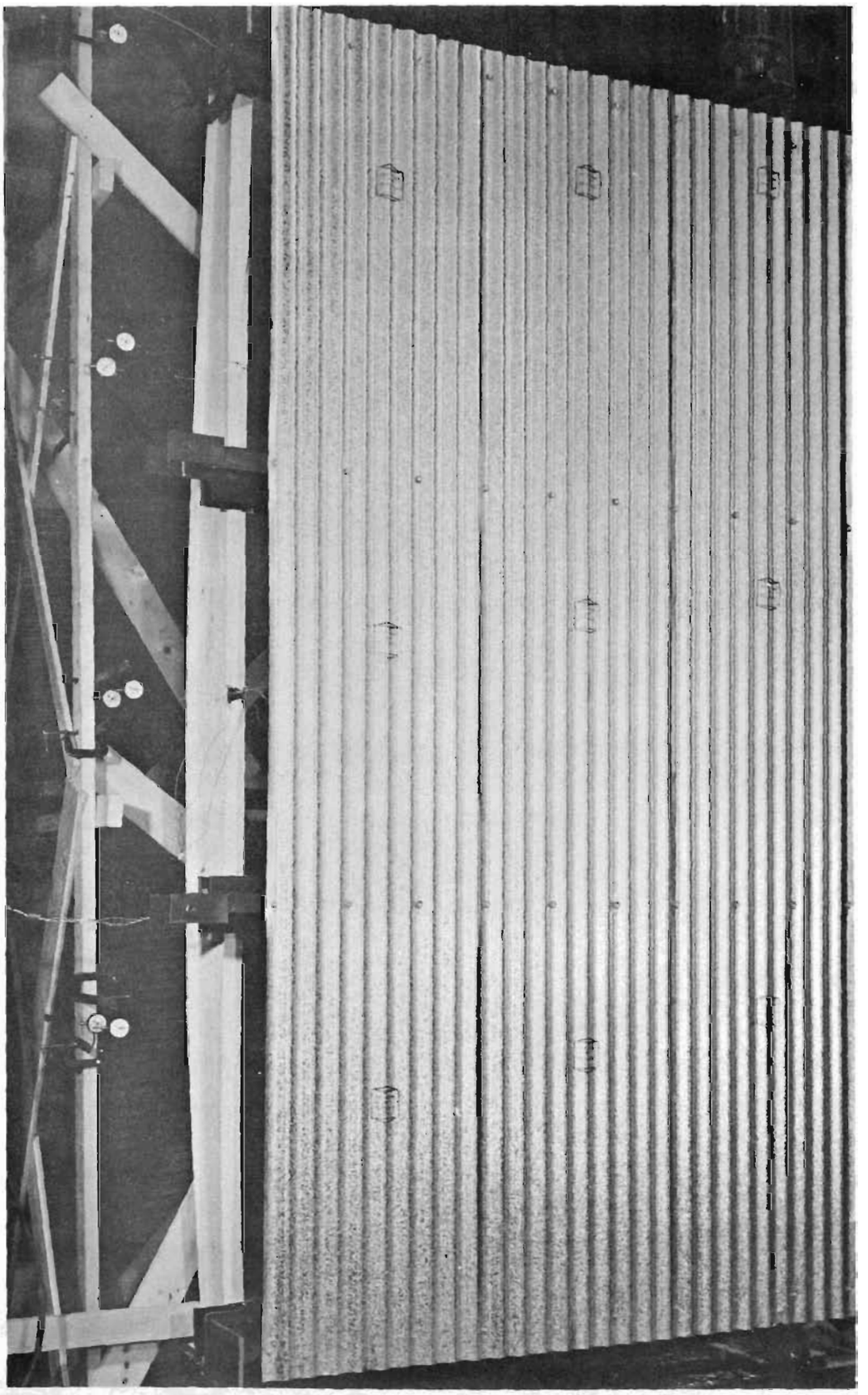

FIG. 3-22 COLUMN-GIRT-DIAPHRAGM ASSEMBLY AFTER FAILURE, TEST GT-1

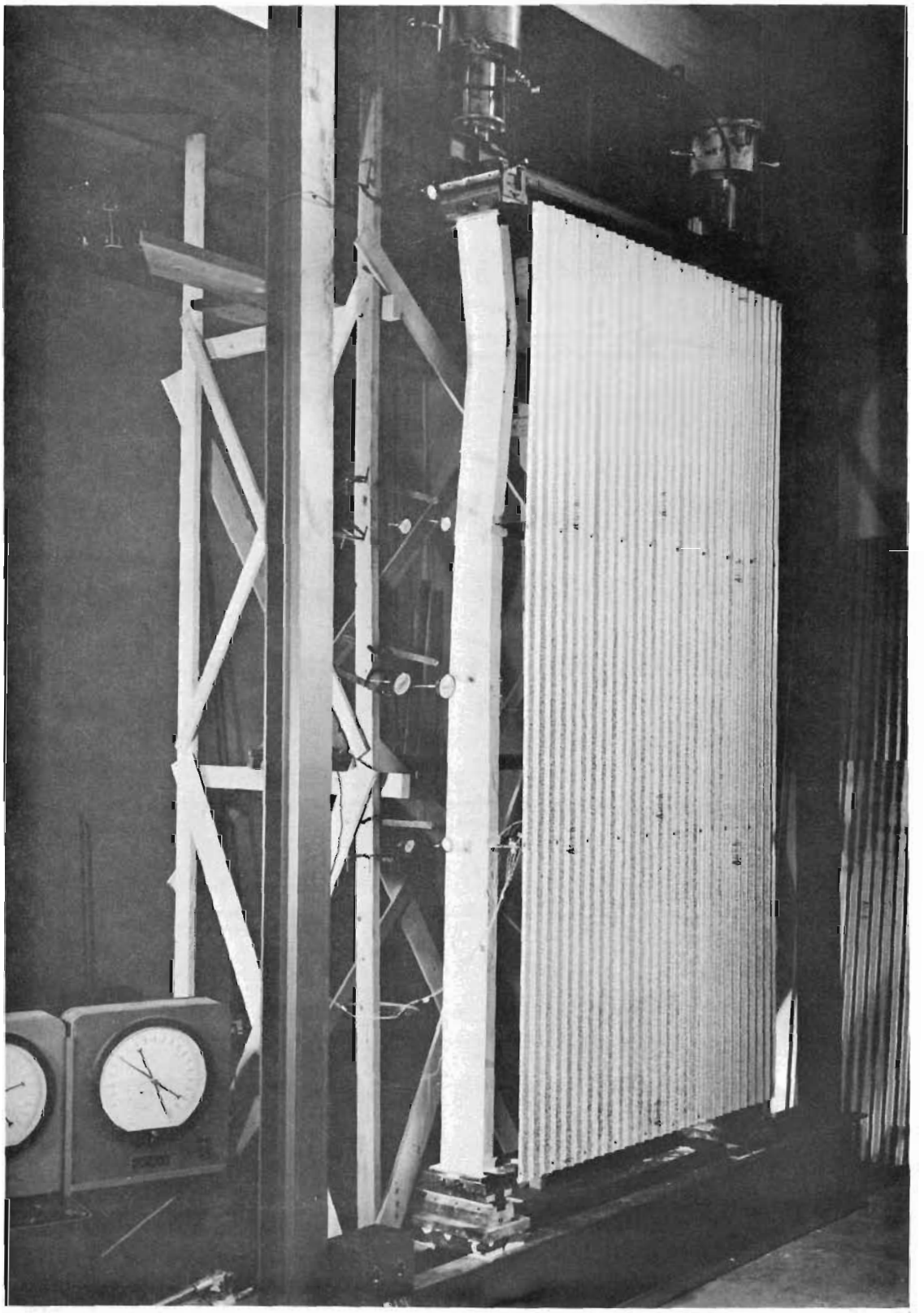

FIG. 3-23 COLUMN-GIRT-DIAPHRAGM ASSEMBLY AFTER FAILURE, TEST GT-2

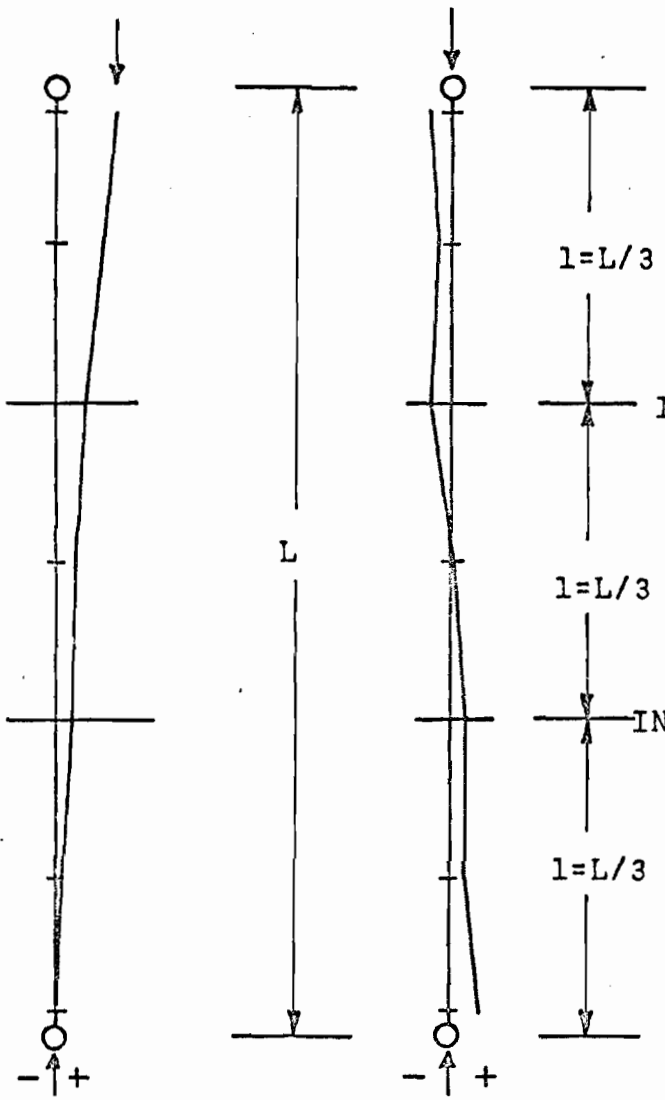

LATERAL DEFLECTION
SCALE 1"=2"

TWIST
SCALE 1"=0.1 RAD.

FIG. 3-24 IMPERFECTIONS AT 0.2 KIP LOAD OF 8JR6.5 I-SECTION COLUMN IN TEST GT-3

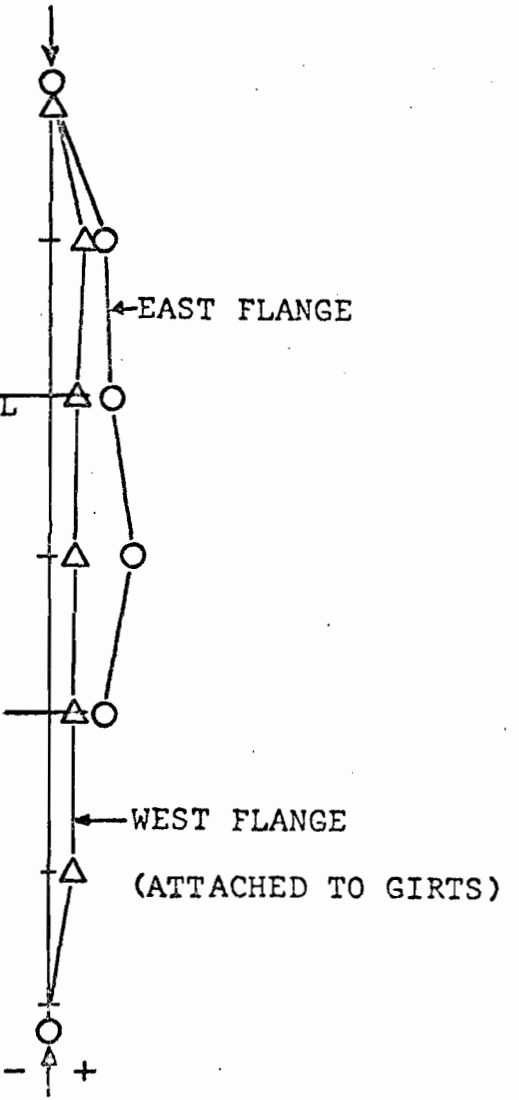

LATERAL DEFLECTION
SCALE 1"=2"

FIG. 3-25 DEFLECTION PATTERN AT 23 KIP LOAD LEVEL OF 8JR6.5 I-SECTION COLUMN IN TEST GT-3

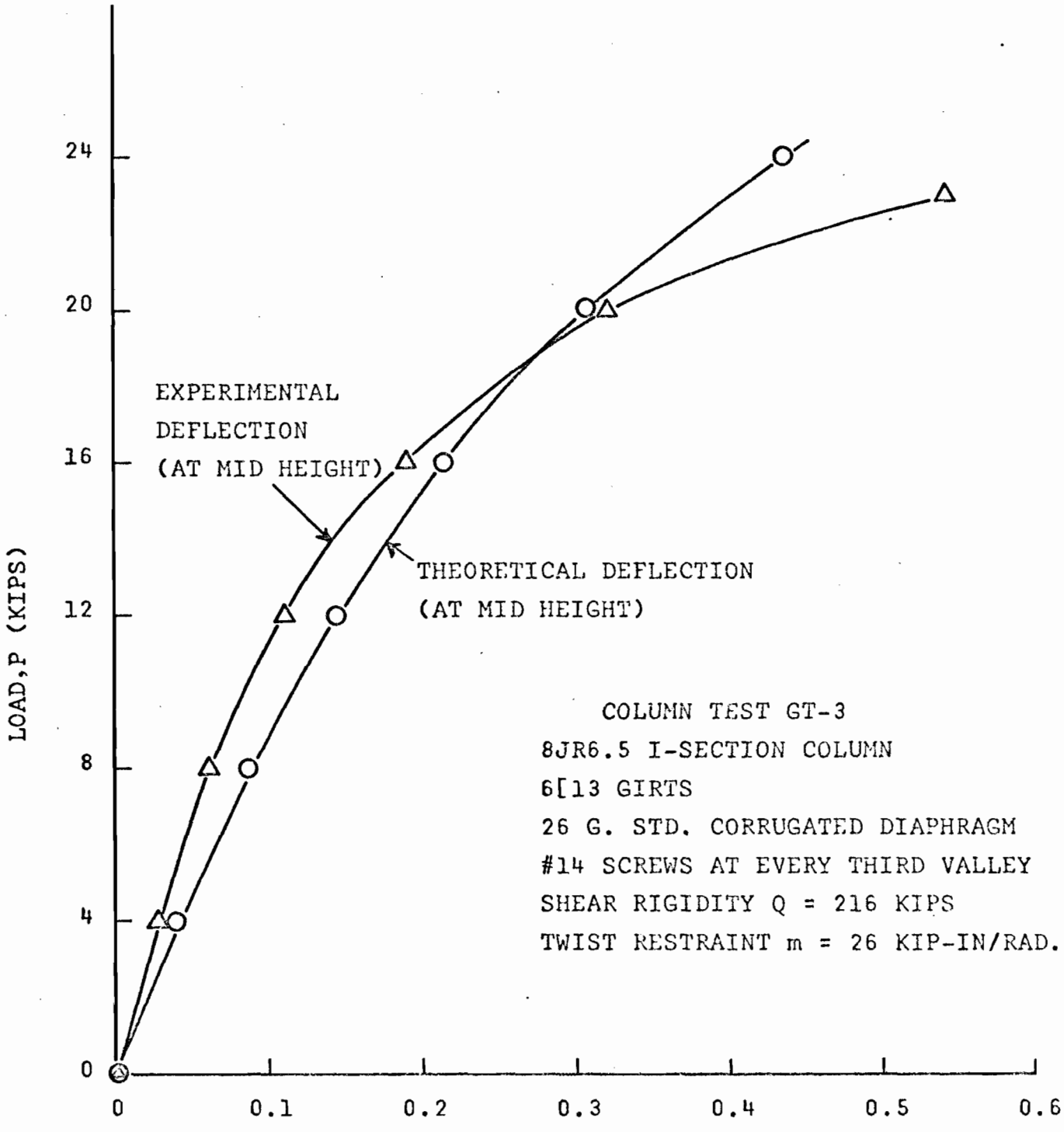

FIG. 3-26 LOAD-DEFLECTION CURVES FOR NORTH COLUMN, COLUMN TEST GT-3

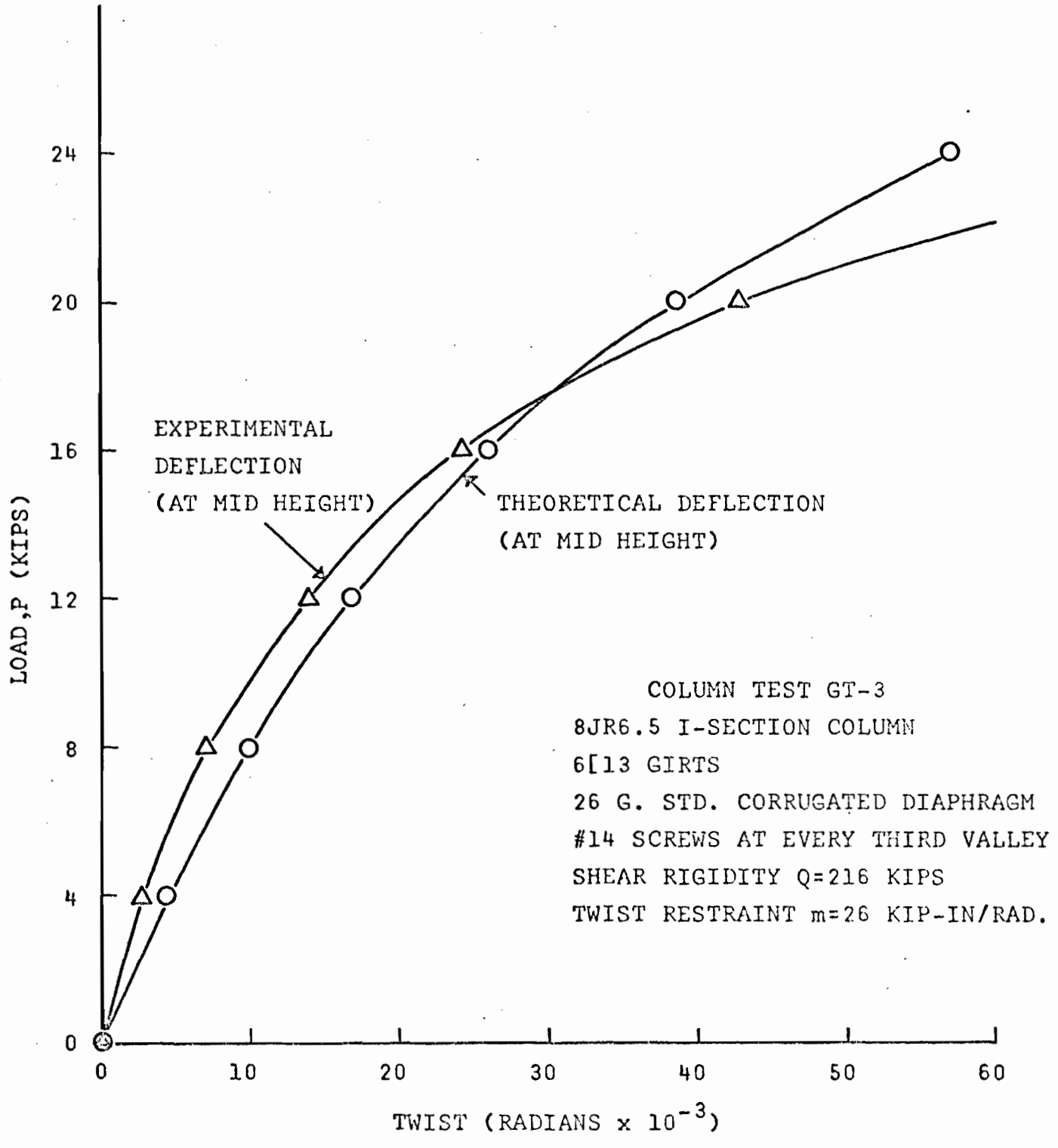

FIG. 3-27 LOAD-DEFLECTION CURVES FOR NORTH COLUMN, COLUMN TEST GT-3

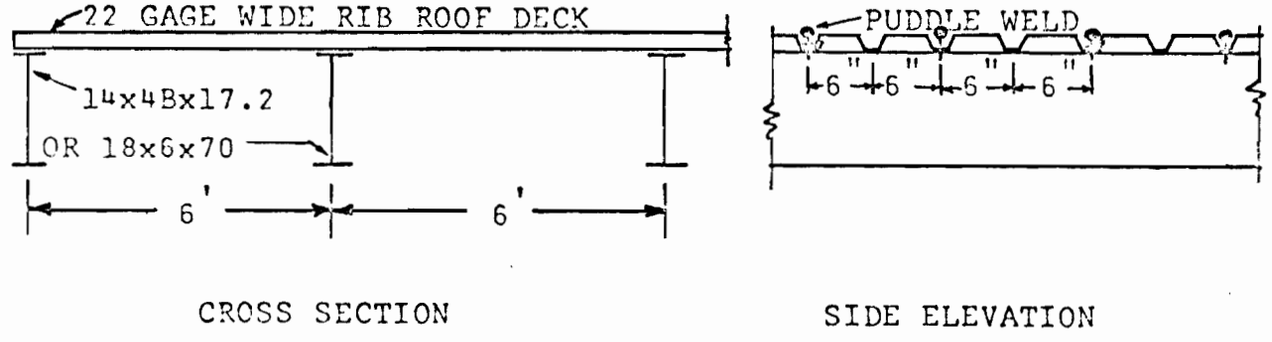

FIG. II-1 ARRANGEMENT OF BEAMS AND DIAPHRAGM

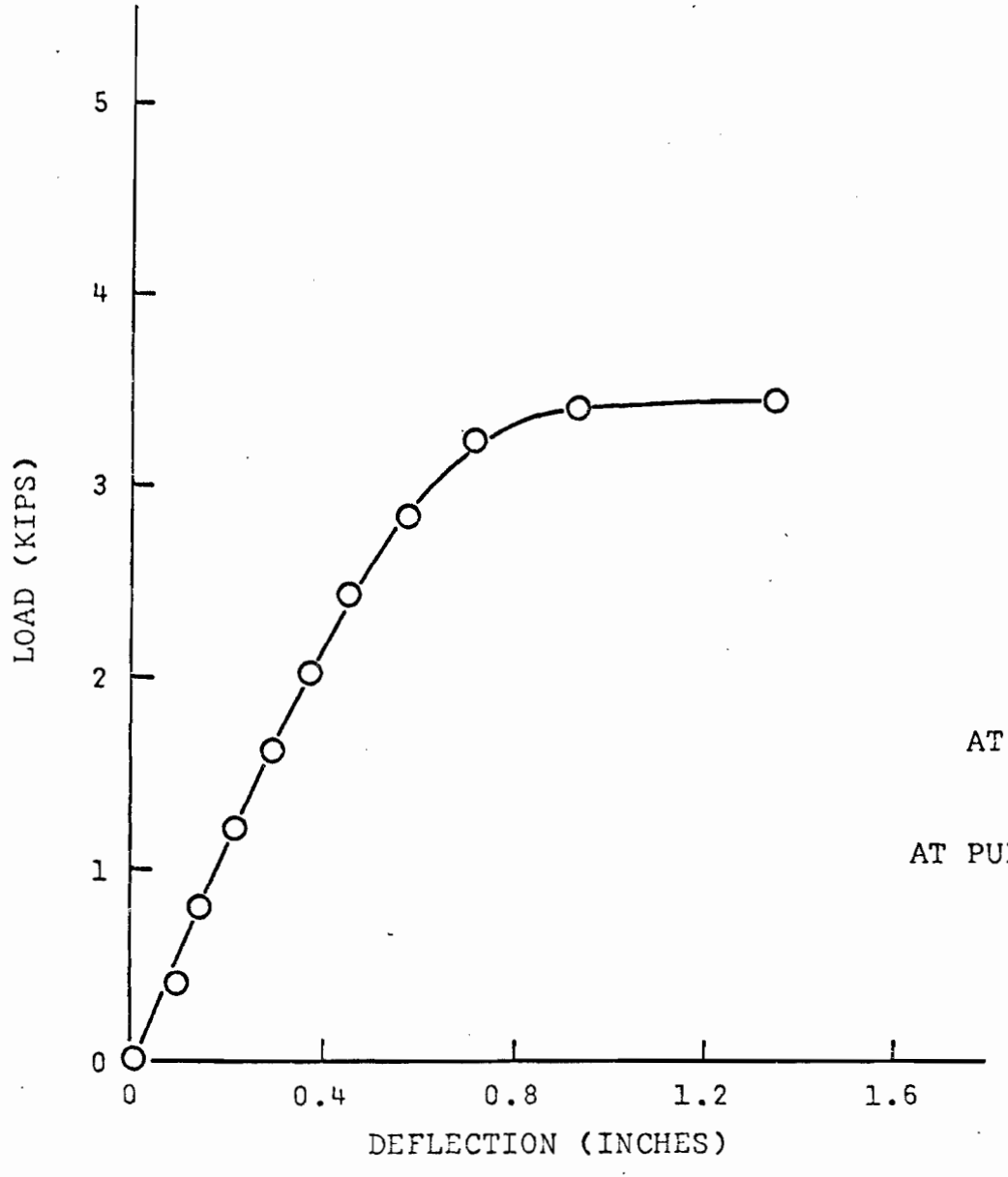

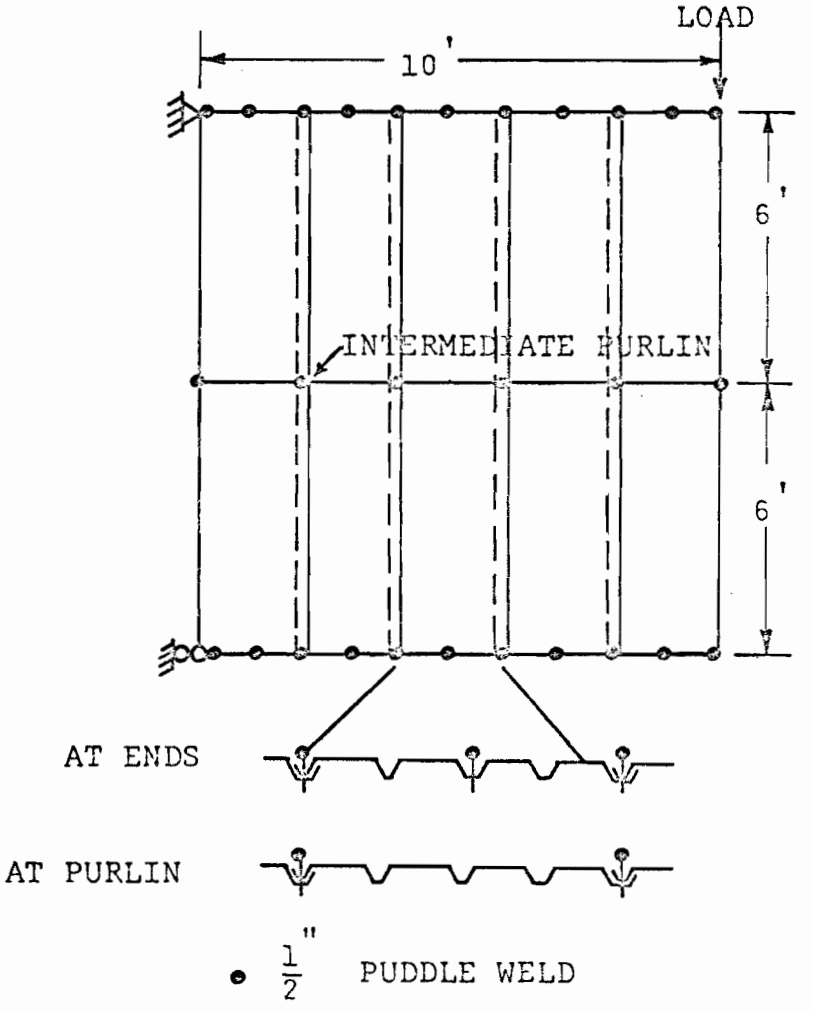

FIG. II-2 22 GAGE WIDE RIB ROOF DECK

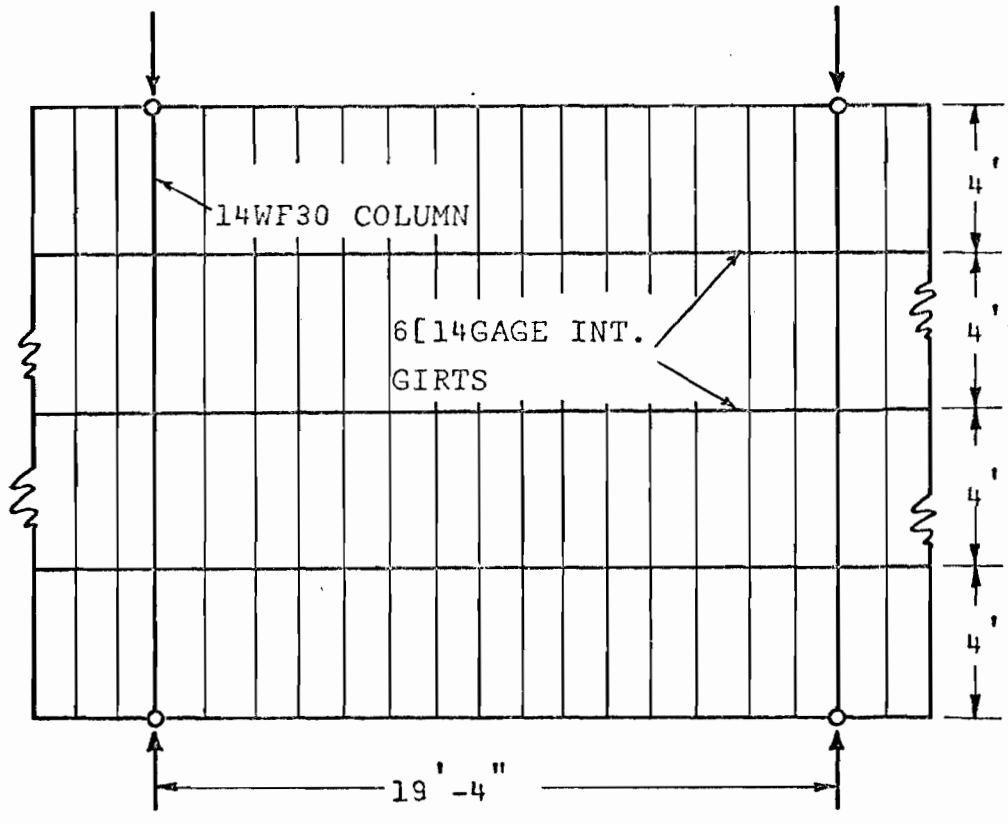

ELEVATION

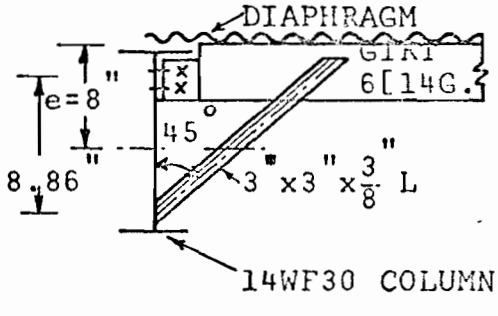

CONNECTION TYPE - I

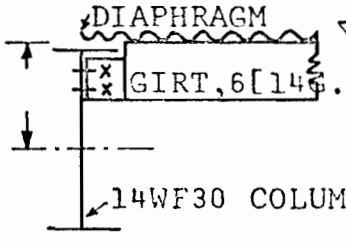

CONNECTION TYPE - II

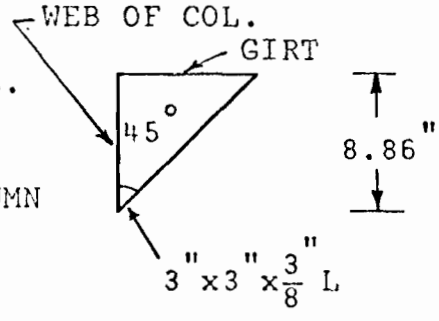

MODEL OF CONNECTION TYPE-I

FIG. III-1 SKETCH FOR EXAMPLE - 1

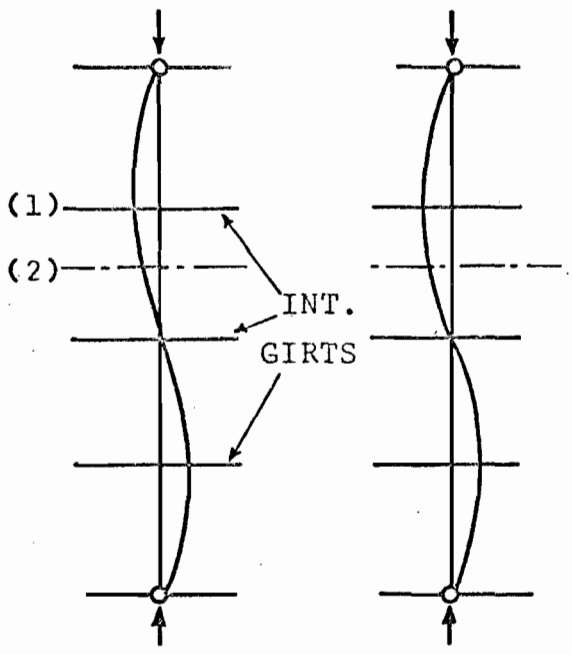

FIG. III-2 DEFLECTION OF THE COLUMN IN EXAMPLE 1, m=2325 K-IN/RAD.

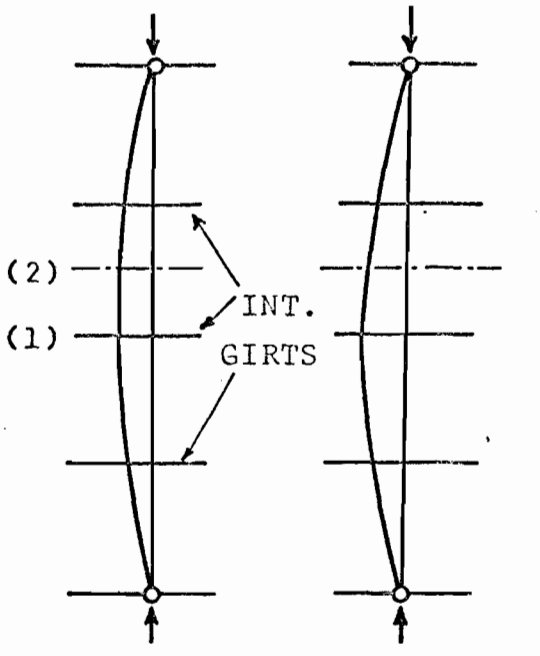

FIG. III-3 DEFLECTION OF THE COLUMN IN EXAMPLE 1, m=0 K-IN/RAD.

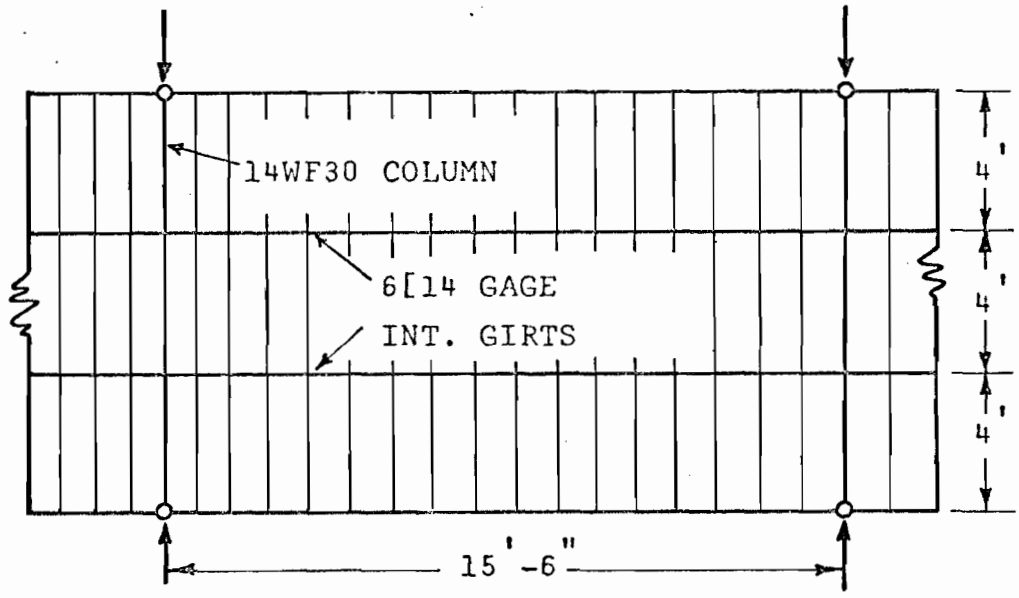

ELEVATION

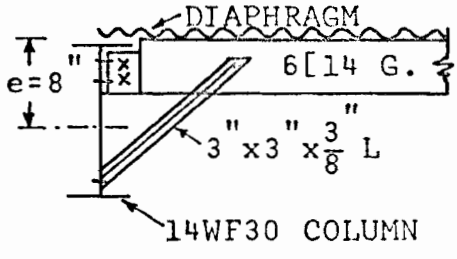

GIRT-COLUMN CONNECTION

FIG. III-4 SKETCH FOR EXAMPLE - 2

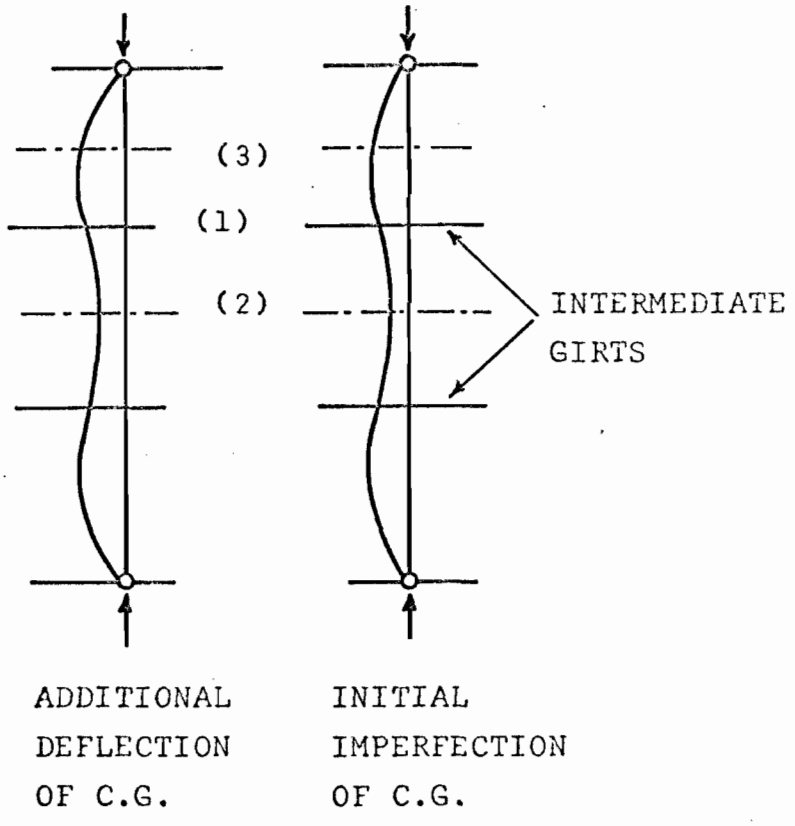

FIG. III-5 DEFLECTION OF THE COLUMN IN EXAMPLE-2

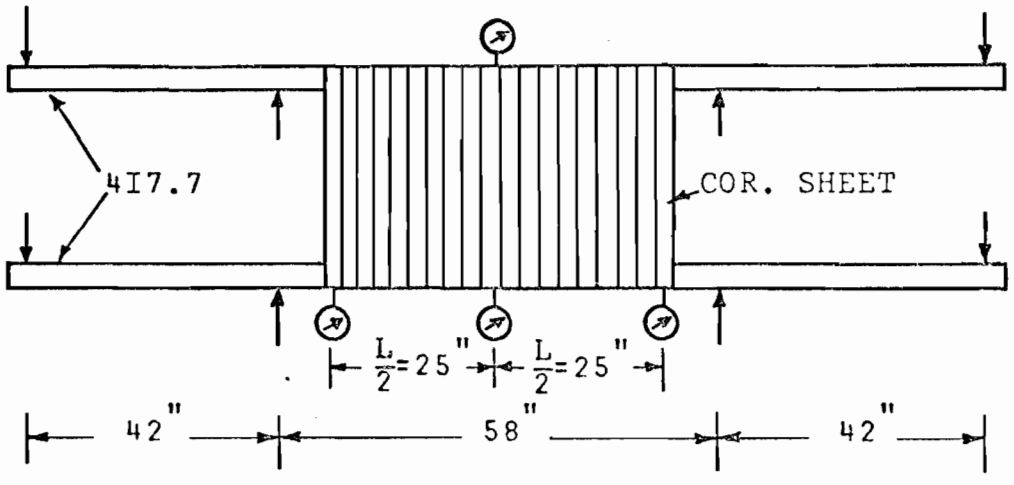

FIG. IV-1 SKETCH OF DOUBLE-BEAM SHEAR TEST SETUP

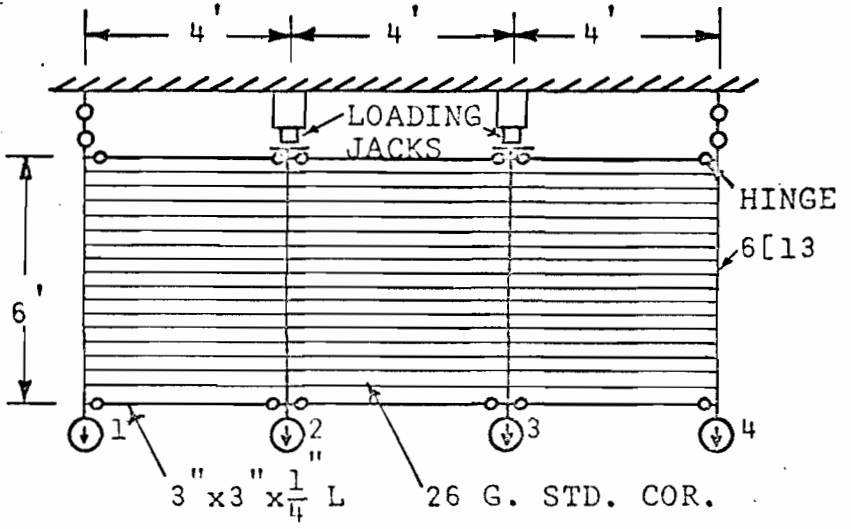

CONNECTION: #14 SCREWS AT EVERY THIRD VALLEY

FIG. IV-2 SIMPLE BEAM SHEAR TEST ARRANGEMENT

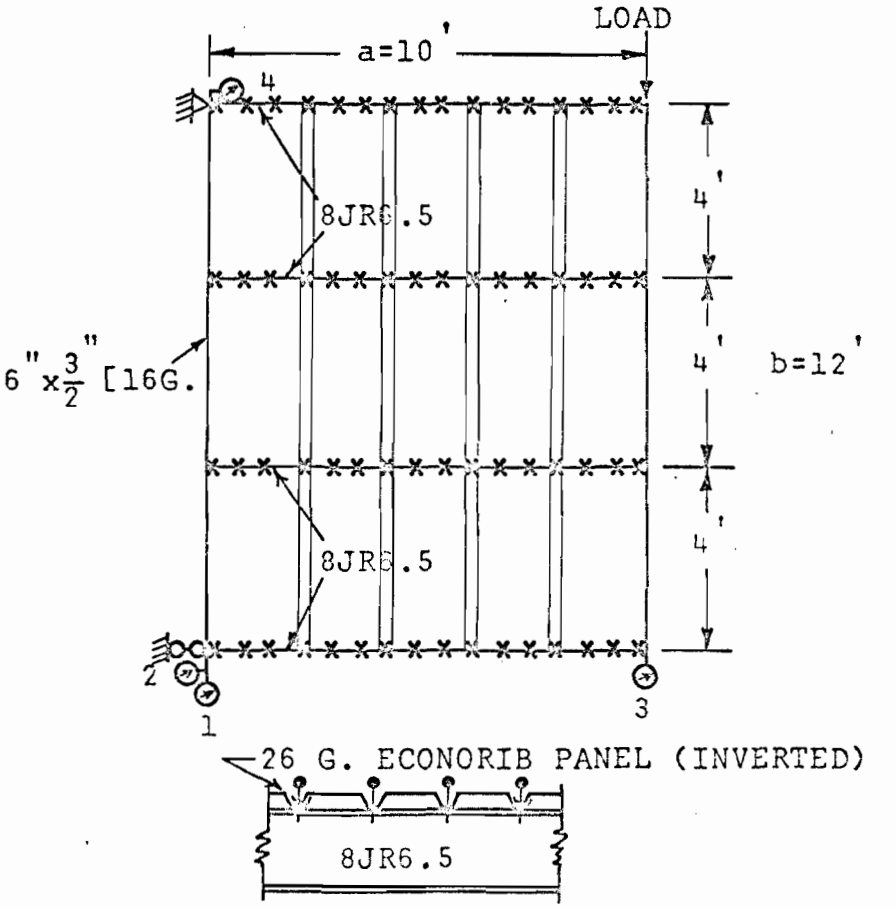

x #14 SCREWS

FIG. IV-3 CANTILEVER SHEAR TEST ARRANGEMENT

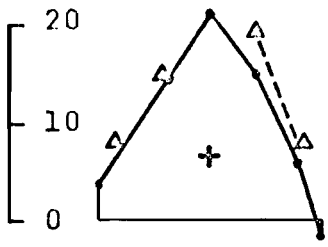

STRIPS

(+) = TENSION

(—) = COMPRESSION

△ = PRIMED POINTS

• = OTHER POINTS

STRESS SCALE 1" = 20 KSI

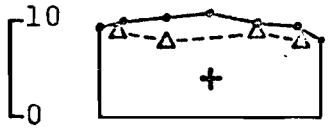

11" CUT

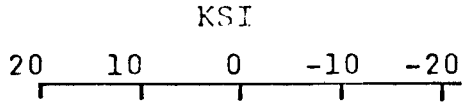

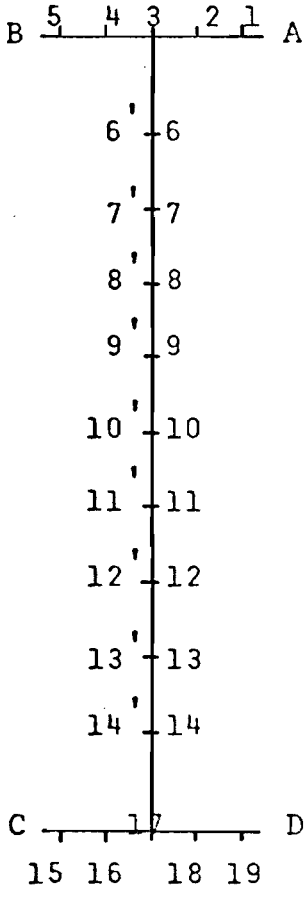

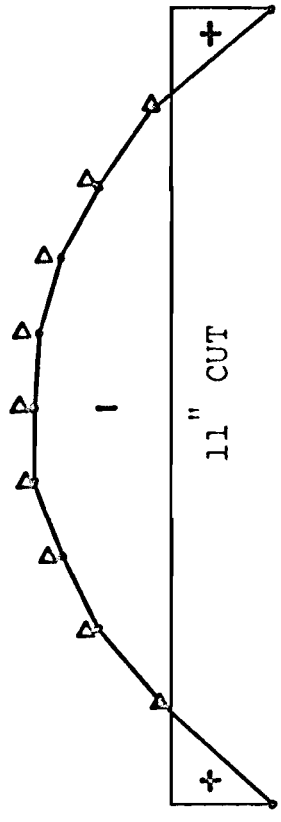

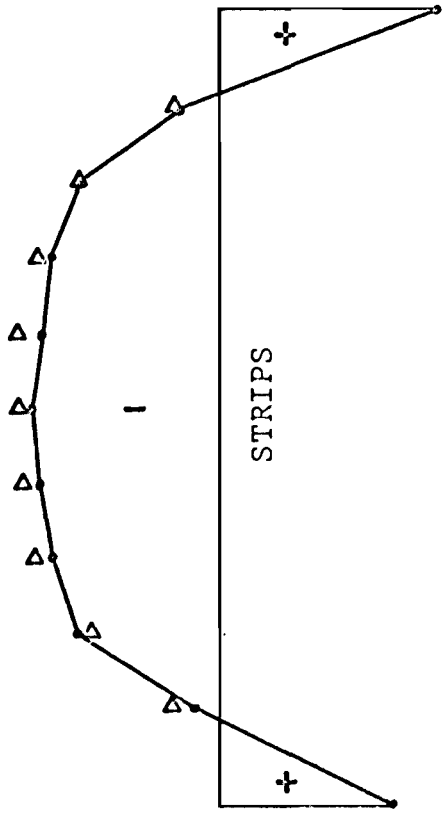

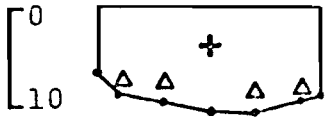

11" CUT

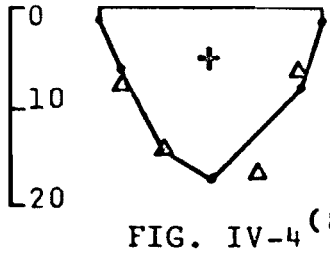

STRIPS

FIG. IV-4[8] RESIDUAL STRESSES IN 8JR6.5 SECTION, BEAM A

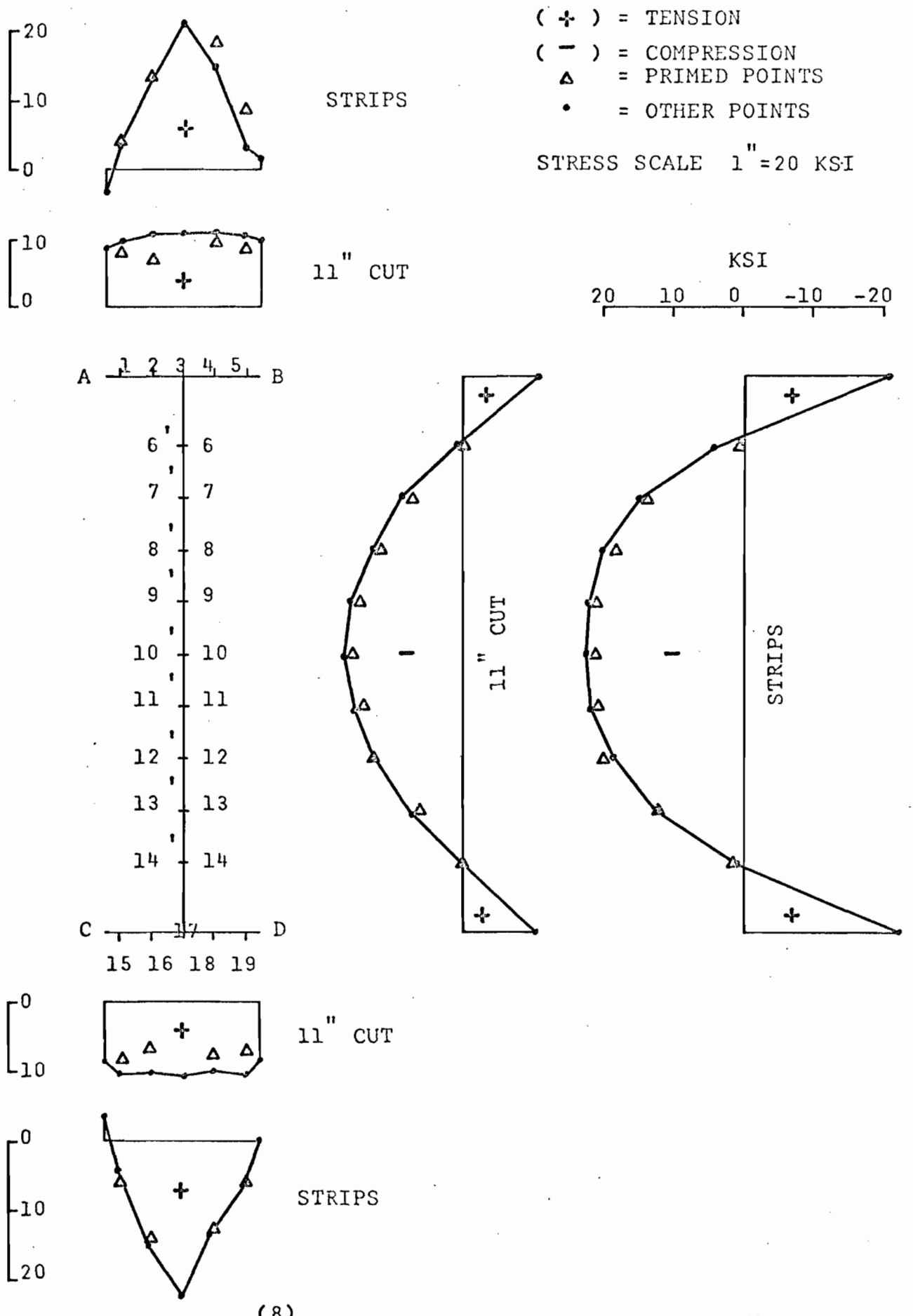

FIG. IV-5[8] RESIDUAL STRESSES IN 8JR6.5 SECTION, BEAM D

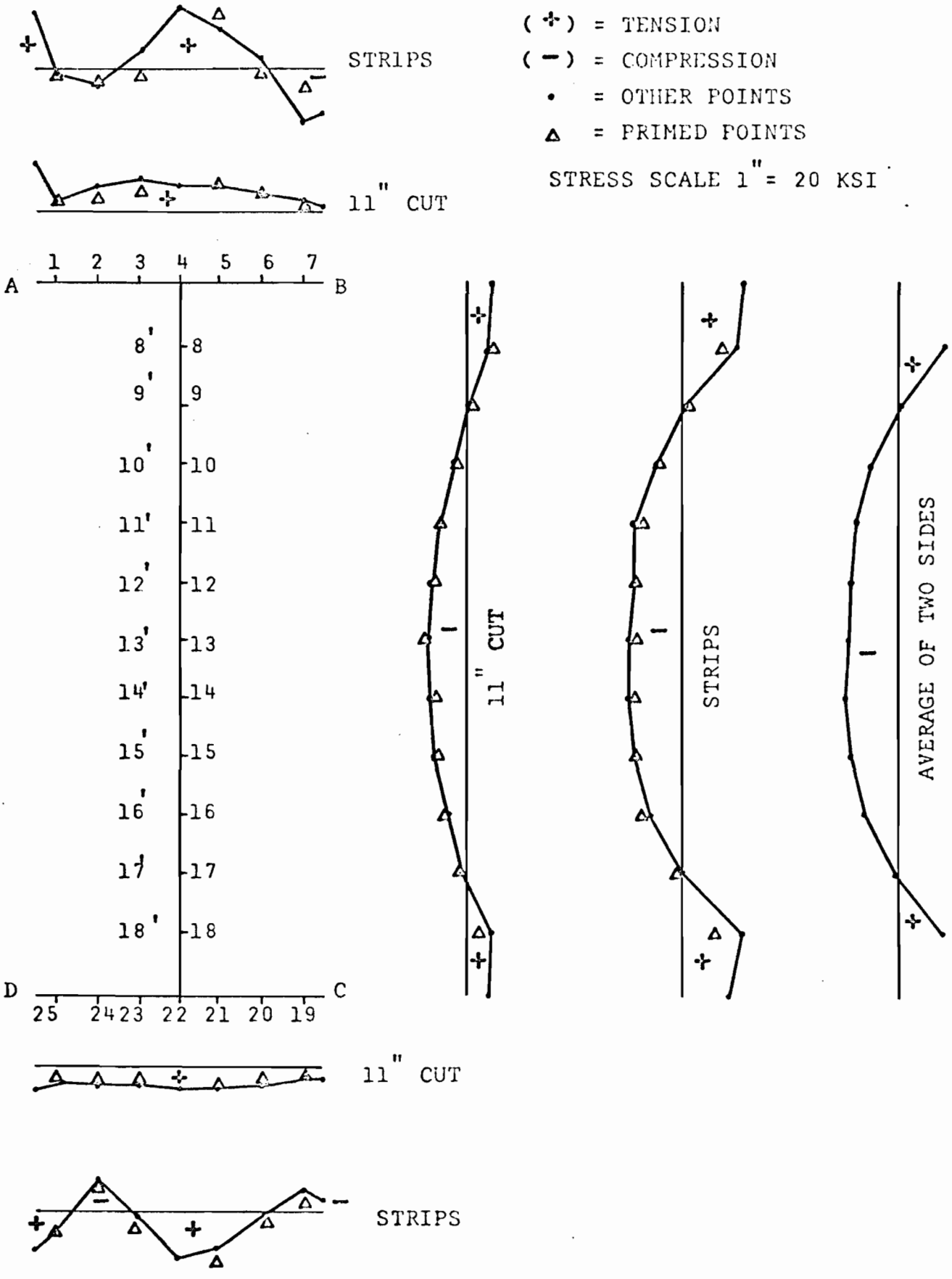

FIG. IV-6[8] RESIDUAL STRESSES IN 10B17 I-SECTION, BEAM A

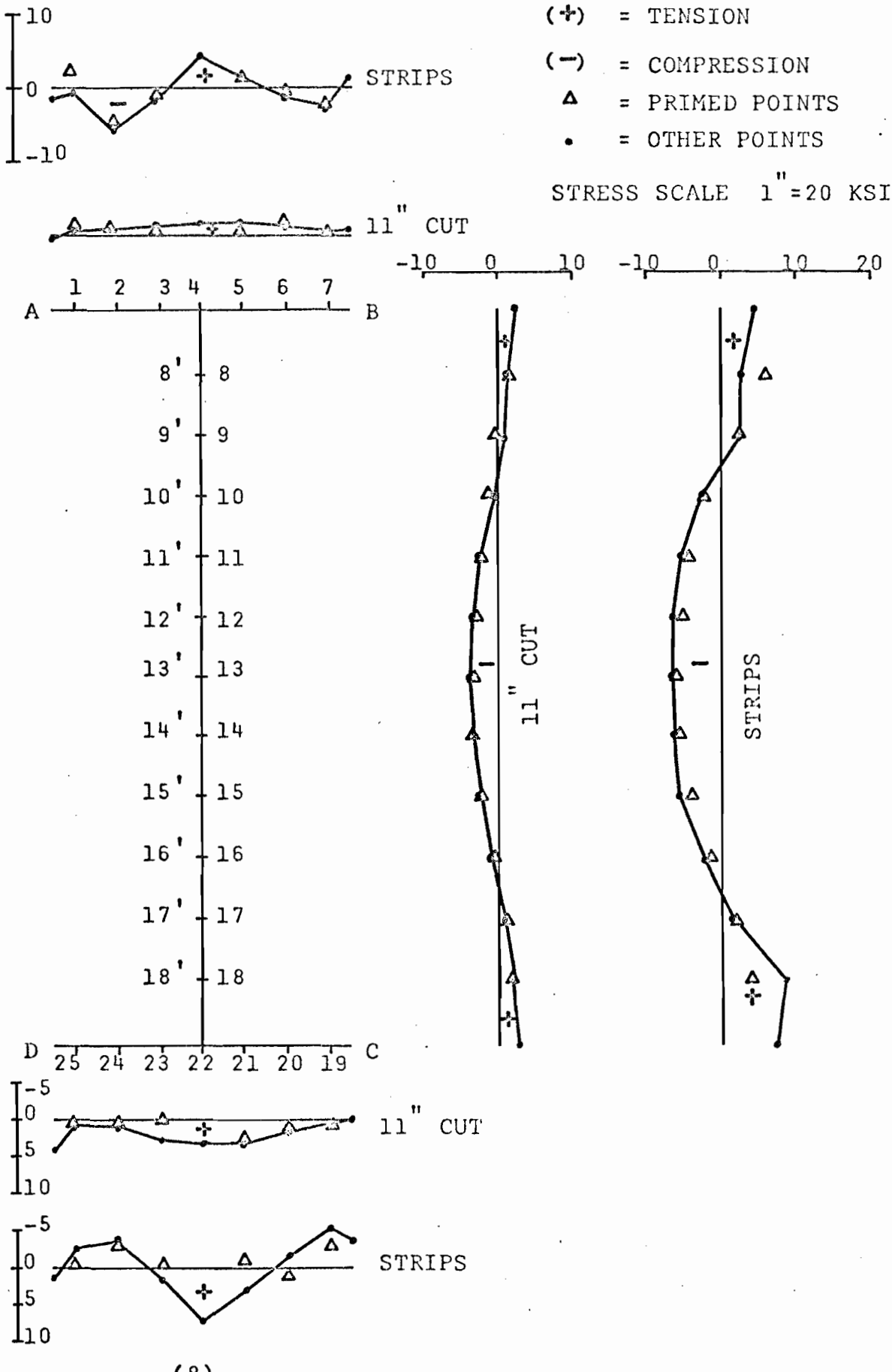

FIG. IV-7[8] RESIDUAL STRESSES IN 10B17 I-SECTION, BEAM G

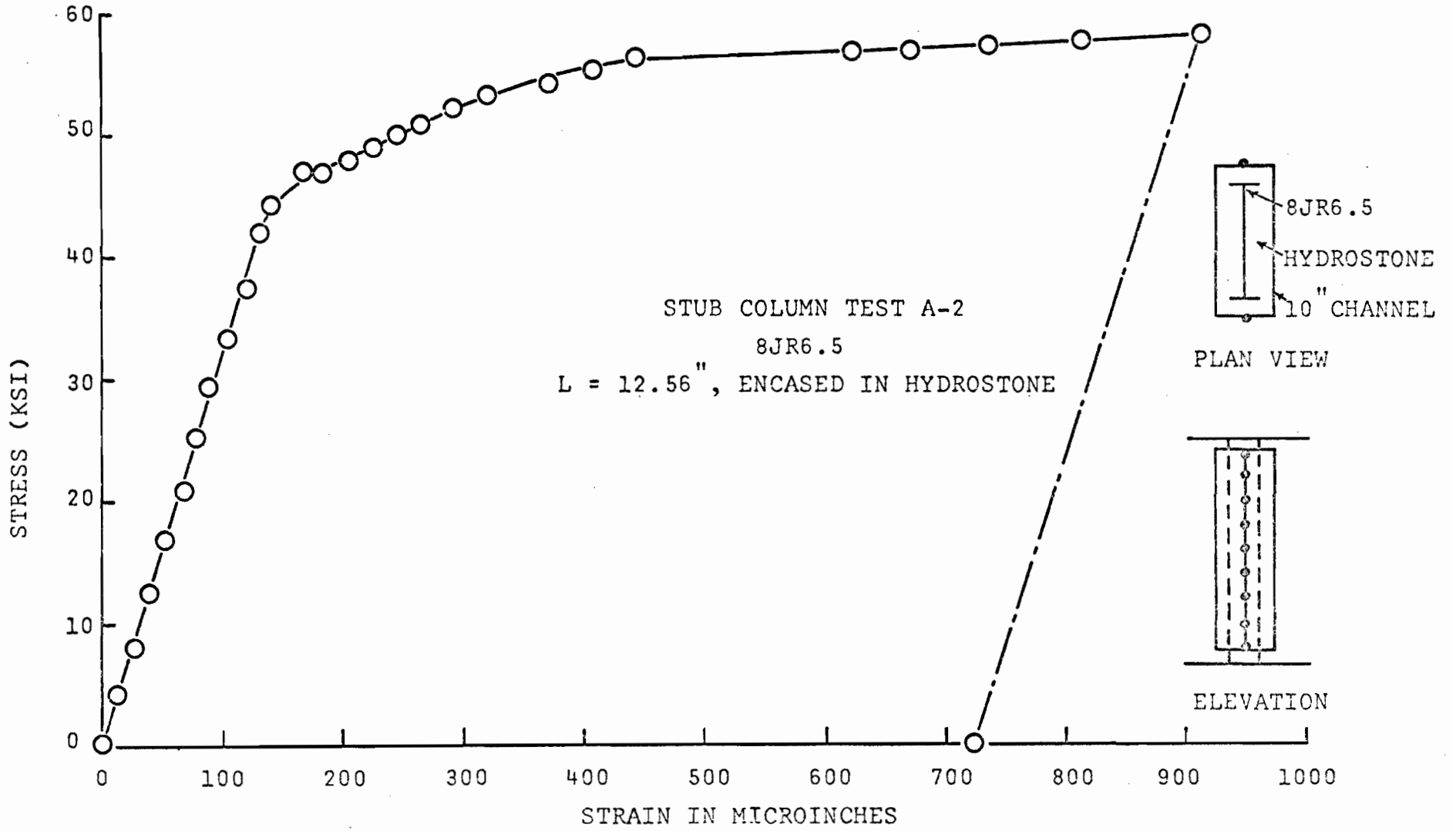

FIG. IV-8[8] 8JR6.5 STUB COLUMN TEST, WITH HYDROSTONE ENCASEMENT

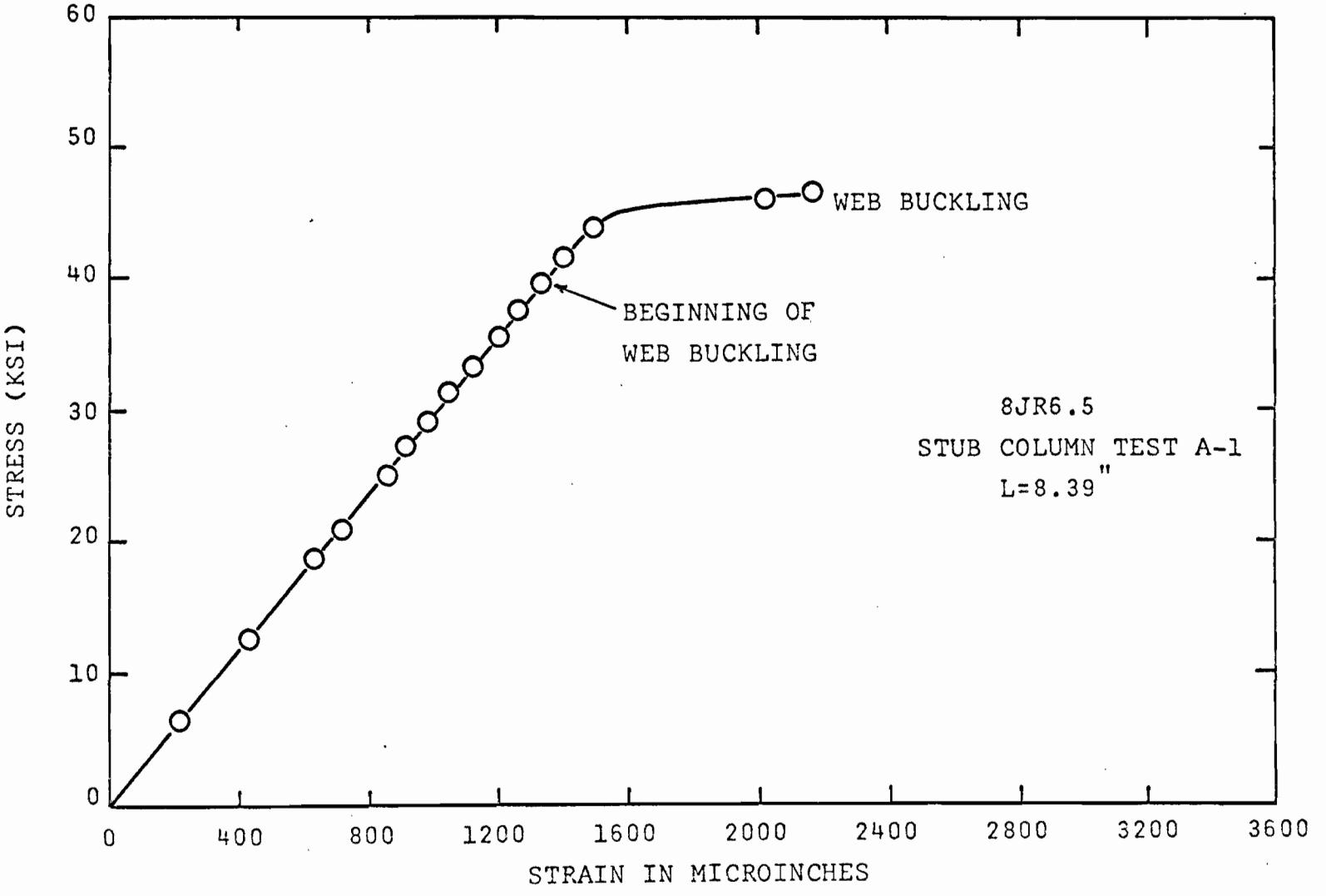

FIG. IV-9[8] 8JR6.5 STUB COLUMN TEST, WITHOUT ENCASEMENT